

**Dynamic proteomics reveals the mitochondrial permeability transition pore can be formed by multiple proteins**

Ziyu Ren

A dissertation submitted in partial fulfilment of the requirements for

**Doctor of Philosophy**

of

**University College London**

Supervisor: Prof Gyorgy Szabadkai

Department of Cell and Developmental Biology

University College London

## Declaration

I, Ziyu Ren, confirm that the work presented in this thesis is my own. Where information has been derived from other sources, I confirm that this has been indicated in the thesis.

## Acknowledgements

I would like to extend my utmost gratitude to my supervisor, Prof Gyorgy Szabadkai, for all his guidance and support, in both academic and personal areas. His experience and expertise are invaluable in helping me develop as a scientist as well as progressing the project. I would also like to thank my graduate tutor Prof Michael Duchon and my secondary supervisor Prof David Selwood for their guidance and expertise on my project. I would like to extend extra gratitude to Prof Michael Duchon for pastoral support during the PhD.

I would like to thank UCL for their faith in me and the Overseas Research Scholarship award. I am also deeply grateful to the BHF (British Heart Foundation) for their recognition of my project design and award of the BHF Doris Baer PhD Studentship.

I am indebted to Dr Gauri Bhosale who patiently taught me many research techniques and guided my progression as a scientist. I thank Dr Chih-yao Chung for wonderful discussions and expertise inputs.

I would like to offer extra thanks to Dr Bill Andrews for all his patient assistance in molecular cloning projects. I would like to thank Jamie Evans for assistance in flow cytometry work and Dr Riccardo Zenezini Chiozzi for his assistance in mass spectrometry work. I thank Erika Bernardini for her help with plasmid cloning. I thank Sam Ranasinghe for all his help in microscopy. I have been helped by so many people in my PhD it is hard to list them all and these people are the ones without whom my PhD project would not be possible.

I would also like to thank all members of the Duchon-Szabadkai labs for all of their daily support, assistance, useful discussions as well as making the lab a fun place to be.

I am very grateful to my family for all their support and understanding during this PhD. Finally, I would like to thank all my friends who have supported me during this period and anyone who have helped me in one way or another.

# Abstract

## Background:

Mitochondrial permeability transition (mPT) is a sudden increase in conductance across mitochondrial membrane (MM). The process is thought to be facilitated by the opening of a physical mega channel known as the mitochondrial permeability transition pore (mPTP). Irreversible opening of the mPTP leads to bioenergetic collapse and cell death which is thought to contribute heavily to ischemia-reperfusion (IR) injury following myocardial infarction. There have been repeated efforts to develop mPTP inhibiting drugs to treat IR injury, but clinical success has yet to be achieved. A major roadblock in the process of developing clinically relevant mPTP inhibitors is the yet unknown molecular identity of the mPTP. There are many suggested candidates for the mPTP where experimental evidence showed that they can modulate the mPTP. However, genetic ablation of any of these candidates failed to abolish mPTP activity, leading to the problem remaining unresolved.

## Aims:

This project aimed to find the channel forming component of the mPTP. CypD is the only undisputed regulatory component of the mPTP. I hypothesised that I could find the mPTP channel by screening for protein interactors of CypD. Although such screens have been done before, I carried out a dynamic screen where I induced mPTP opening via  $\text{Ca}^{2+}$  and compared the CypD interactome with/out mPTP opening. This was only possible with recently developed proteomics techniques and have never been carried out for CypD and the mPTP.

## Results:

The project returned the ATP Synthase, ANT, PiC, VDAC, HSPE1 as relevant CypD interactor hits. I also observed that CypD displayed increased interaction with the ATP Synthase, ANT, PiC and VDAC following mPTP induction via  $\text{Ca}^{2+}$  treatment, this increase is abolished when CsA is added. Additionally, I observed that HSPE1 showed increased interaction with CypD following mPTP induction when CsA is added or when

CypD is desensitized to CsA. This suggest HSPE1 might be involved in a CypD regulated mPTP pathway that is insensitive to CsA.

### **Conclusions:**

The data here would suggest that multiple proteins can form the mPTP channel. I showed that the ATP Synthase, ANT and PiC displayed increased interaction with CypD following mPTP induction, and this interaction was eliminated in the presence of CsA. Although I did not show the process how these proteins form the mPTP, their ability to form the mPTP have been shown by previous work in the field.

My work provides evidence that CypD interacts with multiple mPTP candidate proteins following  $Ca^{2+}$  induced mPTP which provides support for the multiple protein hypothesis of the mPTP. This would also explain why genetic deletion of any single mPTP candidate failed to abolish mPTP activity.

Additionally, this work suggests the possible existence of a previously unknown CsA insensitive CypD mediated mPTP pathway which HSPE1 might be involved in.

## Impact statement

Cardiovascular disease is a leading cause of death worldwide. Opening of mitochondrial permeability transition pore (mPTP) leads to cell death and thus cardiac tissue damage during ischemia-reperfusion (IR) injury following myocardial infarction. In animal models, it has been repeatedly shown that inhibiting mPTP using either genetic approaches or drugs significantly reduces infarct sizes in hearts in reperfusion injury following myocardial infarction. However, while these drugs are cardioprotective in pre-clinical studies, clinical trials have so far failed to find a cardioprotective mPTP inhibitor in humans. In addition to myocardial infarction, the mPTP has also been implicated in a range of diseases including multiple sclerosis, neurodegenerative diseases, muscular dystrophy and ageing. However, research into mPTP's role in these diseases is not as extensive and pharmacological interest is much lesser.

Effective drug development demands understanding of the molecular mechanism of the underlying process. However, the underlying molecular mechanism behind the mPTP process remains unclear. One of the most important questions that remains to be answered is the molecular identity of the mPTP. The identity of the mPTP remains a controversial topic with many candidates including the ATP Synthase, ANT and PiC. Genetic deletion of any of these candidates failed to abolish mPTP activity, leading many to reject them as the mPTP. Elucidating the exact identity of the mPTP will unlock targeted drug design and discovery. It will also aid troubleshooting of existing mPTP inhibitors and their failure in clinical context.

CypD is a mPTP regulator and the only undisputed component of the mPTP. I hypothesised that I could gain insights into the identity of the mPTP by studying changes in the CypD interactome during mPTP opening which is now possible only with new technical developments. I found that CypD increased its interaction with multiple candidate proteins during mPTP opening. This would suggest the mPTP can be formed by multiple proteins and explain why genetic deletion of any single mPTP candidate protein failed to abolish mPTP activity.

My result here will aid the understanding of the process of mPTP formation. It will help clarify the identity of the mPTP channel whose controversial identity has consumed lots of research resources and slowed progress in mPTP research. Clarity over the

identity of the mPTP also means that drug development can now be more focused and specific.

Additionally, greater understanding of the mPTP mechanism will unlock better understanding of mPTP's role in the other diseases mentioned earlier where research is less extensive. With a clearer understanding of mPTP mechanism and identity, it will be easier to further investigate the links between mPTP and these diseases.

Overall, my work would lead to a better understanding of the mPTP, thus supporting future research in mPTP related diseases and drug development.

# Table of Contents

Cover Page .....	1
Declaration.....	2
Acknowledgements .....	3
Abstract .....	4
Impact statement .....	6
Table of Contents.....	8
List of figures.....	11
List of Tables.....	13
Abbreviations .....	14
<b>1. Introduction .....</b>	<b>16</b>
<b>1.1 Overview of the mPTP.....</b>	<b>16</b>
1.1.1 Mitochondria .....	16
1.1.2 General properties of the mPTP.....	17
1.1.3 History of discovery and research.....	18
1.1.4 Biophysical characteristic of the mPTP.....	19
1.1.5 Types of mPTP opening.....	19
1.1.6 mPTP and cell death.....	20
1.1.7 Physiological role of the mPTP .....	21
1.1.8 Molecular identity of the mPTP.....	23
1.1.9 CypD.....	24
1.1.10 Small molecule regulators of mPT.....	25
1.1.11 Medical implications of the mPTP .....	26
<b>1.2 Disease relevance and drug discovery.....</b>	<b>27</b>
1.2.1 Ischemic reperfusion injury.....	27
1.2.2 Other implicated diseases .....	29
1.2.3 Pharmacological and clinical research .....	30
<b>1.3 Disputed molecular identity of the mPTP .....</b>	<b>33</b>



1.3.1 The classical hypothesis .....	33
1.3.2 mPTP candidates .....	38
1.3.3 Alternative theories .....	46
1.3.4 Concluding remarks .....	50
<b>1.4 CypD interactor screens .....</b>	<b>52</b>
1.4.1 Past CypD interactor screens .....	52
1.4.2 Proximity dependent biotinylation and TurboID .....	56
<b>1.5 Research plan .....</b>	<b>57</b>
1.5.1 Establishment of an experimental model for the CypD protein interactome screen .....	57
1.5.2 Generate KO cell line and re-express CypD-TurboID fusion protein ....	58
1.5.3 Protein interaction screen: dynamic proteomics of the CypD interactome.....	63
.....	63
1.5.3 Interpretation and validation of proteomic results .....	63
<b>2. Methods .....</b>	<b>65</b>
2.1 Cell Culture .....	65
2.2 Transfections.....	65
2.3 Mitochondria Isolation.....	66
2.3 Molecular cloning.....	66
2.5 Bicinchoninic acid (BCA) Assay .....	69
2.6 Calcium Retention Capacity (CRC) assays .....	70
2.7 Western blotting.....	72
2.8 CRISPR-Cas9 Genome editing.....	76
2.9 Genomic DNA extraction .....	75
2.10 Proteomics .....	76
2.11 Biological services used .....	78
2.12 Reagents .....	79
<b>3. Generation of HEK293T Cyclophilin D Knockout cell line via CRISPR-Cas9</b>	<b>80</b>
.....	80
3.1 Background .....	80
3.2 Results and Discussion.....	80

3.2.1 CRISPR workflow .....	80
3.2.2 CypD KO Cell line generation .....	85
3.2.3 Expression of fusion proteins in CypD KO cells .....	89
3.2.4 Troubleshooting CypD-TurboID and KO cell line incompatibility .....	91
3.2.5 New round of CRISPR-Cas9 CypD KO cell line .....	101
3.2.6 Fusion proteins breaking up in cells .....	106
3.2.7 Testing of fusion protein in BE22 CypD KO cells .....	113
<b>3.3 Conclusion .....</b>	<b>117</b>
<b>4. Proteomics screen .....</b>	<b>120</b>
<b>4.1 Background .....</b>	<b>120</b>
<b>4.2 Results and Discussion.....</b>	<b>120</b>
4.2.1 Obtaining proteomic samples .....	120
4.2.2 Overview of proteomics results and analysis.....	123
4.2.3 Proteomics results for WT cells .....	128
4.2.4 Proteomics results for CypD KO cells .....	146
<b>4.3 Conclusion .....</b>	<b>164</b>
4.3.1 Addressing potential limitations of the screen .....	164
4.3.2 New insights from the proteomics data.....	169
<b>5. Perspectives.....</b>	<b>172</b>
5.1 OMM channel identity .....	172
5.2 Future research directions.....	173
<b>6. References.....</b>	<b>179</b>
<b>Appendix 1: Review of past CypD interactor hits .....</b>	<b>209</b>
<b>Appendix 2: Screening results of CypD KO cell lines .....</b>	<b>226</b>

## List of Figures

Figure 1.1: Ischemic reperfusion injury and the mPTP.....	28
Figure 1.2: Classical hypothesis on mPTP regulation and formation .....	34
Figure 1.3: Proximity dependent biotinylation as a protein interactor screening tool.....	55
Figure 2.1: Illustrative diagrams of the CRC assay.....	71
Figure 3.1: Workflow for generating CRISPR mediated CypD KO HEK293T cell line .....	82
Figure 3.2: Identifying a successful CypD KO clone of HEK293T.....	85
Figure 3.3: Experimental confirmation of successful CypD KO at protein expression and functional levels .....	87
Figure 3.4: Examining functionality of CypD-TurboID in CypD KO cells .....	90
Figure 3.5: Examining expression of CypD-TurboID in CypD KO cells.....	92
Figure 3.6: Re-examining WT CypD expression in HEK293T cells transfected with CypD-TurboID .....	94
Figure 3.7: Examining functionality of WT CypD in CypD KO HEK293T cells.....	97
Figure 3.8: Examining expression and functionality of WT CypD in WT HEK293T cells.....	99
Figure 3.9: Generation of new CRISPR cell lines.....	103
Figure 3.10: Analysis of protein cleavage sites of CypD, TurboID and CypD-TurboID using the ExPASy PeptideCutter tool .....	108
Figure 3.11: Testing of fusion protein variant designs .....	111
Figure 3.12: Testing of new CRISPR cell lines .....	115
Figure 4.1: Experimental outline for proteomics screen .....	121
Figure 4.2: Generation of proteomics samples.....	122
Figure 4.3: WT cells - aggregated complexes and isoforms - interactor determination using ANOVA followed by t-tests.....	129

<b>Figure 4.3: WT cells – aggregated complexes and isoforms – volcano plot of multiple t-test .....</b>	<b>136</b>
<b>Figure 4.5: WT cells – individual proteins – interactor determination using ANOVA followed by t-tests .....</b>	<b>139</b>
<b>Figure 4.6: WT cells – individual proteins – volcano plot of multiple t-test ... .....</b>	<b>143</b>
<b>Figure 4.7: KO cells – aggregated complexes and isoforms – interactor determination using ANOVA followed by t-tests.....</b>	<b>148</b>
<b>Figure 4.8: KO cells – aggregated complexes and isoforms – volcano plot of multiple t-test .....</b>	<b>155</b>
<b>Figure 4.9: KO cells – individual proteins – interactor determination using ANOVA followed by t-tests .....</b>	<b>158</b>
<b>Figure 4.10: KO cells – individual proteins – volcano plot of multiple t-test.....</b>	<b>162</b>
<b>Figure 4.11: Schematic for mPTP formation with no CsA present based on my data .....</b>	<b>16</b>
<b>Figure 4.12: Schematic for mPTP formation with CsA present based on my data. ....</b>	<b>168</b>
<b>Figure A2: Screening for response to CypD expression in HEK293T CypD KO lines. ....</b>	<b>228</b>

## List of Tables

<b>Table 1.1: Summary of published studies on the molecular identity of the mPTP</b> .....	<b>38</b>
<b>Table 1.2: Summary of mPTP experiments.....</b>	<b>60</b>
<b>Table 2.1 PCR reaction mix .....</b>	<b>67</b>
<b>Table 2.2 Thermocycling steps.....</b>	<b>68</b>
<b>Table 2.3: Antibodies used and respective dilutions .....</b>	<b>75</b>
<b>Table 2.4: Reagent details .....</b>	<b>79</b>
<b>Table 3.1: Analysis of protein cleavage sites of CypD-TurboID using the Procleave tool.....</b>	<b>109</b>
<b>Table 4.1: Summary of proteomics experiment and analysis results .....</b>	<b>127</b>
<b>Table A1: Summary of past CypD protein-protein interaction hits .....</b>	<b>225</b>

## Abbreviations

ADP: Adenosine di-phosphate

ANT: Adenine nucleotide translocator

ATP: Adenosine tri-phosphate

CsA: Cyclosporin A

CypD: Cyclophilin-D

DTT: Dithiothreitol

ER: Endoplasmic Reticulum

FACS: Fluorescence associated cell sorting

GFP: Green fluorescence protein

HEK293T: Human Embryonic Kidney cells immortalised and expressing mutant version of SV30 large T antigen

HRP: Horse Radish Peroxidase (enzymatic method for western blot visualisation)

iBAQ peptides: mass spectrometry output parameter, number of theoretically observable peptides of the protein in a sample

IMM: Inner mitochondrial membrane

IR: Infrared

KO: Gene knockout

LFQ: Label Free Quantification (relative amount of protein normalised across all samples, accounts for protein concentration differences)

MCU: Mitochondrial Calcium Uniporter

MEF: Mouse Embryonic Fibroblasts

MM: Mitochondrial membrane

mPT: Mitochondria permeability transition (the process)

mPTP: Mitochondria permeability transition pore (the physical pore structure allowing mPT to occur)

NHEJ: Non-Homologous End-joining

OMM: Outer mitochondrial membrane

PDVF: Polyvinylidene difluoride (widely used immunoblot membrane)

PiC: Phosphate carrier protein

PPIF: Peptidylprolyl Isomerase F (official gene name for the CypD protein)

Puro: Puromycin

R.T: Room Temperature

RyR2: Ryanodine receptor 2

SR: Sarcoplasmic reticulum

TMRM: Tetramethylrhodamine Methyl Ester (fluorescent dye used for measuring mitochondrial membrane potential)

TSPO: Translocator protein

UPR: Unfolded Protein Response

UTR: Untranslated Region

VDAC: Voltage dependent anion channel

Vh: Vehicle Control

# 1. Introduction

## 1.1 Overview of the mPTP

This section gives an overview and summary of the key areas surrounding mPTP research. These areas will be discussed in more details in the following sections.

### 1.1.1 The mitochondria

Mitochondria are membrane bound organelles found in almost all eukaryotic cells. Unlike the plasma membrane and other organelles such as the Endoplasmic Reticulum (ER), mitochondria are bound by a double membrane instead of a single membrane layer. The inner mitochondria membrane (IMM) and the outer mitochondria membrane (OMM) are separate phospholipid bilayers with the intermembrane space (IMS) residing between them. Mitochondria are the only organelles in a cell with their own genetic information and operate their own gene expression system. Mitochondrial DNA (mtDNA) is a circular DNA encoding 37 genes involved in mitochondrial gene expression and oxidative phosphorylation (Osellame et al., 2012). Mitochondria bear hallmarks of prokaryotic organisms including their own circular DNA genome which led to the prevailing endosymbiotic hypothesis postulating its descent from bacteria (Gray, 2012).

Mitochondria are often referred to as 'the powerhouses of the cell' as they are the sites where most ATP are generated. This occurs via the electron transport chain and proton gradient generated across the inner mitochondria membrane (Osellame et al., 2012).

In addition to their role as the site of energy generation in the cell, mitochondria have more recently gained prominence as a signalling hub. Mitochondria are postulated to regulate metabolism, stress responses, immunity, autophagy, and cellular fate, playing an essential role in maintaining cellular homeostasis (Shen et al., 2022; Stoolman et al., 2022). This recognition has been a long time coming as mitochondria



have long been known to engage in ER crosstalk to regulate cellular calcium homeostasis and play essential roles in multiple cell death pathways (Rizzuto et al., 2003).

The double membrane structure of mitochondria is key to mitochondrial function, it serves as the site for ATP generation via the ETC and the proton gradient across the inner membrane. Integrity of the IMM and the OMM are of utmost importance to cellular survival. Aside from the disruption to energy generation occurring from loss of mitochondrial membrane (MM) integrity, loss of MM integrity is a precursor for cell death. The mPTP is a major pathway that can trigger loss of membrane integrity and cell death but is shrouded in many mysteries (Massimo Bonora et al., 2021). I will attempt to further explore the biology of the mPTP in this work.

### **1.1.2 General properties of the mPTP**

Mitochondrial permeability transition (mPT) is a sudden increase in the permeability of the MM, allowing solutes in the matrix to pass through, disrupting the vital proton gradient and membrane potential across mitochondrial membrane. This change in MM permeability is known as mitochondrial permeability transition (mPT) whereas the physical mega channel whose opening underlies this phenomenon is called the mitochondrial permeability transition pore (mPTP) (I Szabó & Zoratti, 1992). Irreversible opening of the mPTP leads to bioenergetic collapse and cell death (Briston et al., 2018).

mPT is known to be induced by  $\text{Ca}^{2+}$  overload and is sometimes referred to as a  $\text{Ca}^{2+}$  induced  $\text{Ca}^{2+}$  release channel. In addition to  $\text{Ca}^{2+}$ , ROS is also a key inducer of mPT (Assaly et al., 2012; Bernardi, 1999). Additionally, mPTP opening is also known to be affected by factors such as  $\text{Mg}^{2+}$ , NADH,  $\text{H}^+$ , ADP, ATP and  $\text{P}_i$  levels (Bernardi, 1999). mPTP formation is independent of energy and can occur in the absence of mitochondrial energy substrates or in the presence of an uncoupler (Haworth & Hunter, 1979; Douglas R. Hunter & Haworth, 1979a).

It is generally agreed that mPT is a universally conserved phenomenon as it is found in all eukaryotic species examined thus far, with the exception of one (Azzolin et al., 2010). The crustacean *Artemia franciscana* was found to not contain a Ca<sup>2+</sup> induced mitochondrial channel bearing the characteristics of the mPTP (Konrad et al., 2012; Konrad et al., 2011; Menze et al., 2005).

The molecular components responsible for forming the mPTP remain a controversial topic. Many proteins have been proposed to be involved in mPT, but almost all of them have been challenged in one form or other, except for Cyclophilin D (CypD). CypD is the only undisputed component of the mPTP and is known to be a regulatory component, it is also the target of the canonical mPTP inhibitor, Cyclosporin A (CsA) (Baines et al., 2005; Duchen et al., 1993).

### **1.1.3 History of discovery and research**

The existence of mPT was first proposed in a series of papers by Hunter and Haworth (Haworth & Hunter, 1979; Douglas R. Hunter & Haworth, 1979a, 1979b) in 1979. Originally believed to be an artifact of *in vitro* mitochondria manipulation, the evidence later shifted towards that of an actual molecular process when the mPTP demonstrated the key characteristic of having consistent responses to the same stimuli. These includes consistent opening by Ca<sup>2+</sup> induction (D. R. Hunter et al., 1976), consistent responses to modulators such as CsA and a consistent conductance profile that is suggestive of the same channel forming repeatedly (Bernardi et al., 2006).

In addition to the observation that the mPTP is a Ca<sup>2+</sup> induced Ca<sup>2+</sup> release channel, Hunter and Haworth also established some key properties of the mPTP. This includes the size of the channel (< 1.5 kDa) and energy independent formation (Haworth & Hunter, 1979; Douglas R. Hunter & Haworth, 1979a, 1979b).

#### **1.1.4 Biophysical characteristics of the mPTP**

The maximum size of solute which can pass through the channel was determined to be 1.5 kDa by Hunter and Haworth when they first described the mPTP (Haworth & Hunter, 1979). The mPTP is also thought to have a diameter of around 2–3 nm (Zoratti & Szabò, 1995).

In the context of membrane channels, conductance (often reported in siemens (S)), is a quantitative measure of how easily ions flows across a channel (Bezanilla, 2008). In the case of the mPTP, this would measure how fast ions in the matrix would flow across the IMM following mPTP opening. Electrophysiological approaches were used involving patch clamping of the IMM during mPTP opening (M. A. Neginskaya et al., 2021).

Across multiple studies, the mPTP showed a wide range of conductance. It was measured to display conductance ranging from 35, 120-150, 350, and 1,000 pS (Kinnally et al., 1989) up to levels of 1-1.3 nS (Kinnally et al., 1989). The mPTP was alter termed the mitochondrial multiple conductance channel based on these observations, but it was not yet clear then what was behind this wide range of conductance properties (Kinnally et al., 1996).

More recently, the multiple conductance state in the mPTP has been linked to the controversy surrounding the molecular identity of the mPTP. The mPTP was shown to display alternative conductance when the ANT targeting mPTP inhibitor bongkreikic acid was applied (Neginskaya & Pavlov, 2023) and when the ATP Synthase is absent (Neginskaya et al., 2019). This would suggest that the multiple conductance state of the mPTP might correspond to multiple proteins which forms the mPTP channel. This assumes the multiple channel hypothesis of the mPTP to be true which I will discuss in further detail in later sections.

#### **1.1.5 Types of mPTP opening**

The mPTP is thought to undergo 2 different types of opening. The first and most well characterised is that of an irreversible opening, which acts as a cell death pathway

(CROMPTON, 1999). This is the phenomenon that is commonly referred to as mPT in the literature. When mPT or mPTP opening appears in the literature, it is assumed to be referring to the irreversible opening of the mPTP unless transient opening is specifically stated. In which case the work would be referring to the much lesser studied process of transient opening and closing of the mPTP.

The second state is that of transient opening and closing (Boyman et al., 2019; Jonas et al., 1999, 1997; Lu et al., 2016; Malkevitch et al., 1997; Petronilli et al., 1994). It is thought that this state should not lead to cell death and potentially have physiological relevance (Icha & Mazat, 1998; Petronilli et al., 1999). Transient opening has been suggested to play regulatory roles for Ca<sup>2+</sup> balance and signalling (Agarwal et al., 2017; Elrod et al., 2010). This state is not as widely studied likely due to difficulty involved in measuring transient Ca<sup>2+</sup> pulses. Unlike the irreversible opening, there is no consistent and reliable method for inducing transient mPTP opening, which makes studying the phenomenon even more difficult.

This work focuses on irreversible mPTP opening (instead of transient opening), which is the type of mPTP implicated in disease conditions and all references to mPT and mPTP in this work refers to irreversible mPTP opening.

### **1.1.6 mPTP and cell death**

Mitochondria play an important role in cell death and are known to regulate multiple cell death pathways. The most prominent being that of apoptosis but it is also heavily involved in necrosis. The mPTP has been suggested to play a role in both forms of cell death (Borutaite et al., 2003; Nakagawa et al., 2005).

Sustained mPTP opening results in disruption of the MM membrane potential and ion gradients. This leads to decreased ATP production and an increase in ROS due to ETC dysfunction. The low energy state and high ROS are key triggers for necrotic cell death (Karch & Molkenin, 2015). Additionally, ischemia reperfusion is well characterised as a precursor for necrotic cell death with numerous necrotic promoting

conditions including hypoxia, glucose depletion, Ca<sup>2+</sup> overload and eventually mPTP opening (Eum et al., 2007).

mPTP mediated necrosis is well characterised and generally considered to be the pathway for cell death when mPTP opens (M. Bonora et al., 2014; Galluzzi et al., 2018). On the other hand, apoptosis is also thought to occur following mPTP. This is because the process of mPTP facilitates the initiation of apoptosis. mPTP opening leads to loss of OMM integrity, causing key apoptotic inducers including cytochrome C and AIFM1 to be released (M. Bonora et al., 2014). However, a rather impactful study in 2005 provided experimental evidence against apoptotic cell death as a mPTP downstream pathway (Nakagawa et al., 2005). Which lead to doubts regarding whether apoptosis is a downstream pathway of mPT. On the other hand, the presence of apoptosis following mPT continues to be experimentally reported and argued for (Borutaite et al., 2003; Eum et al., 2007; Precht et al., 2005).

A key argument for the reconciliation of these experimental evidence is the suggestion that the occurrence of apoptosis or necrosis following mPTP opening is determined by the cellular energy state (Galluzzi et al., 2018; Leist et al., 1997). A low energy state in the form of a lack of ATP is a necrosis favouring factor (Karch & Molkentin, 2015) whereas ATP itself required to facilitate apoptosis (Tatsumi et al., 2003). Higher ATP levels have been shown to favour apoptosis over necrosis (Izyumov et al., 2004). Hence it has been argued that mPTP can undergo both pathways with ATP level been the determinant of the exact cell death pathway.

### **1.1.7 Physiological role of the mPTP**

Given that mPT is an almost universally conserved phenomenon in eukaryotic organisms, it seems only reasonable that there might be an evolutionary advantage associated with it. While the mPTP is heavily implicated in ischemic reperfusion (IR) injury, it only serves to add to the damage. As such, it is more likely that the role it plays in IR injury is not its original role, but rather an unintended side effect. It is not yet clear what physiological role or evolutionary advantage mPT might serve, although experimental studies have provided some interesting possibilities.

While there has not been any conclusive consensus in the field on the physiological role of the mPTP. There have been studies looking into this. The earliest suggestion was that the mPTP was involved in Ca<sup>2+</sup> efflux and regulation (Altschuld et al., 1992), CypD KO mice were also suggested to be more susceptible to heart failure as a result of stress due to deregulation of mitochondrial Ca<sup>2+</sup> homeostasis (Elrod et al., 2010). However, the role mPTP might play in Ca<sup>2+</sup> efflux has been questioned (E. De Marchi et al., 2014) and CypD KO mice has normal lifespan compared to WT mice (Baines et al., 2005). Nevertheless, Ca<sup>2+</sup> regulation remains a top contender with regards to possible physiological functions of the mPTP, with neuronal plasticity been an interesting area where mPTP might play a role.

#### **1.1.7.1 Neuronal Plasticity**

As part of their role in Ca<sup>2+</sup> regulation, the mPTP was suggested to regulate neuronal plasticity (Mnatsakanyan et al., 2016). In squid axons, it was demonstrated that mitochondria was key to the process of short term potentiation (Jonas et al., 1999). During action potential, Ca<sup>2+</sup> enters the synaptic terminal to trigger release of neurotransmitters. Some of these Ca<sup>2+</sup> were then taken up by the mitochondria. Following these, arrival of new action potential causes another wave of Ca<sup>2+</sup> to enter the synaptic terminal. During this new Ca<sup>2+</sup> wave, Ca<sup>2+</sup> previously stored in the mitochondria was released, leading to a greater amount of Ca<sup>2+</sup> and hence larger amounts of neurotransmitter release. The end result of greater neurotransmitter release is neuronal plasticity and the Ca<sup>2+</sup> induced Ca<sup>2+</sup> release channel of the mitochondria strongly implicates the mPTP, specifically transient opening of the mPTP since no cell death occurs. This evidence formed the basis for the argument that mitochondria is key to neuronal plasticity (Jonas et al., 1999; Jonas & Elizabeth, 2006; Neher & Sakaba, 2008).

More recently, it has been shown that mPTP activity (with manipulations using CsA and atractyloside) was able to regulate neuroplasticity (Stockburger et al., 2016). The evidence suggest that it would be interesting to further investigate the role of the mPTP in neuronal plasticity as a potential physiological function of the mPTP.

### **1.1.7.2 Metabolic regulation**

The main candidates for the mPTP channel are the ATP Synthase, the ANT and PiC. They are some of the most important enzymes involved in energy production in the mitochondria (Jennifer Q. Kwong & Molkentin, 2015). Additionally, the mPTP is also regulated by ADP/ATP, Pi and H<sup>+</sup> which are the main players in the energy production process (Bernardi, 1999). Opening of the mPTP is highly regulated by these metabolic proteins and molecules, the result of its opening also severely and unavoidably affects energy production due to disturbance of the mitochondria membrane potential. Additionally, evidence have shown that in CypD KO models, TCA cycle is heavily affected with altered enzyme activity (Elrod et al., 2010; Menazza et al., 2013). It is clear that mPTP can regulate metabolism and is also in turn regulated by the cell's metabolic state. What we do not yet know is what purpose mPTP serves in the overarching picture of metabolic regulation, which would also be an interesting area to investigate potential physiological roles of the mPTP.

### **1.1.8 Molecular identity of the mPTP**

Ever since the discovery of the mPTP by Hunter and Haworth, the molecular identity of the mPTP has remained a controversial topic. Numerous different proteins were suggested to form the mPTP but every proposed candidate has experimental evidence that disputes its validity. As such, there is no consensus within the field as to which protein constitute the actual channel forming unit of the mPTP. However, there is consensus on the fact that Cyclophilin D is a regulatory component of the mPTP (Briston et al., 2018; Carraro et al., 2020; Chinopoulos, 2018).

The mPTP have to be a membrane protein for it to be able to form a channel across the MM. As such, known mitochondria membrane proteins have attracted the most attention and investigation as possible candidates for the mPTP. The 2 candidates with the most support in the field includes the Adenine nucleotide translocator (ANT) and the ATP Synthase, while other candidates include the mitochondrial phosphate

carrier (PiC), Voltage dependent anion channel (VDAC), Metalloprotease spastic paraplegia 7 (SPG7), Translocator protein 18 kDa (TSPO), as well as BCL-2 proteins Bax and Bak (Baines & Gutiérrez-Aguilar, 2018; Carrer et al., 2021; Jonas et al., 2015). The various evidence for and against these candidates will be discussed in more detail in section 1.3. Novel theories that suggest alternative explanations to the mPTP identity mystery other than putting forth various proteins as candidates will also be considered.

### **1.1.9 CypD**

Cyclophilin-D is a 21-kDa protein located in the mitochondrial matrix. It belongs to the Cyclophilin family and is a peptidyl-prolyl cis-trans isomerase. It catalyses proline imidic peptide bonds and might have roles in assisting protein folding (Baines et al., 2005).

The drug CsA was initially observed to be able to increase the amount of Ca<sup>2+</sup> mitochondria can accumulate (Fournier et al., 1987). It was later shown that this effect of increased Ca<sup>2+</sup> retention was due to the ability of CsA to inhibit mPT (M. Crompton et al., 1988). Using a photoactive version of CsA, CypD was identified as a target of CsA (Tanveer et al., 1996). This led to the hypothesis that CypD is a key component of the mPTP. Strong evidence confirmed this when a knockout (KO) mice model of CypD was shown to significantly reduce mPTP activity and result in loss of CsA sensitivity of the mPTP (Baines et al., 2005).

CypD undergoes multiple post-translational modifications that has all been suggested to affect its ability to regulate the mPTP. These modifications include acetylation (Hafner et al., 2010), phosphorylation (Rasola et al., 2010) and S-nitrosylation (Nguyen et al., 2011).

Similarly to the mPT, the physiological function of CypD remains unclear but experimental work have provided insight into some possible roles. CypD KO mice are healthy and lack any significant observable phenotype with normal lifespan (Baines et



al., 2005). Reported observable phenotypes during animal husbandry include possible adult onset obesity and elevated anxiety levels (Luvisetto et al., 2008).

However, studies at the molecular level reveals that there are many changes at this level in CypD KO mice even if they didn't have significant effects on lifespan and animal husbandry of these mice. They show dysregulated Ca<sup>2+</sup> homeostasis and upregulation of Ca<sup>2+</sup> activated pyruvate dehydrogenase and  $\alpha$ -ketoglutarate dehydrogenase, there was also increased cardiac hypertrophy and reduced cardiac function in response to stress (Elrod et al., 2010). Additionally, CypD KO mice also displayed altered TCA cycle enzyme activity and levels of pyruvate and branched-chain amino acid (Menazza et al., 2013).

CypD is the most important protein when it comes to studying mPT. It established this status through the sheer consistency among experimental studies when it comes to how CypD manipulation can affect mPT. It is also consistent throughout various species and types of models, from mitoplasts to cells to animals. This is in sharp contrast to other proposed components of the mPTP. All other proposed components of the mPTP have contradictory evidence arguing against their role in mPT. Studying these proteins under different experimental models/assays have often lead to inconsistent and often contradictory results (Baines & Gutiérrez-Aguilar, 2018; Massimo Bonora et al., 2021; Briston et al., 2018).

#### **1.1.10 Small molecule regulators of the mPT**

mPT is regulated by Mg<sup>2+</sup>, NADH, H<sup>+</sup>, ADP, ATP, Pi and is affected by a range of different drugs (Bernardi, 1999; Novgorodov et al., 1992). Of these drugs, the earliest to be discovered and most commonly used include the CypD targeting CsA and the Adenine nucleotide translocator (ANT) targeting atractyloside (ATR) and bongkreikic acid (BKA). Small molecule screens have since then discovered many more mPT modulators. However, their target and effect on mPTP are less where characterised whereas the aforementioned drugs have long been established and has been repeatedly used in mPTP research. CsA has emerged as the standard mPTP inhibitor used in research. This is in part due to its effectiveness, consistency and in part

because it targets CypD, the only universally undisputed component of the mPTP (Briston et al., 2018).

### **1.1.11 Medical implications of the mPTP**

The mPTP has been implicated in a range of diseases from muscular dystrophy to neurodegenerative diseases such as Alzheimer's disease. The evidence linking mPTP to Ischemic Reperfusion (IR) injury in the heart and ischemic strokes has been the most convincing and has attracted attention from many researchers (Davidson et al., 2019). A large amount of work has been done to study the possibility of targeting the mPTP for cardio-protection in IR injury. Unfortunately, consistent success in animal models has yet to be translated to clinical success (Massimo Bonora et al., 2021; Briston et al., 2018).

## **1.2 Disease relevance and drug discovery**

The mPTP has been suggested to be a causal mechanism in multiple diseases, most notably IR injury. Inhibition of mPTP via drug or genetic means have achieved repeated success in reducing IR injury in preclinical models. However, clinical success with an mPTP inhibitor have yet to be achieved (Briston et al., 2018).

### **1.2.1 Ischemic reperfusion injury**

The Global Burden of Disease (GBD) study estimates that Cardiovascular diseases continue to be the leading cause of death worldwide in 2017, with ischaemic heart disease accounting for nearly 50% of these deaths (Roth et al., 2018). In light of this, any improvement in treatment of ischaemic conditions would bring significant benefits. Ischemic Reperfusion (IR) injury is the damage which occurs to cardiac tissues upon restoration of blood flow following an ischaemic episode. It is an important contributor to infarct size following an ischaemic and reperfusion episode and is mechanistically heavily linked to the mPTP (Davidson et al., 2018, 2019; Duchon et al., 1993; Griffiths & Halestrap, 1993).

A large amount of evidence has supported the role of the mPTP as a possible target for cardio-protection in IR injury. This is based on numerous studies measuring infarct size in animal hearts or cell death in cardiomyocytes. These studies showed that experimental models where mPT activity is suppressed (via genetic or pharmacological methods) can effectively protect against IR injury (Argaud et al., 2005; Baines et al., 2005; Davidson et al., 2015, 2006; D. Hausenloy et al., 2003; D. J. Hausenloy et al., 2004; S. A. Javadov et al., 2003; Nakagawa et al., 2005; Staat et al., 2005).

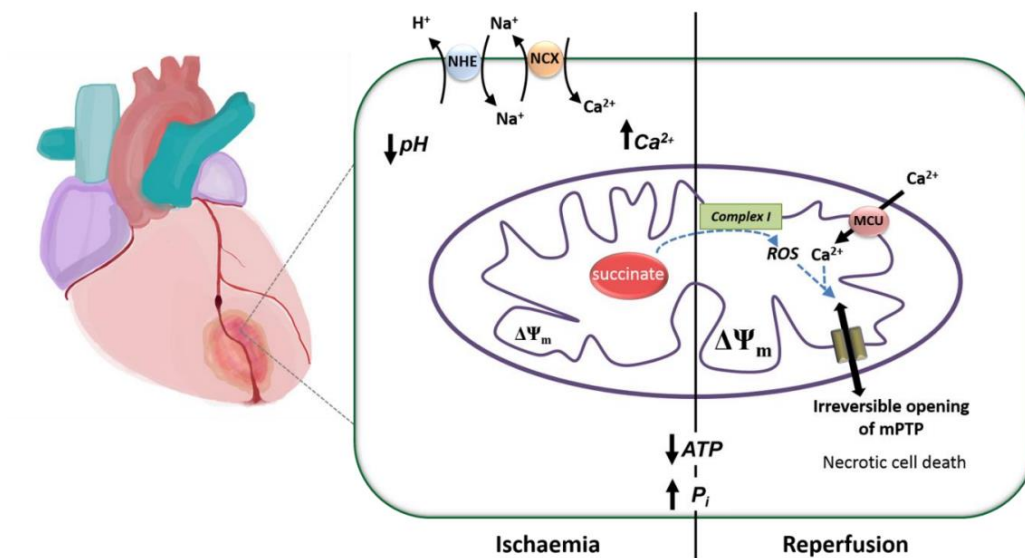


**Figure 1.1: Ischemic reperfusion injury and the mPTP** (Bhosale et al., 2015)

During ischemia  $\text{Ca}^{2+}$  concentration increases which would normally trigger mPT but is offset by increased  $\text{H}^+$ , succinate also accumulates. Following reperfusion,  $\text{H}^+$  concentration decreases removing mPT inhibition, the accumulated succinate drives complex 1 reversal to produce ROS which combines with high  $\text{Ca}^{2+}$  to drive mPT.

Fig 1.1 illustrates how mPT is primed during ischemia and subsequently triggered during reperfusion. During ischemia,  $\text{H}^+$  accumulates in the cytosol. The  $\text{H}^+$  is then exchanged for  $\text{Na}^+$  via the NHE and the  $\text{Na}^+$  is subsequently exchanged for  $\text{Ca}^{2+}$ , thus overloading the cells with  $\text{Ca}^{2+}$  which is taken up into mitochondria via the MCU (Murphy & Steenbergen, 2011). While  $\text{Ca}^{2+}$  overload in the matrix would normally be enough to trigger mPT immediately, the mPTP is thought to be inhibited by the high levels of  $\text{H}^+$  in the matrix which have accumulated due to shut down of ETC as a result of ischemia and lack of oxygen (Murphy & Steenbergen, 2008). During ischemia, reversal of succinate dehydrogenase also converts large amount of fumarate to succinate. This oversupply of succinate then drives reverse operation of Complex 1 following reperfusion which is responsible for generating large amounts of ROS in a

short time period (Briston et al., 2017; Chouchani et al., 2014). Additionally, rapid re-supply of oxygen and ATP to cells leads to hyperactivation of Ryanodine receptor 2 (RyR2), the sarcoplasmic reticulum (SR) Ca<sup>2+</sup> release channel. This results in rapid cycles of SR Ca<sup>2+</sup> uptake and excessive SR Ca<sup>2+</sup> release, further fuelling Ca<sup>2+</sup> accumulation in mitochondria (Davidson et al., 2020). As such, following reperfusion, the reduction of the inhibitory levels of H<sup>+</sup>, the large increase in ROS and the accumulated Ca<sup>2+</sup> in the matrix is thought induce mPT during IR leading to cell death (Bauer & Murphy, 2020).

Based on numerous experimental evidences, cell death due to mPT has been attributed to be a key factor for infarct size determination in IR injury (Bauer & Murphy, 2020). This means that a drug that can inhibit mPT and thus reduce IR injury infarct size can have potentially huge benefits in treating myocardial infarction.

### **1.2.2 Other diseases linked to mPTP**

In addition to IR injury, a range of other diseases have also been linked to mPT. However, evidence for the role of mPT in these diseases are not as extensive and well established as that of IR injury. As such, most pharmaceutical development efforts have focused on targeting the mPTP for IR injury. Nonetheless, some of the work which implicates the mPTP in other diseases are listed below to give a brief overview of the scope of disease mPTP might be involved in.

With regards to multiple sclerosis, CypD KO have been shown to protect against axon damage in a mice model (Forte et al., 2007). In Alzheimer's Disease (AD), CypD has been suggested to interact with Amyloid-beta and CypD deficiency is able to alleviate AD phenotypes in mice AD models (Du et al., 2008, 2011; Du & Yan, 2010). In Amyotrophic Lateral Sclerosis (ALS), CypD KO delayed onset and increased survival of an ALS mice model (Martin et al., 2009).

Inhibition of CypD has been shown to improve dystrophic conditions in a mice model of Duchenne muscular dystrophy (DMD) (Reutenauer et al., 2008). CypD has also been shown to rescue disease phenotype in a mice model of muscular dystrophy

(Millay et al., 2008). Patient myoblasts have been shown to be more susceptible to mPT in Ullrich congenital muscular dystrophy compared to healthy controls (Angelin et al., 2008). Genetic ablation of CypD also offered protection against collagen VI deficiency diseases including Ullrich congenital muscular dystrophy (UCMD) and Bethlem myopathy in a mice model (Palma et al., 2009).

The mPTP has also been suggested to play a role in beta-cell death in diabetes caused by Pdx-1 deficiency (Fujimoto et al., 2010).

The mPTP is also suggested to play a role in aging (Rottenberg & Hoek, 2017). It has been shown to influence lifespan of *C.elegans* (B. Zhou et al., 2019) and modulate age-related osteoporosis (Shum et al., 2016). Recently, mPTP has been suggested to regulated ageing via the Unfolded Protein Response (UPR) (Angeli et al., 2021).

### **1.2.3 Pharmacological and clinical research**

#### **1.2.3.1 Cyclosporin A (CsA)**

CsA is the canonical Cyclophilin D inhibitor and originally shown to protect against cardiac injury even before its role in the mPTP has been established. Following the discovery of CsA as a mPTP inhibitor, it was soon shown that the cardio-protective effects of CsA is dependent upon its ability to inhibit the mPTP (Griffiths & Halestrap, 1993; Nazareth et al., 1991).

CsA was shown to reduce infarct size following IR even when administered after onset of ischemia in mice models (Weinbrenner et al., 1998). In addition to mice models, the protective effects of CsA has also been demonstrated in isolated rat hearts (Griffiths & Halestrap, 1993) and even *in vivo* in minipigs (Skyschally et al., 2010). Although CsA has multiple targets, it was shown that its binding to Cyclophilin D is responsible for this protective effect. This provided further evidence for mPT's involvement in IR injury (Halestrap et al., 1997).

Following the success of CsA in reducing cardiac tissue damage in preclinical models, clinical trials were set up to test whether this success can be translated to better clinical

outcomes for patients. Initially, CsA showed promise when it was found to reduce infarct size in patient with acute myocardial infarction in a phase 2 trial (Piot et al., 2008). However, a follow-up phase 3 trial with a much larger number of patients showed no benefit in terms of IR injury following CsA administration (Cung et al., 2015).

It should also be noted that CsA is an immunosuppressant often used in organ transplantation, its long term use brings undesirable long term immune deficiency effects (Matsuda & Koyasu, 2000) and potential for renal damage (Klintmalm et al., 1981). This prevents its potential use as a long-term drug for patients with cardiovascular problem so it can offer protection before ischemia sets in. Additionally, this also shuts off any chance for application in the other implicated diseases discussed above such as neurodegenerative diseases.

### **1.2.3.2 Difficulties in drug design and discovery**

mPTP inhibition has failed to deliver clinical benefits despite numerous successes in animal studies (Briston et al., 2018). Although CypD is an undisputed regulatory component, attempts to utilize the classic inhibitor Cyclosporin A (CsA) and its analogues to target CypD have all failed to deliver clinical benefits (Briston et al., 2018; S. Javadov et al., 2017). This is a puzzling result that led scientists to look for potential explanations. It must be noted that even complete genetic elimination of CypD results only in partial desensitisation of mPTP opening to conditions of IR injury (Baines et al., 2005). As such, one proposed explanation is that if the stimulus coming from IR is too great (e.g too much ROS or Ca<sup>2+</sup> overload), the partial desensitization of the mPTP would not be enough to be able to afford the necessary protection (Bauer & Murphy, 2020). This would explain why clinical trial results are ambiguous and failed to show statistically significant protection against IR injury. On this line of reasoning, elucidating the identity of the mPTP channel becomes even more important as targeting the actual channel itself instead of a regulatory component will afford much greater inhibition of the mPTP and potentially achieve clinical success.

Another important point to note is that CypD have been much of the focus on drug development not only because it has the strongest supporting evidence in IR injury

protection, but also that the other proposed mPTP components are difficult to target. The strongest candidates for the mPTP channel components are ANT and ATP Synthase. Proper function of both of them are essential for survival and their inhibition might lead to disastrous results for human health. As such the current mPTP candidates does not really offer any good drug targets that can be targeted, leading to additional headwinds in mPTP drug development.

While it is not possible to rule out that the systemic set-up of the mPTP pathway simply does not offer proper drug targets, we cannot know in any certainty whether that is the case given our lack of knowledge regarding the actual components of the mPTP and the dynamics of the pore forming process. The success in animal models has maintained hopes that the mPTP has the potential to bring about health benefits as a treatment target. As such, clarifying the molecular identity of the mPTP remains a priority.

### **1.2.3.3 MCU inhibition as indirect mPTP inhibition**

Given a lack of success in targeting the mPTP components directly, researchers explored whether it would be beneficial to inhibit the mPTP indirectly. As discussed earlier, Ca<sup>2+</sup> overload in the mitochondrial matrix is a primary driver for mPT in IR. Hence preventing Ca<sup>2+</sup> overload might remove mPT stimulus and protect against mPT induced IR injury. This became possible with the discovery of the MCU as the main channel for mitochondrial Ca<sup>2+</sup> import (De Stefani et al., 2011).

Experimental studies thus far were unclear regarding whether MCU inhibition could offer any promise when it comes to treating IR injury. The results from MCU KO studies in mice has been mixed. In 2 separate studies, one with a germline MCU KO (Pan et al., 2013) and one with a cardiac specific MCU KO that turns on at birth (Rasmussen et al., 2015), infarct size of KO hearts were no different from WT hearts when exposed to IR injury . However, in 2 separate studies, tamoxifen-induced MCU KO in adult hearts provided cardio-protection when exposed IR injury (Jennifer Q. Kwong et al., 2015; Luongo et al., 2015). A new study has suggested that constitutive MCU KO results in desensitization of mPTP to Ca<sup>2+</sup> (the main mPTP inducer during IR) via



phosphorylation of CypD-S32, thus resulting in the absence of cardio-protection in the constitutive KO models. The induced KO models did not undergo this adaptation process and hence still retains cardioprotective capabilities (Parks et al., 2019). A such, targeting the MCU for mPTP inhibition remains a possibility. However, more work is required to fully understand the mechanism and resolve the discrepancy in preclinical studies before further developments can proceed.

## 1.3 Disputed molecular identity of the mPTP

### 1.3.1 The classical hypothesis

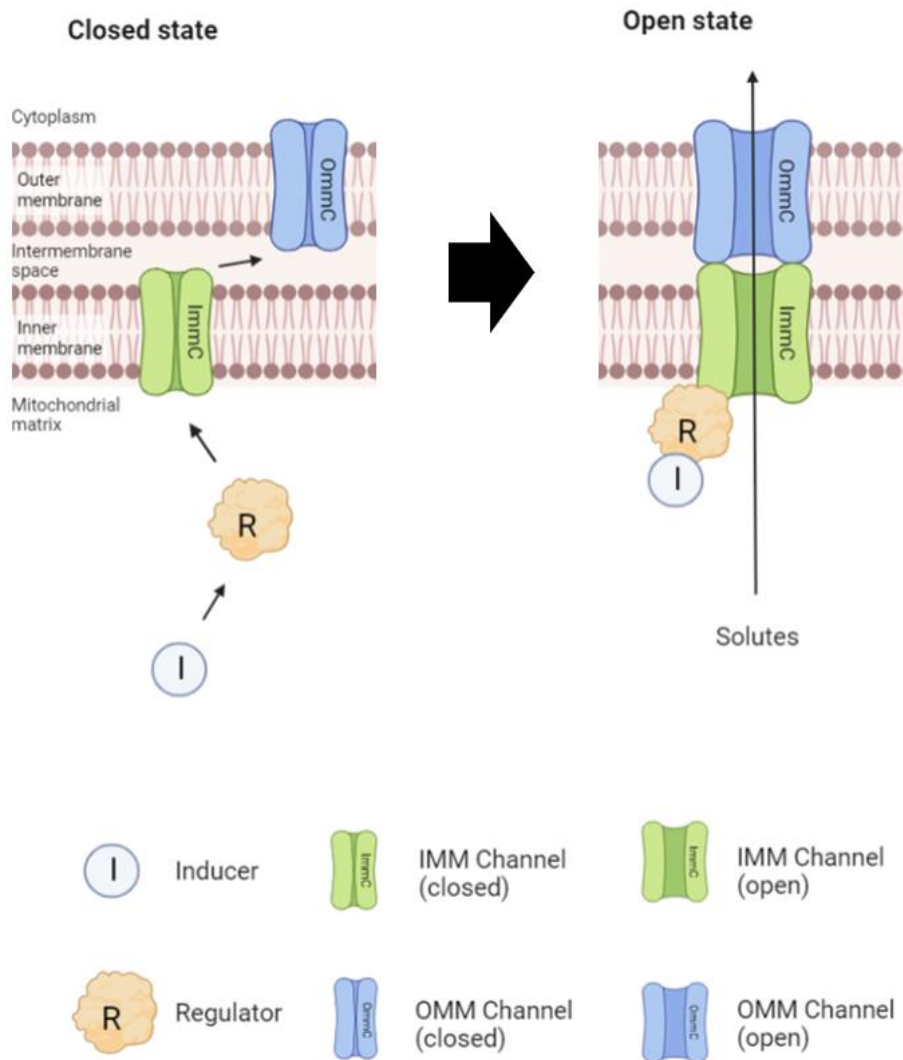


**Figure 1.2: Classical hypothesis on mPTP regulation and formation**

The classical hypothesis of the mPTP is what research on mPTP identity have been based upon for the past few decades. However, growing evidence suggest that it should be rejected. I will discuss how this hypothesis has led to the controversy

surrounding the identity of the channel forming component of the mPTP and why rejecting it in favour of the multiple protein hypothesis is something that should be considered.

The hypothesis basically follows the standard inducer-regulator-effector structure that permeates molecular biology. First, an inducer in the form of some sort of signal will have to come along. The inducer interacts with a regulator which then goes on to cause a conformational change in the final effector proteins which leads to a response. A classic example of a typical molecular pathway would be the  $\text{Ca}^{2+}$  - Troponin C – muscle contraction pathway (Bagur & Hajnóczky, 2017). A similar structural pathway can be applied to a host of different biological pathways ranging from gene expression regulation to hormone release to neurotransmission, another example being the Wnt pathway (Gordon & Nusse, 2006).

As seen in Fig 1.2, in the case of the mPTP, the hypothesis that has been in operation for many years starts with  $\text{Ca}^{2+}$ /ROS acting as Inducer molecules which interact with the Regulator, CypD. The Regulator CypD then interacts with the IMM Channel. The IMM Channel goes on to recruit an OMM Channel and a complex involving the Regulator, IMM Channel and the OMM Channel forms. This hypothesised channel complex is the mPTP which will allow solutes below a certain size to pass through, thus leading to mPT and cell death as discussed earlier.

While the role of  $\text{Ca}^{2+}$ /ROS as inducers and CypD as the key regulator have been repeatedly confirmed experimentally, the identity of the IMM Channel and the OMM Channel have been a topic of much debate. As mentioned earlier, despite being the protein with the strongest and most consistent data on mPT regulation, CypD KO only desensitizes the mPTP to  $\text{Ca}^{2+}$ /ROS induced opening but does not prevent it. Combined with the fact that it is a matrix protein and would need some sort of enormous and incredible conformational changes to insert itself into the MM and become a pore, CypD has been ascribed the role of the regulator in this view.

That still leaves the identity of the IMM and OMM channel to be deciphered. However, unlike a regulator element like CypD, the mPTP cannot possibly form without the IMM or OMM channel protein according to the classical view. As can be seen in the diagram in Fig 1.2, there needs to be a physical channel pathway for the hydrophilic solutes to

cross the 2 hydrophobic MM. Hence the hypothesised channel forming protein has been called the indispensable core component of the mPTP. In hypothesis, if a protein is the IMM or OMM channel of the mPTP, a KO model of that protein should completely erase mPTP activity since there would be no way for the channel to form and hence solutes to pass through. This is the hypothesis the field has adopted and every proposed channel component of the mPTP have been put to the test with KO models. However, in practice, this has caused huge amounts of problems for the field. None of the proteins that has been proposed to be the IMM or OMM channel passed the KO test where their KO erases mPTP activity.

What makes things even more complicated is that most of the proposed candidate proteins for the channel component of the mPTP have strong evidence supporting their role in mPT. This can include evidence where their genetic manipulation modulates mPTP activity. Which creates a puzzling scenario where KO of all of the candidates appears to reduce mPTP activity but never fully abolish it. Table 1.1 includes a summary of the experimental evidence that supports or rejects the possibility of a particular protein being the core channel unit of the mPTP. The candidates are also discussed in more detail in the following sections.

Candidate	Location	Supporting evidence	Contradicting evidence
Adenine nucleotide translocator (ANT)	IMM	(Andrew P. Halestrap et al., 1997)  (Martin Crompton et al., 1998)  (Rottenberg & Marbach, 1990)  (Andrew P. Halestrap & Pasdois, 2009)  (Brustovetsky et al., 2002; Rück et al., 1998)  (Karch et al., 2019)	(Costantini et al., 1998)  (Brustovetsky & Klingenberg, 1996)  (Woodfield et al., 1998)  (Kokoszka et al., 2004)  (Rottenberg & Marbach, 1990)  (Doczi et al., 2016)
ATP Synthase	IMM	(Giorgio et al., 2009)  (Chinopoulos et al., 2011)  (Giorgio et al., 2013)	(J. He, Carroll, et al., 2017)  (Carroll et al., 2019)  (Gerle, 2016)

		<p>(Carraro et al., 2014)</p> <p>(Giorgio et al., 2017)</p> <p>(Urbani et al., 2019)</p> <p>(Massimo Bonora et al., 2013)</p> <p>(Massimo Bonora et al., 2017)</p> <p>(Alavian et al., 2014)</p> <p>(Neginskaya et al., 2019)</p> <p>(Antoniol et al., 2018)</p> <p>(Carrer et al., 2021)</p>	<p>(W. Zhou et al., 2017)</p> <p>(J. He, Ford, et al., 2017)</p>
PiC	IMM	<p>(Leung et al., 2008)</p> <p>(Alcalá et al., 2007)</p> <p>(Büttner et al., 2011)</p> <p>(J. Q. Kwong et al., 2014)</p>	<p>(Alcalá et al., 2007)</p> <p>(Büttner et al., 2011)</p> <p>(Varanyuwatana &amp; Halestrap, 2012)</p> <p>(Gutiérrez-Aguilar et al., 2014)</p> <p>(J. Q. Kwong et al., 2014)</p> <p>(Basso et al., 2008)</p>
SPG7	IMM	<p>(Shanmughapriya et al., 2015)</p>	<p>(Bernardi &amp; Forte, 2015)</p> <p>(Klutho et al., 2020)</p>
VDAC	OMM	<p>(Martin Crompton et al., 1998)</p> <p>(Ildikó Szabó et al., 1993)</p>	<p>(Krauskopf et al., 2006)</p> <p>(Baines et al., 2007)</p>
TSPO	OMM	<p>(Mcenery et al., 1992)</p> <p>(Kinnally et al., 1993)</p> <p>(Chelli et al., 2001)</p>	<p>(Kokoszka et al., 2004)</p> <p>(Krauskopf et al., 2006)</p> <p>(Šileikyte et al., 2014)</p>

Bak and Bax	OMM	(Marzo et al., 1998)  (Narita et al., 1998)  (Karch et al., 2013)	(U. De Marchi et al., 2004)  (Whelan et al., 2012)  (Carraro et al., 2014)

**Table 1.1: Summary of published studies on the molecular identity of the mPTP.**

*The table is divided according to candidate proteins and where they are proposed the form the mPTP channel (IMM or OMM). The studies which provide experimental support for the particular protein as the channel forming component of the mPTP is listed under supporting evidence while studies which discredit the protein as the channel forming of the mPTP is listed under contradicting evidence.*

### 1.3.2 mPTP candidates

#### 1.3.2.1 Adenine nucleotide translocator (ANT)

ANT was the first protein suggested to be the mPTP channel component. This view dates all the way back to when Hunter and Haworth first discovered the mPTP. Based on the observation that drugs targeting the ANT such as atractyloside (ATR) and bongkreikic acid (BKA) can modulate mPT, they suggested that ANT forms the mPTP (Haworth & Hunter, 1979; Douglas R. Hunter & Haworth, 1979a, 1979b).

One of the earliest theories involves a model where ANT dimerization is required for mPTP opening (Andrew P. Halestrap et al., 1997). However, this model was soon challenged by another study which showed that oxidative stress induced mPT does not require dimerization of ANT (Costantini et al., 1998).

Following the establishment of CypD as a key component of the mPTP, it logically follows that a good starting point for discovering other components of the mPTP is to screen for CypD interactors. A CypD affinity matrix made from glutathione S-transferase/Cyclophilin D fusion protein bound to glutathione agarose was used to screen for binding partners of CypD. This experiment pulled down ANT and VDAC as

possible interactors of CypD (Martin Crompton et al., 1998). Given existing theories hypothesising ANT as the pore forming component of the mPTP, ANT gained strong traction as a possible candidate.

It was also observed that drug-protein interactions which favoured the ANT conformation facing the cytosol sensitised the mPTP, whereas drug-protein interactions which favoured ANT facing the matrix inhibited mPTP opening (Andrew P. Halestrap & Pasdois, 2009; Rottenberg & Marbach, 1990). This would suggest that conformational changes of ANT affects mPT, which adds to evidence that ANT is the mPTP channel itself.

Additionally, restitution of ANT in *E.coli* and liposomes showed it could form a channel similar to the mPTP as measured by patch-clamp and allowance for solutes to pass through (Brustovetsky et al., 2002; Rück et al., 1998). However, the conductance profile of these channels varies from that of mPTP when measured with patch-clamp. This has been suggested to be due to reconstitution of the protein and insertion into an artificial membrane such as a liposome (Brustovetsky & Klingenberg, 1996; Woodfield et al., 1998).

In 2003, the ANT hypothesis was put into serious doubt when a mouse model with ANT1 and ANT2 knockout continued to display quintessential mPTP activity (Kokoszka et al., 2004). For a while the ANT hypothesis seems to have been overturned by this discovery. However, a new paper in 2019 put forth the idea that the previous study with ANT1 and ANT2 knockout was not definitive as there is still the presence of ANT3, even though ANT1 and ANT2 remain the dominant forms of ANT (Karch et al., 2019). The authors generated a ANT1, ANT2, and ANT3 knockout mice and demonstrated that a triple ANT knockout mouse was far less sensitive to Ca<sup>2+</sup> induced mPTP opening than the ANT1 and ANT2 double knockout. However, even in the triple knockout model, not only mPTP opening is still possible, it can be further delayed by the addition of CsA (Karch et al., 2019). As such, ANT cannot possibly be the indispensable core channel forming unit of the mPTP.

One hypothesis that has been suggested was that ANT only plays a regulatory role in mPT. ANT is responsible for ADP and ATP exchange across the IMM and ADP is a known modulator of the mPTP. The effect of ANT on ADP and thus mPTP has not

been properly investigated. ADP level changes has been reported in the ANT KO model and it is possible ADP could play a role in the mPT desensitization in the ANT KO model (Karch et al., 2019). Furthermore, it was also suggested that ANT might be affecting mPT by regulating the IMM potential (Rottenberg & Marbach, 1990) or by sensitising the mPTP to changes in the electrochemical gradient across the IMM (Doczi et al., 2016).

### **1.3.2.2 ATP Synthase complex**

In 2009, a new study showed that CypD, the only undisputed regulatory component of the mPTP, interacts with the ATP Synthase in a CsA dependent manner (Giorgio et al., 2009). More evidence also soon emerged in support of the interaction between CypD and ATP Synthase, where CypD was shown to be able to modulate the activity of ATP Synthase (Chinopoulos et al., 2011). Since it is an IMM protein, the ATP Synthase immediately attracted attention a possible candidate for the mysterious pore forming component of the mPTP. Following which, more studies lead to the formation of 2 main hypothesises on how the ATP Synthase could form the mPTP channel.

#### **1.3.2.2.1 ATP Synthase complex - Dimer hypothesis**

The first hypothesis suggests that dimerization of the ATP Synthase forms the mPTP channel, with the OSCP (Oligomycin sensitivity conferring protein) subunit of the ATP Synthase being key to CypD-ATP Synthase interaction and pore formation (Giorgio et al., 2013). It was found that reconstituted ATP synthase dimers but not monomers were able to form a channel in lipid bilayers with similar properties to the mPTP (Carraro et al., 2014; Giorgio et al., 2013).

This ATP Synthase hypothesis was challenged by KO studies. CsA sensitive mPTP activity were shown to be present in an ATP Synthase peripheral stalk and OSCP KO model (J. He, Carroll, et al., 2017). To reconcile this finding with the ATP Synthase dimer hypothesis, it was argued that the mPTP activity measured could be due to the formation of a smaller channel based on vestigial ATP Synthase structure that remained after the KO, rather than the usual mPTP (Bernardi, 2018). This was based



upon the experimental result where KO cells had slower rate of swelling compared to WT (J. He, Carroll, et al., 2017). However, further studies on ATP Synthase KO cells would appear to invalidate the counter argument. mPTP activity was also shown to be present in a ATP Synthase KO model with 5 subunits deleted and where no assembled ATP Synthase complex was present and no dimerization could occur (Carroll et al., 2019).

#### **1.3.2.2.2 ATP Synthase complex - c-ring hypothesis**

The second hypothesis suggests that the c-subunit of the ATP Synthase could be the channel forming component of the mPTP (Beutner, Alavian, et al., 2017). It was found that knockdown (KD) and overexpression of the c-ring is able to modulate mPT by measuring various factors such as H<sub>2</sub>O<sub>2</sub> mediated membrane potential dissipation, cytochrome c release and cell death (Massimo Bonora et al., 2013). Reconstitution of the c-ring in liposomes showed that it can form a voltage sensitive channel whose prolonged opening can dissipate membrane potential. It was also shown that c-ring depletion protects against ROS induced cell death and Ca<sup>2+</sup> induced IMM depolarisation (Alavian et al., 2014). Mutation in the c-ring that changes its conformation has also been shown to sensitize the mPTP to opening (Massimo Bonora et al., 2017).

The first challenge to this hypothesis came from analysis of the biochemical and structural feasibility of the c-ring forming a channel. The inner surface of the c-ring is lipophilic and occupied by a lipid plug, this makes it very unlikely to be able to allow solutes to pass through (Gerle, 2016). Furthermore, an atomic level stimulation of channel formation by the c-ring also suggest that it is biochemically very unlikely to occur (W. Zhou et al., 2017). KO studies have also challenged this ATP Synthase hypothesis. CsA sensitive mPTP activity were shown to be present in a ATP Synthase c-subunit KO cell model (J. He, Ford, et al., 2017). However, this KO study was in turn challenged by an electrophysiology study on the same KO cells which showed that there was a different conductance profile between the WT and KO channels measured. The authors thus argued that the Ca<sup>2+</sup> release channel activity measured in the KO was a channel that was not the mPTP based on differential conductance profiles (Neginskaya et al., 2019).

### **1.3.2.2.3 ATP Synthase complex - Summary**

In addition to those discussed above, there were other evidence in support of ATP Synthase playing a role in the mPTP. For instance, the T163S mutants of the  $\beta$  subunit of ATP Synthase displayed resistance to  $\text{Ca}^{2+}$  induced mPT (Giorgio et al., 2017). It was also shown that mutation of H112 of the ATP Synthase OSCP subunit prevented low pH from having a mPTP inhibitory effect (Antoniell et al., 2018). Evidence also suggest that the ATP Synthase can form a  $\text{Ca}^{2+}$  sensitive channel that was also sensitive to a OSCP ligand when reconstituted in liposomes (Urbani et al., 2019).

On the other hand, the strongest evidence against the ATP Synthase forming the channel component of the mPTP would be the KO studies. These studies showed that KO of multiple ATP Synthase subunits failed to remove the presence of the mPTP (Carroll et al., 2019; J. He, Carroll, et al., 2017; J. He, Ford, et al., 2017). Although there is still debate around what the result of the studies actually mean (Bernardi, 2018; Walker et al., 2020).

Relating to both theories, there is also always the concern that changing ATP Synthase levels will affect ADP and  $\text{P}_i$  levels which are known modulators of the mPTP, so any effect of ATP Synthase manipulation should take this into account (Andrew P Halestrap & Richardson, 2015). Overall, these studies suggest that while it is unlikely that ATP Synthase forms the core channel forming component of the mPTP as these 2 hypothesis might suggest, it is very much likely that ATP Synthase is involved in mPT in some way.

### **1.3.2.3 Mitochondrial phosphate carrier (PiC)**

PiC was suggested to be a component of the mPTP based on the observation that it can interact with CypD in a CsA dependent manner (Leung et al., 2008). As with ANT and ATP Synthase, PiC is also a membrane channel protein. This increases the probability that PiC could be the channel forming component of the mPTP. Later, in a

mouse heart specific model of PiC KD, desensitization of mPT was observed (J. Q. Kwong et al., 2014).

Some secondary and less convincing support for PiC also cited studies which showed PiC KD reduced staurosporine induced cell death (Alcalá et al., 2007) as well as cell death caused by BH3-protein overexpression and oxidative stress (Büttner et al., 2011). However, these studies might point more towards the effect of PiC on cell death in general than any effect on mPT in particular.

On the other hand, genetic studies on PiC argues against PiC as the core component of the mPTP. One study reported no change in mPTP activity following PiC KD (Varanyuwatana & Halestrap, 2012). Another study reported no change in mPTP activity with either over expression or KD of PiC (Gutiérrez-Aguilar et al., 2014).

It has long been known that Pi can modulate mPT (Bernardi, 1999). Further study also suggests that phosphate is essential for the effect of CsA and CypD ablation on mPTP activity (Basso et al., 2008). It is important to note that PiC regulates Pi directly and ADP/ATP levels indirectly in mitochondria. Changes in PiC levels would lead to drastic changes in these key metabolites which are also modulators of mPTP. As such, any change resulting from PiC manipulation needs to be carefully considered before any claims can be made. Experimental work also showed that the protective effects of PiC KD in mPT are lost when mitochondria was incubated with other anions (J. Q. Kwong et al., 2014). Overall, PiC is viewed as more likely to be regulating mPT indirectly rather than being the core channel forming component of the mPTP, and this regulation might even be coming from influencing availability of molecules such as ADP and Pi which are known modulators of the mPTP.

#### **1.3.2.4 Metalloprotease spastic paraplegia 7 (SPG7)**

More recently, an RNAi based knockdown screen of mitochondria proteins identified SPG7 as a possible component of the mPTP (Shanmughapriya et al., 2015). The screen used CRC as a measure of mPTP activity and showed that SPG7 KD resulted in desensitization of the mPTP to Ca<sup>2+</sup>. The authors promptly went on to suggest that

SPG7 formed the IMM component of the mPTP and forms the complete pore together with VDAC on the OMM.

However, despite claims by the author that SPG7 is an essential component of the mPTP, it was duly pointed out that the evidence presented only shows a decrease in mPTP sensitivity, and thus only supports SPG7 to be a regulator of mPT (Bernardi & Forte, 2015). Additionally, further investigation into SPG7 and mPT showed that siRNA KD of SPG7 made no difference to mPT as measured by oxidative stress-induced cell death and Ca<sup>2+</sup> retention capacity (Klutho et al., 2020), casting further doubt on the involvement and role of SPG7 in mPT. The presence of these studies and the lack of any further study in support of SPG7 makes a weak case for its involvement in mPT, with it being a regulator at best.

#### **1.3.2.5 Voltage dependent anion channel (VDAC)**

As mentioned earlier, a CypD interactor screen pulled down both ANT and VDAC (Martin Crompton et al., 1998). Since CypD is a matrix protein and cannot interact directly with VDAC, this led to the hypothesis that VDAC formed the outer mitochondrial membrane (OMM) portion of the mPTP, together with ANT which formed the IMM portion and CypD as the matrix regulator, making up the whole mPTP. This hypothesis also drew support from the fact that VDAC showed electrophysiological properties similar to that of the mPTP (Ildikó Szabó et al., 1993), although later studies showed that the mPTP can have a range of different conductance, weakening the case of this argument.

On the other hand, studies on VDAC KO models suggests that the presence of VDAC was not necessary for mPT to occur and whether it was able to modulate mPT also remains unclear (Baines et al., 2007; Krauskopf et al., 2006). Hence arguing against VDAC as an OMM channel component of the mPTP.

### **1.3.2.6 Translocator protein 18 kDa (TSPO)**

TSPO was first thought to play a role in mPT when ANT and VDAC were leading candidates for the mPTP. TSPO was found to associate with ANT and VDAC (Mcenery et al., 1992). Further evidence came along when it was shown that TSPO ligands can affect mPT activity, for example electrophysiological properties of the channel (Chelli et al., 2001; Kinnally et al., 1993).

However, the role of ANT and VDAC in mPT was called into serious doubt by gene KO experiments (Kokoszka et al., 2004; Krauskopf et al., 2006). TSPO, which was originally suggested to be part of the mPTP based on its association with ANT and VDAC also faced more scrutiny. Further investigation subsequently showed that genetic ablation of TSPO does not affect mPTP activity (Šileikyte et al., 2014). The support for TSPO as a component of the mPTP is limited and more evidence would be needed to support any involvement in mPT.

### **1.3.2.7 Bax and Bak**

Bax was first suspected to be a component of the mPTP when it was found that Bax interacts with ANT by co-immunoprecipitation and yeast two-hybrid. It was also shown that both proteins are required to form an atractyloside sensitive channel in artificial membranes (atractyloside has previously been shown to modulate mPT) and ectopic expression of Bax appears to only induce cell death in presence of ANT (Marzo et al., 1998). Other work also suggest that BCL2 family proteins such as Bak and Bax can regulate cytochrome c release and cell death pathways via the mPTP (Narita et al., 1998). More direct evidence emerged later when ablation of Bax and Bak was shown to protect against oxidative stress induced cell death and modifies OMM permeability during mPT but not IMM permeability (Karch et al., 2013). Bax and Bak were then suggested to form the OMM components of the mPTP based on this study.

The role of Bax in mPT has also been challenged when it was shown that Bax is not required for mPT (U. De Marchi et al., 2004). Further experimentation also suggests that any role Bak and Bax may appear to play in mPT is due to their involvement in

cell death pathways which followed mPT (Whelan et al., 2012). Additionally, the role for Bax in mPT has also been questioned on the basis that organisms naturally lacking Bax still undergoes mPT (Carraro et al., 2014). Overall, more work is needed to determine if Bax and Bak play any roles in mPT.

### **1.3.3 Alternative hypotheses**

As discussed earlier, the classical hypothesis requires the KO of a protein to completely abolish mPTP activity in order for it to be considered an essential component of the mPTP. Since the IMM and OMM channels have to be essential components of the mPTP, none of the proposed proteins for these 2 channels satisfy this requirement as discussed in the previous section.

It is worth noting that many studies with seemingly contradictory conclusions used different experimental models and techniques to study the mPTP (Alavian et al., 2014; Massimo Bonora et al., 2013; Carroll et al., 2019; J. He, Carroll, et al., 2017; J. He, Ford, et al., 2017). Different experimental models including mitoplasts, animals, and different cell types were used in many papers. The apparent inconsistency observed across different studies naturally raises questions regarding the homogeneity of mPT mechanism across experimental models and experimental techniques.

However, if we are considering the classical mPTP hypothesis and the search for the elusive channel forming core component of the mPTP, problems with differential experimental set-ups and models should not change any of our conclusions thus far. This is because mPT is supposed to be a universal phenomenon across almost all eukaryotic organisms with specific exceptions reported only in the crustaceans, *A. franciscana* (Menze et al., 2005), *C. crangon* and *P. serratus* (Konrad et al., 2012). This means that the same mPTP responses should prevail in all experimental models studied. Indeed, we have observed the consistent performance of CypD and CsA across all experimental set-ups and models to an extent that they have almost become standard control set-ups in any publication regarding the mPTP. As such, if mPT can be observed in any experimental set-up following KO of a particular protein, it is strong evidence against that protein as the channel component of the mPTP.

Given the current available evidence, the most logical conclusion is that we have not found a channel component that satisfies the requirements of the classical hypothesis. This remains the case despite large amounts of investigation and numerous screens in one way or another. Furthermore, there is strong evidence that the current proposed candidates are involved in mPTP formation in some way, just not in the way the classical hypothesis hypothesises them to be. As such, alternative hypotheses have been proposed to reconcile how these proteins can all be involved in mPTP formation but none of them is the actual channel component as proposed by the classical hypothesis.

### **1.3.3.1 Multiple protein hypothesis**

Apart from the classical view, the idea that the mPTP is not formed by a single protein or a single 'channel forming component' in either the IMM or the OMM has been proposed quite a while ago (L. He & Lemasters, 2002; Zoratti et al., 2005) but hasn't gained much traction until the recent few years (Bauer & Murphy, 2020; Massimo Bonora et al., 2021; Carraro et al., 2020). This was because many attempts to elucidate the identity of the mPTP have failed to yield any conclusive results. As mentioned earlier, none of the mPTP candidates passed the KO model phenotype assessment required for the classical hypothesis, with mPTP present in KO models of any of the suggested mPTP candidates. Despite this, the large amounts of evidence in support of these candidates being involved in mPTP cannot be discounted. One possible scenario that can account for all this is that multiple different proteins could form the mPTP, which would explain the evidence observed thus far. For example, mPTP activity was still observed following ATP Synthase KO. If multiple proteins can form the mPTP, this would simply mean that the ANT or some other protein will now form the mPTP. However, since ATP Synthase is missing, the mPTP becomes harder to form due simply to a reduce number of available proteins that can form the mPTP. The mPTP would thus have extra or multiple redundant capacity for its formation and our past KO studies only affected a portion of this capacity but not all of it. This will allow us to reconcile the puzzling experimental results observed where KO of candidate proteins delays mPTP opening but do not abolish it.

In addition to the 'simple' view that a few specific proteins can form the mPTP and substitute for each other in the event one of them is unavailable, there are suggestions of more 'structured' multiple protein theories where the multiple proteins suggested to form the mPTP follow a specific pattern or mechanism. Below is a quick overview of some of the more 'structured' multiple protein theories that have been proposed.

One hypothesis proposes that oxidative stress and Ca<sup>2+</sup> bound CypD are able to perturb protein structure and conformation of amphipathic membrane proteins, causing misfolding of membrane proteins which can all form the mPTP. This misfolding of the membrane proteins would be assisted by chaperon proteins such as CypD (L. He & Lemasters, 2002). A criticism of this hypothesis was that the mPTP is modulated in a structured manner by factors such as Pi, ADP and pH. Misfolding of proteins would be unlikely to be regulated by these factors in a structured manner (Baines, 2009; Bernardi, 2013).

Another hypothesis suggested that the channel could be formed by any of the 53 proteins in mitochondrial carrier family (MCF), which includes ANT and PiC, as they all share transmembrane helices and can shift between inward and outward facing conformations (Richardson & Halestrap, 2016). However, this hypothesis did not account for the ATP Synthase, which is not part of the MCF.

A third hypothesis suggests that the mPTP could be formed by synthasomes which include the ATP Synthase, ANT and PiC. The mPTP would be a result of synthasome assembly/disassembly. CypD, with its intrinsic PPIase function which can assist with protein folding, would regulate mPTP by regulating this assembly/disassembly (Beutner, Alanzalon, et al., 2017).

A fourth hypothesis suggests that any member of the SLC25a family can form the mPTP. 2 candidates with strong experimental support as components of the mPTP, ANT and PiC, make up most of the SLC25a family proteins on the IMM. This would explain their experimental involvement in mPT (Richardson & Halestrap, 2016). However, this hypothesis also did not account for the ATP Synthase.

A fifth hypothesis proposes that the components of mitochondria protein import machinery form the mPTP (Zoratti et al., 2005). Studies showed that mitochondrial



signal peptides can increase mitochondria permeability (Sokolove & Kinnally, 1996). It was also showed that the wasp peptide mastoparan could induce a CsA sensitive channel reminiscent of the mPTP (Pfeiffer et al., 1995). The hypothesis was that the ability of peptides to induce mPT was suggestive of involvement of mitochondria protein import machinery in mPT as this machinery is the one that is activated by the peptides.

It should be noted that no direct experimental evidence has emerged in support of the multiple protein hypothesis until very recently. In 2021, Paolo Bernardi's group showed that the ANT can form the mPTP in a ATP Synthase KO model (Carrer et al., 2021). This was the first experimental evidence supporting the multiple entity hypothesis which could potentially resolve the debate around the identity of the mPTP. However, more work is needed to fully validate the multiple entity hypothesis and possibly full resolution of the molecular identity of the mPTP in the future.

### **1.3.3.2 Role for non-protein molecules**

Since the discovery of the mPTP, it has always been assumed that a protein of some sort would form the physical channel that allows solutes to pass through during mPT. This assumption has never really been questioned and for good reason. For starters, proteins can naturally form channels and pores in lipid membranes and all of the solute channels discovered thus far are made up of proteins. Furthermore, molecular pathways are almost always made up of protein effectors and regulators. The fact that we discovered CypD, a key regulator which also appears to have protein folding assistance properties further reinforce the likelihood that proteins are what makes up the mPTP.

However, the possibility of non-protein molecules causing mPT cannot be completely discounted, despite being a very unlikely scenario. There has been little investigation regarding the possibility of non-protein molecules forming the mPTP. The only hypothesis that has attracted some attention and investigation is that of polymers such as Polyphosphate and Polyhydroxybutyrate forming the mPTP. These polymers have been hypothesised to be involved in mPT due to their ability to form channels in

mitochondria with properties somewhat similar to that of mPTP (P A Elustondo et al., 2016; Pavlov et al., 2005; Solesio et al., 2016). There is also evidence suggesting that depletion of Polyphosphate from mitochondria inhibits mPTP (Abramov et al., 2007) and addition of Polyhydroxybutyrate can induce a CsA dependent decrease in mitochondria membrane potential (Pia A. Elustondo et al., 2013). However, there has been no concrete evidence showing their ability to affect mPT in standard mPT assays such as the CRC and ROS induced cell death. Making their case a weak one at the moment. Additionally, a key drawback that needs to be resolved is that if non-protein molecules were to form the mPTP, they would need to be regulated in some way as mPTP formation is a highly regulated process via  $Ca^{2+}$  and a range of different factors. However, being regulated would most likely mean that proteins are involved in the regulation especially with CypD a known regulator. As such, this will bring us back to looking for proteins again as components of the mPTP even if a non-protein molecule forms the mPTP. Unless the hypothesis is  $Ca^{2+}$ /ROS directly reacts with these non - protein molecules to result in formation of the mPTP, which appears unlikely given how regulated processes in cells work and a lack of any evidence for such a possibility.

#### **1.3.4 Concluding remarks**

The experimental efforts to elucidate the identity of the channel forming component of the mPTP according to the classical hypothesis have been evaluated above. If the classical hypothesis is right and such a protein do exist, we have yet to discover it despite decades of effort. As such, we would need to continue to look for new protein candidates which might form the mPTP core channel component. It is also worth noting that there is actually no experimental evidence which supports the classical hypothesis as the basis for how the mPTP operates. The classical hypothesis sort of developed as researchers made assumptions of standard biological pathway behaviour during their investigations of the mPTP.

As discussed earlier, alternative hypothesis surrounding the mPTP are starting to emerge. If the view that multiple proteins can form the mPTP is right, then we are likely to have already found many of these proteins since there are convincing evidences that many of the current candidate proteins are involved in mPT. This hypothesis

recently received support from the first experimental data showing that multiple proteins are able to form the mPTP (Carrer et al., 2021).

In conclusion, the classical hypothesis cannot fully explain the experimental results the field have accumulated. As such, it might be promising to examine alternative multiple channel hypotheses to explain the seemingly conflicting experimental results. However, the alternative hypotheses do not have enough experimental support to conclusively establish itself and resolve the debate surrounding mPTP channel identity. More work is needed before a conclusion can be drawn which is what this project has set out to accomplish.

## 1.4 CypD interactor screens

If we know the identity of a protein in a particular pathway, we can look among its protein interactors for other members of the pathway. This approach has been applied to the mPTP since the discovery of CypD as a mPTP regulator. The ANT, ATP Synthase and PiC were all shown to be CypD interactors before they attracted interest as potential mPTP channel components. Protein screening technology have come a long way since the last CypD interactor screen was carried out. New technologies offer improvement in a host of areas and will allow for previously impossible dynamic interactome analysis when it comes to mPTP. I believe that a CypD protein interactors screen with the newly developed fast version of the proximity dependent biotinylation method (TurboID) would be a promising project.

### 1.4.1 Past CypD interactor screens

Indeed, there have been a number of prior works trying to find the components of the mPTP by looking at CypD interactors. A CypD affinity matrix was used to capture proteins isolated from mitochondria (Martin Crompton et al., 1998), leading to identification of the ANT (Adenine Nucleotide Translocator) and VDAC (Voltage-dependent anion channel) as candidates for forming the mPTP. A decade later, cross-linking and immunoprecipitation experiment identified ATP Synthase components as binding partners of CypD (Giorgio et al., 2009).

Although the role of both the ANT and the ATP Synthase in mPTP are still disputed till this day, so is every single other proposed protein and the uncertainty is likely more to do with the nature of the mPTP itself. ANT and ATP Synthase are by far the strongest candidates for the mPTP at the moment and there are hypothesises of a dual protein model where they form different types of channels of the mPTP (Massimo Bonora et al., 2021). This past success goes to show that the approach of looking at CypD interactors for mPTP components has much merit to it.

#### 1.4.1.1 Curation of proteomic databases

In addition to studies which set out to find mPTP components, there were also studies which did not have any specific hypothesis in mind. Instead, these studies aimed to provide a database of protein-protein interactions for other researchers to use as a reference. They typically apply a specific protein interaction screening technique to all applicable proteins in a cell model. The techniques for which such databases have been created include the 2-hybrid assays (Rolland et al., 2014), chemical protein crosslinking mass spectrometry (Liu et al., 2018; Maly et al., 2017), and affinity purified (AP)/immune-purified (IP) mass spectrometry (X. Li et al., 2015; Maly et al., 2017; Richter et al., 2010) and proximity dependent biotinylation (Roux et al., 2018).

Given these resources, I curated the results in interactome databases which capture these studies (STRING, BioGRID and IntAct). There are a total of 111 hits for CypD interactors recorded in all the proteomic papers archived in these databases. I examined every protein on the list and created a spreadsheet with relevant information. These includes gene name, function, sub-cellular localization and whether they were membrane proteins. Those without experimental information were evaluated using localisation, folding and functional information predicted by bioinformatic tools. The full table and analysis can be found in Appendix 2.

When examining the hits from this database, the first step I carried out was to exclude non-mitochondria proteins. This is determined using Mitocarta 2.0. There were 31 non-mitochondrial proteins with means 80 proteins are left. Since I am looking for the mPTP channel, the target would most likely be an existing membrane channel protein/protein complex, like the main candidates ATP Synthase and ANT. This criterion eliminates all the protein hits but one, the MCU complex.

Interestingly, MCU KO models have already been studied in relation to the mPTP (Jennifer Q. Kwong et al., 2015; Luongo et al., 2015; Pan et al., 2013; Rasmussen et al., 2015). This is not because of its suspected role as the channel component as the mPTP but simply because it is the Ca<sup>2+</sup> import channel that basically controls mPT induction. As discussed in more detail in the MCU section of 1.2.2 and Appendix 2, the relationship between MCU KO and mPT is not very straightforward and it makes any investigation of MCU as a component of the mPTP very difficult in practice.

### **1.4.1.2 Limitations**

Regarding the screens used to create the databases, a one size fits all approach was used where the function of individual proteins was not tested after genetic or chemical manipulation. This was a problem because many of the procedures could alter protein function. The 2-hybrid and proximity dependent biotinylation assays both require fusion proteins to be made which introduces complications regarding protein conformation and function. Chemical crosslinking also directly alters amino acids and potential protein function.

Additionally, these screens do not control for temporal specificity. They only examine CypD interactors under resting state conditions, which might differ from CypD interactors during mPTP forming conditions. This might prevent us from finding the mPTP components since CypD have unknown physiological functions and these screens might just be detecting interactors involved in other CypD functions. Given that resting state CypD interaction studies have failed to provide a conclusive candidate for the mPTP, it would be useful to investigate CypD interactors under mPTP forming conditions.

The methods by which ANT and ATP Synthase were discovered suffer from many unavoidable limitations due to technological availability at the time. (Martin Crompton et al., 1998; Giorgio et al., 2009). The sensitivity of these methods was limited to stable complex formation with CypD, and transient interactions cannot be detected. These proteins were not detected under mPTP forming conditions due to lack of temporal specificity. The studies were not carried out in the natural environment of CypD and CypD protein have been extracted and isolated for these studies.

More recently, new technologies have emerged that will allow us to overcome many of the shortcomings discussed above. This brings with it the potential to carry out more accurate and relevant CypD interactor screens with regards to mPTP. I will elaborate the new technique I have decided to use to achieve this, TurboID, in the following section.

### **1.4.2 Proximity dependent biotinylation and TurboID**

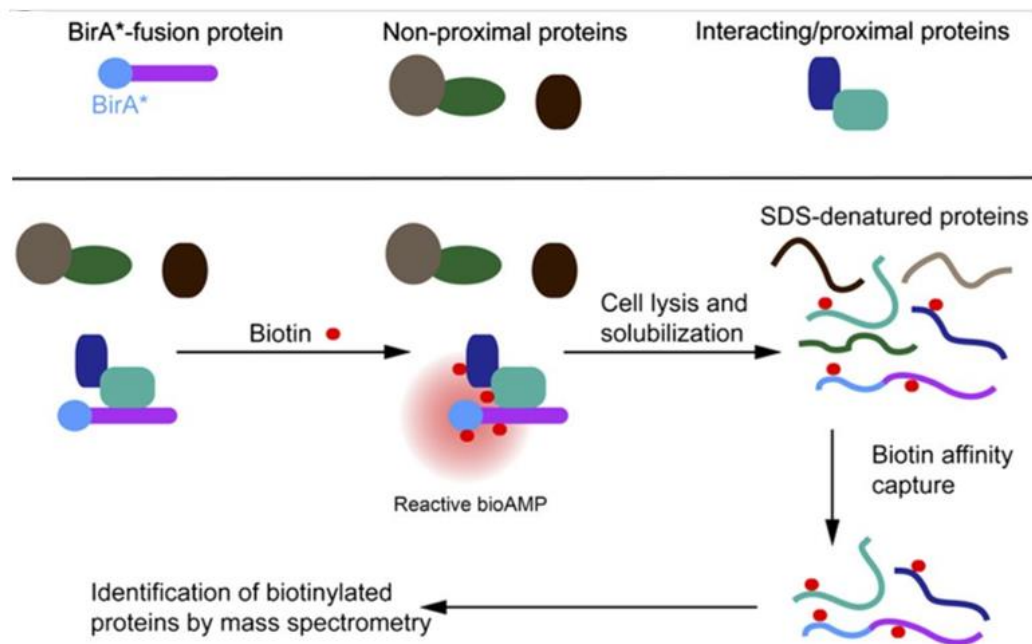


**Figure 1.3: Proximity dependent biotinylation as a protein interactor screening tool** (Roux et al., 2012)

As the name suggest, the basis of proximity dependent biotinylation is to tag proteins with biotin based on how close they are to the protein of interest. This makes use of the fact that the proteins located next to a protein of interest are much more likely to be their interactors than proteins further away. The relative enrichment of biotin-tagged protein can then provide a list of possible protein interactors.

The technique was first introduced as BioID in 2012 and the general process is shown in Figure 1. The screen uses a fusion protein (BirA\*-fusion protein) where a specifically designed biotin-ligase (BirA\*) is fused to the protein of interest. Upon addition of biotin to cells expressing the fusion protein, the biotin-ligase enzyme (BirA\*) will tag Interacting/proximal proteins with biotin, while Non-proximal proteins will not be tagged. The cell is then lysed and solubilized, and the protein denatured with SDS. Biotin tagged proteins are then extracted and isolated via Biotin affinity capture (streptavidin pull-down) and identified by mass spectroscopy (Roux et al., 2012).

BioID was an improvement on previous methods in terms of non-toxicity, the potential for measuring protein interactome under physiological environments, and even allowing animal models to be used in proteomics. However, the original BioID method

had a very significant drawback that limits its use in a mPTP study. The original BioID was a very slow process, it took upwards of 16hrs for labelling to complete following biotin addition. Hence it can only be used for steady state measurements which as we have discussed is a limitation of previous CypD screens (Roux et al., 2012). In 2018 a new version of proximity dependent biotinylation was developed and termed TurboID. The most significant advantage of TurboID is that it allows for ultrafast biotin labelling (under 10mins) and has the potential to allow us to resolve CypD proteomic changes during mPTP formation instead of simply measuring steady state CypD interactions (Branon et al., 2018).

TurboID can overcome most of the limitations regarding previous CypD interactor screens discussed earlier. Firstly, it can be carried out under physiological conditions within cells/mitochondria that are still functioning. This reproduces the natural interactions of CypD much better than methods where extracted CypD has been used. Secondly, it can detect transient interactions due to its fast speed of labelling (under 10 mins) where previous methods all involve much longer incubation time and stable protein complex formation. This allows us to detect mPTP components even if CypD only briefly interacts with it. Lastly and most importantly, TurboID allows us to carry out screens under mPTP forming conditions. This is due to its super-fast labelling capabilities while remaining non-toxic to cells, making it the first proteomics technique to be able to do so. This will allow us to study the change in CypD interactome during mPTP by inducing mPT and then measuring the CypD interactome. Such a screen has never been conducted before and offers the possibility for time resolved evolution of the CypD interactome during mPTP opening, which can offer insight into mPTP identity and formation.



## 1.5 Research plan

### 1.5.1 Project aim and hypotheses

The aim of the project is to identify the channel forming component of the mPTP. I hypothesised that the mPTP can be formed by multiple proteins which likely includes the current candidates such as ATP Synthase and the ANT. This would resolve the apparent conflicting evidence where KO of any one mPTP candidate failed to abolish mPTP activity. Furthermore, this also fits into the multiple conductance characteristic of the mPTP where different conductance states can be explained by different proteins forming the mPTP.

In order to investigate this hypothesis, I designed a project where I would use proteomics to identify CypD interactors during different states of mPTP opening. This in turn have secondary hypotheses themselves that needs to hold true for the project to yield accurate results as intended.

Firstly, I hypothesis that CypD would increases its interaction with the channel forming component of the mPTP during mPTP formation. This is an absolute requirement for the project as I would rely on comparing the difference between CypD interactors when the mPTP is closed vs that when the mPTP is open in order to determine the mPTP channel. Although this have never been experimentally proven, it was a highly likely scenario as CypD have been shown to interact extensively with the mPTP candidates ATP Synthase and ANT which are likely to form the mPTP channels. This assumption is thus supported by past experimental evidence.

Secondly, I hypothesis that the proteomics method that I would use here, TurboID, can be accurately applied to the mPTP model. Although this was untested and have no previous supporting evidence, I would carry out experiments in this project to verify this hypothesis before I carry out the final proteomics experiment. This would involve verifying that the CypD-TurboID fusion protein can replicate the function of CypD in HEK293T cells and label proteins with biotin to allow for the final proteomics experiment.

In terms of more technical experimental goals, I aimed to characterise the CypD interactome under different states of mPTP opening using the TurboID proximity labelling approach. CypD interactome data before and after mPT induction was obtained in order to reveal insights on the role of CypD in mPTP formation and potential candidates for mPTP components. This would be achieved through the following steps:

- 1) *Establishment of a model for the CypD protein interaction screen*
- 2) *Generate KO cell line and re-express CypD-TurboID fusion protein*
- 3) *Protein interaction screen: dynamic proteomics of the CypD interactome*
- 4) *Interpretation and validation of proteomic results*

### **1.5.2 Establishment of an experimental model for the CypD protein interactome screen**

The experimental system used would form the underlying basis and backbone of any project. Hence, I carefully set-up a system that would best fit my purpose. The system would consist of 2 parts that were equally important to ensure that the screen can be properly carried out. The first was a biological model and the second was the CypD-TurboID fusion protein to be used. Both of them would need to fulfil certain key criteria.

The TurboID technique required the introduction of a fusion protein consisting of the protein of interest (CypD) fused to a biotin-ligase enzyme. The presence of endogenous CypD would compete with the fusion protein for interactors and thus reduce the sensitivity of the screen. Using a CypD KO model eliminates this problem. I would generate a CypD KO model and express CypD fused to the biotin ligase enzyme using a plasmid. The CypD component of the fusion protein will interact with endogenous CypD interactors which would consequently be tagged with biotin by the biotin ligase domain of the fusion protein. The interactors would then be affinity purified and identified via mass spectrometry. This brings me to the first key criteria - the model chosen should have established molecular tools for genetic manipulation for generation of a CypD KO model and tools for easy introduction of exogenous genetic sequences to allow expression of the CypD-TurboID fusion protein.

For this project, the ability to induce mPT in a temporally controlled manner was critical in order to capture dynamic changes in CypD interactions as mPT happens. As discussed above, this was so that I can make use of the fast-labelling capabilities of TurboID to look at the CypD interactome under different states of mPT opening. As such, the second key criteria would be that the model must allow for mPT induction in a highly temporally controlled and specific manner.

Finally, I would also need an experimental readout from the model which can effectively measure mPT. This would ensure I could properly verify that any genetic or experimental manipulation introduced to the model was not impacting mPT itself. As such, the best way to develop a model for the screen would be to pick an experiment that has been consistently used in the literature and the model that comes along with it. I studied the most frequently used mPTP experiments in the literature to see which one would best satisfy the two criteria described above. Table 1.2 list the mPTP experiments that were frequently used and their details.

<b>Experiment</b>	<b>mPT inducer</b>	<b>Summary of method</b>	<b>Model type</b>	<b>Example Publications</b>
CRC-Isolated mitochondria	Ca <sup>2+</sup>	Repeated Ca <sup>2+</sup> additions are delivered to isolated mitochondria to induce mPT, the amount of Ca <sup>2+</sup> required for mPT is used as a quantitative measurement	Isolated mitochondria	(Karch et al., 2019)  (Bhosale & Duchon, 2019)
CRC-Permeabilised cells	Ca <sup>2+</sup>	The same experiment as that in isolated mitochondria. However, permeabilised cells are used as plasma membrane is Ca <sup>2+</sup> impermeable	Permeabilised cells	(J. He, Ford, et al., 2017)  (Carroll et al., 2019)
Mitochondria swelling assay	Ca <sup>2+</sup>	Mitochondria swells following mPT, this swelling can be quantitatively measured as changes in light absorbance at 530nm following mPT induction	Isolated mitochondria	(W. Li et al., 2018)  (Briston et al., 2016)
Cell death assays	ROS/Ionophores	mPT is induced using ROS (H <sub>2</sub> O <sub>2</sub> ) or ionophores, the	Intact cells	(Karch et al., 2013)

		amount of cell death observed after a set period of time is used as a quantitative measurement of mPT		(Klutho et al., 2020)
Calcein-cobalt quench	Ionophores/ROS	Calcein is used to stain the entire cell including the mitochondria. Cobalt, which quenches calcein is added and non-mitochondria calcein is immediately quenched since only the mitochondria is normally impermeable to cobalt. During mPT, cobalt enters the mitochondria, and the rate at which calcein is quenched by cobalt can be used as a quantitative measurement of mPT	Intact cells	(Petronilli et al., 1998)  (Alavian et al., 2014)
Ischemia reperfusion	IR	mPT is induced in reperfused mice/rat hearts by recreating IR conditions (restricting blood flow before restoring it later), cardiac tissue damage is used as a quantitative measurement of mPT	Reperfused mice/rat hearts	(Baines et al., 2005)  (Littlejohns et al., 2014)

**Table 1.2: Summary of mPTP experiments**

Considering the key criteria of temporally controlled mPT induction, I could essentially eliminate any experiment which relies on ROS or an Ionophore to induce mPT in intact cells. Addition of H<sub>2</sub>O<sub>2</sub> is the most common way by which ROS is used to induce mPT. However, experiments involving H<sub>2</sub>O<sub>2</sub> are essentially only used in cell death assays where the outcome of H<sub>2</sub>O<sub>2</sub> addition followed by mPT triggered cell death can often only be measured hours after the initial treatment (Klutho et al., 2020). This would not satisfy our criteria for temporal specific control as we cannot be certain of when the mPT actually occurs. Ionophores such as ionomycin induce mPT by transporting Ca<sup>2+</sup> across the plasma membrane and the endoplasmic reticulum has also been used to induce mPT. Despite the fact that ionomycin induces mPT via Ca<sup>2+</sup> overload instead

of ROS, it is actually also mainly used only in cell death assays and can take hours for effects to show (J. Q. Kwong et al., 2014). As such it suffers a similar draw back as ROS induced mPT. These are the only experiments where intact cells are utilised and essentially means intact cells would not be a suitable model for the screen.

Using a mouse animal model would probably offer the most clinical and physiologically relevant picture. Such a model would involve creating a transgenic mouse line expressing a CypD-TurboID fusion protein. I could then induce mPT using an ischemic reperused heart model (Baines et al., 2005), this would allow the induction of mPT in a manner as described in 1.2.1. This model has the potential to allow for temporal control of mPT induction as I would be able to control for timing of reperfusion and mPT should be occurring immediately following reperfusion. However, there would be a few significant drawbacks. Firstly, a transgenic mice line needs to be created. There was a possibility that the CypD-TurboID fusion protein have unforeseen problems regarding subcellular localization/function preservation which would require multiple fusion proteins to be tested. This would mean multiple mice lines might need to be generated, which was not feasible. Additionally, optimization of the experiment might involve a large number of repeats and a large number of mice might need to be used which was not compatible with the idea for reducing the use of animals in research. As such, using a reperused mice heart model does not appear to be a straightforward option here as genetic manipulation is costly and time consuming.

Using swelling assays as a readout will not work for this project as swelling assays do not report a specific point of time where mPT occurs. This would be problematic as I will need to be able to control the exact onset of mPT to resolve the difference between the CypD interactome before and after mPT.

That basically leaves us with carrying out the project in permeabilised cells or isolated mitochondria using the CRC assay as an experimental readout. Since mPT is a basic molecular process, carrying out the project in isolated mitochondria or permeabilised cells should not be a problem and any findings should be transferrable. The CRC assay is also a time-tested standard assay for measuring mPT. However, while most CRC assays use mitochondria isolated from mice liver, I would not be able to use a mice model due to limitations mentioned earlier. As such, I would need to isolate mitochondria from cell lines should I wish to use isolated mitochondria. Alternatively,

permeabilised cells can also be used but it also presents its own challenges. The use of either isolated mitochondria or a permeabilised cell model was required so that the  $\text{Ca}^{2+}$  can reach mitochondria almost instantly as the plasma membrane is largely impermeable to  $\text{Ca}^{2+}$ . Using this method, mPT should occur almost immediately following  $\text{Ca}^{2+}$  addition, giving us a high level of control over mPT induction.

The cell line selected for this work is the human embryonic kidney HEK293T cell line, where TurboID was first optimised (Branon et al., 2018). This cell line allows efficient transfection, fast growth, and relatively easy genetic manipulation with CRISPR-Cas9. Since it has been shown to work with the TurboID method, it removes concerns regarding compatibility of the method and the cell type. Additionally, HEK293T has been used in mPT experiments before and was shown to produce consistent results with respect to mPT, further supporting its suitability for my use case (Alavian et al., 2013; Massimo Bonora et al., 2017). HEK293T cells were used in conjunction with isolated mitochondria CRC assays, with works well together to give consistent experimental readouts of the mPTP.

Additionally, I had to ensure the functionality of the CypD-TurboID fusion protein that was created and its relevance to the screen. This basically revolves around ensuring that fusing two proteins together does not disturb their conformation to an extent where their original functions were affected. The following 3 criteria had to be met.

- 1) The fusion protein was properly imported to mitochondrial matrix – this was verified using organelle isolation and western blotting
- 2) The fusion protein retains the ability of the biotin ligase to tag proximal proteins with biotin – this was verified using a western blot stain with specifically detects biotinylated proteins
- 3) The fusion protein retains its ability to modulate mPT – this was verified using CRC assays

A model that fulfilled the above benchmarks would produce a reliable set of proteomics data that recaptures the physiological interactors of CypD. The first criterion ensures

proper localization of the fusion protein, this ensures that we are not receiving noise signal from non-relevant areas such as the cytoplasm. The second criterion ensures that the sensitivity and underlying interactor 'hits' identification method for the screen is properly retained. The third criterion ensures the applicability of the screen by ensuring that the fusion protein retains its ability to regulate mPT, this would allow me to be confident that the screening results were relevant to mPT.

### **1.5.3 Generate KO cell line and re-express CypD-TurboID fusion protein**

No matter what cell line I choose and whether I use isolated mitochondria or permeabilised cells, the next step would be to generate a KO model and re-expressing the CypD-TurboID fusion protein in the KO model. As discussed earlier, the KO model removes competition for CypD interactors from endogenous CypD. This allows the CypD-TurboID fusion protein access to all of the available CypD interactors.

A KO model of the HEK293T cell line will be created using CRISPR-Cas9. Since the discovery of CRISPR, its ease of use and efficiency has quickly made it the preferred tool for gene editing. The Zhang lab protocol and plasmids will be used here (Ran et al., 2013). The gRNAs will target the 5'UTR and 3'UTR for gene KO, an alternative set of gRNAs targeting the 5 exons of CypD was also created. The KO cell line will be verified using western blots, CRC and sanger sequencing.

### **1.5.4 Protein interaction screen: dynamic proteomics of the CypD interactome**

CypD protein interaction screens will be carried out under different conditions. This includes, before and after inducing mPTP opening, with or without addition of CsA. The ability to temporally resolve protein interactions is a special feature of TurboID technology and will be fully utilised here. By comparing the protein interaction data of CypD under various states of mPTP opening, I aim to gain insight into the molecular identity of the mPTP.

Once the CypD KO HEK293T cell model expressing the CypD-TurboID fusion protein is set-up, the proteomics will be carried out. mPT will be induced in these cells with/out

CsA and compared to control groups with no mPT with/out CsA. Protein samples will be collected from these conditions and a mass spectrometry with label free quantification detection capabilities will be used to determine relative protein abundance and thus the CypD interactors under each of these conditions.

### **1.5.5 Interpretation and validation of proteomic results**

The data will be analysed using Python using appropriate statistics including multiple t-tests and ANOVA which takes into account large number of samples and tests. If any potential candidates for the mPTP are identified in the proteomics screen, I would analyse the likelihood that they are actually part of the mPTP.



## 2. Methods

\* *Please refer to reagents list for details.*

### 2.1 Cell Culture

All cells were grown in Dulbecco's modified Eagle's medium Glutamax (with 3.5g/L glucose and pyruvate supplementation, Life technologies: 31966-021) supplemented with 10% Fetal bovine serum (Gibco #16130071), and 1% Antibiotic-Antimycotic (Gibco #15230096) and incubated at 37 °C with 5% CO<sub>2</sub>. Trypsin (Life technologies: 15300053) was used to detach cells for passaging. When freezing cell stocks, cells were centrifuged at 800 rpm for 3 mins, the media was removed, and cells were resuspended in freezing buffer (10% DMSO in FBS). 1ml of the resuspended cells were then placed in freezing vials with is placed in a freezing container filled with isopropanol solution at RT. The cells were left overnight in -80°C before being transferred to a liquid nitrogen storage.

The HEK293T cells used were in stock in our lab and originally obtained from the American Type Culture Collection (ATCC). CypD KO and Control MEF cell lines were obtained from Gauri Bhosale, UCL.

### 2.2 Transfections

Transfection of cells were carried out using Lipofectamine 3000 reagent (Invitrogen Catalog number: L3000008) for all plasmids. When transfecting 10 cm dishes, 30ul of Lipofectamine™ 3000 Reagent, 20ul of P3000™ Reagent and 10ug of Plasmid DNA are diluted in 1ml Opti-MEM GlutaMAX media (life technologies: 51985033) before being added to 10ml of Cell culture DMEM media in a 10 cm dish.

### **2.3 Mitochondria Isolation**

Functional mitochondria were isolated from cultured HEK293T cells for use in CRC assays and western blots. The media was first removed, and the cells were washed once with trypsin (Life technologies: 15300053). Following which, the cells were resuspended in PBS and placed in a 15mL Conical Centrifuge Tube. The cells were centrifuged at 600g for 10 mins to obtain a cell pellet. The supernatant was removed, and the pellet was resuspended in 3 ml of ice-cold Isolation Buffer (IBc)\* and transferred into a glass test tube. The suspension was then homogenised using a Teflon Pestle by stroking the cell it 5-times with the Teflon pestle, this process breaks down the plasma membrane and releases the organelles from the cells. The homogenate was then centrifuged at 600g for 10 mins and the supernatant containing the cellular contents was collected, the pellet containing the broken-up plasma membrane was discarded. The supernatant was then centrifuged at 5000g for 10 mins in a 15mL Conical Centrifuge Tube to obtain a pellet containing mitochondria, the supernatant containing cytosolic fraction was then removed. The pellet was resuspended in 200ul IBc\* and transferred to a 1.5ml Microcentrifuge Tube. The resuspended pellet was then centrifuged at 7000g for 10 mins, this was done to increase the purity of mitochondria and remove any remaining cytosolic content. The supernatant is removed, and the resulting pellet contains mitochondria can then be resuspended in RIPA Buffer\* (for western blotting) or MSK Buffer\* (for CRC assays).

### **2.4 Molecular cloning**

The subsequent protocols including PCR, Restriction Digest, Plasmid Ligation, Plasmid amplification, Agarose gel electrophoresis and Site directed mutagenesis were adapted from addgene (<https://www.addgene.org/protocols/>) and NEB (<https://international.neb.com/>) protocols.

Non-CRISPR plasmids were propagated in DH5alpha *E.coli* which has been optimised for plasmid propagation. However, CRISPR plasmids were propagated in Stbl3 *E.coli* which are less affected by the presence of CRISPR plasmids compared to DH5alpha as they have been engineered for reduced homologous recombination.

Should DNA concentration measurements be needed, these are done using a Thermo Fisher Nanodrop Spectrophotometer.

### 2.4.1 PCR

For each PCR reaction, a reaction mix was created as shown in Table 2.2. The reaction mix was then placed in a thermocycler for a series of PCR amplification steps as described in table 2.3. The final DNA product was then processed using a PCR clean up kit (NEB: T1030S) before use in any future experiments.

<b>Component</b>	<b>Amount (for a 50ul reaction)</b>
Template DNA	200ng
Forward Primer	500nM
Reverse Primer	500nM
100 mM dNTP solution (NEB: N0336S)	1 ul
Q5® Reaction Buffer (NEB: B9027S)	10ul
Q5® High-Fidelity DNA Polymerase (NEB: M0391S)	0.2 ul
Sterile dH2O	Fill up to 50ul

**Table 2.1 PCR reaction mix**

<b>Step</b>	<b>Function</b>	<b>Time (mins)</b>	<b>Temperature (°C)</b>
1	Initial Denaturation	2	94
2	Denaturation	0.5 (30 cycles)	94
3	Primer annealing	0.5 (30 cycles)	55

3	DNA extension	2 (30 cycles)	72
5	Final extension	5	72

**Table 2.2 Thermocycling steps**

For PCR reactions, steps 2-3 are repeated for 30 cycles as a set.

### **2.4.2 Restriction digestion**

20 units of the corresponding restriction enzyme was mixed with 1ug of target DNA, 5ul of 10X rCutSmart Buffer (NEB: B7204S). The reaction was allowed to stand for 15-30 mins. A DNA clean-up was done using a DNA clean up kit (NEB: T1030S) following the digest.

### **2.4.3 Plasmid ligation**

1ul T4 DNA ligase was mixed with 2ul of T4 DNA Ligase Buffer (10X), 0.020 pmol of vector DNA, 0.060 pmol of insert DNA and made up to 20ul with nuclease free water. The reaction was allowed to stand at RT for 1hr.

### **2.4.4 Plasmid amplification**

500 ng of plasmid DNA was mixed with 200 ul of competent bacteria cells in a 1.5 ml microcentrifuge tube and incubated on ice for 30 mins. A heat shock was then carried out as the microcentrifuge tube was partially submerged in a 42°C water bath for 45 secs. The mixture was then place on ice for 2 mins. A mini bacteria amplification step was done here as 800ul of LB broth was added to the mixture and the mixture was placed on a shaking incubator at 37°C for 45 mins. A 1000ul pipette tip was then dipped in the bacteria mixture and spread over a 10cm<sup>2</sup> agar plate with the corresponding antibiotic (e.g Ampicillin infused) to create single cell colonies. The plate was then incubated at 37°C overnight to allow the individual colonies to form. Multiple colonies were then picked using a 1000ul pipette tip with the tip subsequently swirled in a 15ml falcon tube filled with LB broth. The bacteria in LB broth was placed

overnight in a 37°C shaking incubator to allow for bacteria growth. A mini/midi prep was then carried out on the bacteria and plasmid DNA was then amplified.

#### **2.4.5 Agarose Gel Electrophoresis**

DNA gels were carried out for troubleshooting and diagnostic purposes.

An agarose solution was first made up by heating and dissolving 1g of agarose in 100ml of TAE\* buffer. The solution was then poured into a gel tray with the well comb in place. The agarose was allowed to cool so a gel was formed. The gel was moved to an electrophoresis unit and TAE\* buffer was added to the unit. DNA was mixed with loading buffer and loaded into each well, a DNA ladder was also loaded. The gel was run at 110v until the dye front reaches 80% of the gel. The gel was then removed, washed, and stained with SYBR Safe DNA Gel Stain (Thermo Fisher: S33102). The gel was then visualised using a Biorad Chemidoc system.

#### **2.4.6 Site directed mutagenesis**

Site directed mutagenesis is a method used to make small changes base pair changes to plasmid DNA. This can include substitutions, deletions, and insertions. A pair of overlapping primers is created with the intended mutation and complementary sequences to the target sites. The primers would anneal to the plasmid and be extended by DNA polymerase. The extended strands would then anneal together, and ligation would result in a new plasmid with the intended mutation.

Site directed mutagenesis was carried out using the NEB Q5® Site-Directed Mutagenesis Kit (NEB: E0553S). The primers used are designed using the NEBaseChanger® web tool (<https://nebasechanger.neb.com/>).

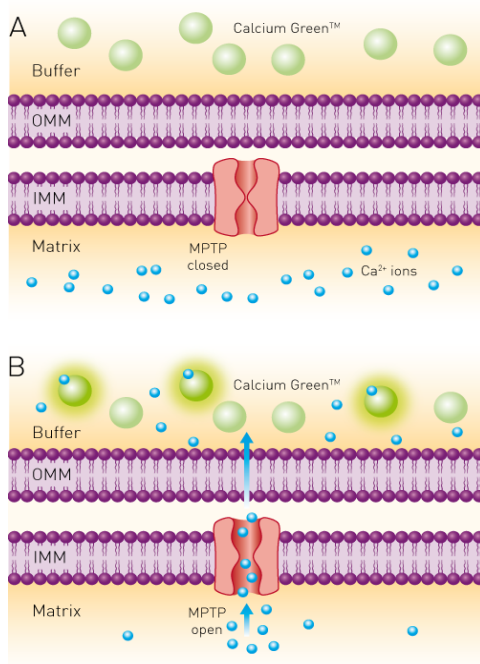
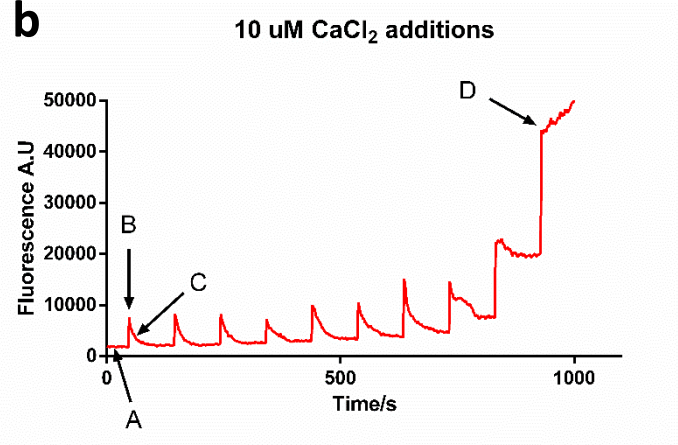
#### **2.5 Bicinchoninic acid (BCA) Assay**

Pierce™ BCA Protein Assay Kit (Thermo Scientific: 23227) was used to measure protein concentration. A series of 9 protein standards with the following concentrations were made using BSA (Bovine serum albumin):

2000/1500/1000/750/500/250/125/25/0 ug/ml. During each protein concentration measurement, 5ul of each standard and 5ul of each sample were pipetted into a clear 96 well plate. Following which, 200ul of the BCA working reagent (50 parts reagent A and 1 part reagent B) was pipetted into each well containing sample/standard. The 96 well plate was then covered in foil and incubated for 30 mins at 37°C. Following the incubation, absorbance at 562 nm was read in a plate reader. The absorbance data obtained from the protein standards were used to plot a  $y=mx+c$  standard curve where  $y$ =protein concentration and  $x$ =absorbance. Curves with  $R^2$  value  $>0.95$  were deemed sufficiently accurate for predicting protein concentration. The absorbance values of the samples were inputted as  $x$  values into the equation and the  $y$  value gave the corresponding protein concentration.

## **2.6 Calcium Retention Capacity (CRC) assays**

Isolated mitochondria or cell pellets were resuspended in MSK buffer\* and placed on ice. A BCA assay was done. An appropriate amount of mitochondria (30-35ug) or cells (5-10 million) (exact amount used differs between different experiments) were resuspended in 45/90ul of MSK buffer\* and placed in a 96 well clear bottom imaging plate (Corning™ 353219). 1uM Thapsigargin was added to the mixture to block  $Ca^{2+}$  uptake from the endoplasmic reticulum and ensure that all measured  $Ca^{2+}$  changes were a result of mitochondria activity. 1uM Fluo-5N, a  $Ca^{2+}$  sensitive fluorescent dye was also added to the mixture. If CsA is added, it was at this stage. A 50-200uM (depending on experiment)  $CaCl_2$  stock in MSK is prepared, 1uM Thapsigargin and 1uM Fluo-5N were also added to the stock solution. A fluorescence time series capable plate reader (CLARIOstar by BMG Labtech) was used to measure the fluorescence intensity of Fluo-5N as sequential injections of  $CaCl_2$  were added to each well.

**a****b**

**Figure 2.1: Illustrative diagrams of the CRC assay**

a) Diagram showing the mechanism of the CRC assay (diagram by BMG Labtech)

b) Example readout of a CRC assay

Fig 2.1.a shows the set-up and mechanism of the CRC assay. The CRC assay makes use of the Ca<sup>2+</sup> uptake capability of mitochondrial and plasma membrane impermeable Ca<sup>2+</sup> dyes. The Ca<sup>2+</sup> level in each well is monitored using a Ca<sup>2+</sup> sensitive dye, Calcium Green 1-N (ThermoFisher: C3011MP) or Fluo-5N (ThermoFisher: F13203). The intensity of the Ca<sup>2+</sup> sensitive dye reveals when mPT occurs. Before mPT occurs, Ca<sup>2+</sup> was stored in mitochondria and fluorescence intensity of the dye was low. When mPT occurs, Ca<sup>2+</sup> quickly flows out of mitochondria via the mPTP and a huge increase in fluorescence intensity of the dye occurs, indicating mPTP opening.

The fluorescent intensity of each well was constantly monitored, and a measurement is made every 2 seconds. Each well containing mitochondria would produce a single

curve as shown in Fig 2.1.b. Usually, multiple wells containing mitochondria with different experimental conditions are run.

Fig 2.1.b shows an example CRC curve, the fluorescence intensity of the  $\text{Ca}^{2+}$  dye was plotted against time. Since measurements were taken repeatedly at 2 second intervals, I could observe how the fluorescence level and hence  $\text{Ca}^{2+}$  content of the extra-mitochondria buffer changes in real time. This changes in extra-mitochondria  $\text{Ca}^{2+}$  which is made up of 3 phases as labelled in Fig 2.1.b.

A: Basal  $\text{Ca}^{2+}$  Fluorescence Levels

B: Spike in  $\text{Ca}^{2+}$  levels following injection of  $\text{Ca}^{2+}$

C: Decrease in  $\text{Ca}^{2+}$  levels as the newly added  $\text{Ca}^{2+}$  is taken up by mitochondria

D: Point at which mitochondria can no longer take up newly added  $\text{Ca}^{2+}$ , the mPTP opens and all  $\text{Ca}^{2+}$  stored in mitochondria is released

In a CRC assay, point A, B and C was repeated as  $\text{Ca}^{2+}$  is continuously injected until point D was reached. The number of injections taken to reach point D gave an indication of how sensitive mitochondria was to mPTP opening under various conditions. For example, the classical CypD inhibitor CsA would decrease the sensitivity of mPTP to  $\text{Ca}^{2+}$  overload and more  $\text{Ca}^{2+}$  injections would be required to induce mPTP opening relative to untreated mitochondria. During CRC assays, multiple conditions were often run at once and analysis involved comparing how many  $\text{Ca}^{2+}$  injections a particular condition takes to reach mPTP opening as compared to a control condition. Each experiment was first normalised to a control condition before experiments from different runs were collated and analysed.

## **2.7 Western blotting**

When doing whole cell protein extractions, the media was removed from cells and the cells washed with phosphate buffered saline (PBS). The cells were then detached using a cell scraper and resuspended in RIPA buffer\*+ (with added 1 mM



phenylmethane sulfonyl fluoride (PMSF) and PhosSTOP phosphatase inhibitors (Roche, 04906837001)) for lysis. When extracting proteins from mitochondria, the solution containing mitochondria is centrifuged at 7000g for 10 mins. The supernatant was removed, and mitochondria pellet was then resuspended in RIPA buffer\*+ for lysis.

When studying mitochondria vs cytosolic proteins, a mitochondria isolation was carried out. During which, the cytosolic column obtained in the differential centrifugation step was kept in -20°C for future western blots. The isolated mitochondria fraction was resuspended in RIPA Buffer for lysis.

The lysis process involves leaving the proteins in RIPA Buffer on ice for approximately 30 mins. Following which, 1.5 ml microcentrifuge tubes containing the proteins were centrifuged at 16,000g for 10 mins. The supernatant containing the proteins were transferred to a fresh 1.5ml Microcentrifuge Tube and stored at -20°C for future use.

Before running the blot, a BCA assay was done to determine the protein concentration for each sample. 10-30 ug (depending on experimental use case) of protein was mixed with 3X Protein Sample Loading Buffer (Licor: 928-30003) and boiled at 95 °C for 5 mins.

Samples were then separated on pre-cast 4%–12% Invitrogen Bis-Tris gels (Invitrogen, NP0321BOX) in MOPS running buffer (Invitrogen, NP0001). After the proteins have been separated on the gel, they were transferred onto a PVDF membrane (Millipore #IPFL00010) in NuPAGE transfer buffer (Invitrogen, NP0006) supplemented with 20% methanol using semi-dry transfer. The membrane was then blocked with Blocking buffer\* (3% BSA in TBS-T\*) for 1 hour at R.T on a shaker.

If a standard western blot utilizing primary and secondary antibodies was to be carried out, the membrane was incubated with primary antibodies overnight at 4°C on a shaker. All primary and secondary antibodies were diluted in Blocking buffer\*. After incubation with primary antibodies, the membrane was washed 3 times with TBS-T\* and incubated with secondary antibodies for 1 hour at RT.

Alternatively, if a streptavidin stain was to be carried out. After the blocking step, the membrane was washed 3 times with TBS-T\* and incubated with streptavidin conjugated antibodies diluted in blocking buffer for 30 mins at R.T.

Occasionally, the membrane might be stripped and re-probed using different antibodies. If this was done, the membrane is incubated for 20 mins with Restore™ Western Blot Stripping Buffer (Thermo Scientific: 21059) followed by washing 3x with TBS-T\*. The experiment then proceeds again from the membrane blocking step.

The membrane was washed 3 times using TBS-T\* before visualisation. Depending on the secondary antibodies used, the membranes were visualised using either a ChemiDoc system (BioRad) (for HRP-conjugated antibodies (substrate: Thermo Scientific: 31491)) or a Licor Odyssey CLx system (for IR dye conjugated antibodies).

Densitometry analysis were carried out using ImageJ (NIH) or Image studio lite (Licor) and statistical analysis was carried out using Graphpad Prism.

<b>Antibodies</b>	<b>Catalogue information</b>	<b>Dilution</b>
<b>Primary</b>		
anti-PPIF mouse monoclonal	Abcam: ab110324	1:10,000
anti-Tom20 rabbit monoclonal	Abcam: ab186735	1:10,000
anti-β-actin mouse polyclonal	Santa Cruz: #sc-47778	1:10,000
<b>Secondary</b>		
anti-rabbit 680	Licor (P/N: 926-68071)	1:10,000

anti-mouse 800	Licor (P/N: 926-32210)	1:10,000
<b>Others</b>		
HRP-Conjugated Streptavidin	Thermofisher: N100	0.3 µg/mL
IRDye® 680RD Streptavidin	Licor P/N: 926-68079	1:3,000

**Table 2.3: Antibodies used and respective dilutions**

## 2.8 CRISPR-Cas9 Genome editing

CRISPR-Cas9 was used to create CypD KO cells lines. Complementary gRNA targeting CypD gene sequence was designed using Benchling (<https://www.benchling.com/>). They were then cloned into the plasmids pSpCas9(BB)-2A-Puro and pSpCas9(BB)-2A-GFP depending on use case. The CRISPR plasmids were then transfected into HEK293T cells in 6 well plates. Puromycin selection was carried out 2 days after transfection. 5 days after transfection, the cells were sorted into single cell colonies using FACS into 96 well cell culture plates. Once the single cell colonies have grown, they were expanded into a 24 well plates followed by 6 well plates. Proteins were then extracted from the 24 well plate and the 6 well plates were used to continue the cell lines. The extracted proteins were tested for CypD using western blotting and further tested with Sanger sequencing and CRC to verify that a successful KO cell line was obtained.

## 2.9 Genomic DNA extraction

gDNA was extracted from cultured cells using the Qiagen DNeasy Blood & Tissue Kits (Qiagen: 69504). The manufacturer's instructions were followed which basically involved the following steps. The cells were lysed, and a nuclei pellet was obtained via centrifuging at 1300g and discarding the supernatant. The nuclei pellet was then lysed

in a buffer containing protease and placed in a filter microcentrifuge tube. The gDNA will bind to the resin on the tube and the flow through is discarded. Following which, the gDNA can then be eluted using elution buffer (e.g isopropanol).

## **2.10 Proteomics**

### **2.10.1 Sample generation**

Cells were transfected with the CypD-TurboID fusion protein as described in Section 2.2. After 48 hours, mitochondria isolation was carried out on the transfected cells as described in Section 2.3. For each biological replicate, 4 confluent 10cm<sup>2</sup> dishes of cells are used. The isolated mitochondria are kept in 1.5ml microcentrifuge tubes and at 37°C in a thermomixer, 1uM CsA or a corresponding volume of DMSO is added at this stage. Biotin is then added to the isolated mitochondria. Following which, 250uM of Ca<sup>2+</sup> is added to some samples to induce mPT. Mitochondria are then left for 15mins at 37°C to allow biotin labelling to occur, this starts from the moment biotin is added. Following which, mitochondria is centrifuged at 7000g and the MSK buffer containing biotin is removed. Mitochondria are then resuspended in RIPA buffer\*+ and left on ice for 30 mins to lyse mitochondria and release the proteins.

For each replicate, the lysed mitochondria mixture is mixed with 20ul of Pierce™ Streptavidin Magnetic Beads (Thermo Fisher: 88816) that has been prewashed with RIPA buffer. 500 µL RIPA lysis buffer is added to the bead + lysed mitochondria mixture and the resulting mixture is incubated at 4 °C overnight on a rotator. The material is then store at -20 °C for future use.

The biotinylated proteins of interest should now be located on the streptavidin beads. The magnetic beads are pelleted using a magnetic rack and the rest of the mixture can be discarded or retained for analysis. The beads are then washed twice with RIPA buffer\*+ (1 mL, 2 min at RT), once with 1 M KCl (1 mL, 2 min at RT), once with 0.1 M Na<sub>2</sub>CO<sub>3</sub> (1 mL, ~10 s), once with 2 M urea in 10 mM Tris-HCl (pH 8.0) (1 mL, ~10 s), and twice more with RIPA buffer\*+ (1 mL per wash, 2 min at RT). Following this

washing steps, the proteins on the beads can be eluted for analysis or proceed directly to on-bead digestion for mass spectrometry.

If analysis of the pulled-down proteins is desired. The proteins on the beads are eluted by boiling each sample in 30  $\mu$ L of 3 $\times$  protein loading buffer supplemented with 2 mM biotin and 20 mM Dithiothreitol (DTT) at 95  $^{\circ}$ C for 10 min. If mass spectrometry is carried out, the beads are washed twice with Tris-HCL pH 8.0 before on bead digestion.

### **2.10.2 Mass spectrometry**

Mass spectrometry is carried out from the on-bead digestion step with assistance from our collaborators at the Thalassinos lab (<http://www.homepages.ucl.ac.uk/~ucbtkth/>). The output is returned as an excel sheet with relevant proteomics data.

### **2.10.3 Data analysis**

Python is used for analysis of the proteomics data. The pandas, numpy, re, plotly, matplotlib and scipy libraries are used. During pre-processing of the data, the LFQ intensity of each hit is normalised by dividing LFQ with the iBAQ peptides to account for the number of possible peptides that can be generated by trypsin digest. Any protein with a NaN/0 value in any biological repeat was also removed to increase robustness of data. Following this, non-mitochondrial proteins were excluded using Mitocarta 3.0 as a reference. 2 methods of data processing were used, the normalised LFQ for protein complexes and different isoforms of a protein is either combined into a single signal or left as separate signals. For each set of the 2 processed data, 2 types of analysis were carried out.

The first type of analysis was to start by statistically determining the interactor hits of CypD before measuring whether the interaction levels of these hits differ between different states of mPTP opening. To determine the protein hits, I carried out an ANOVA test followed by Tukey's HSD test for all proteins in the dataset. This serves to separate the background biotinylation labelling from actual CypD interactions. The difference between conditions was then calculated by comparing samples with Ca<sup>2+</sup> addition over ones without to study effect of mPT on the CypD interactome. A one-

way ANOVA followed by Tukey's HSD was then used to determine statistical significance among the interactors.

The second type of analysis would be to carry out a multiple t-test for each pair of conditions, with/out mPT induction and with/out CsA addition. The Bonferroni correction is applied to account for the fact that multiple p-values has been calculated for each biological repeat. A standard volcano plot was generated for this type of analysis.

## **2.11 Biological services used**

### **Sequencing**

Sanger sequencing was carried out using the Eurofins Genomics Tubeseq (<https://www.eurofinsgenomics.eu/en/custom-dna-sequencing/eurofins-services/tubeseq-service/>) service. PCR was first used to amplify the target region of interest, and the PCR product was purified and sent for sequencing with the PCR primers used for amplification.

### **FACS**

All FACS was carried out with the assistance of Jamie Evans at the Flow Cytometry core facility in the division of medicine at UCL (<https://www.ucl.ac.uk/medicine/research/core-facilities>).

### **Gene Synthesis**

Gene synthesis was carried using the Genscript's services ([https://www.genscript.com/gene\\_synthesis.html?src=pullmenu](https://www.genscript.com/gene_synthesis.html?src=pullmenu)). All sequences were verified via sequencing and cloned into pcDNA3.1+ vectors.

## 2.12 Reagents

Reagent	Catalogue information
RIPA Buffer	Sigma-Aldrich: R0278  (150 mM NaCl, 0.5% sodium deoxycholic acid, 0.1% SDS, 1% Triton X100, 50 mM Tris pH 8)
Thermo Fisher BCA assay kit	Thermo Scientific™: 23227
Recording Buffer	HEPES buffered phenol red-free DMEM (Gibco #A1443001) with 10 mM glucose, 1 mM glutamine
MSK Buffer	75mM Mannitol, 25mM sucrose, 5mM potassium Phosphate monobasic, 20mM Tris-HCL, 100 mM Potassium Chloride, 0.1% BSA, 10mM Glutamate, 10mM Succinate, 5mM Malate
Isolation Buffer	0.01M Tris-MOPS, 0.001 M EGTA/Tris, 0.2 M sucrose. pH 7.4
TBS-T	TBS (20 mM Tris-HCl, 140 mM NaCl) + 0.1% Tween-20

**Table 2.4: Reagent details**

### 3. Generation of HEK293T Cyclophilin D Knockout cell line via CRISPR-Cas9

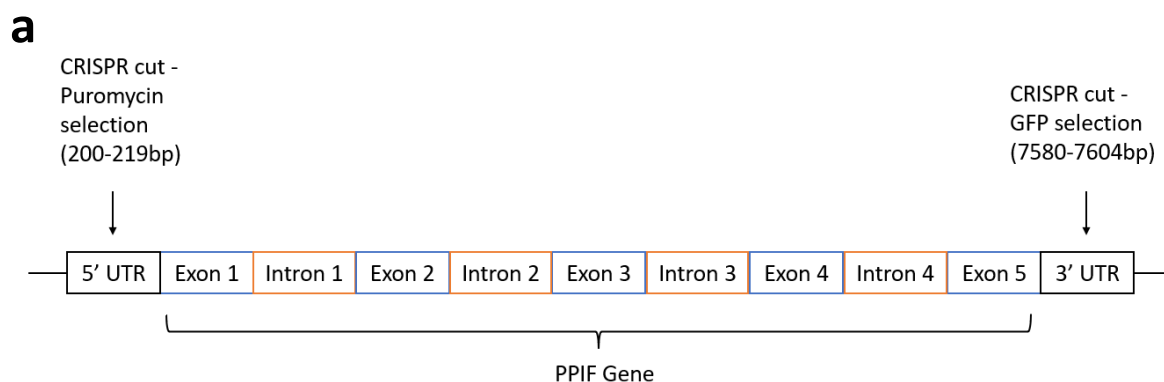
#### 3.1 Background

As discussed earlier, I would like to express the CypD-TurboID fusion protein in a CypD KO cell line in order to prevent possible competition for interactors between the fusion protein and endogenous WT CypD which might interfere with the screening results. HEK293T does not have a CypD KO line available, so I decided to create one myself using CRISPR-Cas9 gene editing. I will verify successful genetic CypD KO via sanger sequencing and ensure the loss of any CypD effect in mPT regulation via CRC assays.

#### 3.2 Results and discussions

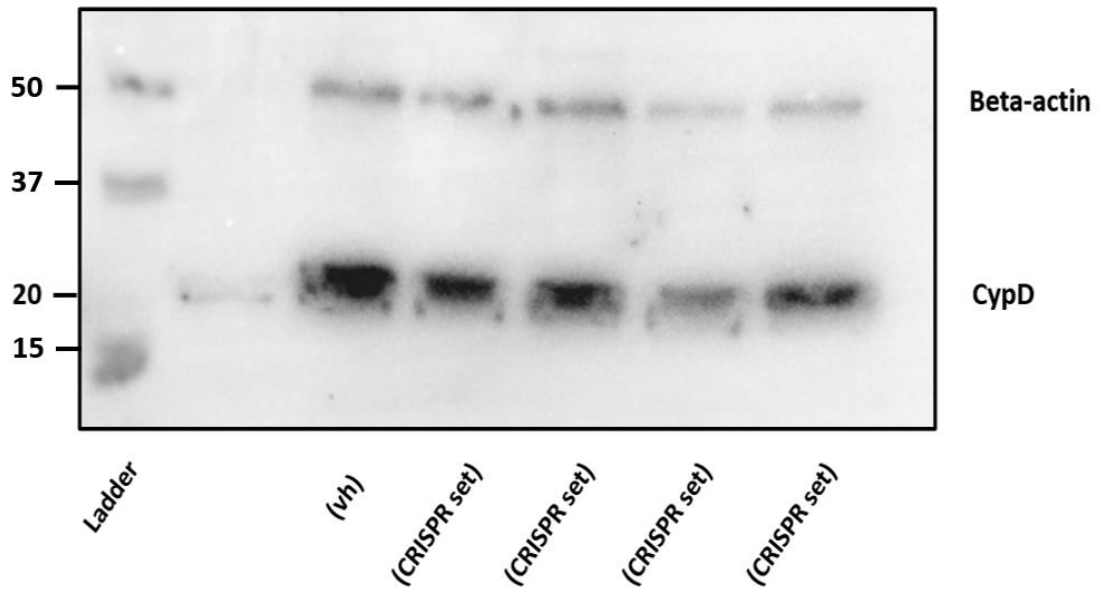
##### 3.2.1 CRISPR workflow

The CRISPR workflow I used to generate CypD KO HEK293T cell lines is adapted from the Zhang lab protocol (Ran et al., 2013). The CRISPR plasmids used are also made by his lab and obtained via addgene (<https://www.addgene.org/browse/article/7375/>). The 2 plasmids used were pSpCas9(BB)-2A-GFP and pSpCas9(BB)-2A-Puro. In order to ensure complete gene KO, I planned to introduce a deletion mutation where the entire CypD coding region is deleted.

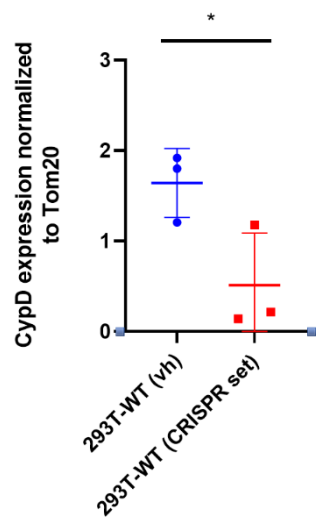




**b**



**c**



**d**

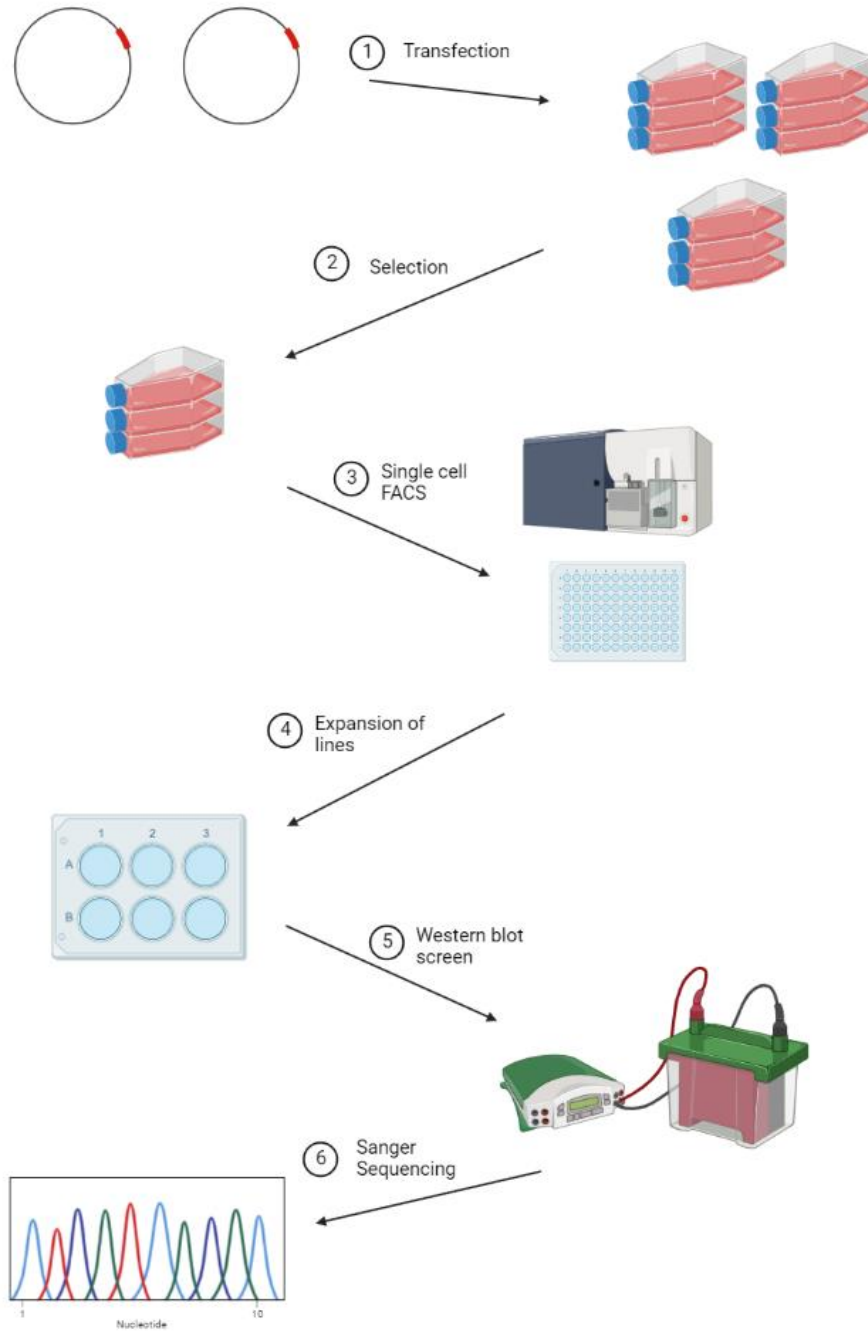


**Figure 3.1: Workflow for generating CRISPR mediated CypD KO HEK293T cell line**

a) Schematic diagram for CRISPR cut sites and selection markers applied

b) Representative western blot for HEK293T cells transfected with predesigned gRNA (in pSpCas9(BB)-2A-Puro or pSpCas9(BB)-2A-GFP) or vh (vehicle control: empty pSpCas9(BB)-2A-Puro or pSpCas9(BB)-2A-GFP), n=3

c) Quantification of CypD protein expression for HEK293T cells transfected with predesigned gRNA (in pSpCas9(BB)-2A-Puro and pSpCas9(BB)-2A-GFP) or vh (vehicle control: empty pSpCas9(BB)-2A-Puro and pSpCas9(BB)-2A-GFP), n=3

d) Monoclonal CRISPR cell line generation workflow

All quantification analysis are represented as mean  $\pm$  SD and were analysed using unpaired t-test (\* :  $p < 0.05$ ).

Two gRNAs were designed to target the Untranslated Regions (UTR) flanking the PPIF gene, one targeted the 5' UTR and the other targeted the 3' UTR. If both targets were cleaved successfully by the CRISPR plasmid, the DNA repair mechanism might join the 2 cleaved sites together leaving out the PPIF coding region in between. This would result in KO of the PPIF gene. Each of the 2 CRISPR plasmids had a different selection marker. One had a GFP and the other had a puromycin resistance gene. The 5'UTR gRNA was cloned into pSpCas9(BB)-2A-Puro, while the 3'UTR gRNA was cloned into pSpCas9(BB)-2A-GFP. The cleavage positions of the CRISPR plasmids were shown in Fig 3.1.a. As can be seen, selecting for presence of both plasmids can theoretically result in full deletion of the CypD gene.

The gRNAs used here were designed using the benchling web portal (<https://www.benchling.com/>). In terms of gRNA selection, we would need to take into account on target specificity and off target activity. Possible gRNA sequences in the respective UTR regions were assessed using the scoring model described in (Doench et al., 2016) and the gRNAs with the best scores were selected with balancing on vs off target activity in mind.

Before the full CRISPR process for generating a new cell line was carried out, I conducted preliminary testing of the gRNA and plasmids. This was to ensure that the gRNA and CRISPR plasmids I am using was indeed capable of knocking out CypD as

designed in our cell line of choice. The actual CRISPR process will take months and we will not know whether the KO is successful until the final step. I designed this new set of PPIF targeting gRNAs using theoretical concepts alone and it was important to ensure they work as expected in empirical contexts before committing to a lengthy experiment. HEK293T cells were transfected with both plasmids and grown in 2.5ug/ml puromycin containing media 2 days after transfection to select for the puromycin resistant plasmid. Following which, FACS was used to collect all the cells with GFP present to select for the second plasmid. Proteins are then extracted from cells and a CypD western blot is carried out.

Fig 3.1.b shows the western blot results when comparing the CRISPR plasmid transfected cells and untransfected cells, the results are quantified in Fig 3.1.c. As expected, cells transfected with the CRISPR plasmid set showed significantly lower level of CypD relative to Tom20. This means that the transfected CRISPR set was able to successfully delete the CypD gene as planned in a fraction of cells. This deletion will not be consistent all the time due to the inherent nature of the DNA repair mechanism and non-homologous end joining (NHEJ). As such, I would expect a mixed population of cells with some cells retaining WT CypD and some cells with CypD KO. Overall, this would result in a lower level of CypD in the population if CypD KO cells was present in the population at a high enough proportion. The result here would suggest that this combination of gRNA and CRISPR plasmid transfection should be able to create successful CypD KO HEK293T cells.

After ensuring that the plasmid set can achieve the desired CypD KO, I proceeded to carry out the full process of generating a CypD KO cell line. The process consisted of 6 steps and is depicted in Fig 3.1.d.

In step 1, the two CRISPR plasmids containing the designed gRNAs were transfected into HEK293T cells. In step 2, puromycin selection was carried out to ensure the cells contained the 5'UTR targeting CRISPR plasmid. In step 3, FACS was carried out to select for GFP and thus cells containing the 3'UTR targeting CRISPR plasmid. The FACS process also sorted the cells into single cell colonies in 96 well plates to ensure a monoclonal cell line is obtained. In hypothesis, the single cell colonies now contain both the 5'UTR and 3'UTR targeting plasmids. In step 3, the sorted monoclonal cell lines were then grown and expanded. In step 5, once there were enough cells for each

line, some cells were kept to progress the line while other cells were used for a western blot to screen for successful CypD KO. In step 6, any cell line that appeared to be a CypD KO line in the western blot screen were sequenced to confirm successful KO of CypD.

### 3.2.2 CypD KO Cell line generation

Range 1: 7590 to 7869 [Graphics](#) [▼ Next Match](#) [▲ Previous Match](#)

Score	Expect	Identities	Gaps	Strand
518 bits(280)	3e-150	280/280(100%)	0/280(0%)	Plus/Plus
Query 116	TACGAGGTGTTTGGATCATGGGGACGGGTATTTTCATGGCTTGGTGC	TGTTTTCTTGATGG	175	
Sbjct 7590	TACGAGGTGTTTGGATCATGGGGACGGGTATTTTCATGGCTTGGTGC	TGTTTTCTTGATGG	7649	
Query 176	TGAATTATTGCAAGATACGGTCATTTAAAATTGTGTGGCACCTCC	CCCTGCCCTTCTT	235	
Sbjct 7650	TGAATTATTGCAAGATACGGTCATTTAAAATTGTGTGGCACCTCC	CCCTGCCCTTCTT	7709	
Query 236	GCTCCTGCTTTTACCATGTGACATGCCTGATCCCCCTTACCTTTT	GCCATGGTCATAAG	295	
Sbjct 7710	GCTCCTGCTTTTACCATGTGACATGCCTGATCCCCCTTACCTTTT	GCCATGGTCATAAG	7769	
Query 296	CTTCCTGAGGCCTCCCTGGAAGCTGAGCAGATGCCAGCACCATG	CTTCCTGTACATCCTG	355	
Sbjct 7770	CTTCCTGAGGCCTCCCTGGAAGCTGAGCAGATGCCAGCACCATG	CTTCCTGTACATCCTG	7829	
Query 356	CAGAACCATAAGCCAATTAACCTTTTTAATAATAAATTA	395		
Sbjct 7830	CAGAACCATAAGCCAATTAACCTTTTTAATAATAAATTA	7869		

Range 2: 96 to 210 [Graphics](#) [▼ Next Match](#) [▲ Previous Match](#) [▲ First Match](#)

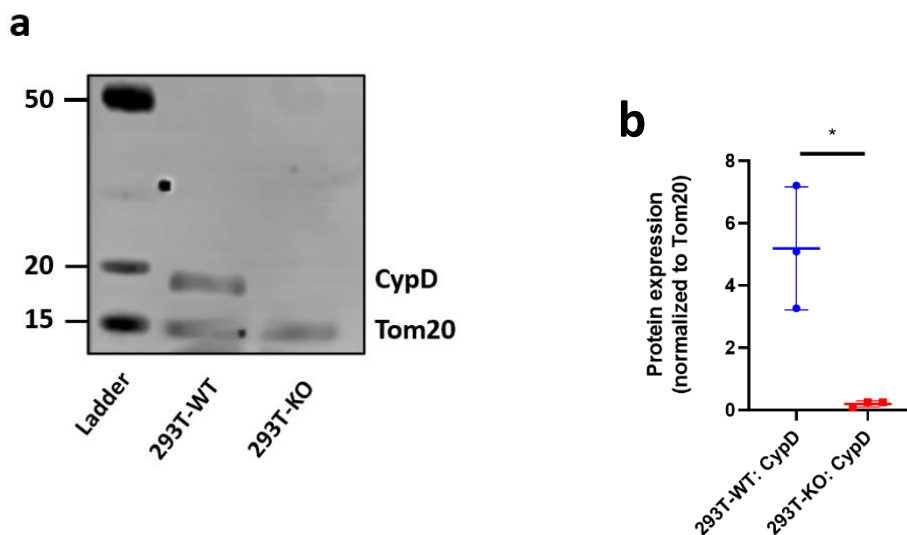
Score	Expect	Identities	Gaps	Strand
213 bits(115)	2e-58	115/115(100%)	0/115(0%)	Plus/Plus
Query 1	TGCGGCTCCCGCTGGCTCGGCTGCTCTCCGTCCC	GCGCTCCGTGCCGCTGCGCCTCCCC	60	
Sbjct 96	TGCGGCTCCCGCTGGCTCGGCTGCTCTCCGTCCC	GCGCTCCGTGCCGCTGCGCCTCCCC	155	
Query 61	GCGGCCCGCGCTGCAGCAAGGGCTCCGGCGACCCGTCCTTTCCTCCTCCTCCG	115		
Sbjct 156	GCGGCCCGCGCTGCAGCAAGGGCTCCGGCGACCCGTCCTTTCCTCCTCCTCCG	210		

**Figure 3.2: Blast-alignment analysis of the sanger sequencing results for clone 11 vs the human PPIF genetic sequence**

The CypD KO HEK293T cell line was generated according to the procedure described in Fig 3.1.d. At step 5, a western and one cell line was identified as a potential. CypD

KO line. This line was then sent for sanger sequencing following DNA extraction and PCR amplification.

Sanger sequencing was carried out using the Eurofins genomics service. Once the result was returned, a NCBI Blast alignment was carried out between the original PPIF genomic region and the corresponding region in the KO cell line. Fig 3.2 shows the result of this alignment. Two 100% sequence similarity regions were found between the KO and WT regions. In Range 1, the 116-395 base pair region of the KO cell line corresponds to the 7590-7869 base pairs region in the WT. In Range 2, the 1-115 base pair region of the KO cell line corresponds to the 96-210 base pairs region in the WT. This shows that a sequence deletion of 7380 base pairs occurred between the 210 and the 7590 nucleotides of the PPIF gene in this CypD KO line, resulting in deletion of all 5 Exons. This whole gene deletion was also exactly the optimal expected result from the CRISPR gRNA design.



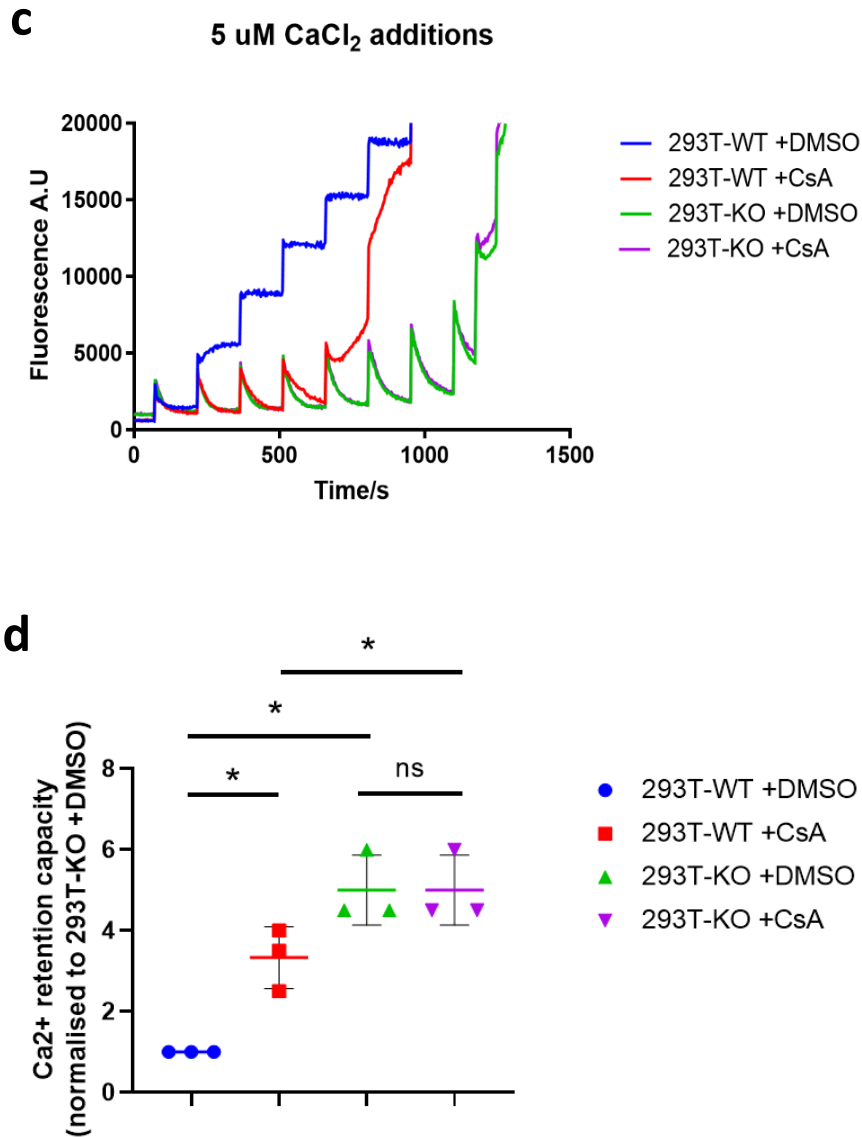


**Figure 3.3: Experimental confirmation of successful CypD KO at protein expression and functional levels**

a) Representative western blot for HEK293T WT vs HEK293T KO clone 11,  $n=3$

b) Quantification of CypD expression levels for HEK293T WT vs HEK293T KO clone 11, normalised to Tom20, an unpaired  $t$ -test is carried out,  $n=3$

c) Representative CRC assay data for HEK293T WT vs HEK293T KO clone 11, with 2uM CsA or an equivalent volume of DMSO added prior to measurement,  $n=3$

*d) Quantification of CRC assay data for HEK293T WT vs HEK293T KO clone 11, with 2 $\mu$ M CsA or an equivalent volume of DMSO added prior to measurement, a one-way ANOVA followed by Tukey's multiple comparisons test was carried out, n=3*

*All quantification analysis are represented as mean  $\pm$  SD, (\* :  $p < 0.05$ ).*

More western blot experiments were also carried out to confirm the absence of the CypD protein in this new CypD KO cell line. The results of the western blots were shown in figure 3.3.a and the statistical analysis in 3.3.b. I observed the absence of CypD in the blot itself which was double confirmed by measuring band intensities and using statistical analysis to compare the KO and WT CypD band regions on the blot.

Finally, there was one last property of the KO cell line that needs to be verified before I could use it as the CypD KO line for my screen. The aim of the project was to identify CypD interactors that might be involved in mPT. As such, I needed to verify that the effect of CypD on mPT was absent in the KO cells as this was the most important phenotype with respect to the project. I carried out CRC assays to characterise the mPTP of the CypD KO cell line.

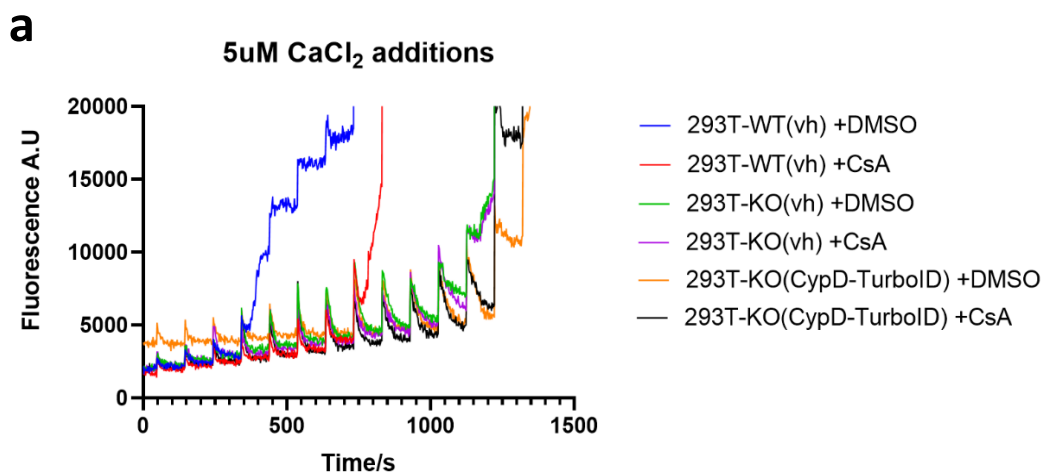
From Fig 3.3.c, it can be observed that the CypD KO cell line required much more Ca<sup>2+</sup> for mPT to occur, this was also statistically confirmed in Fig 3.3.d. This was the expected result as CypD KO causes the mPTP to have decreased Ca<sup>2+</sup> sensitivity owing to the absence of the positive mPTP regulator CypD. As discussed earlier in Chapter 1, CsA inhibits mPT by binding to CypD. As such, successful KO of CypD should cause CsA to lose any effect it had on inhibiting the mPTP. As can be seen in Fig 3.3.c, CsA decreased Ca<sup>2+</sup> sensitivity of the mPTP in WT mitochondria, this showed that the CsA drug is working well and as expected, whereas it failed to decrease the Ca<sup>2+</sup> sensitivity in KO cells. As expected, CsA had no effect on mPT in KO cells. This observation was consistently observed and statistically quantified in Fig 3.3.d.

From the results in Fig 3.3, I concluded that the CypD KO line was verified at the genetic, protein expression, and the functional level. This means it should make a good model for the screen.



### 3.2.3 Expression of fusion proteins in CypD KO cells

Before the screen can be carried out, I would need to verify the functionality of CypD-TurboID in the new CypD KO HEK293T cells. This would be very similar to the preliminary experiments carried out in Chapter 3 on the WT HEK293T cells but needed to be repeated here on the CypD KO HEK293T cells since it was a newly created cell line. The CypD-TurboID fusion protein would be transfected into the HEK293T CypD KO cells using previously optimised transfection protocol. I would then carry out CRC assays to determine if CypD-TurboID can replicate the function of WT CypD by increasing Ca<sup>2+</sup> sensitivity and re-establishing CsA sensitivity of the mPTP in CypD KO cells. Following which, I would test if the CypD-TurboID fusion protein can properly biotinylate proteins upon a short exposure to biotin.



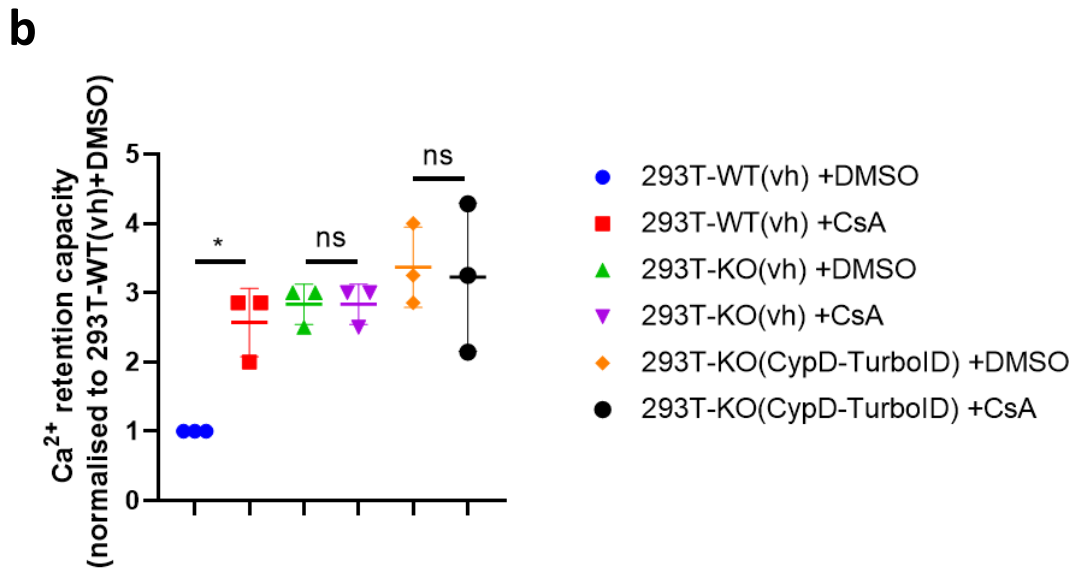


**Figure 3.4: Examining functionality of CypD-TurboID in CypD KO cells**

a) Representative CRC assay data for HEK293T KO cells transfected with CypD-TurboID (in pcDNA3.1+) or vh (vehicle control: an empty plasmid backbone of pcDNA3.1+) and HEK293T WT cells transfected with vh, with 2 $\mu$ M CsA or an equivalent volume of DMSO added prior to measurement, n=3

b) Quantification of CRC assay data for HEK293T KO cells transfected with CypD-TurboID (in pcDNA3.1+) or vh (vehicle control: an empty plasmid backbone of pcDNA3.1+) and HEK293T WT cells transfected with vh, with 2 $\mu$ M CsA or an equivalent volume of DMSO added prior to measurement, a one-way ANOVA followed by Tukey's multiple comparisons test was carried out, n=3

All quantification analysis are represented as mean  $\pm$  SD, (\*:  $p < 0.05$ )

The CRC assay was used to investigate whether the CypD-TurboID fusion protein functionally replicates WT CypD. Fig 3.3.a shows a representative trace of such a CRC experiment. The CRC assay results were further validated via repeat experiments and statistical analysis in Fig 3.3.b. As Fig 3.3.b shows, there was no significant difference between KO (vh) and KO (CypD-TurboID) as well as between DMSO and CsA treated KO (CypD-TurboID). This result had 2 major implications on the function of CypD-TurboID in CypD KO cells. Firstly, the CypD-TurboID fusion protein did not increase

the Ca<sup>2+</sup> sensitivity of the mPTP in KO cells. Secondly, the CypD-TurboID fusion protein failed to restore any sensitivity of the mPTP to CsA. If the CypD-TurboID fusion protein was replicating the function of WT CypD at the molecular level, one would expect it to increase the Ca<sup>2+</sup> sensitivity of the mPTP in KO cells and restore CsA dependent mPTP inhibition. However, that was not the case here. This suggested that the fusion protein is not properly replicating the effect of WT CypD in the KO cells with respect to mPTP sensitivity.

The inability of the CypD-TurboID fusion protein to restore WT CypD function in the KO cell line was a major obstacle to the project and I could not continue with the screen until I resolved the issue. This was important because the aim of the project was to identify possible components of the mPTP. If the CypD fusion protein in the system was no longer able to regulate mPT in a Ca<sup>2+</sup> dependent manner, the screen would not be producing any result relevant to the mPTP. This result was unexpected, since the same fusion protein was able to produce the desired result in WT HEK293T cells and the data in Fig 3.3 suggest that the fusion protein can successfully replicate the effect of CypD in regulating mPTP. Further experiments would need to be conducted to investigate and potentially resolve the problem.

### **3.2.4 Troubleshooting CypD-TurboID and KO cell line incompatibility**

The results in Fig 3.3 suggest that CypD-TurboID and the CypD KO cell line were incompatible when it comes to restoring CypD function. This was a rather unexpected observation, and I did not have a reasonable hypothesis explaining the results at this stage. As such, I decided to adopt a systemic approach to troubleshoot the issue by checking every point where this functional restoration could have gone wrong.

The first possibility that I needed to rule out was inadequate protein expression in the CypD KO HEK293T cells. Although the transfection protocol has been optimised in WT HEK293T cells, it had not been tested in the new KO cell line. In theory the protocol should perform equally well in both cell lines as the KO cell line was derived from the original WT HEK293T cell line and CypD KO should not have any effect on transfection and foreign transgene expression. However, CRISPR-Cas9 was known to introduce

unwanted off-target effects. There was a possibility that an off-target effect occurred which affected a gene that is essential for transfection or transgene expression.

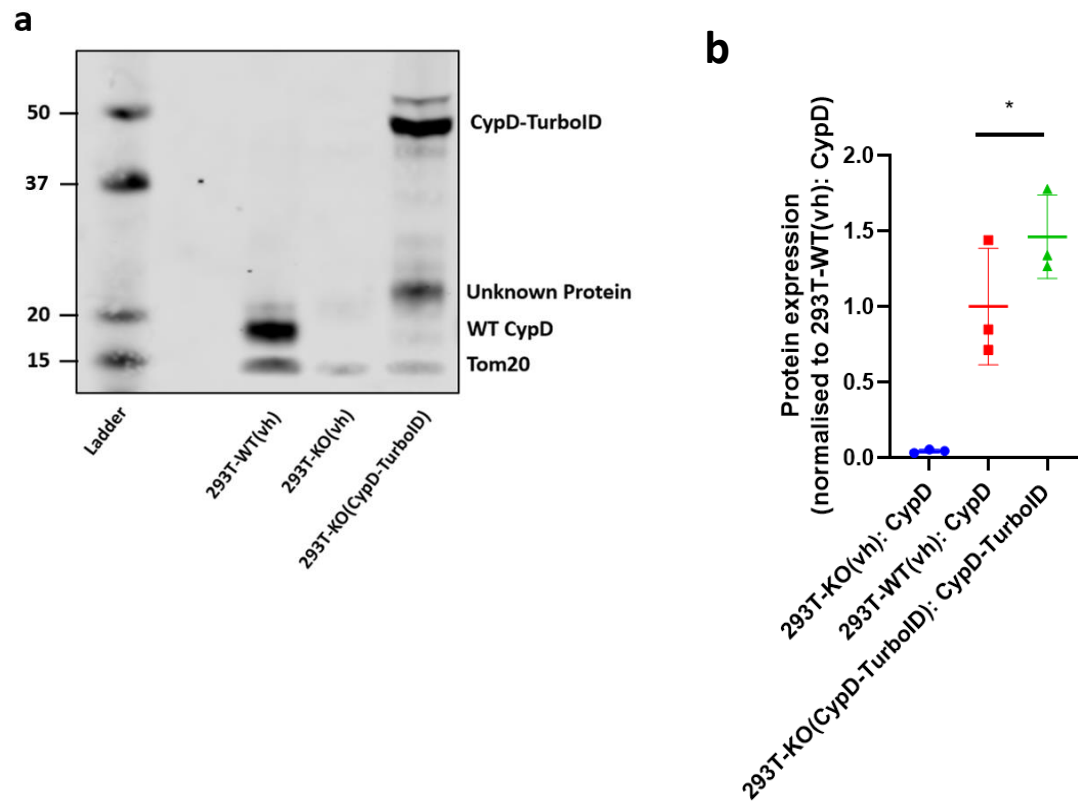


**Figure 3.5: Examining expression of CypD-TurboID in CypD KO cells**

a) Representative western blot for HEK293T KO cells transfected with CypD-TurboID (in pcDNA3.1+) or vh (vehicle control: an empty plasmid backbone of pcDNA3.1+) and HEK293T WT cells transfected with vh,  $n=3$

b) Quantification of CypD-TurboID expression for HEK293T KO cells transfected with CypD-TurboID (in pcDNA3.1+) vs WT CypD expression for HEK293T KO and WT cells transfected with vh (vehicle control: an empty plasmid backbone of pcDNA3.1+), normalised to WT CypD expression levels in WT HEK293T cells transfected with vh, a one-way ANOVA followed by Tukey's multiple comparisons test was carried out,  $n=3$

All quantification analysis are represented as mean  $\pm$  SD, (\* :  $p < 0.05$ ).

From Fig 3.5.a, it can be observed that there was proper expression of the CypD-TurboID fusion protein. This was double confirmed using statistical analysis shown in Fig 3.5.b. The western blot was carried out using isolated mitochondria. As such, I could safely assume proper mitochondrial localization here as well. This allowed me to rule out insufficient protein expression as the cause for the lack of CypD functionality as shown in Fig 3.3. While proper expression of the CypD-TurboID fusion protein would be suggestive of other problems stemming from the KO cell line, the western blot data obtained after transfecting the CypD KO HEK293T cells with the CypD-TurboID fusion protein was problematic and introduces new issues I must now consider.

As can be seen in Fig 3.5.a, there were 2 bands detected by the anti-CypD antibody in CypD KO cells transfected with CypD-TurboID. One band was around 35kDa in size and corresponds to the fusion protein. The second band was approximately 25kDa in size and only slightly larger than WT CypD which was approximately 20kDa. Given that the anti-CypD antibody was supposed to specifically detect CypD, it can be assumed that this new band was structurally very similar to CypD. Given the context of CypD KO cells and fusion protein expression, I drew the conclusion that this was likely a result of the CypD part of the fusion protein breaking off from the main protein. As to why it was slightly larger than WT CypD, this might be due to the unknown 25 kDa 'CypD' retaining some amino acids from the other components of the fusion protein, most likely the GS linker.

Having made this observation, I now needed to determine whether the observed unknown protein band and potential breakage of the CypD-TurboID fusion protein was exclusive to CypD KO HEK293T cells and hence possibly causing the lack of functional restoration in CypD KO cells. If this problem was not exclusive to CypD KO cells, I would need to re-visit the fusion protein design and look elsewhere for the lack of functional restoration in CypD KO cells. I carried out western blotting experiments for WT HEK293T cells which were transfected with the CypD-TurboID fusion protein to help evaluate the problem.

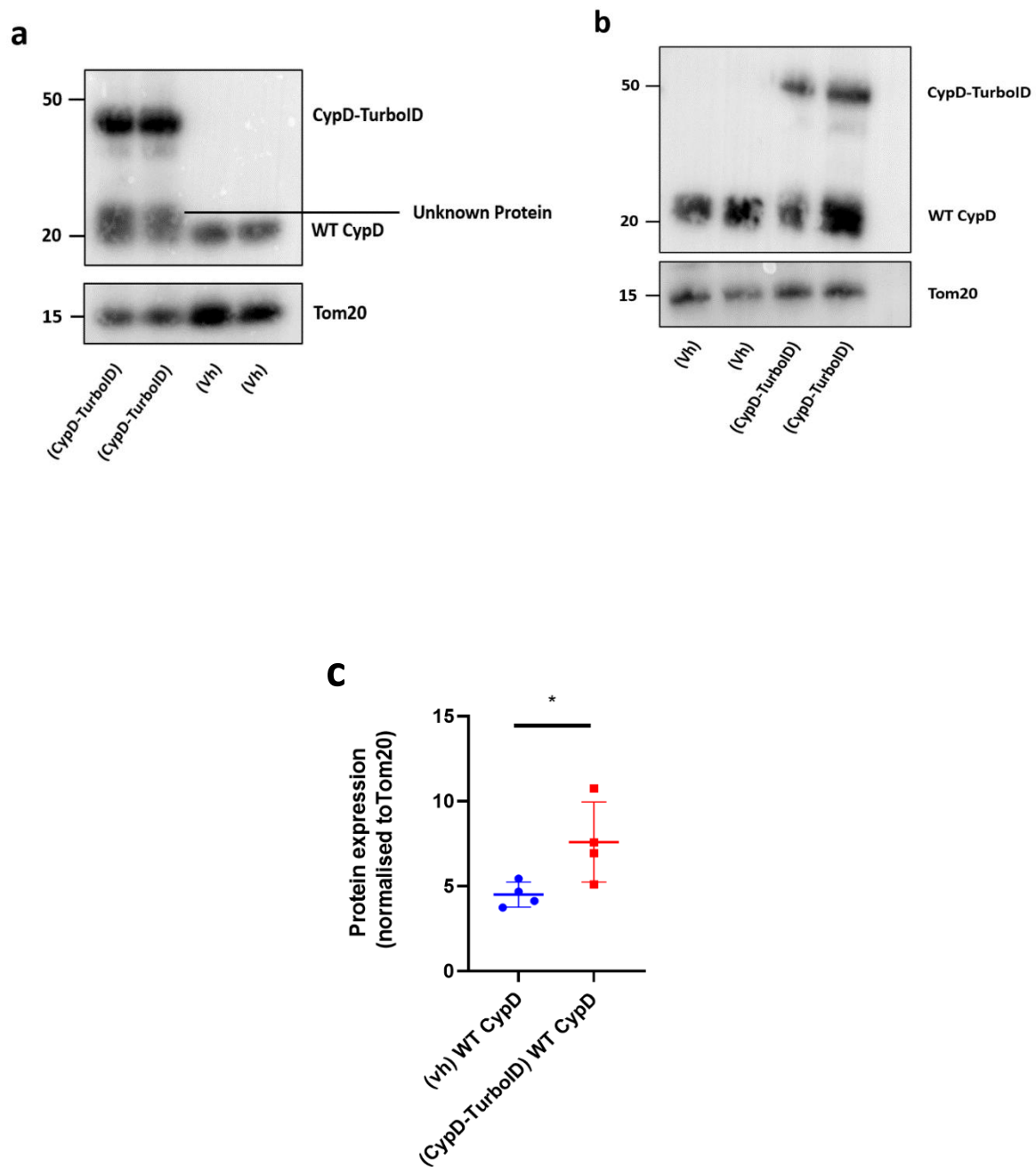


**Figure 3.6: Western blots of WT HEK293T cells transfected with CypD-TurboID**

a) Representative western blot for HEK293T WT cells transfected with CypD-TurboID (in pcDNA3.1+) or vh (vehicle control: an empty plasmid backbone of pcDNA3.1+), n=3

*b) Representative western blot for HEK293T WT cells transfected with CypD-TurboID (in pcDNA3.1+) or vh (vehicle control: an empty plasmid backbone of pcDNA3.1+), n=3*

*c) Quantification of WT CypD band expression levels in HEK293T cells transfected with CypD-TurboID as compared to HEK293T cells transfected with vh control, normalised to Tom20, an unpaired t-test is carried out, n=3*

*All quantification analysis are represented as mean  $\pm$  SD, (\* :  $p < 0.05$ ).*

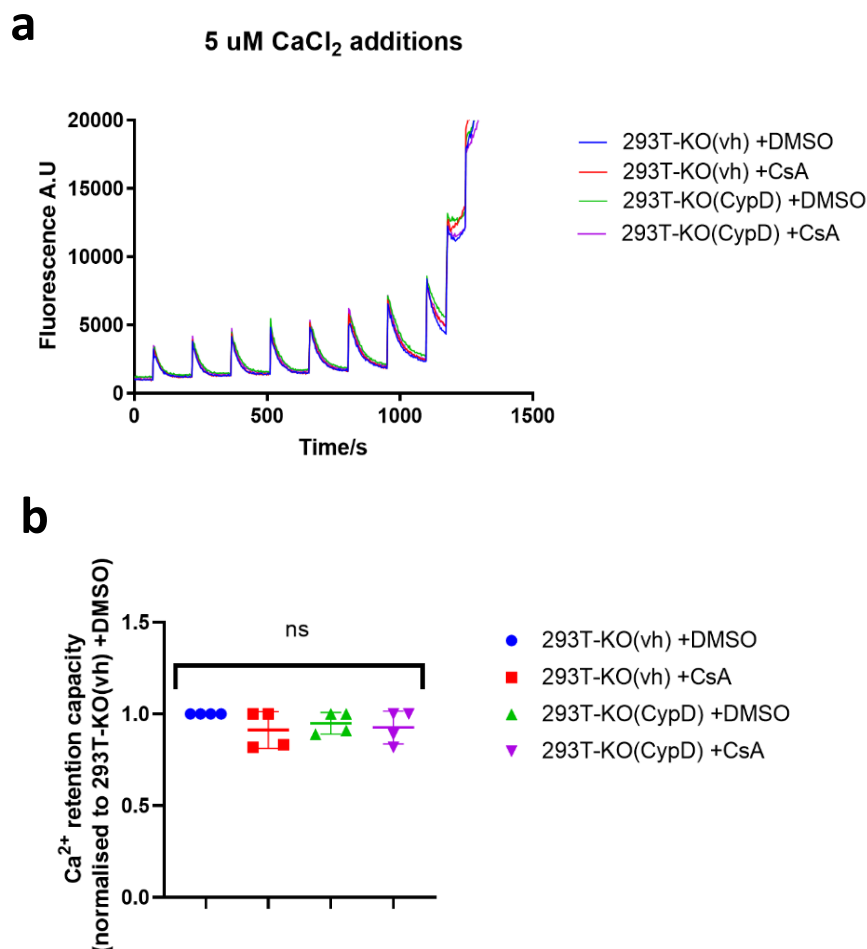
Looking at Fig 3.6.a, 2 very close bands around the size of WT CypD can actually be observed in WT HEK293T cells transfected with CypD-TurboID. This was much more obvious when compared to vehicle transfected cells. Since the experiments were all conducted in WT HEK293T cells, the 25 kDa 'CypD' protein which was very close in size to WT CypD were mixed together with the endogenous CypD bands on the same western blots. On the other hand, looking at Fig 3.6.b, it was actually not possible to conclude that 2 bands were present around the CypD bands region in WT HEK293T cells transfected with CypD-TurboID. Based on observations across multiple blots, I found that although the 2 bands were often observed, it was not always discernible by simple qualitative examination. As such, I proceeded to perform some statistical analysis by comparing the WT CypD band in WT HEK293T cells transfected with CypD-TurboID and vh. The result of this analysis in Fig 3.6.c showed that CypD-TurboID transfected cells have a statistically higher amount of protein around the WT CypD region than vehicle transfected cells. This suggest that possible breakage of the fusion protein occurs consistently around the linker region, which was the most likely way of breakage that will lead to the observed bands.

This possible breakage of the fusion protein brings to light hidden potential shortcomings of the project that needed to be resolved. Given that there was breaking of the fusion protein, I would not be able to make accurate conclusions regarding the effect of expressing the CypD-TurboID fusion protein in any cell line. It might be possible that any effects observed following transfection of the fusion protein were due to the function of the broken off parts of the fusion protein instead of the whole protein itself. This introduces the possibility that the biotin labelling process became dissociated from CypD and thus its interactors, rendering the screen less reliable.

The result from the experiments here suggest that I needed to deal with 2 potential problems. Firstly, I would need to continue to troubleshoot the issue where expression of the CypD-TurboID fusion protein failed to have any effect on mPT. Additionally, I would also need to troubleshoot the breakage problem observed in the fusion protein. The two issues were separate and were investigated in separate following sections.

### 3.2.4.1 Expression of WT CypD in CypD KO cells

The lack of effect in mPT from expression of the fusion protein in CypD KO cells was surprising. As discussed earlier, there does not appear to be any clear explanation for this. In order to further investigate the issue, I tested the effect of expressing WT CypD into CypD KO cells. This was to conclusively pin down the problem onto the cells, especially after it was discovered earlier that the fusion protein might not be as reliable as previously thought.





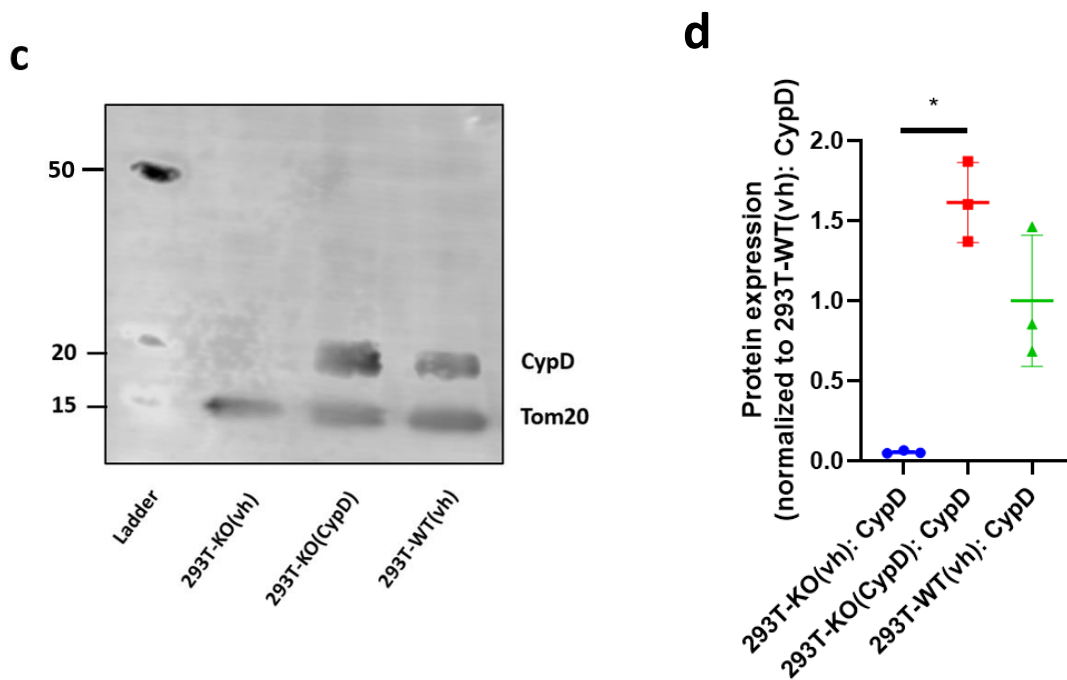


**Figure 3.7: Examining functionality of WT CypD in CypD KO HEK293T cells**

a) Representative CRC assay data for CypD KO HEK293T cells transfected with WT CypD (in pcDNA3.1+) or vh (vehicle control: an empty plasmid backbone of pcDNA3.1+) with 2uM CsA or an equivalent volume of DMSO added prior to measurement, n=3

b) Quantification of CRC assay data for CypD KO HEK293T cells transfected with WT CypD (in pcDNA3.1+) or vh (vehicle control: an empty plasmid backbone of pcDNA3.1+) with 2uM CsA or an equivalent volume of DMSO added prior to measurement, one-way ANOVA followed by Tukey's multiple comparisons test was carried out, n=3

c) Representative western blot for CypD KO HEK293T cells transfected with WT CypD (in pcDNA3.1+) or vh (vehicle control: an empty plasmid backbone of pcDNA3.1+), n=3

d) Quantification of western blot for CypD KO HEK293T cells transfected with WT CypD (in pcDNA3.1+) or vh (vehicle control: an empty plasmid backbone of pcDNA3.1+), a one-way ANOVA followed by Tukey's multiple comparisons test was carried out, n=3

All quantification analysis are represented as mean  $\pm$  SD, (\*:  $p < 0.05$ ).

A WT CypD cDNA sequence was cloned into the same expression plasmid as the CypD-TurboID fusion protein, pcDNA3.1+. It was then transfected into the CypD KO HEK293T cell line. The resulting data should give me insight into where the problem observed in Fig 3.5 lied. If the problem lied with the fusion protein, I should be able to restore CypD function by using WT CypD. If that was the case, a CRC assay should show that CypD KO cells transfected with WT CypD required less Ca<sup>2+</sup> for mPT and ability of CsA to regulate mPT would be restored. However, if the problem lied with the KO cell line, I would continue to observe the same problems. This means that the CRC assays would show that even transfection with WT CypD could not confer additional Ca<sup>2+</sup> sensitivity to the mPTP and the effect of CsA would not be restored.

Fig 3.7.a shows that transfection of WT CypD into CypD KO cells had no effect on Ca<sup>2+</sup> sensitivity of the mPTP, it also did not restore CsA sensitivity of the mPTP. Quantification of the CRC assay data in Fig 3.7.b confirmed the observations in Figure 3.7.a. Furthermore, western blot was used to assess expression level of WT CypD in CypD KO cells. Fig 3.7.c shows high levels of WT CypD expression in CypD KO cells transfected with WT CypD. Quantification of the western blot data (CypD protein levels relative to Tom20 levels) in 3.8.d also shows that there was a high level of CypD WT expression transfected KO cells compared to WT cells. The western blot data excluded any possibility that there were problems with expression of WT CypD in these cells.

The results here suggested that the problem lied with the KO cell line itself. However, I needed to first ensure that the new WT CypD plasmid can properly replicate the function of CypD in WT HEK293T cells before making the final conclusion. This was because the plasmid had not been previously tested in HEK293T cells and there was no baseline to compare the effect of its expression in these new CypD KO cells to.

### 3.2.4.2 Testing of WT CypD plasmid in WT HEK293T cells

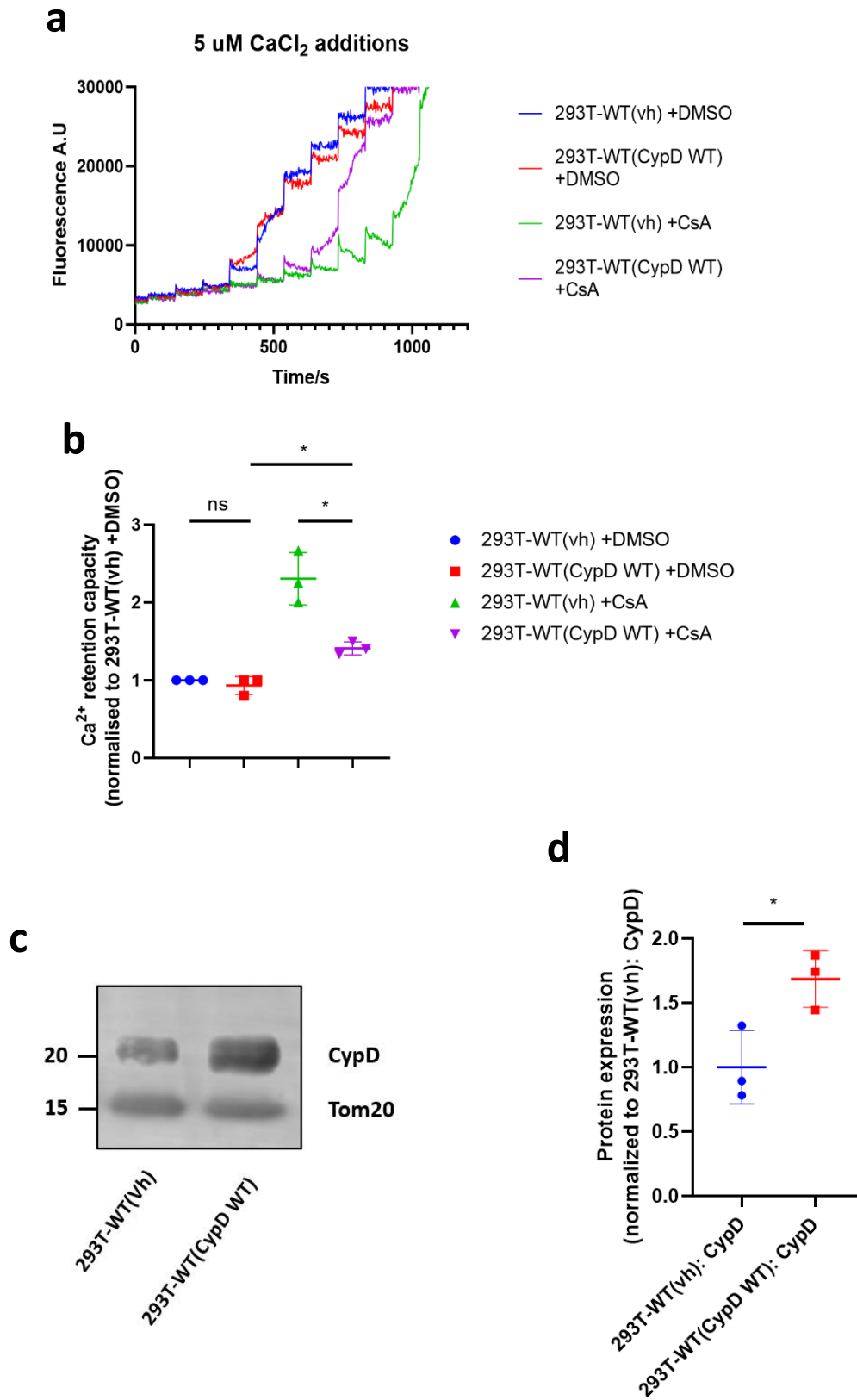


**Figure 3.8: Examining expression and functionality of WT CypD in WT HEK293T cells**

a) Representative CRC assay data for WT HEK293T cells transfected with CypD WT (in pcDNA3.1+) or vh (vehicle control: an empty plasmid backbone of pcDNA3.1+) with 2 $\mu$ M CsA or an equivalent volume of DMSO added prior to measurement, n=3

b) Quantification of CRC assay data for WT HEK293T cells transfected with CypD WT (in pcDNA3.1+) or vh (vehicle control: an empty plasmid backbone of pcDNA3.1+) with 2 $\mu$ M CsA or an equivalent volume of DMSO added prior to measurement, one-way ANOVA followed by Tukey's multiple comparisons test was carried out, n=3

c) Representative western blot for WT HEK293T cells transfected with CypD WT (in pcDNA3.1+) or vh (vehicle control: an empty plasmid backbone of pcDNA3.1+), n=3

d) Quantification of western blot for WT HEK293T cells transfected with CypD WT (in pcDNA3.1+) or vh (vehicle control: an empty plasmid backbone of pcDNA3.1+), a t-test was carried out, n=3

All quantification analysis are represented as mean  $\pm$  SD, (\* :  $p < 0.05$ ).

As can be seen in Fig 3.8.a, CRC assay results showed that expression of WT CypD in WT HEK293T cells had no effect on the amount of Ca<sup>2+</sup> required to induce mPT. However, the expression of WT CypD reduced the effect CsA had on desensitizing mPTP to Ca<sup>2+</sup> induced opening in WT HEK293T cells. This observation was statistically confirmed in Fig 3.8.b. In hypothesis, one would expect overexpression of CypD (as was the case of expressing WT CypD in WT HEK293T cells that already have physiological levels of CypD) to increase the Ca<sup>2+</sup> sensitivity of the mPTP and decrease the sensitivity of mPTP to CsA. The increase in Ca<sup>2+</sup> sensitivity was not observed whereas the reduction in effect of CsA was. This was unexpected but there could be a theoretical explanation for this. If I assume that the physiological amount of CypD in HEK293T was saturated in terms of facilitating Ca<sup>2+</sup> induced mPT, then an increase in the amount of CypD would not confer additional Ca<sup>2+</sup> sensitivity. The effect of CsA would still be reduced because the additional CypD would compete in CsA binding with the original CypD, thus reducing the effect of CsA on mPT.

Given that the WT CypD had an effect on mPT in WT HEK293T cells while it had no effect on mPT in CypD KO HEK293T cells, I can conclusively say that that there was

an unknown phenotypic change in the CypD KO cell line that caused CypD to lose its function in mPT. The CRISPR gene editing process might have caused changes in HEK293T phenotype that rendered CypD unable to regulate Ca<sup>2+</sup> dependent mPT. This could come in the form of CRISPR off target effects or potentially from adaptation during the experiment, for example during the monoclonal cell line selection process.

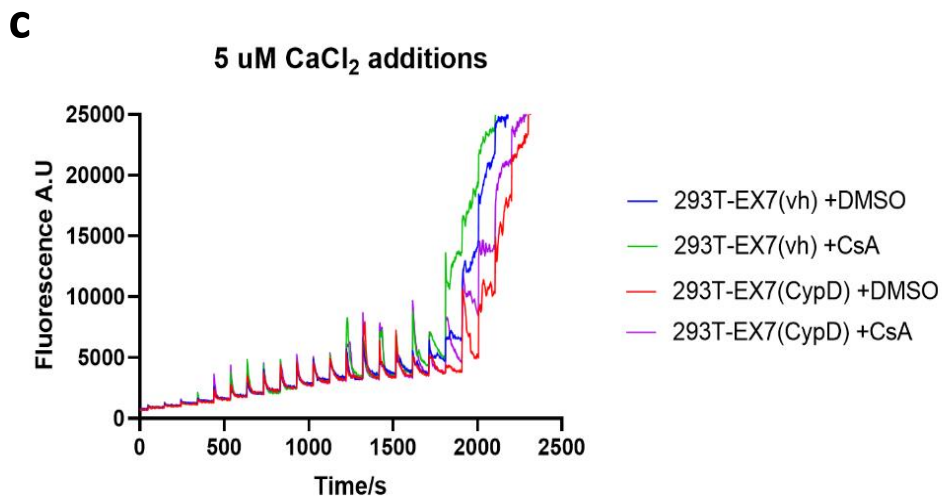
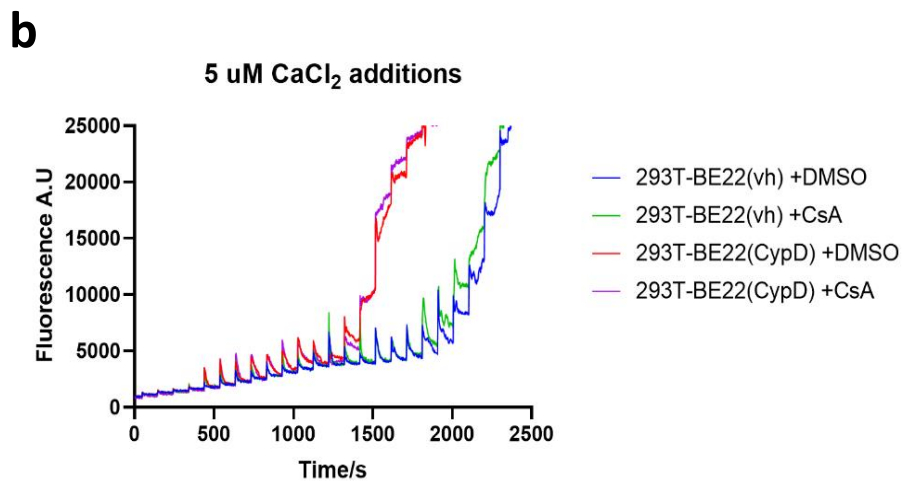
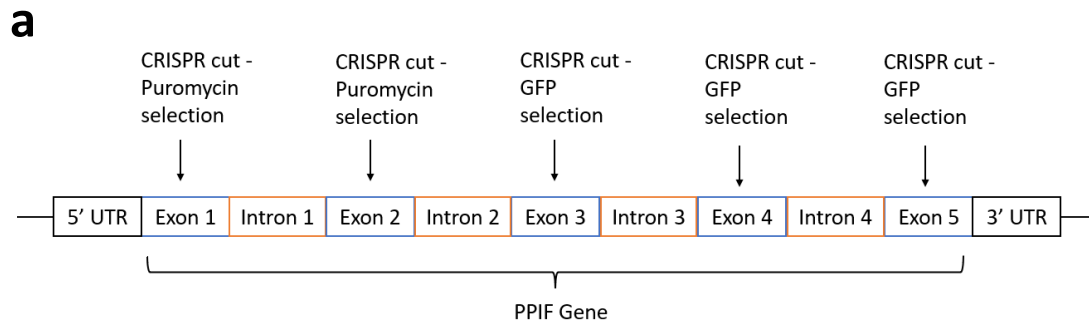
### **3.2.5 New round of CRISPR-Cas9 CypD KO cell lines**

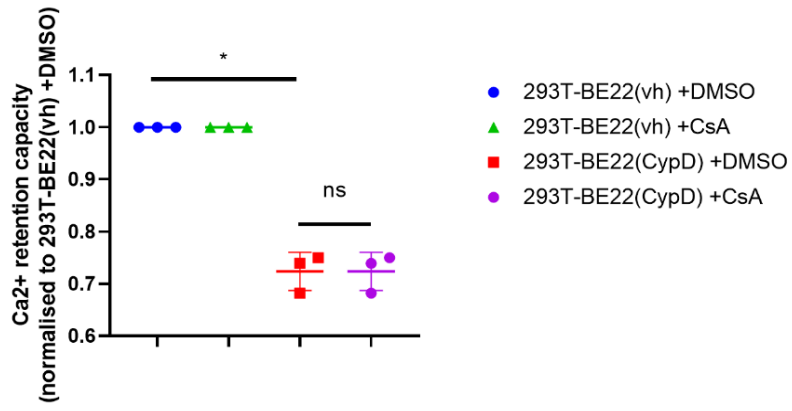
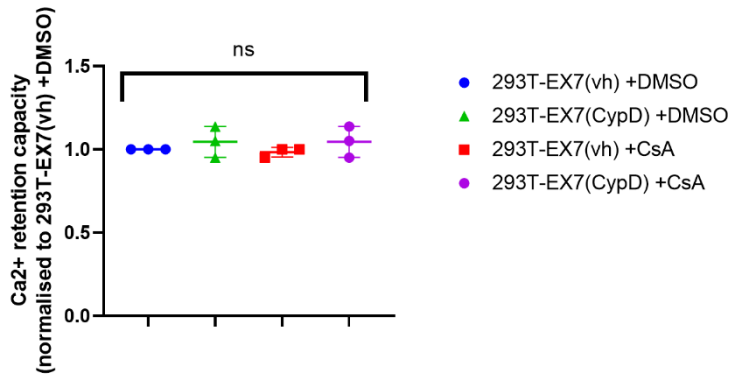
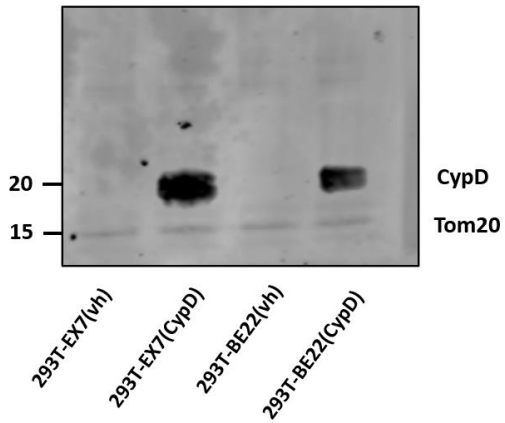
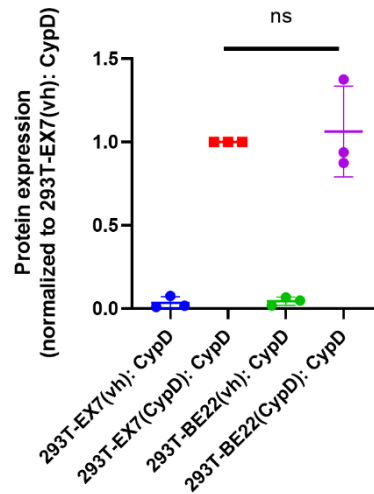
In light of the issues discussed above facing the CypD KO cell line. It was decided a potential solution was to generate more KO cells lines to sidestep the problem. If the problem was indeed due to unintended side-effects of the CRISPR-cas9 gene-editing process, in theory it can be avoided by using different gRNAs in the CRISPR process and testing more KO lines as side-effects of CRISPR behave in a probability like manner.

In the second round of CRISPR, in addition to the gRNAs targeting the 5'UTR and 3'UTR of the PPIF gene as used in the previous round of CRISPR, I also utilised 5 new gRNAs each targeting an exon of the CypD gene. This was to sidestep the possibility that the old gRNA sequences used have any specific unintended off target effects that was causing the problem in the current CypD KO cell line. The same procedure as described earlier was used to generate the KO cell lines. The cells were transfected with the CRISPR plasmids, sorted into single cell colonies using FACS and the expanded colonies were then screened for CypD KO using western blots. The targeting sites and selection markers of the new CRISPR plasmids are shown in Fig 3.7.a.

This time round dozens of cells lines were generated using both the old gRNAs targeting the 5'UTR and 3'UTR of the PPIF gene (BE) and new gRNAs targeting the exons (EX). The cell lines were named according to which set of gRNAs was used to generate them. This was to keep track of whether the BE gRNAs were indeed causing undesired off-target effects. However, these new KO cell lines needed to be further tested for their ability to allow restoration of CypD function following introduction of exogenous CypD genes. A CRC screen was carried out for this purpose on these

cell lines. The candidate KO lines were transfected with WT CypD plasmid and a CRC assay was carried out to determine if the function of CypD in mPTP regulation can be restored. Since this was the experiment that revealed issues with the original CypD KO cell line, I would like to exclude any problems here before committing more resources to any of the new cell lines.



**d****e****f****g**

**Figure 3.9: Generation of new CRISPR cell lines**

a) Schematic diagram for CRISPR cut sites and selection markers applied for exon targeting gRNAs

a) Representative CRC assay data for BE22 cells transfected with CypD WT (in pcDNA3.1+) or vh (vehicle control: an empty plasmid backbone of pcDNA3.1+) with 2uM CsA or an equivalent volume of DMSO added prior to measurement, n=3

b) Representative CRC assay data for EX7 cells transfected with CypD WT (in pcDNA3.1+) or vh (vehicle control: an empty plasmid backbone of pcDNA3.1+) with 2uM CsA or an equivalent volume of DMSO added prior to measurement, n=3

c) Quantification of CRC assay data for BE22 cells transfected with CypD WT (in pcDNA3.1+) or vh (vehicle control: an empty plasmid backbone of pcDNA3.1+) with 2uM CsA or an equivalent volume of DMSO added prior to measurement, n=3

d) Quantification of CRC assay data for EX7 cells transfected with CypD WT (in pcDNA3.1+) or vh (vehicle control: an empty plasmid backbone of pcDNA3.1+) with 2uM CsA or an equivalent volume of DMSO added prior to measurement, n=3

e) Representative western blot for BE22 and EX7 cells transfected with CypD WT (in pcDNA3.1+) or vh (vehicle control: an empty plasmid backbone of pcDNA3.1+), n=3

f) Quantification of western blot for BE22 and EX7 cells transfected with CypD WT (in pcDNA3.1+) or vh (vehicle control: an empty plasmid backbone of pcDNA3.1+), n=3

All quantification analysis are represented as mean  $\pm$  SD and were analysed using one-way ANOVA followed by Tukey's multiple comparisons test, (\* :  $p < 0.05$ ).

I screened the new KO cell lines sequentially for changes in mPTP following WT CypD transfection. If a cell line demonstrates a change in CRC following WT CypD transfection, it was retained for further experimental repeats. If no change is observed, the cell line was excluded as a candidate and another cell line was tested. I screened 5 cell lines which showed no change in CRC following WT CypD transfection (results in appendix) until cell line BE22 showed positive results. Fig 3.9.c shows the CRC result of one of these 5 cell lines, EX7, with quantification shown in Fig 3.9.e.



Following identification of BE22 as a possible working CypD KO cell line, I carried out experimental repeats to make sure WT CypD re-expression was indeed having an impact on mPT in BE22. From Figure 3.9.b, it was observed that in the BE22 line, transfection with WT CypD increased sensitivity of the mPTP to Ca<sup>2+</sup> induced opening. This decreased Ca<sup>2+</sup> retention capacity was statistically significant as shown in Figure 3.9.d. In theory, the addition of CsA should desensitise the mPTP and increase Ca<sup>2+</sup> retention capacity by interacting with the plasmid expressed CypD. However, from the same CRC assay results, it was observed that there was no significant difference with or without CsA treatment for BE22 cells transfected with WT CypD.

Given the lack of response to CsA, there were 2 possibilities, either CypD could no longer bind CsA for some reason or that CypD was not actually responsible for the increase in mPTP sensitivity to Ca<sup>2+</sup>. It was very difficult to attribute the increase in Ca<sup>2+</sup> retention capacity to something else other than CypD. The control groups were transfected with an empty vehicle plasmid pcDNA3.1+ which was also the same plasmid used as the vector for all the transgenes. As such, there should be no biological difference between the 2 groups other than the amount of CypD. The ability of this CypD plasmid to increase mPTP sensitivity to Ca<sup>2+</sup> was also statistically confirmed in both WT and KO cells, making the results reliable. This would suggest that the plasmid expressed WT CypD somehow lost its ability to interact with CsA. Although this was quite puzzling, the experimental result would suggest this to be the most likely scenario.

This was unexpected as transfection with the same plasmid in WT HEK293T cells lead to desensitisation of the mPTP and an increase in Ca<sup>2+</sup> retention capacity under the presence of CsA, as discussed earlier in Fig 3.8. The results in Fig 3.8 would thus suggest that the plasmid expressed WT CypD retained its ability to interact with CsA. Although the results in Fig 3.8 and Fig 3.9 seems to contradict each other, it was possible to reconcile them. What might be happening was that the CsA was binding the nuclear genome expressed CypD in WT cells in Fig 3.8 which led to desensitization of the mPTP to Ca<sup>2+</sup>. However, the plasmid expressed CypD was making up this difference by increasing the Ca<sup>2+</sup> sensitivity of the mPTP at the same time. As such, what I observed in Fig 3.8 was the reduced effect of CsA on mPTP Ca<sup>2+</sup> sensitivity not due to extra plasmid expressed CypD interacting with CsA but extra plasmid

expressed CypD making up for the nuclear expressed CypD that were interacting with CsA in mPTP regulatory functions.

If this was the case, it would suggest that the expression process of CypD itself might be crucial to some part of CypD function. A key difference between the CypD transgene and the genomic CypD is the lack of introns in the transgene, although it is not clear how this can affect function of CypD. A possible way of testing this is to express CypD transgene with introns present to observe if there are any differences. There might also be differences in post-translational modification between nuclear and plasmid expressed CypD and these modifications, for example acetylation, has been suggested to be important for CypD function (Hafner et al., 2010). However, all of this remains hypothetical, and it would take a full investigation to get to the root of the problem.

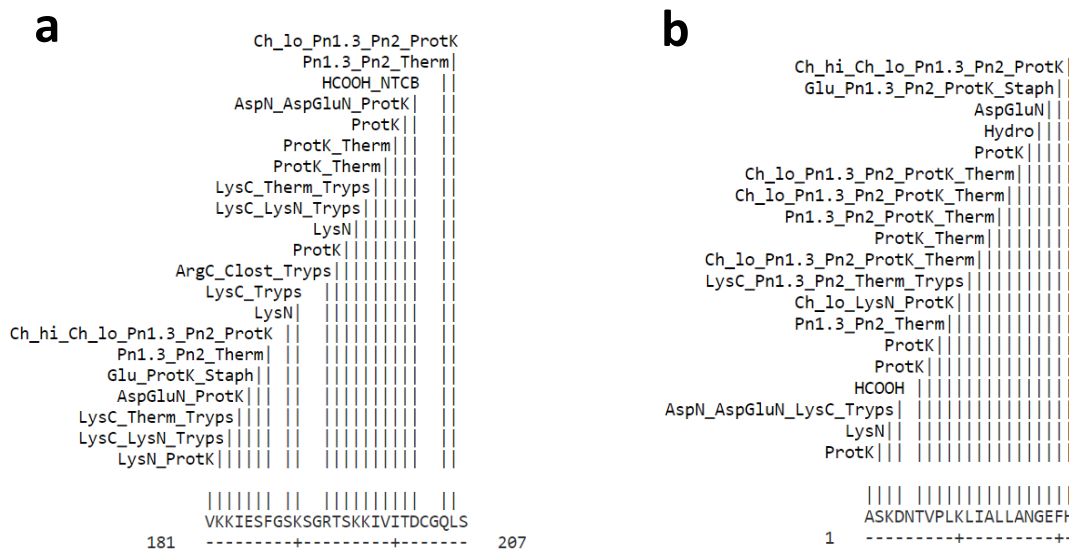
Additionally, the majority of the CypD KO cells cannot have their CypD sensitivity and mPTP regulation restored from re-expression of CypD. This was very puzzling because this was normally a very straightforward experiment in many studies. It was worth noting that restoration of CypD sensitivity via expression of exogenous CypD had been shown before. CypD KO MEF cells were re-exposed to CypD via lentiviruses and when their mPTP activity was measured using H<sub>2</sub>O<sub>2</sub> cell death assays, there was successful re-establishment of CypD regulation of mPTP in the experiment (Baines et al., 2005). However, this was somewhat different from my context since I used CRISPR and HEK293T cells. It would be very difficult to get to the root of the problem especially since changing the gRNA used did not appear to make any difference. Nonetheless, a possible starting point could be to conduct whole genome sequencing of the KO cells to see what other genetic changes there might be which could account for the observed phenomenon. Both of these are out of the scope of the project and were not investigated further here.

### **3.2.6 Fusion proteins breaking up in cells**

While troubleshooting the problem with the first CypD KO cell line, it was discovered that the fusion protein might be breaking into 2/multiple fragments. This was confirmed

with western blotting data in Figure 3.6. The first possibility that came to mind was that a protease cleavage site had been accidentally introduced when designing the CypD-TurboID fusion protein which uses a GS linker as a connector sequence between the 2 proteins. However, the GS linker sequence had been extensively used in the creation of fusion proteins and one would expect that it should not create such an obvious shortcoming. Nonetheless, the size of the observed unknown band which can be detected by the CypD antibody is very close in size to that of WT CypD so much so that the two bands were sometimes difficult to distinguish on a western blot, suggesting breakage around the linker. There was also no new band of any other size that can be detected by the CypD antibody, suggesting only one specific type of breakage was occurring. These would support the protease breakage hypothesis. On the other hand, there was still a large amount of the CypD-TurboID fusion protein intact, this flies against the possibility of protease cleavage as a cleavage site would likely result in consistent breakdown of the protein.

Nonetheless, the first thing to do would be to look further into the protease site hypothesis. I ran the CypD-TurboID fusion protein sequence as well as the CypD and TurboID sequence separately against databases containing potential protease cleavage sites. I could only find 2 such tool, the ExPASy PeptideCutter (Gasteiger et al., 2005) and Procleave (F. Li et al., 2020), the results obtained are shown below.



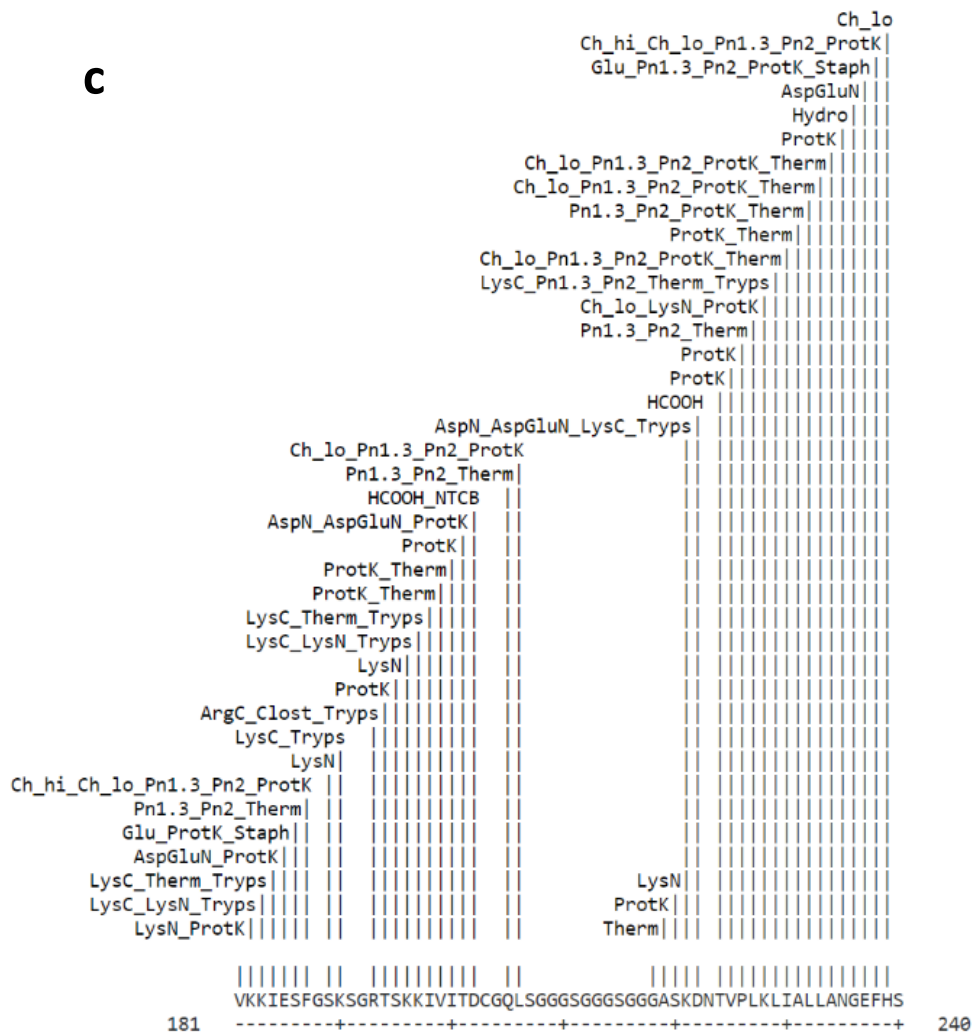


**Figure 3.10: Analysis of protein cleavage sites of CypD, TurboID and CypD-TurboID using the Expsy PeptideCutter tool**

- a) Protease cleavage site for the last 181-207 amino acids of CypD
- b) Protease cleavage site for the first 1-21 amino acids of TurboID
- c) Protease cleavage site for the last 181-230 amino acids of CypD-TurboID

Fig 3.10 shows the protease sites as analysed by the Expsy PeptideCutter. Only the relevant amino acid regions are shown as only adjacent amino acids contribute to cleavage site sequences. The GS linker was placed at the end of the CypD sequence

and before the start of the TurboID sequence, so only the adjacent sequences should matter. The last 181-207 amino acids of CypD shown in Fig 3.10.a and the 1-21 amino acids of TurboID shown in Fig 3.10.b were the amino acid sequences flanking the GS linker. By comparing the protease cleavage sites in these regions to the protease cleavage sites in the 181-230 amino acids region of CypD-TurboID in Fig 3.10.c, which contained the GS linker region flanked by the same sequences in Figure 3.10.a and 3.11.b, I would be able to tell if the addition of the GS linker introduced any new cleavage sites. As expected, there was no protease cleavage site in the GS linker itself. In the amino acid regions surrounding the GS linker, the addition of the linker did introduce 1 new 'Therm' cleavage site. However, this is irrelevant as the thermolysin enzyme is only found in the bacteria *Bacillus thermoproteolyticus*. The nature of these site prediction makes it easier to include all enzymes instead of manually selecting those of interest, hence the presence of non-human enzymes here.

Enzyme	Relevance
necepsin-1	None: C.elegans enzyme
Cathepsin family of proteases	Little: Found almost exclusively in lysosomes and only activated by low pH with the exception of cathepsin K, which works extracellularly
Falcipain-2, Falcipain-3	None: P. falciparum enzyme
matrix metalloproteinase-2 (MMP-2)	Little: Extracellular enzyme
Astacin	Little: Either extracellular or plasma membrane bound
Lactocepin I, Lactocepin-3	None: Lactococcus lactis enzyme

**Table 3.1: Analysis of protein cleavage sites of CypD-TurboID using the Procleave tool**

Another protein cleavage prediction tool, Procleave, was also consulted. Table 3.1 shows the result obtained from Procleave. The original data was difficult to display, and the result had been summarized in Table 3.1. Procleave assigns a probability score of 0-1 when predicting cleavage sites and every new protease site with p-score > 0.5 following introduction of the GS linker is included in this table. The relevance of each of these protease hits was also analysed. In summary, there was nothing that was likely to cause any issue in the CypD-TurboID fusion protein.

Although the bioinformatic tools can only function as a guide, the lack of any relevant protease site as predicted by the tools, coupled with the fact that GS linkers are widely used in fusion protein generation, implied that the accidental introduction of a new protease cleavage site was unlikely to be the cause of the problem here. An alternative hypothesis was that the linker length was too short or long, resulting in an unstable protein structure potentially due to steric hinderance. Although this length was determined following consultation with the literature where 9-22 (Chen et al., 2013) was found to be among the most commonly used linker length, it is possible that specific tweaks needed to be applied for each individual case. In order to further troubleshoot the problem, I decided to vary the GS linker length to see if that results in any improvement of the issue. Two CypD-TurboID fusion proteins, one with a 7 amino acid (GGGSGGG) linker and one with a 31 amino acid (GGGS- repeated till 31 amino acids) were created. They were then transfected into CypD KO HEK293T cells and western blots were carried out to examine the protein fragmentation.

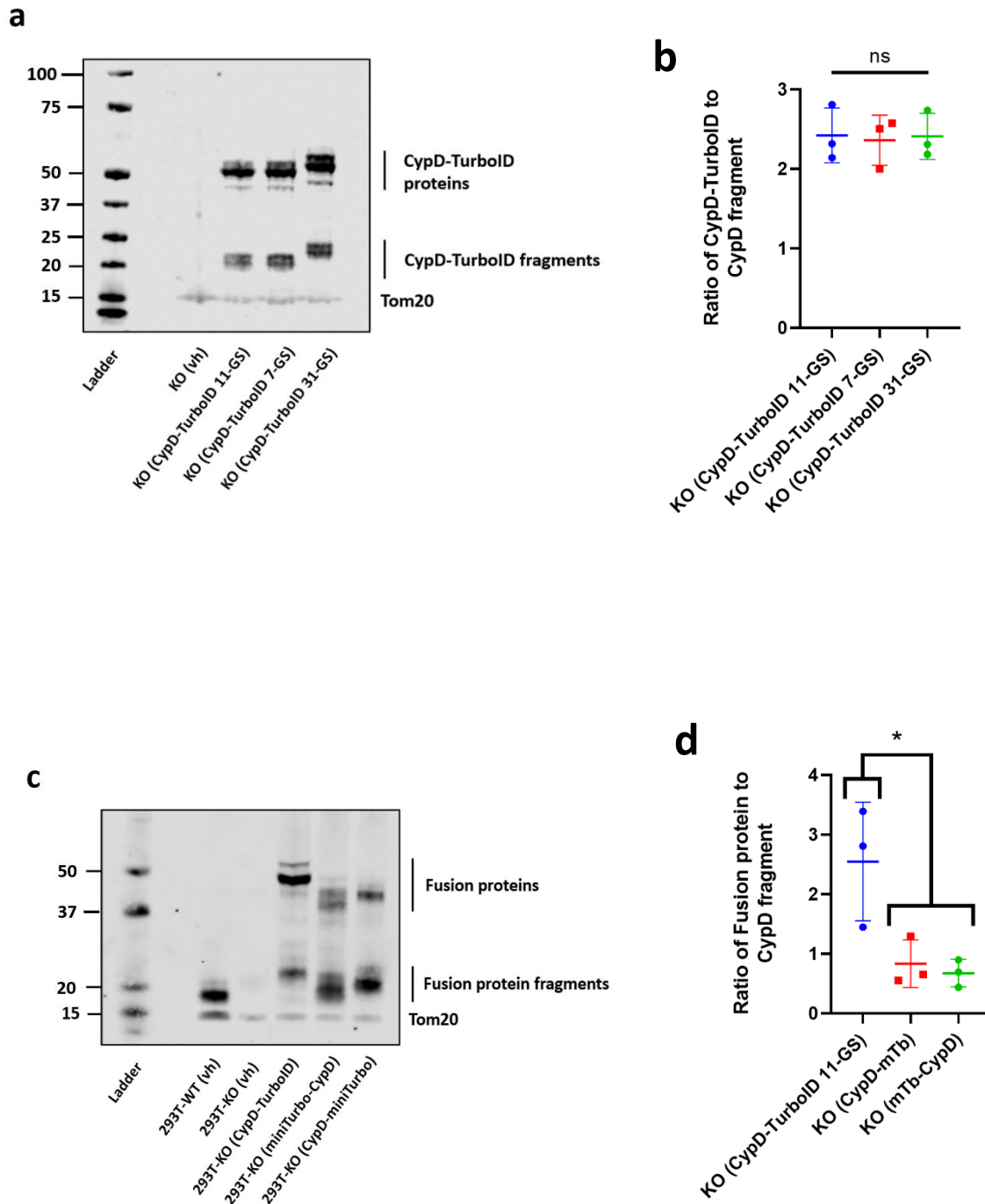


**Figure 3.11: Testing of fusion protein variant designs**

a) Representative western blot for CypD KO HEK293T cells transfected with CypD-TurboID GS linker length variants (in pcDNA3.1+) or vh (vehicle control: an empty plasmid backbone of pcDNA3.1+), n=3

b) Quantification of western blot for CypD KO HEK293T cells transfected with CypD-TurboID GS linker length variants (in pcDNA3.1+) or vh (vehicle control: an empty plasmid backbone of pcDNA3.1+), n=3

c) Representative western blot for CypD KO HEK293T cells transfected with fusion protein variants (in pcDNA3.1+) or vh (vehicle control: an empty plasmid backbone of pcDNA3.1+), n=3

d) Quantification of western blot for CypD KO HEK293T cells transfected with fusion protein variants (in pcDNA3.1+) or vh (vehicle control: an empty plasmid backbone of pcDNA3.1+), n=3

All quantification analysis are represented as mean  $\pm$  SD and were analysed using one-way ANOVA with Tukey's multiple comparisons test when analysing more than 2 conditions, (\* :  $p < 0.05$ ).

Fig 3.11.a shows the western blot data for CypD KO HEK293T cells transfected with CypD-TurboID with different GS linker length variants. For all 3 GS linker lengths, a CypD fragment protein could be detected. Additionally, Fig 3.11.b shows the ratio of the intact CypD-TurboID protein to the broken CypD fragment, this data gave a quantitative assessment of how much protein was breaking up. Fig 3.11.b shows that there was no significant difference between the CypD-TurboID: CypD fragment ratio between the 3 GS linker length variants. This suggested that neither increasing nor decreasing the linker length appeared to have any effect on the protein breakage problem.

This suggested that linker length had no effect on the stability of the fusion protein and bioinformatic analysis suggest the problem was unlikely to lie with the GS linker sequence. From here, I hypothesised that it might be worthwhile to investigate whether the sequences and arrangement of CypD and TurboID themselves were contributing to an unstable structure. In order to test this, I generated two additional fusion protein variants, CypD-mTb and mTb-CypD. The CypD-mTb fusion protein swapped the TurboID sequence for the miniTurbo sequences, miniTurbo was an alternative version of the TurboID biotin ligase developed by the same group (Branon et al., 2018). This switch aimed to test if there might be some incompatibility between the TurboID and CypD protein biochemistry. mTb-CypD consisted of the CypD (MTS region only) followed by miniTurbo followed by GS linker followed by CypD (minus the MTS region). mTb-CypD inverts the order of the fusion proteins, it aimed to test if switching the proteins around might lead to more stability and better folding. Fig 3.11.c shows the



western blot result for the original CypD-TurboID and the 2 new fusion protein variants. The western blot data appeared to show that the 2 new variants had a much worse protein breakage problem compared to CypD-TurboID. This was confirmed in Fig 3.11.d where the ratio of intact fusion protein to CypD fragment was quantified, CypD-mTb and mTb-CypD both had a significantly lower ratio of intact protein to CypD fragment as compared to CypD-TurboID. While the result here confirmed the hypothesis that the specific protein combination and arrangement of CypD and the biotin ligase matters for fusion protein stability, CypD-TurboID was already the best option available.

In the end, despite creating multiple fusion protein and linker length variants, I was not able to eliminate the protein breakage problem. Furthermore, none of the modifications offered any improvement in the breakage problem in anyway and some made thing worse. This was not promising as it even deprives me of any direction where I can try to work on to solve the issue. However, CypD-TurboID did allow for most (> 66%) of the fusion protein to stay intact. This was encouraging as it means my original rational design resulted in the best available fusion protein design. Given a lack of time for further troubleshooting, I decided to proceed with the project with the CypD-TurboID 11-GS which appears to be the most stable among the different fusion protein variants tested.

### **3.2.7 Testing of the fusion protein in BE22 CypD KO cells**

Having decided on a cell line and on the fusion protein to be used, I needed to ensure that they were compatible before the final screen as CypD-TurboID had not been tested in the new BE22 CypD KO cell line. I needed to verify 2 things, that the CypD-TurboID fusion protein was properly replicating the function of CypD in BE22 and regulating the mPTP, and that CypD-TurboID was properly labeling proximal proteins with biotin.

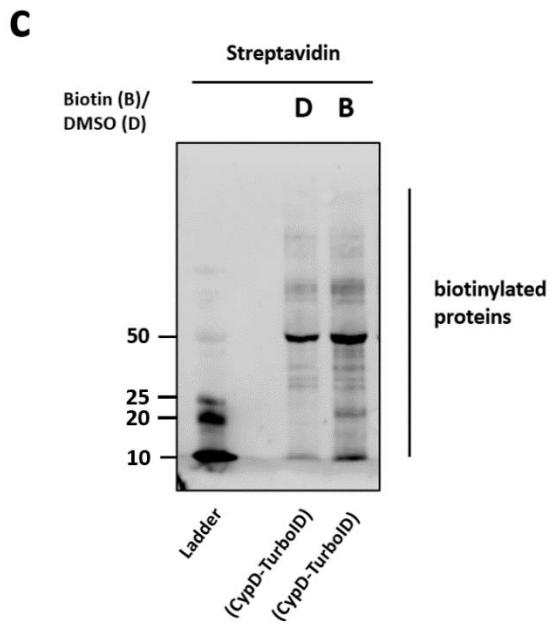
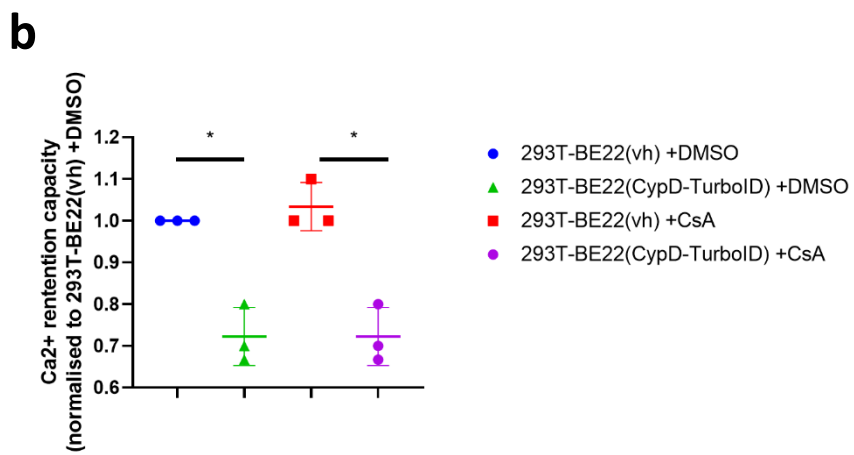
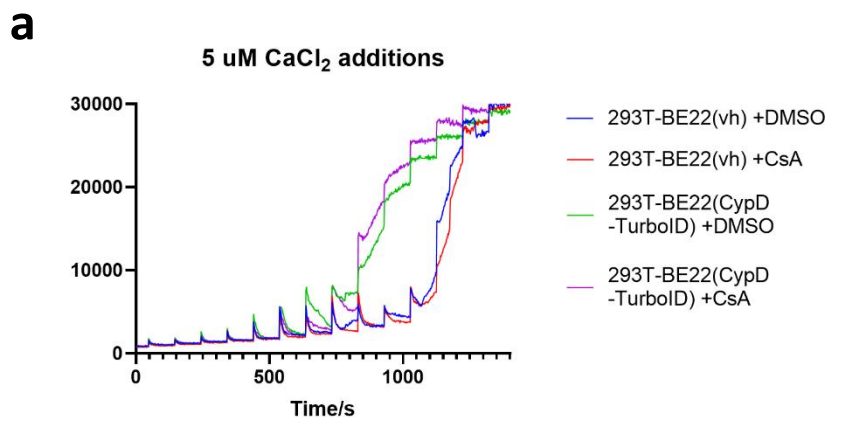


**Figure 3.12: Testing of new CRISPR cell lines**

a) Representative CRC assay data for BE22 cells transfected with CypD-TurboID (in pcDNA3.1+) or vh (vehicle control: an empty plasmid backbone of pcDNA3.1+) with 1 $\mu$ M CsA or an equivalent volume of DMSO added prior to measurement, n=3

b) Quantification of CRC assay data for BE22 cells transfected with CypD-TurboID (in pcDNA3.1+) or vh (vehicle control: an empty plasmid backbone of pcDNA3.1+) with 1 $\mu$ M CsA or an equivalent volume of DMSO added prior to measurement, one-way ANOVA followed by Tukey's multiple comparisons test was carried out

c) Representative streptavidin-IR680 western blot for HEK293T cells transfected with CypD-TurboID (in pcDNA3.1+) or vh (vehicle control: an empty plasmid backbone of pcDNA3.1+), with B (50 $\mu$ M biotin) and D (volume of DMSO equal to amount of biotin added) addition 5 mins prior to protein extraction

All quantification analysis are represented as mean  $\pm$  SD, (\*:  $p < 0.05$ ).

Fig 3.12 shows the CRC assay results of transfecting BE22 CypD KO cells with CypD-TurboID. As can be seen from 3.13.a, introduction of CypD-TurboID decreased CRC in BE22 cells, this was consistent with the expectation that CypD would sensitise mPTP to Ca<sup>2+</sup> induced opening and was supportive of CypD-TurboID replicating the effect of CypD in BE22 cells. This decrease in CRC and hence increase in mPTP Ca<sup>2+</sup> sensitivity is statistically verified in Fig 3.12.b. On the other hand, the addition of CsA failed to result in any changes in CRC for BE22 cells transfected with CypD-TurboID which cast doubts on the ability of CypD-TurboID to replicate the effect of CypD. However, looking back at the effect of expressing WT CypD in the BE22 line in Fig 3.10, there was also no restoration of the effect of CsA on CRC following re-introduction of WT CypD. This would mean that the CypD-TurboID was replicating the effect of WT CypD in BE22 perfectly well here. The lack of effect of CsA, as we have discussed earlier, was likely due to some other unknown problem with the BE22 KO cell line itself and should not interfere with WT CypD and hence CypD-TurboID's regulation of the mPTP.

Fig 3.13.c shows that CypD-TurboID was properly labelling with biotin. Addition of biotin leads to a large increase in biotinylated proteins as detected by streptavidin. Hence the combination of CypD-TurboID and BE22 CypD KO cell line should serve as a good model for the screen.

## 3.3 Conclusion

### 3.3.1 Review of CypD KO cell line generation

The experiments with the CRISPR cell lines led to puzzling results. The CypD KO cells all appeared to be successful CypD KOs verified with western blots and CRC assays. However, I ran into problems when re-expressing CypD in these cells. When CypD-TurboID and WT CypD were re-expressed, the KO cell line generated in the first round of CRISPR failed to display any change in CRC assays. However, the same plasmids resulted in an increase in mPTP sensitivity in WT cells, indicating that the problem lied with the KO cell line. In order to tackle this problem, I carried out a second round of CRISPR and generated a large number of CypD KO cell lines using different gRNAs and cutting strategies. In the second round, I was able to identify a KO cell line (BE22) that responded to CypD re-expression. However, most of the cell lines tested in the second round also did not respond to CypD re-expression, making the only one that responded a rare case. Additionally, even when the CypD KO cell line responded to CypD re-expression by showing increased CRC assay sensitivity, it did not respond to CsA treatment.

It is not yet clear what had caused the unexpected results in the KO cell lines. Initially, when CRC assays of the KO cell line failed to respond to CypD re-expression, the first thing that came to mind was that a CRISPR off target effect had occurred. This was because CRISPR off target effects are a well-known process that is unavoidable in CRISPR experiments. As such, I re-designed a new set of gRNAs and carried out another round of CRISPR KO. However, the same problem where CypD KO cell lines failed to respond to CypD re-expression occurred even with new gRNAs. This suggested that the issue was unlikely to do with CRISPR off target effects as off target effects are gRNA specific and the lack of CypD rescue displayed here was gRNA independent.

Another possible explanation was that the CRISPR cell line generation process itself created permanent changes in the cell lines which changed the relationship between CypD and mPTP regulation. How this change occurred cannot be identified at this point and out of the scope of my project. It is possible that long term absence of CypD has forced the cell line to adapt in an unknown manner where CypD was no longer

needed or was no longer properly processed by the mitochondrial transport and processing machinery, leading to no observable effect of CypD even if it was properly expressed. A possible avenue which could lead to this adaptation was via metabolic regulation changes. It has been found that the absence of CypD causes profound metabolic changes in cells. This includes upregulation of pyruvate dehydrogenase and  $\alpha$ -ketoglutarate dehydrogenase (Elrod et al., 2010), as well as changes in TCA cycle enzyme activity and levels of pyruvate and branched-chain amino acid (Menazza et al., 2013). Additionally, key metabolic products and substrates including ADP/ATP and Pi are known mPTP regulators (Bernardi, 1999). As such, it might make sense for CypD KO to have a feedback effect on CypD and mPTP regulation via metabolic changes.

A further possibility was that permanent changes occurred in mitochondria during monoclonal cell line selection and expansion, this process is highly energy intensive and growth promoting so it is possible mitochondria underwent certain changes which might influence the redox state and ADP/ATP ratios which are all factors that affect the mPTP.

In the end I was able to find a cell line that responded to CypD re-expression which means that the loss of possible CypD rescue effect in CypD KO cells is not completely unavoidable but does occur with very high frequency. I screened 8 cell lines before finding a KO cell line that responded to CypD re-expression. However, the only cell line that responded to CypD re-expression failed to respond to CsA following re-expression of CypD. This cast doubt on the validity of the cell line as a screening model especially since expressing the same CypD plasmid in WT CypD has an effect on CsA mediated mPTP inhibition. In the end, given the lack of time for further troubleshooting and the fact that the main effect of CypD re-expression (increasing mPTP sensitivity) was fulfilled in the BE22 cell line, I decided to continue the project using this cell line.

In addition to the problem encountered with the KO cell lines, I also encountered problems with the CypD-TurboID fusion protein breaking up in cells. In order to troubleshoot this, I tried changing up the linker length as well as using alternate versions of TurboID and mixing the order of protein fusion. None of these changes led to any improvement in the breakage situation. Given a lack of time and troubleshooting

direction, as well as the fact that most of the protein remains intact, I decided to continue with the project.

In the end, the CypD KO cell line screening model consisted of a CypD-TurboID fusion protein with some levels of protein breakage that was expressed in a CypD KO cell line where CypD re-expression does not restore CsA sensitivity. This means that I have to keep in mind the screen result would need to be interpreted considering these limitations. However, as mentioned before, most of the fusion proteins remained intact and that the CypD-TurboID expression in the BE22 KO cell line did increase mPTP sensitivity. As such, it was likely that I could carry out a good screen where mPTP related CypD interactors could be identified.

### **3.3.2 Using WT HEK293T cells in an additional proteomics screen**

In my original research plan, the purpose of using a CypD KO HEK293T cell line was to remove potential competition from endogenous CypD for protein interactors with the CypD-TurboID. However, this does not mean that using the WT HEK293T cell line was not a valid approach. The current CypD KO HEK293T cell line I will be using have a non-standard response to CsA addition, hence it would be wise to include a full set of proteomics experiments on WT HEK293T cells as a control.

The WT HEK293T cells displayed very good responses to CypD-TurboID transfection when it comes to expected CRC response and biotinylation, hence it was very likely to make a good model. Additionally, it displayed the expected response when CsA is added (increased CRC). This means that it might be possible for me to gain insight into why there was a loss of CsA response in the CypD KO cells.

Referring back to the secondary hypothesis that the TurboID method can be applied to HEK293T cells, the experiments here show that it should be applicable in both HEK293 WT and CypD KO models with the two complimenting each other in output results.

## **4. Proteomics screen**

### **4.1 Background**

The ultimate aim of the project was to carry out a CypD protein interactor screen. All the preparation and troubleshooting done previously was to better prepare for the screen and ensure its accuracy. Since I had sorted out the fusion protein and the cell line, I could proceed with the screen.

As discussed earlier, I would be carrying out the experiment on HEK293T CypD KO cells to minimize competition from WT CypD. However, the CypD KO cell line I ended up with was not an ideal model. There remains the issue of a lack of CsA response in the CypD KO line following CypD rescue. I cannot be certain on the cause for this issue. Keeping this shortcoming in mind, I decided to also carry out the screen on the WT HEK293T line and attribute a greater level of importance to the screen using WT HEK293T cells. Additionally, I argued that the result potentially could also help provide more clarity on the state of the mPTP leading to CsA insensitivity in the CypD KO line.

### **4.2 Results and discussions**

#### **4.2.1 Obtaining proteomic samples**

Obtaining the samples was a very important step before the mass spectrometry can occur. For my case, this was even more crucial as I needed to introduce biotin as well as specifically induce mPT in some of the samples right before extracting the samples. This involved a series of troubleshooting step leading to an optimised protocol based on (Cho et al., 2020). The entire process is outlined below.



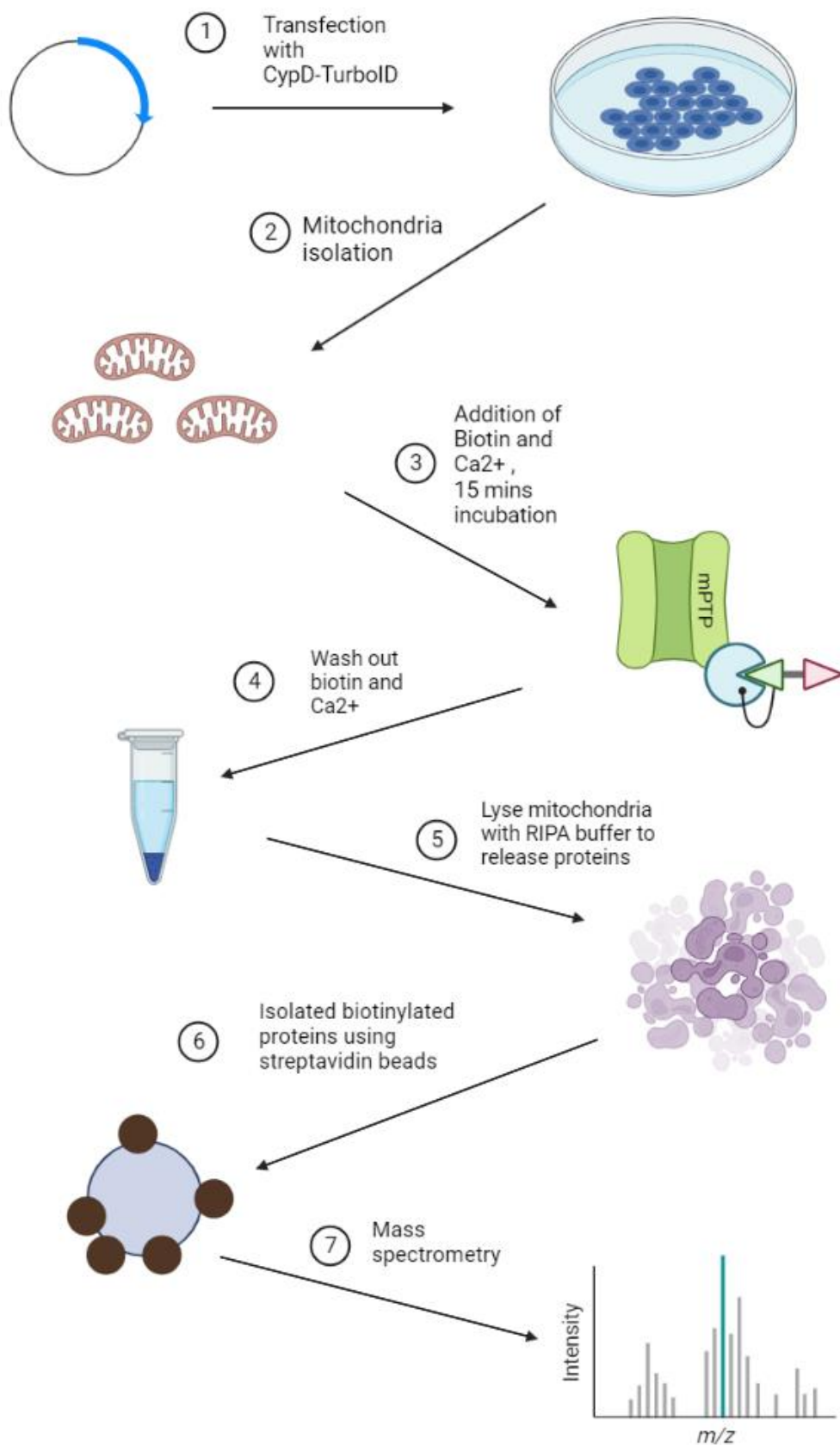


**Figure 4.1: Experimental outline for proteomics screen**

Fig 4.1 shows the 7 steps of the proteomics screen. The exact procedure is detailed in the methods section. There are 2 key steps to take note here for discussion of results and ensuring accurate experimentation. The first is step 3 as this was the step where different mPT conditions were created via additions of DMSO/CsA and DMSO/Ca<sup>2+</sup>. The second was step 6 which ensure only biotinylated proteins (thus ensuring that the CypD-TurboID protein has labelled enough proteins with biotin) were captured and was a key quality control step in the experiment.

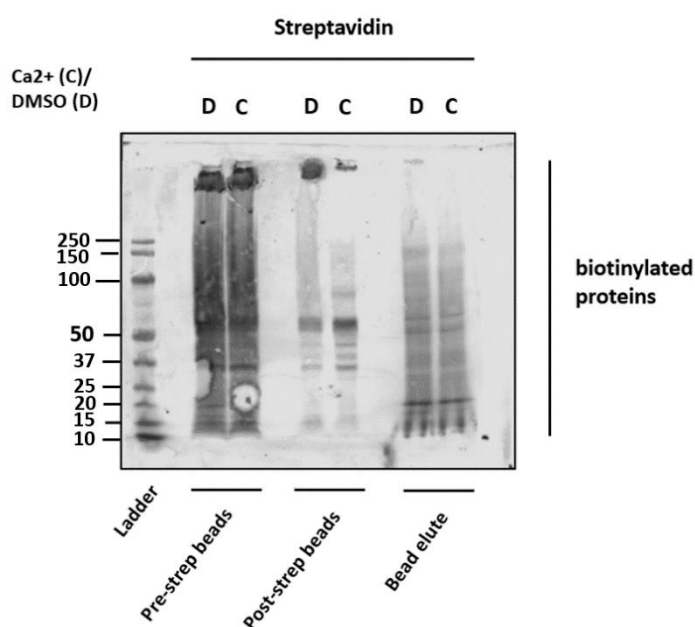


**Figure 4.2: Generation of proteomics samples**

Representative streptavidin-IR680 western blot for HEK293T cells transfected with CypD-TurboID with 50uM biotin added. D (DMSO) and C (Ca<sup>2+</sup>) represents the experimental groups. Pre-strep: sample before streptavidin bead pull down. Post-strep: sample after streptavidin bead pull down. Bead-elute: protein sample extracted from streptavidin beads after pull down. The same volume (15ul) is used for all samples.

The final sample to be processed would be in the form of biotinylated proteins attached to streptavidin beads. As such, I would need to ensure that the proteins were properly

attached to the streptavidin beads in an efficient manner before mass spectrometry can proceed. Fig 4.2 shows a streptavidin-stained western blot for this purpose. As can be seen from the blot, there was a large amount of biotinylated proteins in the Pre-strep beads samples (protein sample before incubation with streptavidin beads). In the Post-strep beads samples (protein sample after incubation with streptavidin beads) there was a large decrease in the amount of biotinylated proteins as the biotinylated proteins have now been pulled to the beads. Finally, if I elute the proteins from the beads, as can be seen in the Bead elute samples, there was a large amount of biotinylated proteins present. From here, I passed the beads with proteins attached to my collaborators in the Thalassinos lab, who carried out the mass spectrometry and returned the results to me in the form of Label Free Quantification (LFQ) of protein enrichment.

#### **4.2.2 Overview of proteomics results and analysis**

The CypD interaction screen was carried out as described earlier. Biotin was added to isolated mitochondria that had been pre-treated with either DMSO or 2uM CsA followed by 250uM Ca<sup>2+</sup> or vehicle treatment. The biotin labelling and Ca<sup>2+</sup> treatment happens simultaneously and was a 15 min incubation before both biotin and Ca<sup>2+</sup> were removed and the mitochondria were further processed for protein extraction. This resulted in 4 conditions for each experiment which I had named as follows, DMSO C- /DMSO C+/CsA C-/CsA C+ and would be referenced in subsequent results. The naming is self-explanatory with DMSO/CsA measuring the effect of CsA and C-/C+ measuring mPTP induction via Ca<sup>2+</sup> addition.

Before analysis of the specific proteins, the data was processed and cleaned. I decided to use the LFQ (Label free quantification) normalised to iBAQ peptides (which is the number of possible peptides for each protein) as the readout for relative abundance of each protein in the samples.

There were many ways to approach such a large dataset statistically and to draw conclusions from it. I analysed the data using a few different approaches that are all statistically valid. They complement each other to give a more complete picture of the results.

Two approaches of summarising the data were used at the data processing level.

The first approach was to combine the signals of protein complexes and protein isoforms with the aim to give a more complete picture of the spectrum of interactions. Summing of signals was in part due to existing knowledge about the mPTP in the literature. It had been shown that the whole ATP Synthase complex was involved in mPTP, so analysing the subunits separately might lead to inaccuracies. Additionally, when interacting with a protein complex, catalytic activity of a biotin ligase would be distributed among all accessible subunits of the complex, hence resulting in lower biotinylation levels for individual subunits as compared to the whole complex. This might lead to a dilution of signal and hence inaccurate results. Combining the signals of different isoforms of a protein was also rooted in the literature. The literature suggests all isoforms of ANT and VDAC might be involved in mPTP. Assuming CypD interacts with them in a similar manner, by analysing them separately I would be distorting the real interaction that was happening. Having explained the reasoning behind the method of data processing, the method also has its downsides. If CypD interacts with the isoforms in different ways or if it interacts with the subunits of complexes independently, the data would again be distorted. However, upon preliminary exploratory analysis my data, most of the hits (regardless of analysis method) were proteins that have already been heavily investigated as part of the mPTP, for example ANT and the ATP Synthase. Past works suggest that their interaction with CypD falls more in line with whole complex (ATP Synthase) and all isoform involvement. Hence this method of data processing should be the primary approach to understand the overall interaction spectrum of CypD.

In the second approach, protein complex subunits and different protein isoforms were treated as separate entities for further analysis. This was also the default way the data is generated and does not require the above-described further processing of the signals.

Apart from the two approaches at the data processing level, I applied also different approaches to the final statistical analysis of the data. The following two approaches were used.

In the first analysis method, I would identify the interactor hits of CypD by applying ANOVA followed by Tukey's HSD with a  $p=0.05$  cut off on the normalised LFQ value.

One-way ANOVA followed by Tukey's multiple comparisons test was then applied across all 4 conditions. A rationale for determining interactor hits of CypD before any comparison was done lied with the proximity dependent biotinylation method that I was using. Using a biotin ligase labelling approach means that a large number of biotinylated proteins would be detected. This was because the biotin ligase would label any protein that comes near CypD and the underlying hypothesis was that interactors would be labelled far more often than non-interactors. Hence there would be a background level of biotinylated proteins due to the experimental process and the presence of naturally biotinylated proteins. Normally when large datasets were analysed a multiple t-test with correction (e.g Bonferroni) to correct for the large number of tests giving rise to false positives is frequently used. However, if I use that here I might be subjecting the interactors to needless statistical correction because most of the proteins here were background noise labels as mentioned earlier and thus might distort the actual statistics.

Using an ANOVA test here would let me know which proteins have significantly higher abundance compared to the rest of the proteins. This would let me determine the interactors of CypD and differentiate them from background labelled proteins. Knowing the interactors themselves is interesting information regardless of mPT related interaction changes. Following the interactor determination, I could apply ANOVA with a multiple comparison test with no need for multiple testing correction since the number of interactors was very small and the large dataset pitfall no longer exists.

As with every method, the approach where the interactors were first determined using ANOVA followed by ANOVA with a multiple comparison test to measure mPTP related changes has its limitations. One clear assumption was that any mPTP relevant CypD interactor would first have a high level of CypD interaction to begin with, by considering only the interactors first, I am likely to eliminate the possibility of detecting a protein where there was a huge jump in CypD interaction following mPTP induction from very low to very high levels. To avoid this bias, I introduced the second statistical approach.

In the second analysis method, I created volcano plots comparing the different conditions, using multiple t-test with Bonferroni correction. This is a common approach to large datasets involving multiple conditions. As mentioned earlier, this would complement a limitation of the first analysis method and allow me to detect cases

where a protein with little basal CypD interaction had a huge increase in interaction following mPT.

Finally, I needed to carry out both analysis methods for each of the 2 types of data processing approach. This will generate 4 sets of analysis results. This sounds like quite a complicated approach, especially since I needed to do 4 sets for both the WT HEK293T cells and CypD KO HEK293T cells, leading to 8 total sets of analysis. However, I have carefully explained the justification of each of these analyses here and I believe that they were all necessary to get a complete and unbiased picture of the study. As I would show later in the results section, many of the analysis compliments each other and, in the end, I was able to get a rather clear view what was happening to CypD interactions following mPTP induction with CsA intertwined in between.

Table 4.1 shows an overview of the analysis results that have been obtained. They will be discussed in detail in the subsequent sections.

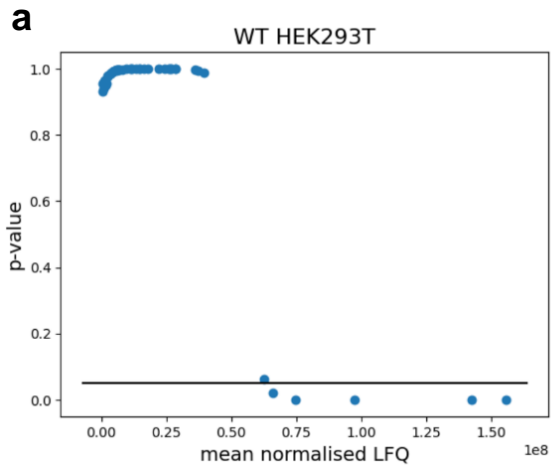
<b>Section</b>	<b>Cell line</b>	<b>Data processing</b>	<b>Statistical approach</b>	<b>Figure</b>
<b>4.2.3.1</b>	<b>WT</b>	<b>Aggregated</b>	<b>ANOVA +</b>	<b>4.3</b>
<b>4.2.3.2</b>	<b>WT</b>	<b>Aggregated</b>	<b>Multiple t-test</b>	<b>4.4</b>
<b>4.2.3.3</b>	<b>WT</b>	<b>Individual</b>	<b>ANOVA+</b>	<b>4.5</b>
<b>4.2.3.3</b>	<b>WT</b>	<b>Individual</b>	<b>Multiple t-test</b>	<b>4.6</b>
<b>4.2.4.1</b>	<b>KO</b>	<b>Aggregated</b>	<b>ANOVA+</b>	<b>4.7</b>
<b>4.2.4.2</b>	<b>KO</b>	<b>Aggregated</b>	<b>Multiple t-test</b>	<b>4.8</b>
<b>4.2.4.3</b>	<b>KO</b>	<b>Individual</b>	<b>ANOVA+</b>	<b>4.9</b>
<b>4.2.4.3</b>	<b>KO</b>	<b>Individual</b>	<b>Multiple t-test</b>	<b>4.10</b>

**Table 4.1: Summary of proteomics experiment and analysis results**

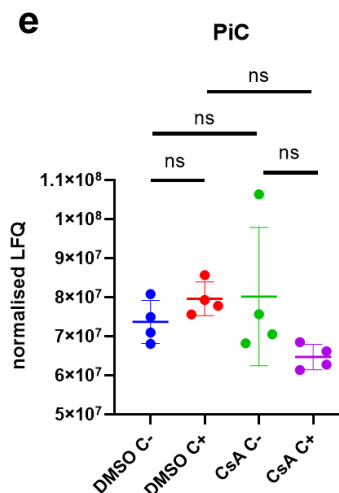
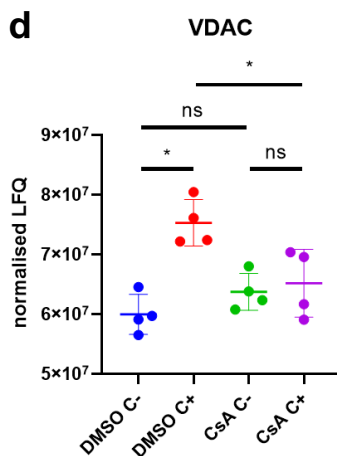
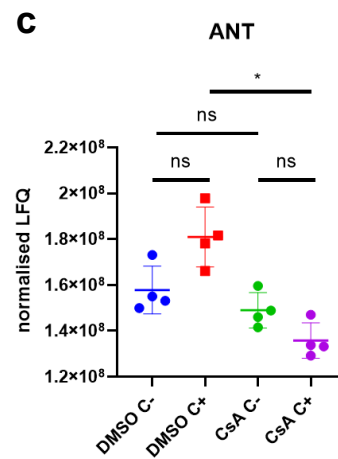
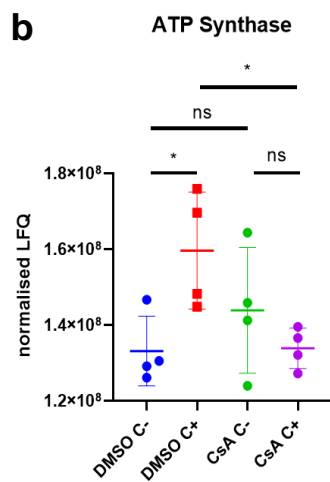
*This table listed the specific analyses of the proteomics data to aid understanding of the proteomics dataset. The section and Figure number of each specific analysis result is listed with the corresponding cell line (WT vs CypD KO), data processing method (Aggregated complex and isoforms vs Individual proteins) and statistical approach (ANOVA followed by paired t-test vs Multiple t-test with Bonferroni's correction)*

## 4.2.3 Proteomics results for WT cells

### 4.2.3.1 WT cells – aggregated complexes and isoforms – interactor determination using ANOVA followed by one-way ANOVA with multiple comparisons



Significant hits at p=0.05	LFQ (1e8)
Peptide synthesis complex -Borderline p-value slightly above 0.05 but in same cluster	0.63
VDAC Isoforms	0.66
PiC	0.75
HSPE1	0.98
ATP Synthase Complex	1.43
ANT Isoforms	1.56





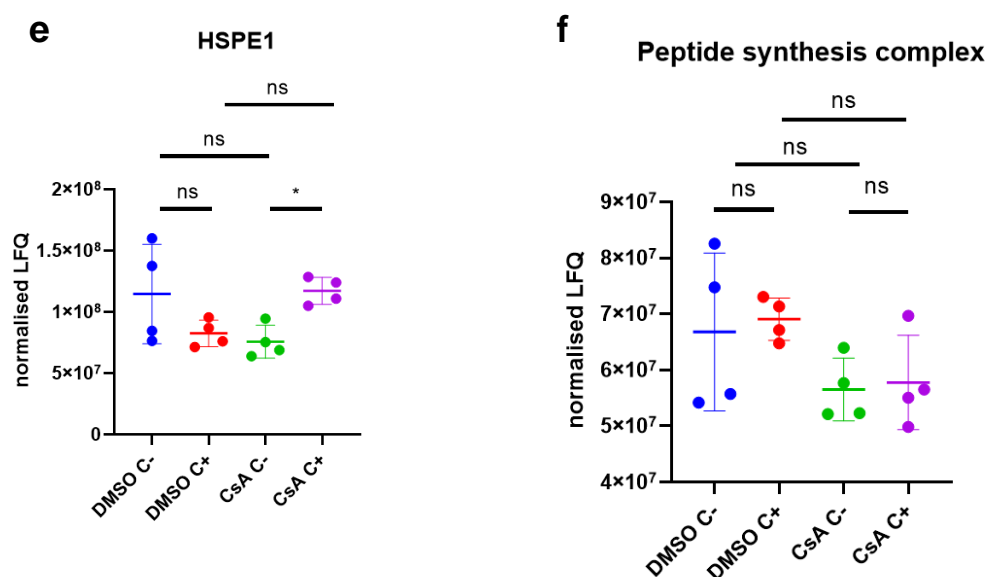


**Figure 4.3: WT cells – aggregated complexes and isoforms – interactor determination using ANOVA followed by one-way ANOVA with multiple comparisons**

a) Determination of CypD interactors using ANOVA followed by Tukey's HSD with  $p=0.05$  as cut off. ANOVA ( $F$  statistic: 350,  $p$ -value: 0.0). Table summarizes the significant hits along with respective interaction level

b) Normalised LFQ data of ATP Synthase complex for DMSO C<sup>-</sup>, DMSO C<sup>+</sup>, CsA C<sup>-</sup>, and CsA C<sup>+</sup> conditions, a one-way ANOVA followed by Tukey's multiple comparisons test was carried out

c) Normalised LFQ data of ANT Isoforms for DMSO C<sup>-</sup>, DMSO C<sup>+</sup>, CsA C<sup>-</sup>, and CsA C<sup>+</sup> conditions, a one-way ANOVA followed by Tukey's multiple comparisons test was carried out

d) Normalised LFQ data of VDAC Isoforms for DMSO C<sup>-</sup>, DMSO C<sup>+</sup>, CsA C<sup>-</sup>, and CsA C<sup>+</sup> conditions, a one-way ANOVA followed by Tukey's multiple comparisons test was carried out

e) Normalised LFQ data of PiC protein for DMSO C<sup>-</sup>, DMSO C<sup>+</sup>, CsA C<sup>-</sup>, and CsA C<sup>+</sup> conditions, a one-way ANOVA followed by Tukey's multiple comparisons test was carried out

f) Normalised LFQ data of HSPE1 protein for DMSO C<sup>-</sup>, DMSO C<sup>+</sup>, CsA C<sup>-</sup>, and CsA C<sup>+</sup> conditions, a one-way ANOVA followed by Tukey's multiple comparisons test was carried out

g) Normalised LFQ data of the peptide synthesis complex for DMSO C<sup>-</sup>, DMSO C<sup>+</sup>, CsA C<sup>-</sup>, and CsA C<sup>+</sup> conditions, a one-way ANOVA followed by Tukey's multiple comparisons test was carried out

Fig 4.3 shows the analysis result obtained when the CypD interactors were first identified before following up with t-test statistics on each interactor hit for the summed protein complex and isoforms dataset.

The first result that could be examined here is that of the CypD interactors. From Fig 4.3.a, it can be observed that the background proteins and the actual interactors were extremely well separated into two clusters based on p-value following ANOVA statistics. All background proteins have p-values above 0.9 and interactors having p-values below 0.05 except for one hit. The peptide synthesis complex, which is made up of mitochondria ribosomal subunits, had a p-value that is marginally above 0.05. However, since this complex clearly aligns with the interactor group in terms of clustering, I have included it here for consideration despite not strictly meeting the p-value cut off.

Surprisingly, almost all detected interactors have been previously shown to interact with CypD, strongly supporting the reliability of the data. Most of the interactors are also implicated in mPTP and comprises many of the strongest candidates for the mPTP, including the ATP Synthase, ANT, VDAC and PiC. HSPE1 and the peptide synthesis complex have not been implicated in mPTP but have also shown up in previous screens for CypD interactors (Refer to appendix for my summary of previous screens).

Following the identification of the interactors, I next analysed the dynamic changes in CypD interactions following mPTP induction with and without CsA blockade.

Given the presence of mPTP candidate proteins here, I first examined their statistical changes. In Fig 4.3.b, I observed that the ATP Synthase complex had a statistically significant increase in CypD interaction following Ca<sup>2+</sup> treatment under DMSO conditions. Importantly, the effect was entirely CsA sensitive, since Ca<sup>2+</sup> addition under CsA conditions resulted in no significant change in ATP Synthase abundance. The same statistical conclusion was obtained for VDAC (Fig 4.3.d). These results are strong evidence supporting VDAC and the ATP Synthase as mPTP components, in concert with previous work showing their role in mPTP.

Based on the statistical analysis, a possible interpretation of these results is that the ATP Synthase complex makes up the IMM component and VDAC makes up the OMM component of the mPTP, since no other protein showed a statistically significant increase in CypD interaction following Ca<sup>2+</sup> under DMSO conditions. However, the ANT and PiC data here could not be discounted purely on the lack of statistical significance on one dataset comparison. The result of numerous previous works in support of ANT and PiC playing a role in mPTP means that I must closely examine their interaction pattern even if they did not meet the standard  $p=0.05$  cutoff for statistically significant change.

Looking closely at Fig 4.3.c and Fig 4.3.e, it can be observed that the interaction of ANT and PiC with CypD follows a similar trend as that of the ATP Synthase complex and VDAC. The interaction of ANT and PiC with CypD showed a clear increase following mPT induction, this increase subsequently disappeared when CsA treatment was added. However, unlike the increases in ATP Synthase and VDAC, the increased interaction levels in ANT and PiC with CypD during mPT was not statistically significant. Hence interaction changes following mPT under DMSO conditions was not strong enough to provide support for the involvement of ANT and PiC in mPTP. On the other hand, for ANT, CsA addition significantly decreased the level of CypD interaction after Ca<sup>2+</sup> addition. This decrease was not present when Ca<sup>2+</sup> was absent, i.e when mPT is not occurring. What this implied was that CsA was only inhibiting the interactions between CypD and ANT during mPT. Given that CsA is a CypD targeting mPT inhibitor, this decreased interaction between ANT and CypD during mPT when CsA was added was strong evidence supporting ANT and PiC as components of the mPTP. Regarding why the increased CypD interaction with ANT and PiC following mPT under DMSO conditions was not significant even though the trend is clearly in the right direction, I would like to refer to the original research plan I had. I hypothesised that the presence of endogenous CypD might interfere with CypD-TurboID hence disrupting the screen results, which might be what was happening here. The CypD KO cell line was created to overcome this limitation, but I had to use the WT HEK293T cell line in the end due to reasons discussed earlier.

The interpretation of the proteomics data here also makes sense on an overarching scale in terms of resolving the contradictory identity of the mPTP. The data here

suggest that the ATP Synthase, ANT, PiC and VDAC are all involved in mPTP formation. This is actually a very noteworthy result. As I have discussed earlier, the ATP Synthase, PiC and ANT have all been shown to modulate mPTP activity and there is a debate on whether any one of them might be the channel forming subunit of the mPTP. However, studies have shown that KO of any of them does not eliminate mPTP activity and does not take away the effect of CsA. Given this, many in the field is suspecting that multiple proteins might be able to form the channel subunit of the mPTP. It was recently shown that ANT can form the mPTP in the absence of ATP Synthase (Carrer et al., 2021), strengthening this school of thought.

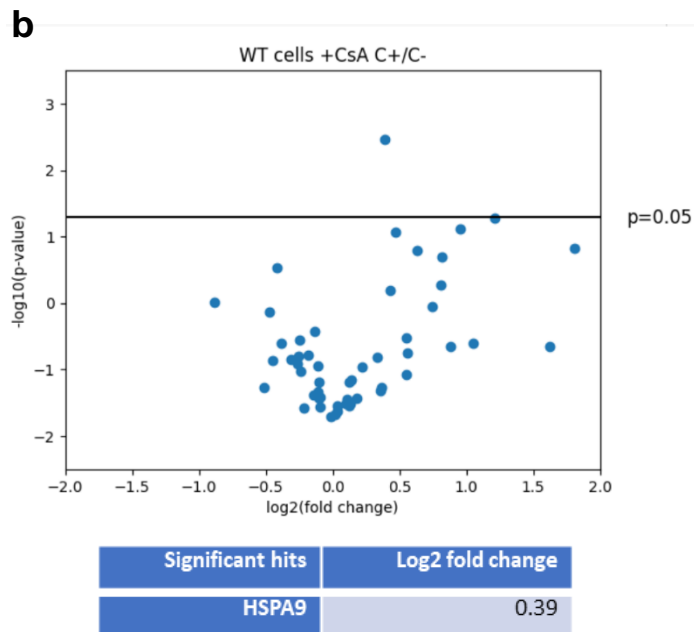
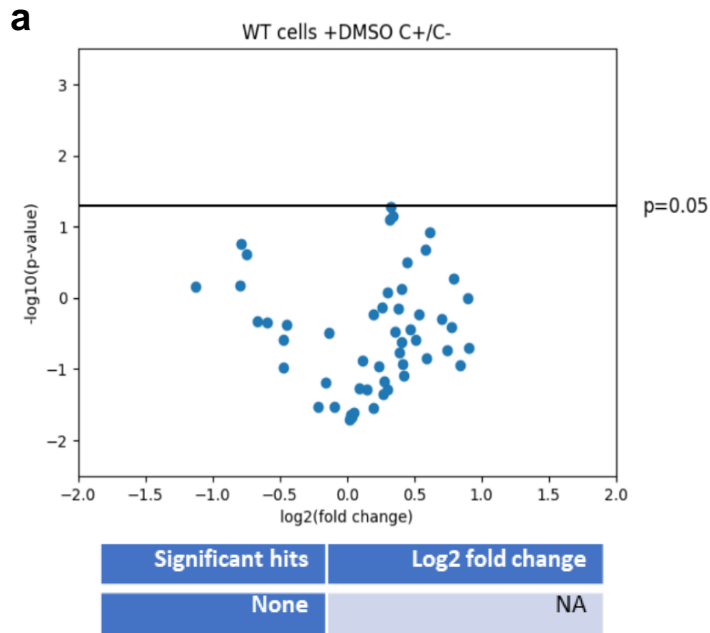
Keeping all of this in mind, the data here very much supports the multiple protein hypothesis of the mPTP. It fits right into the narrative and would help to explain why KO of any of the proteins individually does not abolish mPT.

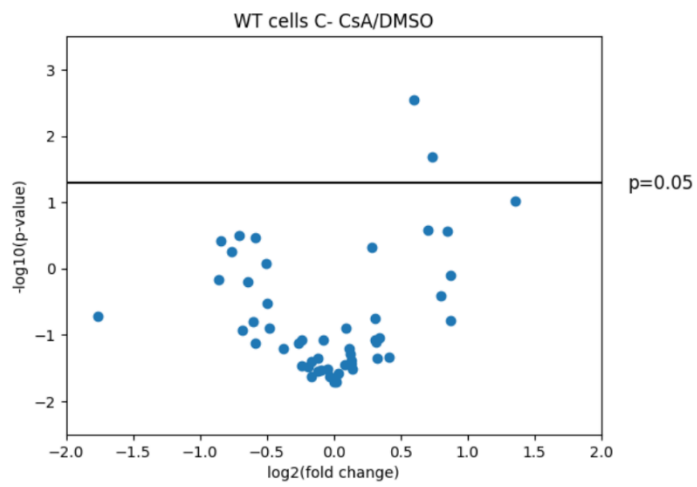
Aside from the known mPTP components I discussed above. Two other CypD interactors had also been identified, HSPE1 and the peptide synthesis complex. For the peptide synthesis complex data in Fig 4.3.g, there were no changes following mPTP induction in either DMSO or CsA conditions. Although there was a statistically significant decrease in interaction between DMSO C+ and CsA C+ conditions, this likely stemmed from the lower levels of interaction in both C- and C+ conditions under CsA treatment as compared to DMSO. Further considering the role and intra-mitochondrial location of the peptide synthesis complex it seemed very safe to conclude that it was not involved in the mPTP and likely relates to other functions of CypD.

HSPE1 in Fig 4.3.f represents a different pattern. Although there was no statistically significant change following mPTP induction under DMSO conditions, there was a statistically significant increase in HSPE1 and CypD interaction following mPTP induction under CsA conditions. This was interesting as it suggests HSPE1 could be involved in mPTP formation in the CypD-CsA bound state. However, under the current paradigm of CsA and CypD interaction, it is assumed that CsA completely inhibits all of CypD's involvement in mPT. This raises the question of the possibility of CypD regulation of mPTP even in the presence of CsA. I would discuss this interesting hypothesis further in later sections where more evidence emerged regarding this topic.

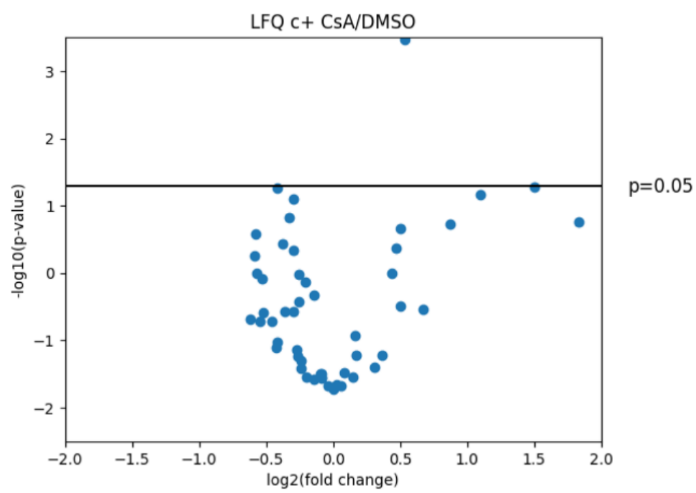
The data here would suggest that the ANT, PiC, VDAC and ATP Synthase are not involved in mPTP opening under CsA conditions, at least not in any way that involves CypD, evident from a lack of increase and even decrease in their interaction with CypD following mPT induction under CsA conditions.

### 4.2.3.2 WT cells – aggregated complexes and isoforms – multiple t-test



**c**

Significant hits	Log2 fold change
HSPD1	0.60
MDH2	0.73

**d**

Significant hits	Log2 fold change
HSPA9	0.53

**Figure 4.3: WT cells – aggregated complexes and isoforms – volcano plot of multiple t-test**

a) Volcano plot of C+/C-  $\log_2(\text{fold change})$  for DMSO treated WT cells and corresponding  $-\log_{10}(\text{p-value})$ , significant hits listed in table next to plot with the specific  $\log_2(\text{fold change})$

b) Volcano plot of C+/C-  $\log_2(\text{fold change})$  for CsA treated WT cells and corresponding  $-\log_{10}(\text{p-value})$ , significant hits listed in table next to plot with the specific  $\log_2(\text{fold change})$

c) Volcano plot of CsA/DMSO  $\log_2(\text{fold change})$  for C- WT cells and corresponding  $-\log_{10}(\text{p-value})$ , significant hits listed in table next to plot with the specific  $\log_2(\text{fold change})$

d) Volcano plot of CsA/DMSO  $\log_2(\text{fold change})$  for C+ WT cells and corresponding  $-\log_{10}(\text{p-value})$ , significant hits listed in table next to plot with the specific  $\log_2(\text{fold change})$

paired t-test at  $p=0.05$  cut off is applied for all 3 plots with significant hits listed in a table next to the plot

Fig 4.3 shows the analysis result I obtained when I applied multiple t-tests with Bonferroni's correction to the summed protein complex and isoforms dataset.

In Fig 4.3.a, under DMSO conditions, the multiple t-test screen failed to find any protein with statistically significant alterations in interactions following mPT induction. This was a clear area of difference with the analysis in 5.3 where ATP Synthase and VDAC were identified as having statistically significant increases. This was primarily due to the different statistical approaches used. Given the divergence in statistical conclusions for the 2 analyses, using multiple analyses here was already paying off, as hypothesised originally. Based on past work and what we know about the mPTP, I would argue that the interactors analysis for complexes and isoforms appear to be the more representative and would be where I would be drawing the primary conclusions from the data.

In Fig 4.3.b, under CsA conditions, the multiple t-test screen identified HSPA9 as having statistically significantly increased interaction following mPT induction. HSPA9 is a heat shock protein with multiple regulatory roles in mitochondria. If this result was meaningful and not an artefact, the only interpretation was that HSPA9 was involved in CypD mediated mPT under CypD-CsA bound conditions since I observed no statistically significant increase in interaction when mPTP opened under DMSO conditions. Interestingly, HSPE1 has been implicated for the same role in the



interactors analysis. They are both heat shock proteins but belong to different families, so it is not clear if any link exists here. The possibility of HSPA9 involvement in mPTP can be considered but evidence here was weak and further support elsewhere in the data was lacking, not to mention no previous work has suggested any involvement of HSPA9 in mPT. Hence, it might only have a limited value as a *bona fide* mPTP candidate.

In Fig 4.3.c, under C- conditions, the multiple t-test screen identified heat shock protein family D (Hsp60) member 1 (HSPD1) and malate dehydrogenase 2 (MDH2) as having statistically significantly higher interaction in the CsA condition as compared to the DMSO condition. HSPD1 is a heat shock protein involved in chaperoning and MDH2 is the mitochondrial isoform of the enzyme involved in the TCA cycle. Neither protein has being implicated in mPTP activity before and did not respond to Ca<sup>2+</sup> treatment in this experiment. Hence, they are unlikely to be involved in the mPTP and any changes here were most likely due to CsA binding changing CypD structure and hence interactions.

In Fig 4.3.d, under C+ conditions, the multiple t-test screen identified HSPA9 as having statistically significantly increased interaction in the CsA condition as compared to the DMSO condition. This basically just reinforces the observation in Fig 4.3.b regarding HSPA9 interaction with CypD and has already been discussed earlier.

### 4.2.3.3 WT cells – individual proteins – interactor determination using ANOVA followed by one-way ANOVA with multiple comparisons

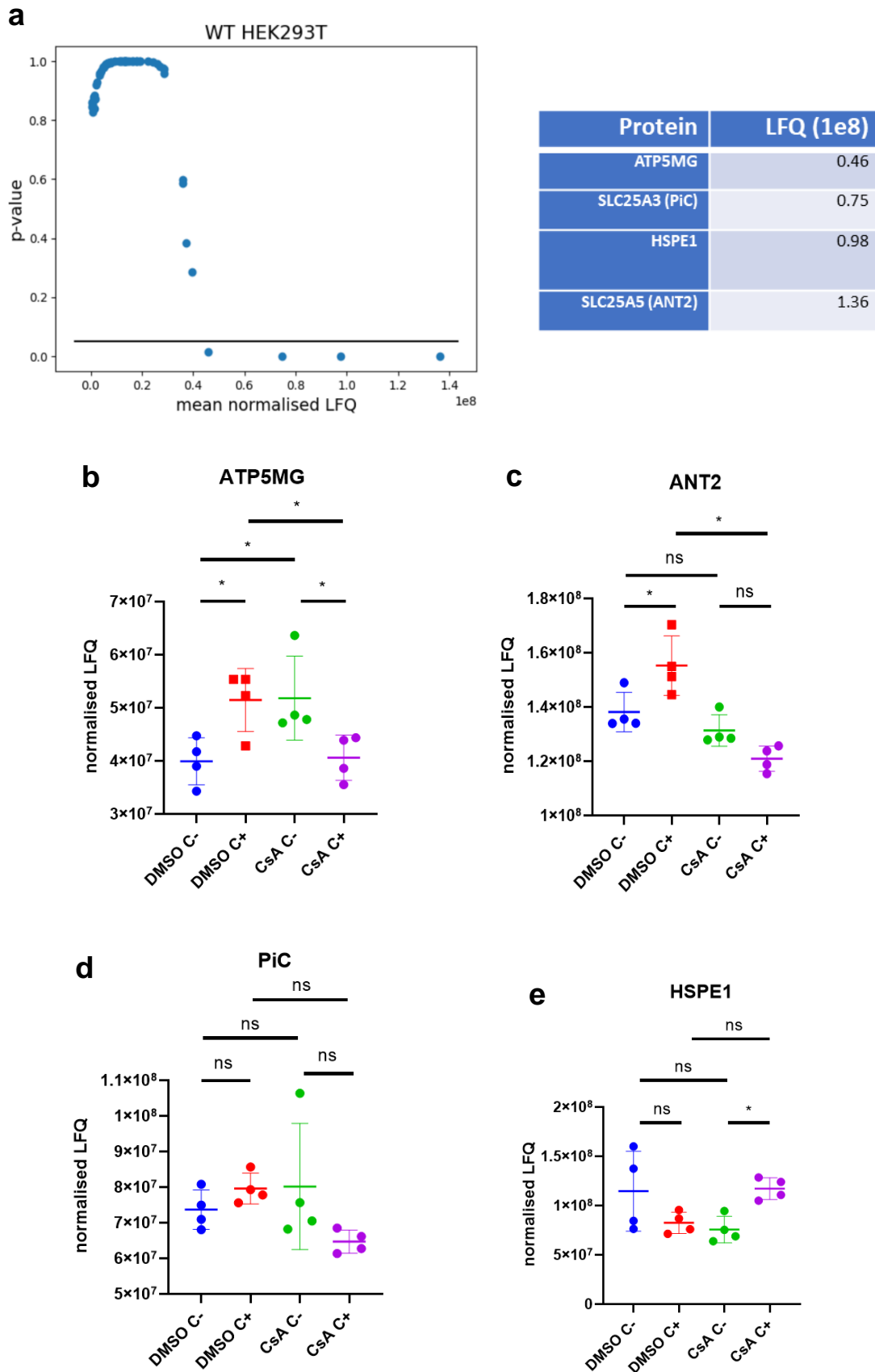


**Figure 4.5: WT cells – individual proteins – interactor determination using ANOVA followed by one-way ANOVA with multiple comparisons**

a) Determination of CypD interactors using ANOVA followed by Turkey's HSD with  $p=0.05$  as cut off. ANOVA (F statistic: , p-value: ). Table summarizes the significant hits along with respective interaction level

b) Normalised LFQ data of ATP5mg protein for DMSO C-, DMSO C+, CsA C-, and CsA C+ conditions, a one-way ANOVA followed by Tukey's multiple comparisons test was carried out

c) Normalised LFQ data of ANT2 protein for DMSO C-, DMSO C+, CsA C-, and CsA C+ conditions, a one-way ANOVA followed by Tukey's multiple comparisons test was carried out

d) Normalised LFQ data of PiC protein for DMSO C-, DMSO C+, CsA C-, and CsA C+ conditions, a one-way ANOVA followed by Tukey's comparisons test was carried out

e) Normalised LFQ data of HSPE1 protein for DMSO C-, DMSO C+, CsA C-, and CsA C+ conditions, a one-way ANOVA followed by Tukey's multiple comparisons test was carried out

Fig 4.5 shows the analysis result obtained when the CypD interactors were identified first before following up with t-test statistics on each interactor hit for the individual proteins dataset.

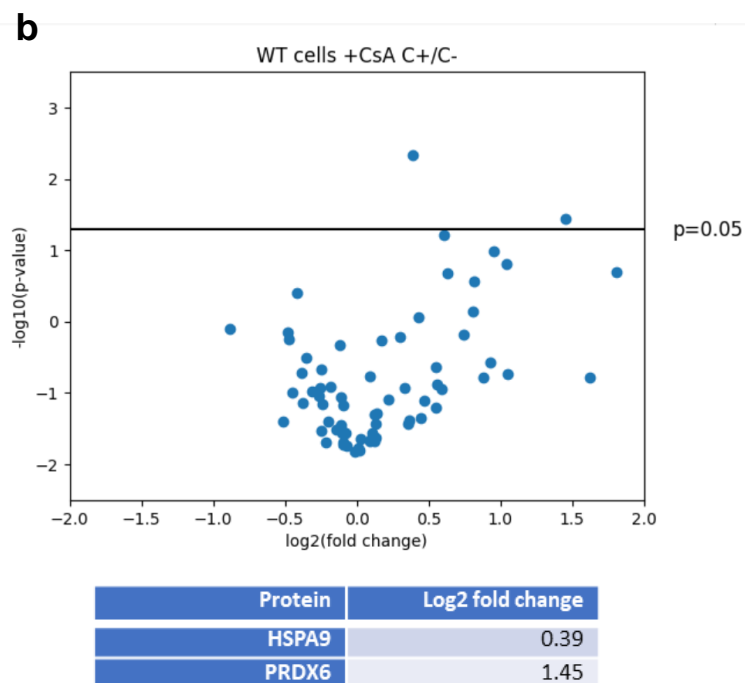
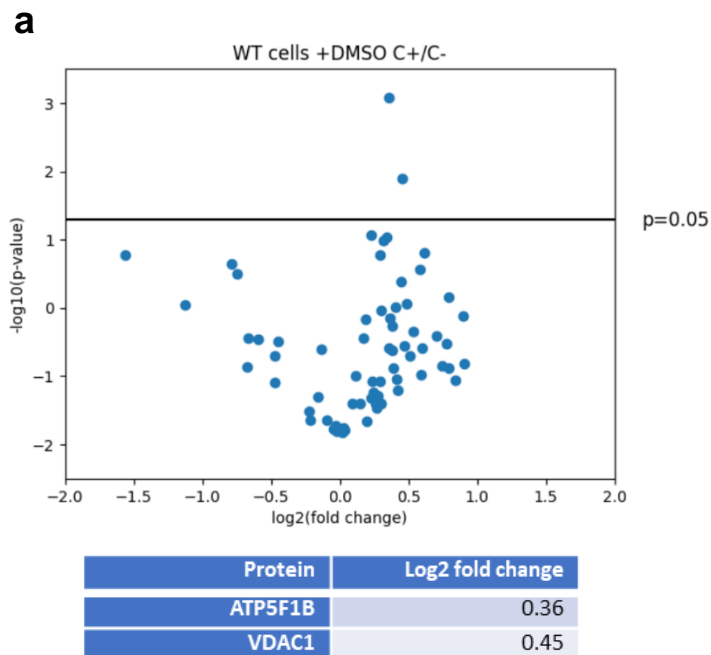
Looking at the interactor analysis for individual proteins data for WT cells in Fig 4.5.a, it seems to be a subset of the combined complex and isoforms data. I observed ATP5mg (a subunit of the ATP Synthase complex), ANT2 (ANT Isoform that is most prevalent in kidney cells which HEK293T originate from), PiC and HSPE1 as interactors, all previously described in the complex and isoforms analysis. I also observed that interactor and background clustering was not as clearly defined as in the complex and isoforms data in Fig 4.3.a. Here I observed a few proteins residing in the p-value spectrum between the clearly defined interactors at  $p<0.05$  and the clear background proteins at  $p>0.8$ . Among these are VDAC isoforms which when summed would increase in statistical strength and be classified as an interactor.

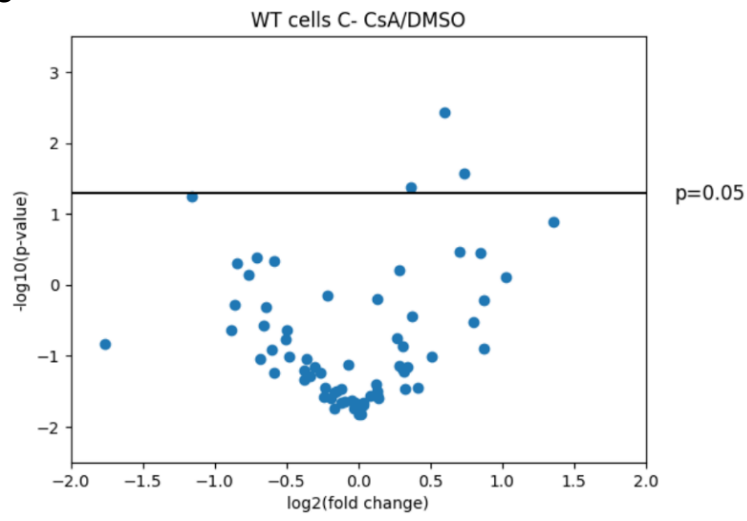
The exact statistical conclusions here were also slightly different for ATP5mg compared to the full ATP Synthase complex in Fig 4.3. When the dynamics of the

interaction was examined by comparing different states of the mPTP, both ATP5mg and ANT2 followed the same trend as the ATP Synthase complex and the ANT isoforms combined data described in Fig 4.3. They showed an increase in CypD interaction following mPTP induction under DMSO conditions which is abolished when CsA is present. The increase in CypD interaction following mPTP opening were statistically significant for both proteins, in contrast to Fig 4.3 where they were only significant for the ATP Synthase Complex. This provides further support for my conclusion in Fig 4.3 that the ANT likely failed to display statistically significant change due to technical limitations. As such the data here supports conclusion I established earlier in Fig 4.3 that the multiple protein hypothesis of the mPTP fits with my data.

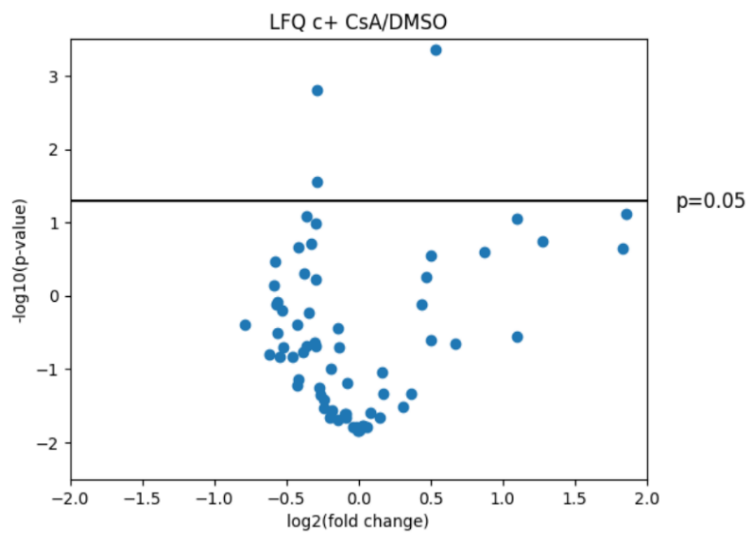
For PiC and HSPE1, since they are individual proteins with no known isoforms, their analysis results here was the same as that in Fig 4.3 and have been discussed earlier.

### 4.2.3.3 WT cells – individual proteins – multiple t-test



**c**

Protein	Log2 fold change
HSPD1	0.60
MDH2	1.73
VDAC1	0.36

**d**

Protein	Log2 fold change
HSPA9	0.53
ATP5F1B	-0.29
ATP5F1A	-0.29

**Figure 4.6: WT cells – individual proteins – volcano plot of multiple t-test**

a) Volcano plot of C+/C-  $\log_2(\text{fold change})$  for DMSO treated WT cells and corresponding  $-\log_{10}(\text{p-value})$ , significant hits listed in table next to plot with the specific  $\log_2(\text{fold change})$

b) Volcano plot of C+/C-  $\log_2(\text{fold change})$  for CsA treated WT cells and corresponding  $-\log_{10}(\text{p-value})$ , significant hits listed in table next to plot with the specific  $\log_2(\text{fold change})$

c) Volcano plot of CsA/DMSO  $\log_2(\text{fold change})$  for C- WT cells and corresponding  $-\log_{10}(\text{p-value})$ , significant hits listed in table next to plot with the specific  $\log_2(\text{fold change})$

d) Volcano plot of CsA/DMSO  $\log_2(\text{fold change})$  for C+ WT cells and corresponding  $-\log_{10}(\text{p-value})$ , significant hits listed in table next to plot with the specific  $\log_2(\text{fold change})$

paired t-test at  $p=0.05$  cut off is applied for all 3 plots with significant hits listed in a table next to the plot

Fig 4.6 shows the analysis result obtained when multiple t-tests were applied with Bonferroni's correction to the individual proteins dataset.

In Fig 4.6.a, when screening for statistically significant changes in DMSO C+/DMSO C- conditions, I found ATP5F1B and VDAC1 as having significantly higher interaction with CypD following mPT. On the other hand, the screen for statistically significant changes in CsA C+/CsA C- conditions shows no significant changes for ATP5F1B (ATP Synthase complex subunit) and VDAC1 (VDAC isoform). This result corroborates the finding in Fig 4.3 where the aggregated ATP Synthase complex and VDAC isoform data also showed the same trend and statistical conclusions, the only difference being that only a subset of the signal in Fig 4.3 is measured here as opposed to the full aggregated signal in Fig 4.3.

In Fig 4.6.b, when screening for statistically significant changes in CsA C+/CsA C- conditions, I found HSPA9 and Peroxiredoxin-6 (PRDX6) as having significantly increased interaction with CypD following mPT. The HSPA9 finding was the same as that in the summed complexes and isoforms data in Fig 4.6.b and has been discussed earlier. PRDX6 is a bifunctional enzyme implicated in redox regulation and phospholipid turnover regulation with no previous links to the mPTP. Given that its interaction only increased following mPT induction under CsA conditions, it could only

possibly be involved in the CypD-CsA bound state mPTP pathway. More investigations are needed to understand the significance of these findings.

In Fig 4.6.c, when screening for statistically significant changes in CsA C-/ DMSO C- conditions, I found HSPD1, MDH2 and VDAC1 as having significantly altered interaction levels. The HSPD1 and MDH2 results were the same as that of Fig 4.3.c and have been discussed earlier. The presence of VDAC1 was unexpected as while it is a strong mPTP candidate, it resides in the OMM. The data suggests that VDAC1 interaction is increased following CsA treatment. This basically means that CypD has great affinity for VDAC1 when bound to CsA. It is not clear what this implies. Additionally, this change was not detected when the VDAC isoforms are summed together in Fig 4.3.c. This makes the VDAC1 result here less convincing as grouped isoform data erases the change. If this was true it would imply VDAC1 behaves differently from VDAC2 and VDAC3 when it comes to CypD binding which is not something that was known and would need further investigation.

In Fig 4.6.d, when screening for statistically significant changes in CsA C+/ DMSO C+ conditions, I found HSPA9, ATP5F1A and ATP5F1B. The result for HSPA9 was the same as that in Fig 4.3 and has already been discussed then. ATP5F1A and ATP5F1B are ATP Synthase subunits and their decreased interaction in CsA C+ conditions compared to DMSO C+ fall in line with their suspected role as a CypD mediated mPTP channel in the absence of CsA.

#### **4.2.3.5 WT cells data summary**

Overall, the results here would support the involvement of ATP Synthase, ANT and VDAC in the mPTP, complement previous work and alternative analyses of my own data. It is interesting to note that three different ATP Synthase subunits were found in the analysis when we analysed individual proteins instead of protein complexes. In Fig 4.5, ATP5MG is the only ATP Synthase subunit identified as an interactor of CypD while in Fig 4.6 ATP5F1B and ATP5F1A are detected in the multiple t-test screens instead of ATP5MG. This shows that it is difficult to view and analyse the ATP Synthase subunits as separate entities when it comes to CypD interaction which would only needlessly complicate the data as is the case here. Hence it would make sense



to provide a summed complex analysis as I have done earlier for a clearer understanding.

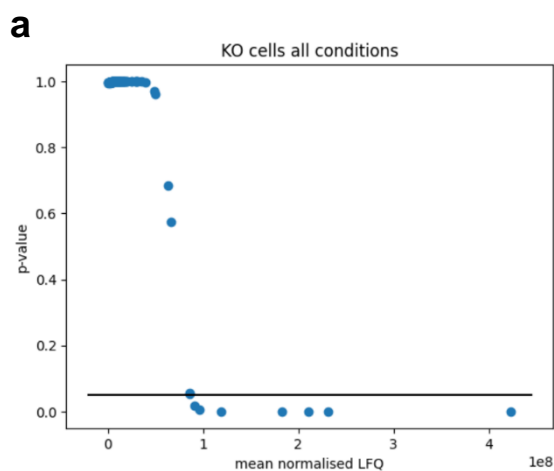
Overall, the proteomics data obtained using WT cells provided realistic and convincing results. It showed evidence supporting the multiple entity hypothesis of the mPTP which helps to resolve the long-standing debate regarding the identity of the mPTP. However, my original concern regarding competition between endogenous WT CypD and CypD-TurboID remains relevant and might have manifested itself in the WT data, reducing the sensitivity of the screen. This might be the reason why even though certain changes (e.g increased ANT interaction following mPT) clearly fits into the overarching narrative as I have discussed earlier, the specific statistical measurement here remains non-significant. This was one area where I aimed to use the CypD KO cells to provide more clarity on.

## 4.2.4 Proteomics results for CypD KO cells

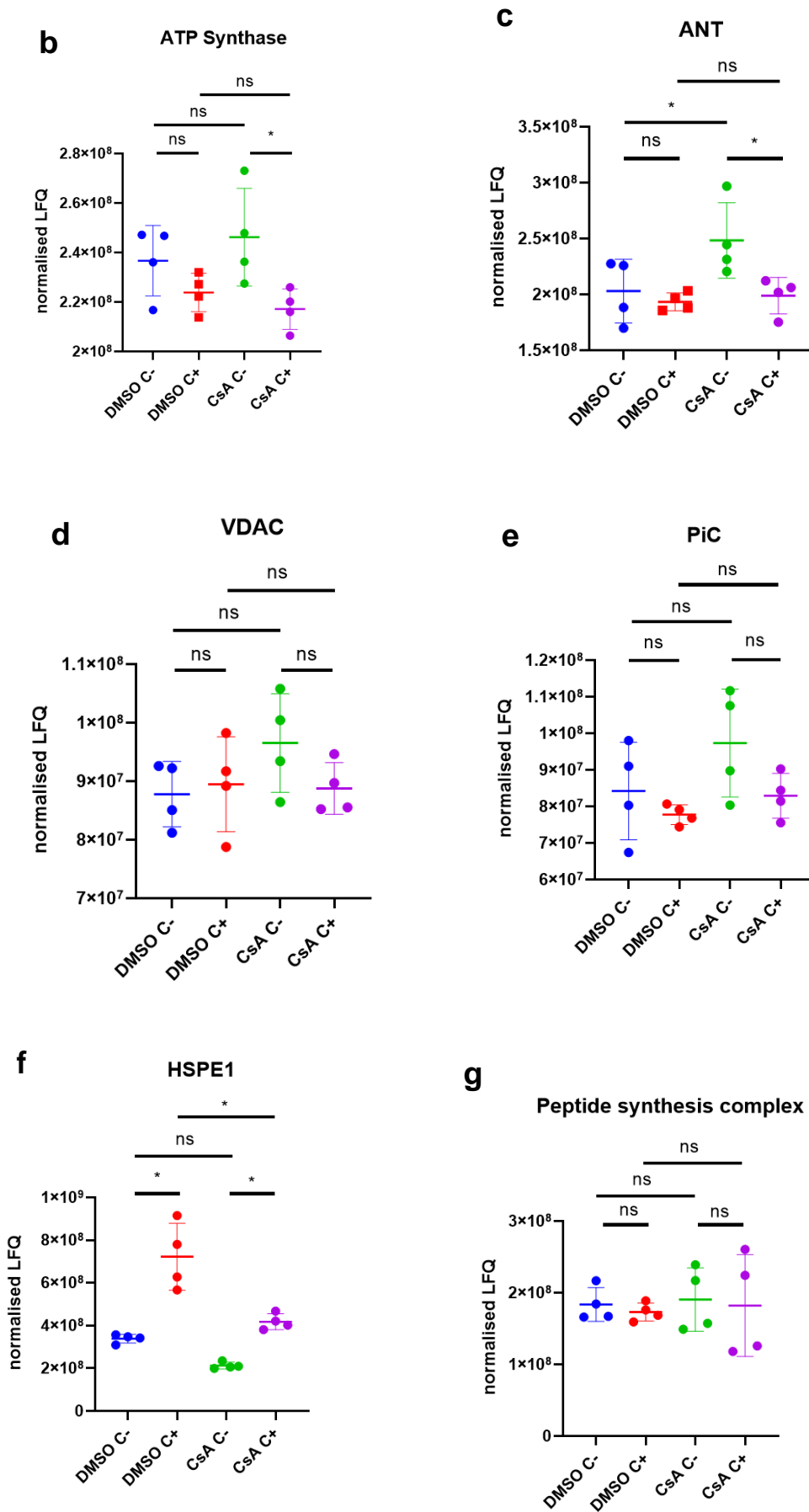
The CypD KO cell line used here has an unexpected characteristic, in that CypD could regulate mPTP but has lost its CsA sensitivity. As discussed earlier, the reason behind this strange phenomenon was not clear. Since CypD can still regulate mPT, I expected that it would still yield some interesting and novel insights. The anticipated results might even provide further clarification on the reason behind the loss of CsA sensitivity.

Furthermore, the WT data provided many interesting insights, providing support and theoretical resolution on old candidates as well as yielding some new candidate proteins with changes during mPT (HSPE1, HSPA9, MDH2 and PRDX6), especially under CsA conditions. I would be on the lookout to see if the CypD KO cells data would be able to corroborate any of these new hits in the WT cells data.

### 4.2.4.1 KO cells – aggregated complexes and isoforms – interactor determination using ANOVA followed by one-way ANOVA with multiple comparisons



Protein	LFQ (1e8)
HSDL1/2 –	0.85
Borderline p-value slightly above 0.05 but in same cluster	
PiC –	0.86
Borderline p-value slightly above 0.05 but in same cluster	
VDAC Isoforms	0.91
PYCR Isoforms	0.96
LDHB	1.19
Peptide synthesis complex	1.82
ANT Isoforms	2.11
ATP Synthase Complex	2.31
HSPE1	4.23



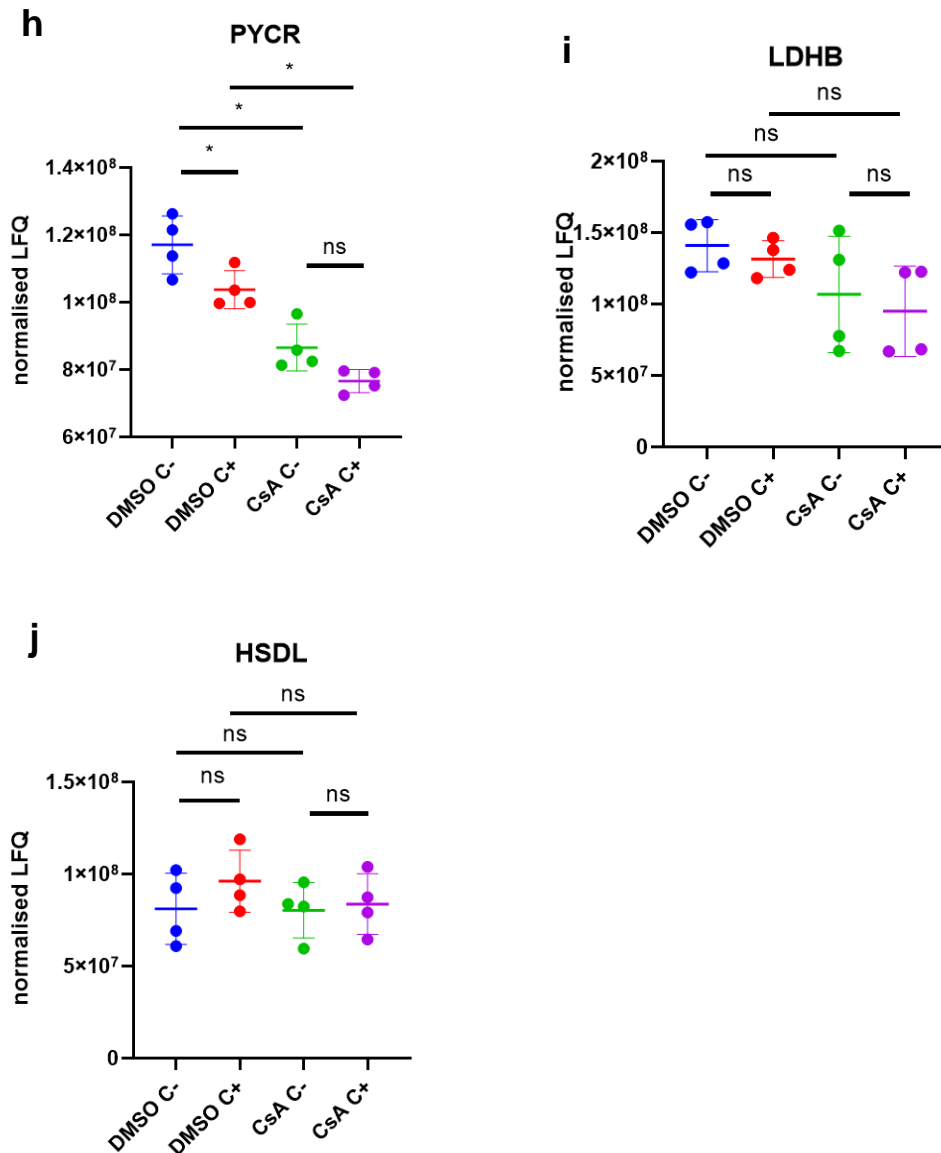


**Figure 4.7: KO cells – aggregated complexes and isoforms –interactor determination using ANOVA followed by one-way ANOVA with multiple comparisons**

a) Determination of CypD interactors using ANOVA followed by Turkey’s HSD with  $p=0.05$  as cut off. ANOVA (F statistic: 350, p-value: 0.0). Table summarizes the significant hits along with respective interaction level

b) Normalised LFQ data of ATP Synthase complex for DMSO C<sup>-</sup>, DMSO C<sup>+</sup>, CsA C<sup>-</sup>, and CsA C<sup>+</sup> conditions, a one-way ANOVA followed by Tukey’s multiple comparisons test was carried out

c) Normalised LFQ data of ANT Isoforms for DMSO C<sup>-</sup>, DMSO C<sup>+</sup>, CsA C<sup>-</sup>, and CsA C<sup>+</sup> conditions, a one-way ANOVA followed by Tukey’s multiple comparisons test was carried out

*d) Normalised LFQ data of VDAC Isoforms for DMSO C-, DMSO C+, CsA C-, and CsA C+ conditions, a one-way ANOVA followed by Tukey's multiple comparisons test was carried out*

*e) Normalised LFQ data of PiC protein for DMSO C-, DMSO C+, CsA C-, and CsA C+ conditions, a one-way ANOVA followed by Tukey's multiple comparisons test was carried out*

*f) Normalised LFQ data of HSPE1 protein for DMSO C-, DMSO C+, CsA C-, and CsA C+ conditions, a one-way ANOVA followed by Tukey's multiple comparisons test was carried out*

*g) Normalised LFQ data of Peptide synthesis complex for DMSO C-, DMSO C+, CsA C-, and CsA C+ conditions, a one-way ANOVA followed by Tukey's multiple comparisons test was carried out*

*h) Normalised LFQ data of PYCR family for DMSO C-, DMSO C+, CsA C-, and CsA C+ conditions, a one-way ANOVA followed by Tukey's multiple comparisons test was carried out*

*i) Normalised LFQ data of LDHB family for DMSO C-, DMSO C+, CsA C-, and CsA C+ conditions, a one-way ANOVA followed by Tukey's multiple comparisons test was carried out*

*j) Normalised LFQ data of HSDL family for DMSO C-, DMSO C+, CsA C-, and CsA C+ conditions, a one-way ANOVA followed by Tukey's multiple comparisons test was carried out*

Fig 4.7 shows the analysis result obtained when CypD interactors were first identified by ANOVA, following up with t-test statistics on each interactor hit for the summed protein complex and isoforms dataset.

Looking at the CypD interactors detected here, all the interactors previously detected in the combined complex and isoforms data for WT HEK293T cells were also detected here. This included the ATP Synthase, ANT, PiC, VDAC, HSPE1 and the peptide synthesis complex. However, looking at the dynamics of the interaction during mPTP, there was a vastly different picture from that of the WT HEK293T cells.

The mPTP candidates, ATP Synthase, ANT, PiC and VDAC, which all shared a single trend and interaction pattern in WT cells also shared a single trend and interaction pattern in CypD KO cells. However, in contrast to WT cells, in KO cells the pattern was rather static. None of the interacting proteins showed any change in CypD interaction following mPTP induction under either DMSO or CsA conditions. This was in sharp contrast with an increase in their interaction following mPTP induction without CsA in

WT cells. Although the KO cell data would appear to argue against the involvement of these proteins in the mPTP at first glance, after taking into account the results of the WT study and the context of these KO cells, it actually fits right into the narrative and supports the full story. In Fig 4.3 the same proteomics data in WT HEK293T cells showed that these mPTP candidates only increased their interaction following mPT induction in the absence of CsA. Under CsA conditions, there was no increase in interactions and I observed even some slight decreases.

In the context of KO cells, as discussed earlier, CsA had lost its effect on modulating the mPTP while CypD was still able to modulate the mPTP. In Chapter 3, I hypothesised that CsA had lost its effect on CypD due to potential changes in CypD molecular properties in the KO cell line, possibly with regard to posttranslational modification changes. However, the data here suggests that this was unlikely to be the case.

If the lack of effect of CsA is due to changes in CypD-CsA interaction for whatever reason, the interaction between CypD and other mPTP candidates should not change, since CRC assay showed that CypD is still able to modulate the mPTP in these KO cells. Instead, what has happened was that there was a drastic difference in CypD interaction between KO cells and WT cells when all other conditions were held equal, as was the case here. The data here actually shows that in the KO cells, CypD interaction with mPTP candidates under DMSO conditions is similar to that of CsA conditions in WT cells. In WT cells, presence of CsA completely abolishes any increase in CypD interaction with the ATP Synthase, ANT, VDAC and PiC. In the KO cell data shown here, there was no change in interaction even without CsA, and CsA has no effect on CypD interaction with these mPTP candidates.

This suggest that the loss of effect of CsA in the KO cells was due to the cells shifting to a mPTP pathway that is similar to a state where CypD is bound to CsA, hence explaining why the DMSO condition of the KO cells showed the same trend of CypD interaction as that of the CsA condition of the WT cells. In this respect, a lack of change in these mPTP candidates fits right into the previously established view that they are only involved in mPT in a CsA dependent manner and are not involved in mPT when CsA was present.

As far as the literature is concerned, the view has always been that CypD is not involved in mPTP formation when CsA is present at a saturation concentration. However, if the mPTP pathway in CypD KO cells proceeds in a similar manner as that in a CsA bound state of CypD, which is what my data is suggesting, this view will be called into question. I have shown that CypD can still regulate mPTP in the KO cells so it would support the idea that CypD is still involved in mPT in a CsA bound state with mPTP possibly proceeding via a different pathway than the established candidates. If this is true, the question would then be what is the CypD dependent mPTP pathway under CsA conditions. Interestingly, the data here actually offers a good candidate. HSPE1 has been shown to increase its interaction with CypD following mPT induction in WT cells under CsA conditions in a statistically significant manner but showed no change under DMSO conditions following mPT induction as seen in Fig 4.3.f. In the KO cells, as seen in Fig 4.7.f, HSPE1 have significantly increased interaction with CypD following mPT induction under both DMSO and CsA conditions. This also fits the view that the DMSO condition in KO is similar to the CsA condition in WT. Thus, importantly, HSPE1 appears to be an attractive candidate for a CypD mediated mPTP pathway in a CsA bound state.

The peptide synthesis complex was the last hit that was also detected in the WT cells. In Fig 4.3, it showed basically no change under any form of treatment and as discussed earlier is likely to do with non-mPTP functions of CypD.

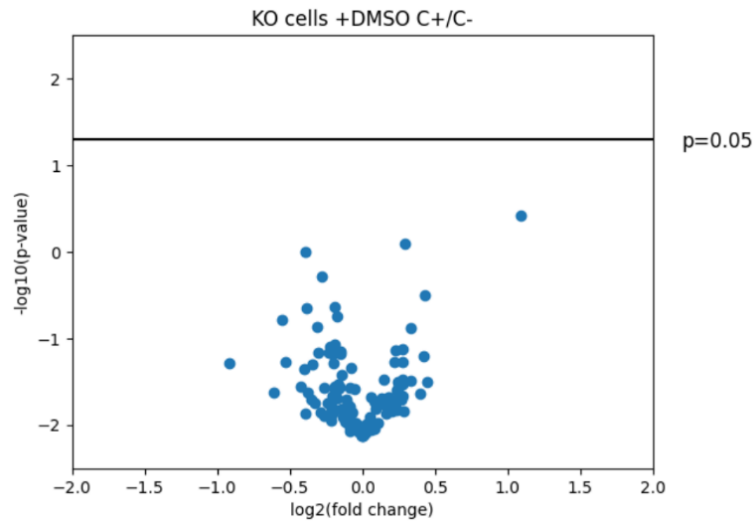
PYCR (Pyrroline-5-Carboxylate Reductase 1 and 2), LDHB (Lactate Dehydrogenase B) and HSDL (Hydroxysteroid Dehydrogenase Like 1 and 2) were new hits that have only surfaced in the KO cells. LDHB and HSDL showed basically no changes of any kind following mPT induction, they have never been suggested to be involved in mPTP and no other analysis of our data suggests they have any role in mPTP. Hence, they were likely to be involved in non-mPTP CypD functions. On the other hand, PYCR showed a multitude of changes when comparing between multiple different conditions. PYCR showed a statistically significant decrease in CypD interaction following mPT induction in DMSO conditions, it also tended to decrease in CypD interaction under CsA conditions although it was not statistically significant. CsA treatment also lowered the interaction levels of PYCR resulting in statistically significant decreases in both CsA treated conditions when compared to their respective DMSO conditions. It was

not clear what was causing these changes. It was possible that CypD had less affinity for PYCR when it is regulating mPTP opening and the CsA bound state of CypD also had less affinity for PYCR, causing these decreases. Nonetheless, it is clear that PYCR was unlikely to be involved in the mPTP in anyway given that it shows decreased interaction with CypD following mPTP induction under both DMSO and CsA conditions. Hence these 3 proteins were not investigated further as mPTP components.



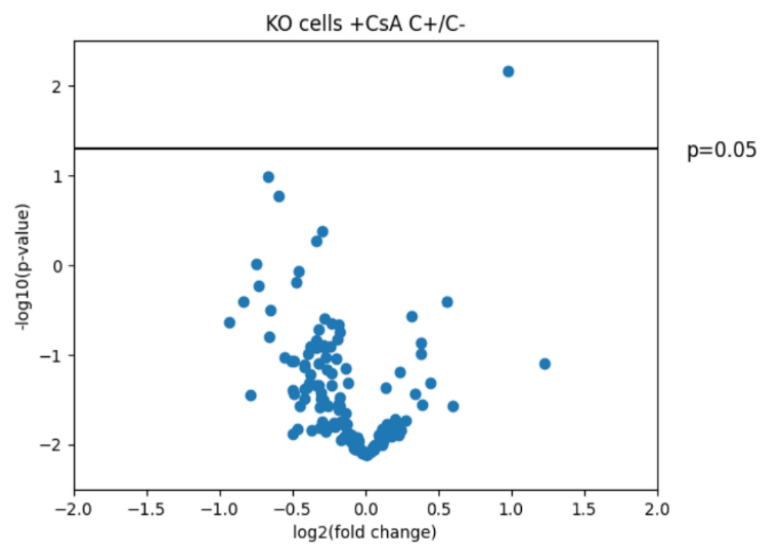
### 4.2.3.2 KO cells – aggregated complexes and isoforms – multiple t-test

**a**

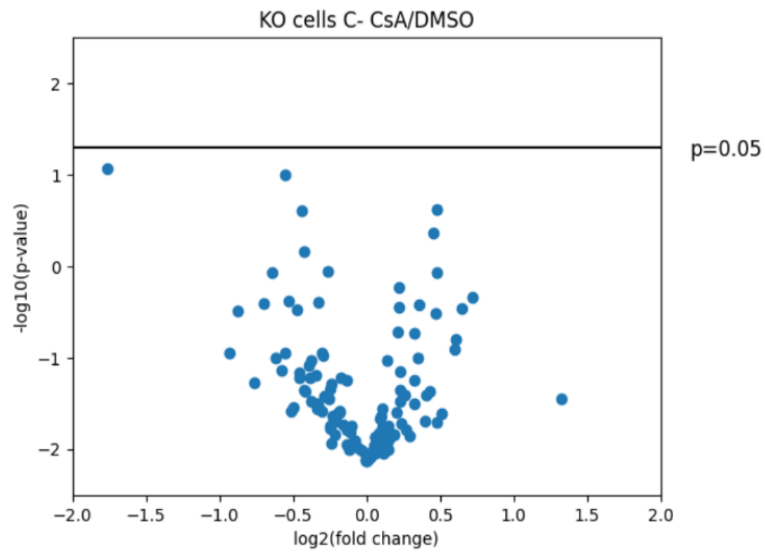


Significant hits	Log2 fold change
None	NA

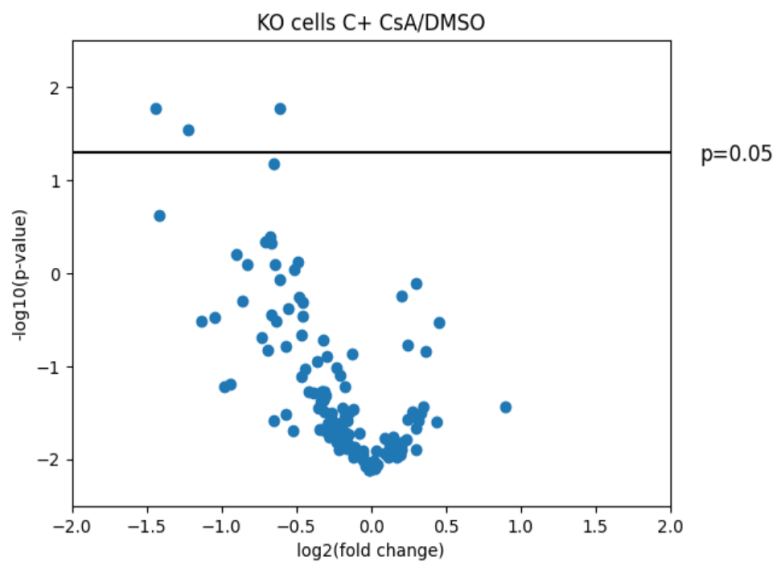
**b**



Protein	Log2 fold change
HSPE1	0.97

**c**

Significant hits	Log2 fold change
None	NA

**d**

Protein	Log2 fold change
PYCR Isoforms	-0.61
FDPS	-1.22
ECHS1	-1.44

**Figure 4.8: KO cells – aggregated complexes and isoforms – volcano plot of multiple t-test**

a) Volcano plot of C+/C-  $\log_2(\text{fold change})$  for DMSO treated WT cells and corresponding  $-\log_{10}(\text{p-value})$ , significant hits listed in table next to plot with the specific  $\log_2(\text{fold change})$

b) Volcano plot of C+/C-  $\log_2(\text{fold change})$  for CsA treated WT cells and corresponding  $-\log_{10}(\text{p-value})$ , significant hits listed in table next to plot with the specific  $\log_2(\text{fold change})$

c) Volcano plot of CsA/DMSO  $\log_2(\text{fold change})$  for C- WT cells and corresponding  $-\log_{10}(\text{p-value})$ , significant hits listed in table next to plot with the specific  $\log_2(\text{fold change})$

d) Volcano plot of CsA/DMSO  $\log_2(\text{fold change})$  for C+ WT cells and corresponding  $-\log_{10}(\text{p-value})$ , significant hits listed in table next to plot with the specific  $\log_2(\text{fold change})$

paired t-test at  $p=0.05$  cut off is applied for all 3 plots with significant hits listed in a table next to the plot

Fig 4.8 shows the analysis result obtained when I applied multiple t-tests with Bonferroni's correction to the summed protein complex and isoforms dataset in KO cells.

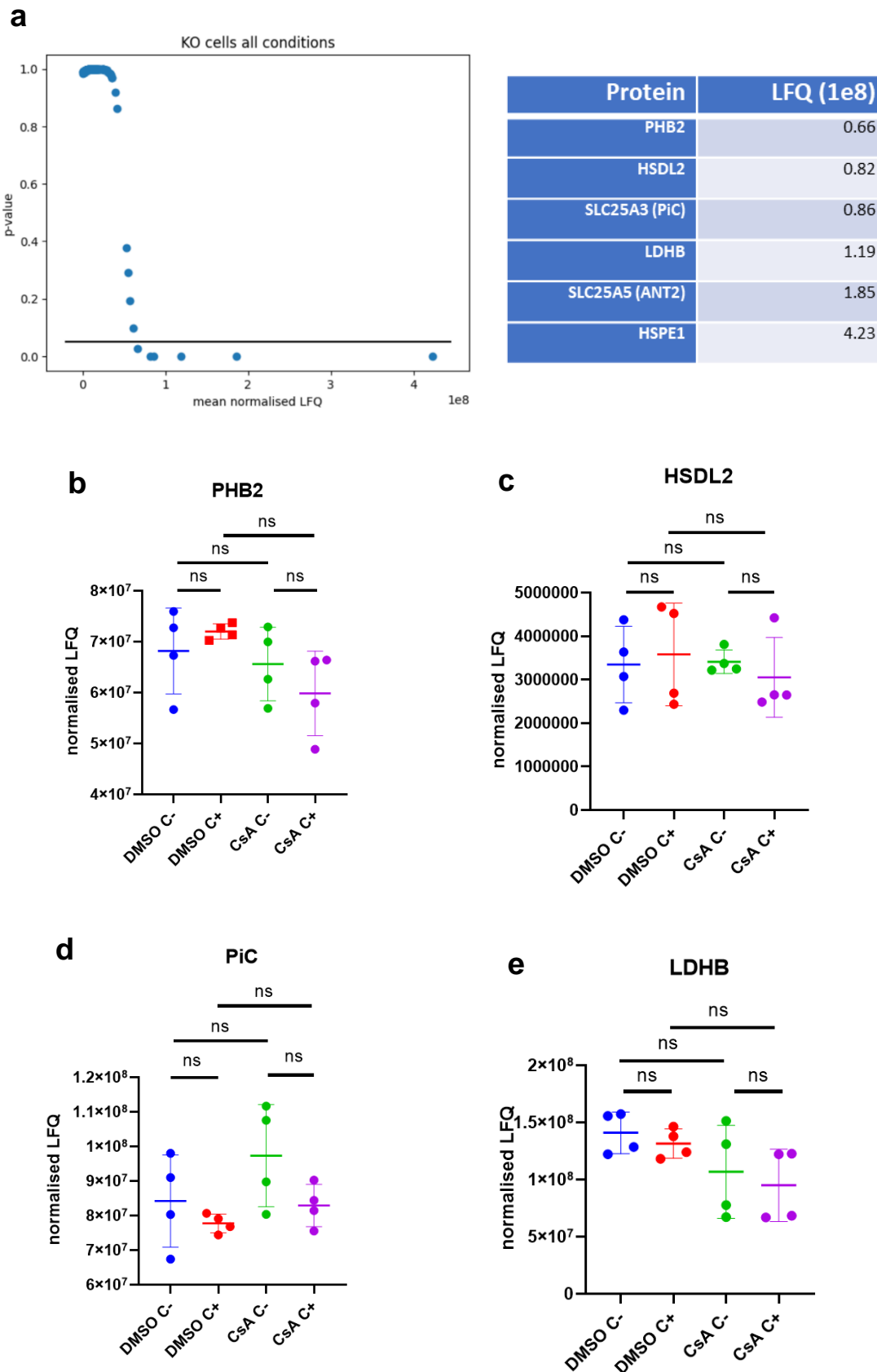
In Fig 4.8.a, when screening for statistically significant changes in DMSO C+/DMSO C- conditions, I found no proteins with any significant changes.

In Fig 4.8.b, when screening for statistically significant changes in CsA C+/CsA C- conditions, I found HSPE1 as having significantly higher interaction with CypD following mPT induction. This supports the narrative where HSPE1 might play a role in CypD dependent mPTP pathway in the presence of CsA. Given that the CypD KO cell DMSO condition should mimic the WT cell CsA condition at least in terms of mPTP activation, one would also expect HSPE1 to be detected in the screen for DMSO conditions in Fig 4.8.a. However, this was not the case. While changes in HSPE1 in the DMSO C+/DMSO C- conditions failed to be recognised as significant in the multiple t-test screen here, it was recognised as significant in Fig 4.7.f under the alternative analysis. This discrepancy was the same as that observed in the ATP Synthase analysis in WT cells and was likely due to limitation of different analyses methods as discussed earlier.

In Fig 4.8.c, when screening for statistically significant changes in CsA C-/DMSO C- conditions, I found no proteins with any significant changes.

In Fig 4.8.d, when screening for statistically significant changes in CsA C+/DMSO C+ conditions, I found PYCR, FDPS (Farnesyl Diphosphate Synthase) and ECHS1 (enoyl-CoA hydratase, short chain 1) as all having decreased interaction with CypD. Changes in PYCR were the same as those described in Fig 4.7.h and has already been discussed then. FDPS is an enzyme that catalyses the formation of geranyl pyrophosphate and farnesyl pyrophosphate and ECHS1 is an enzyme that catalyses the hydration of 2-trans-enoyl-coenzyme A (CoA) intermediates to L-3-hydroxyacyl-CoAs. Neither protein has being implicated in mPTP activity before and has not been shown to respond to Ca<sup>2+</sup> treatment in this experiment. Hence, they were unlikely to be involved in the mPTP and possibly relates to other CypD functions.

### 4.2.3.3 KO cells – individual proteins – interactor determination using ANOVA followed by one-way ANOVA with multiple comparisons



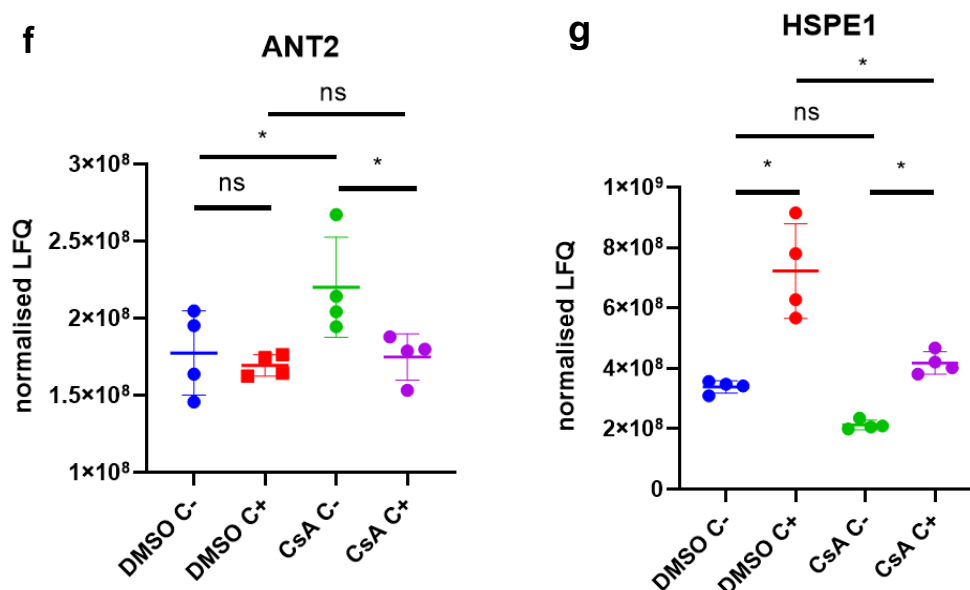


**Figure 4.9: KO cells – individual proteins – interactor determination using ANOVA followed by 2-way ANOVA with multiple comparisons**

a) Determination of *CypD* interactors using ANOVA followed by Tukey's HSD with  $p=0.05$  as cut off. ANOVA (F statistic: , p-value: ). Table summarizes the significant hits along with respective interaction level

b) Normalised LFQ data of *PHB2* protein for DMSO C-, DMSO C+, CsA C-, and CsA C+ conditions, a one-way ANOVA followed by Tukey's multiple comparisons test was carried out results

c) Normalised LFQ data of *HSDL2* protein for DMSO C-, DMSO C+, CsA C-, and CsA C+ conditions, a one-way ANOVA followed by Tukey's multiple comparisons test was carried out

d) Normalised LFQ data of *PiC* protein for DMSO C-, DMSO C+, CsA C-, and CsA C+ conditions, a one-way ANOVA followed by Tukey's multiple comparisons test was carried out

e) Normalised LFQ data of *LDHB* protein for DMSO C-, DMSO C+, CsA C-, and CsA C+ conditions, a one-way ANOVA followed by Tukey's multiple comparisons test was carried out

f) Normalised LFQ data of *ANT2* protein for DMSO C-, DMSO C+, CsA C-, and CsA C+ conditions, a one-way ANOVA followed by Tukey's multiple comparisons test was carried out

g) Normalised LFQ data of *HSPE1* protein for DMSO C-, DMSO C+, CsA C-, and CsA C+ conditions, a one-way ANOVA followed by Tukey's multiple comparisons test was carried out

Fig 4.9 shows the analysis result obtained when CypD interactors were first identified before following up with t-test statistics on each interactor hit for the individual proteins dataset.

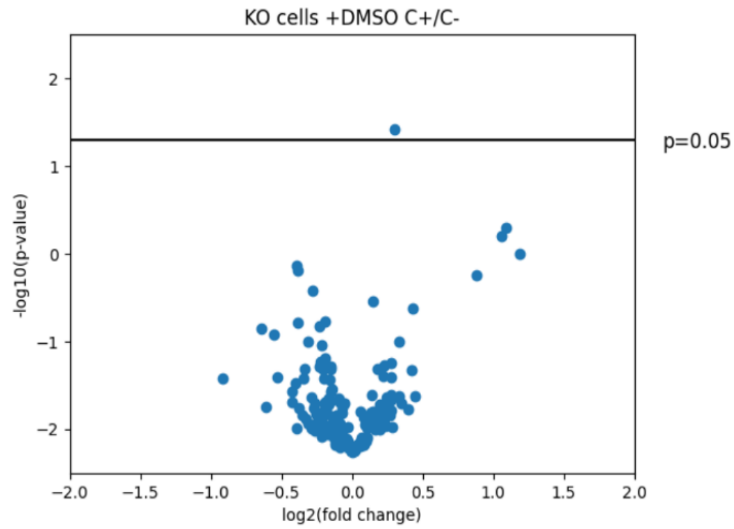
Looking at the detected interactors in Fig 4.9.a, only PiC and ANT2 were previously suggested mPTP candidates. As I have established earlier, these proteins should only be involved in CypD mediated mPT when CsA is not bound to CypD. In Fig 4.9.d and Fig 4.9.f their interaction behaviour was as expected and did not show any increase and even showed some decrease, although not statistically significantly, following mPT induction. This has already been discussed in detail in Fig 4.7.

In Fig 4.9.g, the HSPE1 result was the same as that in Fig 4.7.f and had been discussed earlier.

When examining Fig 4.9.b, Fig 4.9.c and Fig 4.9.e, the data for PHB2 (prohibitin2), HSDL2 (HSDL2hydroxysteroid dehydrogenase-like 2) and LDHB (Lactate Dehydrogenase B) respectively, I observe no statistically significant changes between any of the conditions. None of the proteins have been previously implicated in mPT and their interaction did not change following mPT induction which supports the view that they are not involved in mPTP formation. The result for HSDL2 was the same as the summed HSDL1/2 result in Fig 4.7, this was also true for LDHB. Both proteins had been discussed then and the same conclusion stands.

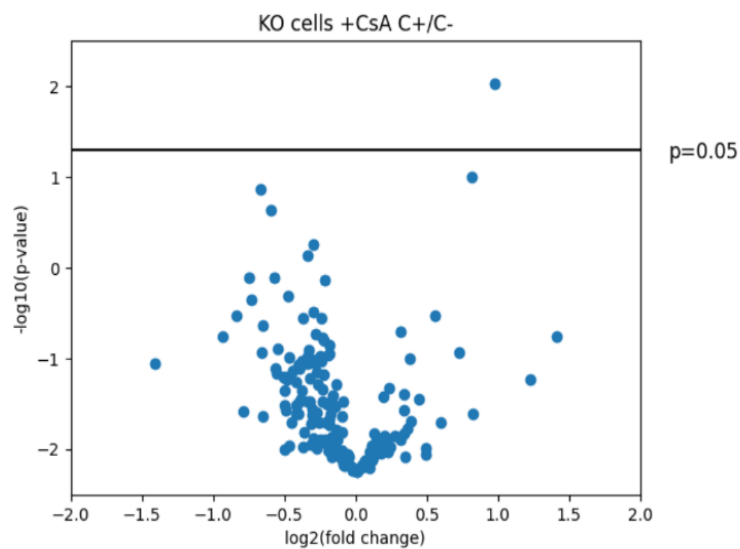
### 4.2.3.3 KO cells – individual proteins – volcano plot of multiple t-test

**a**



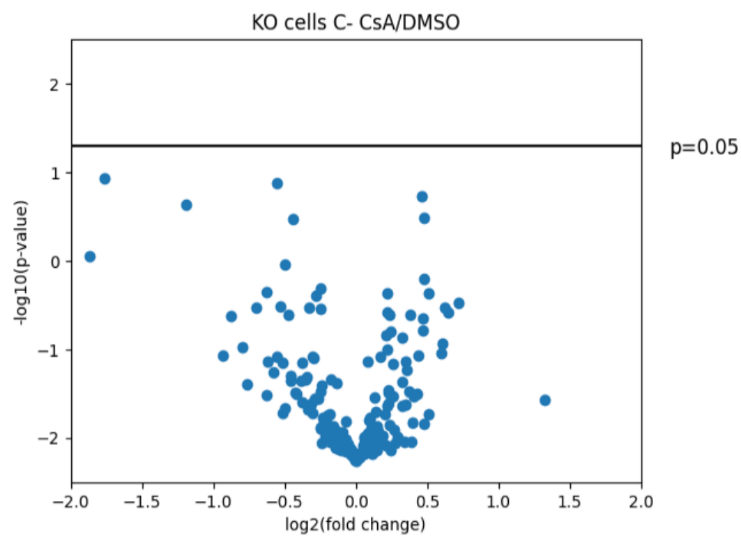
Protein	Log2 fold change
PRDX6	0.30

**b**

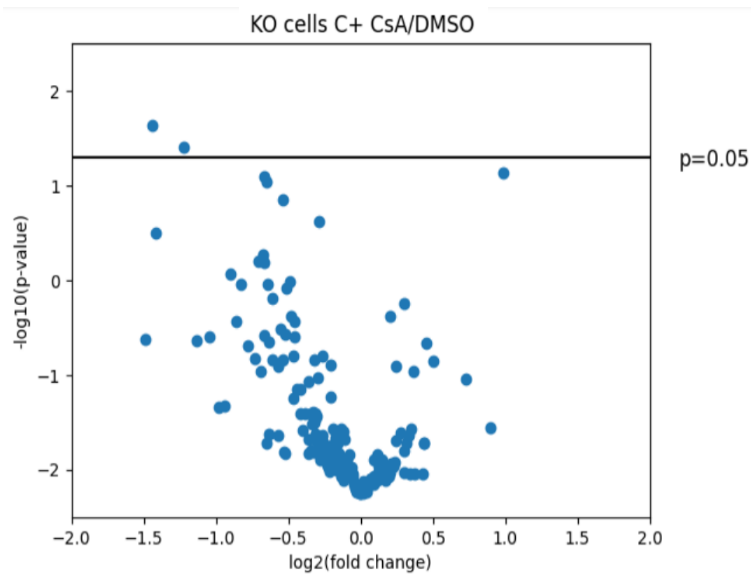


Protein	Log2 fold change
HSPE1	0.97



**c**

Significant hits	Log2 fold change
None	NA

**d**

Protein	Log2 fold change
FDPS	-1.22
ECHS1	-1.44

**Figure 4.10: KO cells – individual proteins – volcano plot of multiple t-test**

a) Volcano plot of C+/C-  $\log_2(\text{fold change})$  for DMSO treated WT cells and corresponding  $-\log_{10}(\text{p-value})$ , significant hits listed in table next to plot with the specific  $\log_2(\text{fold change})$

b) Volcano plot of C+/C-  $\log_2(\text{fold change})$  for CsA treated WT cells and corresponding  $-\log_{10}(\text{p-value})$ , significant hits listed in table next to plot with the specific  $\log_2(\text{fold change})$

c) Volcano plot of CsA/DMSO  $\log_2(\text{fold change})$  for C- WT cells and corresponding  $-\log_{10}(\text{p-value})$ , significant hits listed in table next to plot with the specific  $\log_2(\text{fold change})$

d) Volcano plot of CsA/DMSO  $\log_2(\text{fold change})$  for C+ WT cells and corresponding  $-\log_{10}(\text{p-value})$ , significant hits listed in table next to plot with the specific  $\log_2(\text{fold change})$

paired t-test at  $p=0.05$  cut off is applied for all 3 plots with significant hits listed in a table next to the plot

Fig 4.10 shows the analysis result I obtained when I applied multiple t-tests with Bonferroni's correction to the individual proteins dataset.

In Fig 4.10.a, when screening for statistically significant changes in DMSO C+/DMSO C- conditions, I found PRDX6 as having significantly increased interaction with CypD. A similar hit was found in Fig 4.6.b where PRDX6 showed increased interaction in a CsA C+/CsA C- screen. This corroborates our hypothesis that the DMSO state in the KO cells was similar to the CsA state in WT cells as discussed earlier and this data would support PRDX6 as a possible candidate for playing a role in CypD dependent mPT in the presence of CsA.

In Fig 4.10.b, when screening for statistically significant changes in CsA C+/CsA C- conditions, I found HSPE1. HSPE1 has already turned up in these analyses multiple times and has already been discussed earlier as possibly playing a role in CypD dependent mPTP pathway in the presence of CsA.

In Fig 4.10.c, when screening for statistically significant changes in CsA C-/DMSO C- conditions, I found no proteins with any significant changes.

In Fig 4.10.d, when screening for statistically significant changes in CsA C+/DMSO C+ conditions, I found FDPS and ECHS1 as having decreased interaction with CypD. Both of these changes have been previously observed and discussed in Fig 4.8.d.

### **5.2.3.5 KO cells data summary**

In the WT cells data, I found HSPE1, HSPA9, MDH2 and PRDX6 as potential candidates of interest as they all displayed statistically significant changes in CypD interaction following mPT. However, among them only HSPE1 and PRDX6 were corroborated by the KO cells data. The KO data did not provide any new potential mPTP candidates. Both HSPE1 and PRDX6 showed increased CypD interaction following mPT under CsA conditions in WT cells and increased CypD interaction following mPT under DMSO conditions in KO cells. This fits into my hypothesis where the KO cells has shifted to a mPT pathway similar to a state where CsA is bound to CypD in WT cells.

While both HSPE1 and PRDX6 are corroborated in both studies, the case for HSPE1 was clearly much stronger. PRDX6 only showed up in a specific type of analysis – applying multiple t-test with Bonferroni's correction to individual proteins, whereas HSPE1 showed consistent statistically significant changes following mPT for all types of analysis used here. This means that HSPE1 was much more likely to be involved in mPTP than PRDX6 but the possibility of PRDX6 being involved in mPTP remains a likely case.

## **4.3 Conclusion**

Here I summarize all the analyses and draw the conclusion from the proteomics screen. However, before that is done, I will address the concerns and potential limitations of the screen which I discussed earlier in 3.3. These have been discussed in the previous section but their implication on the proteomics results must be discussed before any conclusion is drawn to avoid any biased or erroneous conclusions. After the known potential limitations are addressed and conclusions are drawn, I will discuss the open questions (old or new) regarding the mPTP that this project brings to my attention. These potential limitations existed due to a lack of resources and time for the project. However, they have been mitigated in various ways before the final proteomics screen was carried out. Furthermore, they were only potential limitations and the actual proteomics results showed that they did not manifest into actual limitations of the study.

### **4.3.1 Addressing potential limitations of the screen**

Before the screen was carried out, I outlined potential limitations that can affect the result of the screen either due to intrinsic properties of the experimental method or potential limitations in the set-up of experimental conditions. I will discuss the possible influence of these effect on the screen results before drawing conclusions about the mPTP from the proteomics results.

#### **4.3.1.1 KO cell line limitations**

One limitation lies within the CypD KO HEK293T cellular model. As shown earlier, the CypD KO HEK293T cell line did not respond to CsA treatment even after CypD had been re-expressed in the CRC assay. The only conclusion I could reach was that the KO cell line generation process had somehow altered the physiology of the KO cell line such that the CsA sensitive CypD mediated mPTP pathway was no longer utilised. However, CypD appeared to still be able to modulate the mPTP even when the CsA sensitive mPTP pathway was shut down as seen from the CRC results.

The result from the proteomics would confirm that the CsA sensitive mPTP pathway was inhibited in the KO cells when CypD was re-expressed. The proteomic results in the absence of CsA mimics that of those in the presence of CsA in the WT cells, and addition of CsA has no influence on the proteomics results when mPTP is considered.

However, while the proteomics results confirmed that the CsA sensitive mPTP pathway was inhibited in KO cells, it provided relatively weak support for the existence and mechanism of a CsA insensitive CypD mediated mPTP pathway. The problem with hypothesising the existence of such a pathway was that there has been no previous report of its existence despite numerous studies focusing on CypD and the mPTP. As such, I am still very cautious regarding its existence and maintain the possibility of considering it as a possible artefact.

The limitation discussed here regarding the KO cells is however not a major limitation of this study. I will be making most of the conclusion regarding the mPTP based on the WT cells data alone, and any conclusion from the KO cells data is made in context of its mPT behavioural shift. In fact, the CypD KO HEK293T cell proteomics data does not call into question any conclusions drawn from the WT HEK293T cell data and only supplement/support it. As such I am confident that there is no risk of drawing wrong conclusions as a result of the strange behaviour of the KO cell line.

#### **4.3.1.2 Fusion protein breakage**

An additional possible limitation was that of the CypD-TurboID fusion protein breaking up. As shown earlier, I discovered that CypD-TurboID had a tendency to break up in mitochondria. As discussed earlier, this presents two possible scenarios that could severely undermine the result of the screen.

The first was that the biotin labelling effect attributed to the CypD-TurboID fusion protein might be due to biotinylation activity from the broken off biotin ligase enzyme instead of the intact, whole fusion protein. If this was true, the proteomic results will show a relatively consistent level of biotinylation across all detected proteins. However, as I have shown earlier there was a clear and statistically significant group of proteins with higher biotinylation levels. Additionally, many of these proteins were also known CypD interactors. Hence this potential limitation did not materialize and can be ignored.

The second was that the effect the CypD-TurboID fusion protein have on mPTP regulation might be due to the broken off part of CypD instead of the whole, intact fusion protein. If this were true, I would expect that there would be no statistically significant change in the interaction level of any protein with CypD following mPTP or CsA addition since the biotinylation and CypD activity would have become disengaged. However, not only did I observe statistically significant changes following mPTP induction in several proteins, but they also contain some of the strongest mPTP candidates. As such, it is clear that this concern was not an issue for the final outcome and interpretation of the proteomic screen results.

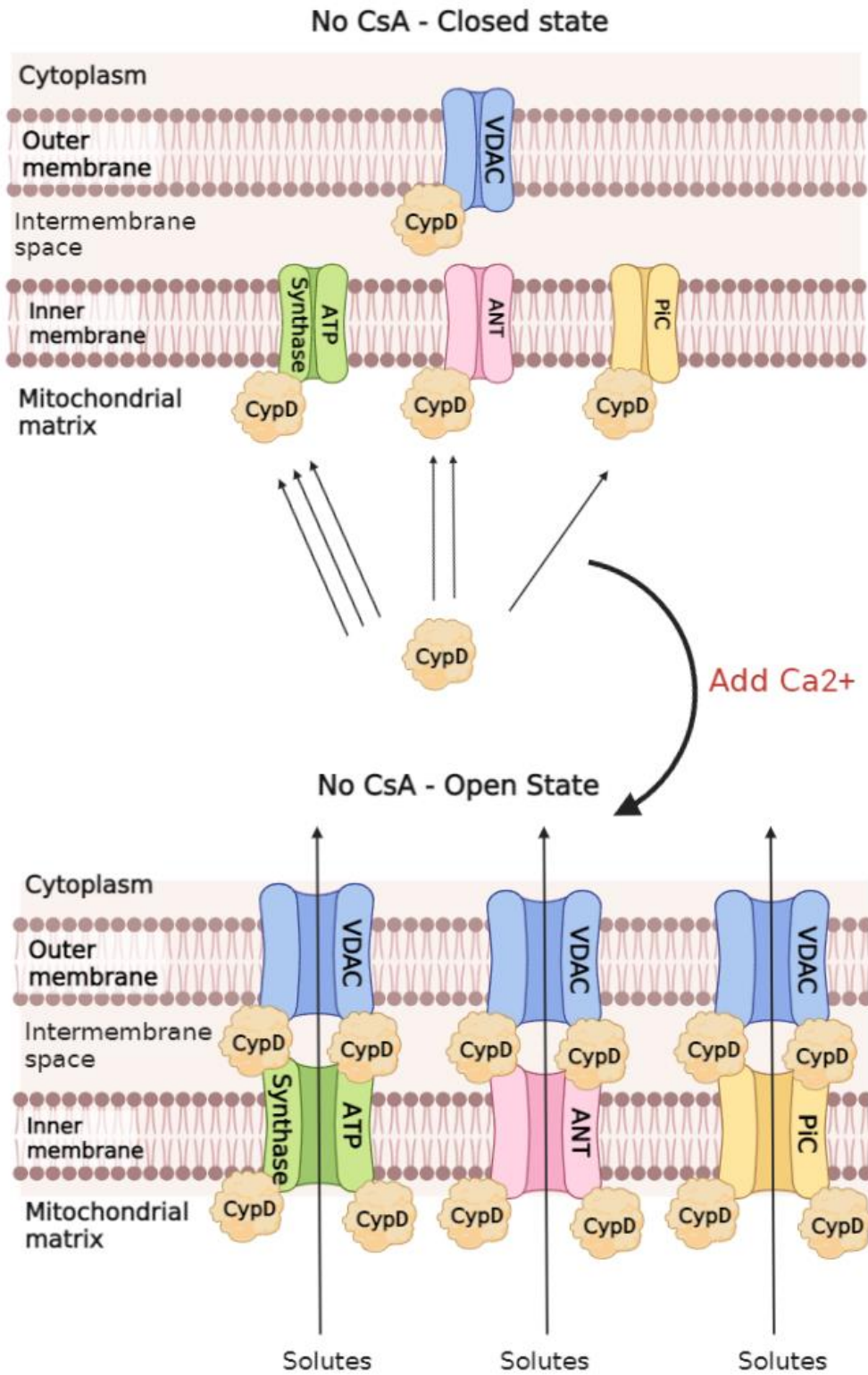


**Figure 4.11: Schematic for mPTP formation with no CsA present based on my data**

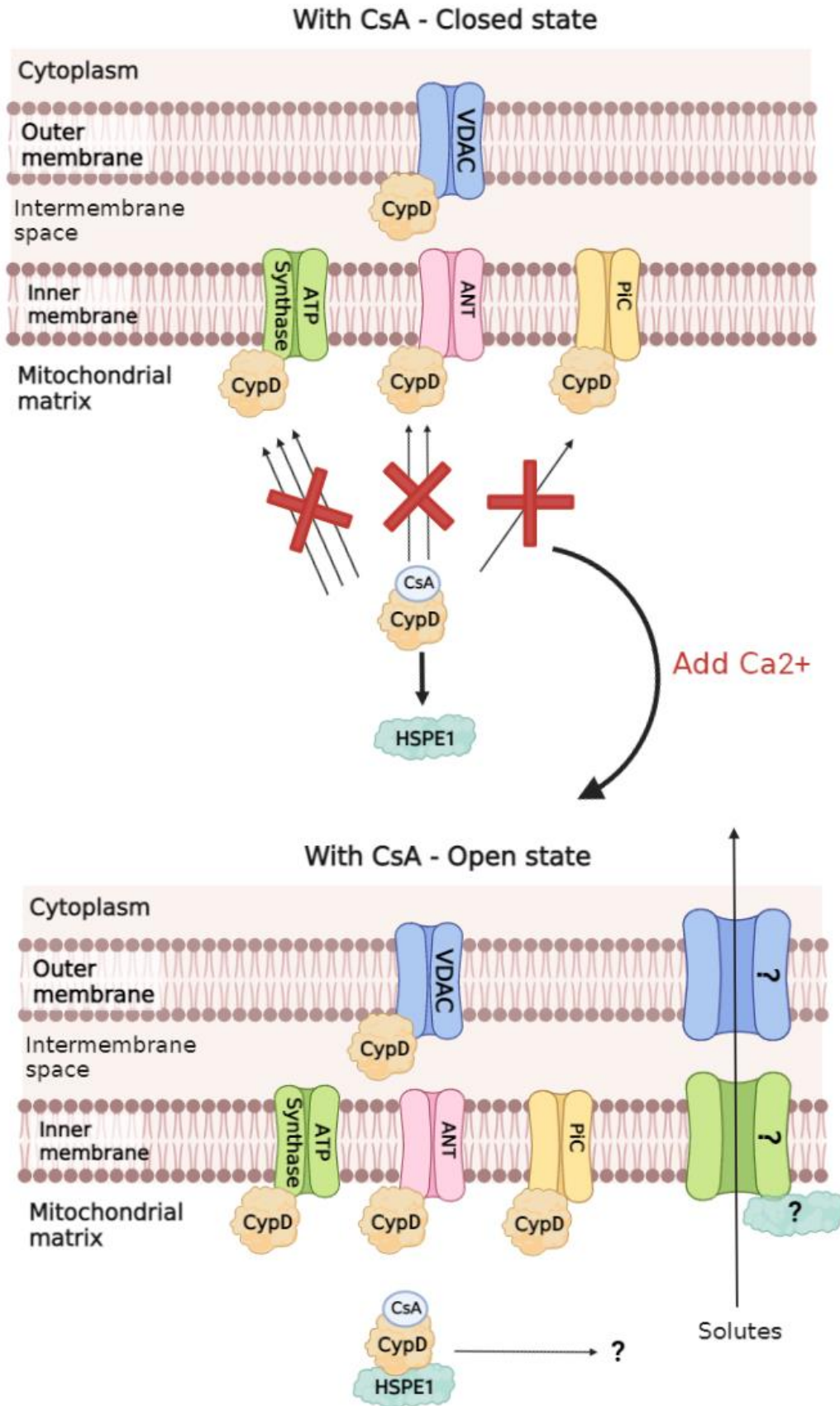


**Figure 4.12: Schematic for mPTP formation with CsA present based on my data**



The proteomics data revealed interesting insights into the CypD dependent mPTP opening process in the presence and absence of CsA. The graphical representation of these findings are detailed in Fig 4.12 and Fig 4.13.

### **4.3.2 New insights from the proteomics data**

Following detailed analysis of the proteomics data from WT and CypD KO HEK293T cells, the data allowed me to make some new conclusions regarding the mPTP channel identity and behaviour with high levels of confidence.

Fig 4.12 shows the pathway for CypD dependent mPTP formation in the absence of CsA. In essence, my data supports the multiple entity hypothesis of mPTP. I observed that CypD increases its interaction with the ATP Synthase, ANT, VDAC and PiC following Ca<sup>2+</sup> addition as a method of mPT induction. This implies that CypD regulates mPTP opening by turning all these proteins into mPTP channels. Hence, I am proposing that the mPTP is not a single channel but rather multiple different channels displaying similar characteristics and regulated by the same protein, CypD. If observed alone, the data here do not make a concrete case for this hypothesis. However, given the results of previous work as discussed in section 1.3 on the identity of the mPTP and the latest result in support of the existence of multiple mPTP channels (Carrer et al., 2021), it gives a logical explanation of the existing data. As discussed in section 1.3, the ATP Synthase, ANT and PiC have all shown to be able to modulate mPTP activity and have been suggested to form the IMM channel of the mPTP. However, their candidacy was dismissed when KO studies showed that mPTP persists in the absence of any one of them (Baines et al., 2007; Carroll et al., 2019; Kokoszka et al., 2004; Varanyuwatana & Halestrap, 2012). This was the classical view where a single mPTP channel has been sought. If the mPTP can be formed by multiple entities, dismissal of these candidates based on KO studies is no longer valid. If one then takes their candidacy to be accurate, which is heavily supported by large amounts of previous experimental data, the new proteomics data here ties everything together for providing evidence for the multiple channel hypothesis and leads to a resolution of seemingly conflicting results.

As such, the proteomics data here makes the case that the IMM channel of the mPTP can be formed by any of these 3 entities under regular conditions. This directly

answers one of the most contradictory questions in mPTP research – the identity of the mPTP channel itself.

Fig 4.13 shows the pathway for CypD dependent mPTP formation in the presence of CsA. Previously I concluded that the ATP Synthase, ANT and PiC can all form the mPTP IMM channel in a CypD dependent manner. Here I make an important conclusion on top of the previous one which is that our data only supports this when CsA is not present. In the presence of CsA, I did not observe any increase in the interaction of these 3 proteins with CypD. This would suggest that these 3 proteins only interact with CypD to form the mPTP when CsA is not present. This is supported by previous evidence which showed that the interaction between ATP Synthase and ANT is inhibited by CsA. In addition to this, the proteomics data show that CypD displays increased interaction with HSPE1 following mPT induction in the presence of CsA. Hence, I can conclude with certainty that CypD do not interact in a Ca<sup>2+</sup> dependent manner with ATP Synthase, ANT and PiC to form mPTP when bound to CsA, CypD instead shifts to interact with HSPE1. How and whether mPTP is initiated by CypD in the presence of CsA and whether HSPE1 has anything to do with this cannot be concluded with certainty from the proteomics data alone.

Finally, there might be an explanation for why the statistical significance was not consistent for changes in CypD interaction of these mPTP channels. Looking at the data, I observe very high levels of interaction between the candidate proteins and CypD even without mPTP induction. This could mean that the simple phenomenon of enzyme kinetics could cause the weakened statistical significance. As the mPTP channels get labelled with biotin, there will be less available sites on the channel protein for biotinylation, thus resulting in lower rate of biotinylation following mPTP induction by Ca<sup>2+</sup>. Hence even if there is a large increase in CypD interaction with the candidate proteins in this case, it might be difficult to observe due to limiting rates of labelling and might explain why the changes are not statistically significant in some cases for these mPTP components. This hypothesis also fits with the data where the ATP Synthase had the strongest statistical significance across all analyses. This might be because ATP Synthase is the largest protein among all the mPTP components with multiple subunits and can provide a larger number of available sites for biotinylation, resulting in a more robust change as observed from the data. Of course, it was entirely possible that the higher statistical significance of the ATP Synthase is due to it being

the preferential CypD interactor target, at least in this cellular model, as compared to other channel components.

As such, I can conclude that my original hypothesis for the project, that the mPTP is formed by multiple candidate proteins, holds true and is supported by my experimental data.

## 5 Perspectives

I do believe I have contributed some interesting findings to the field of mPTP research, especially in terms of helping to clarify the identity of the mPTP. However, the mPTP is still shrouded in many mysteries and lots of areas need more investigation for us to get a better understanding of the mPTP.

In addition to its support for the multiple protein hypothesis of the mPTP. There are also many new directions regarding the mPTP that my work can lead to. Furthermore, my work also re-raised the old question of the possible OMM component of the mPTP which also needs more work before it can be resolved.

### 5.1 OMM channel identity

While the proteomics data provided evidence for a good resolution to the IMM channel debate, it did not appear to provide any potential resolution to the molecular identity of the OMM channel. The proteomics data here would support the old hypothesis that VDAC is the OMM channel of the mPTP, this is also depicted in my diagram. The idea that VDAC makes up the OMM channel was a very old one but has been dismissed when experimental studies showed that mPTP can occur in the absence of VDAC, ruling out the possibility of VDAC as the only indispensable OMM channel of the mPTP. My study failed to detect any other OMM protein in addition to VDAC that could be contenders for the OMM channel. Additionally, there was also no study which shows alternative proteins can form the OMM channel in the event a particular protein has been knocked out, which is the case for ATP Synthase and ANT.

As such, a similar resolution to the OMM channel identity where multiple entities can form the channel still lacks experimental support.

In addition to having multiple OMM channels, another possible resolution to the VDAC experimental evidence might be that the OMM channel is not strictly necessary for the mPTP since mPTP can be observed in mitoplasts devoid of an OMM (Carrer et al., 2021; Šileikyte et al., 2011). However, this would also imply that the VDAC/OMM channel is

an optional addition to aid mPT but not a necessary one. Overall, more work is needed to get a better understanding of the mPTP OMM channel.

My data showed VDAC as the only OMM hit. As I have discussed earlier, it is surprising that any OMM component is returned at all. Nonetheless, in theory if more than one OMM channel exists, the proteomics data should detect all of them instead of just one. Hence more investigation is needed to clarify the OMM component. One possible approach is to return to the VDAC KO cells and investigate whether other OMM proteins is substituting for VDAC. This could come in terms of direct investigation of mPTP forming for OMM candidates such as Bax and Bak or possibly applying a CypD screen as I did in the project.

## **5.2 New research directions**

### **5.2.1 CypD/VDAC localisation**

Here the proteomics data showed high levels of interaction between CypD and VDAC which increased when mPT was induced by Ca<sup>2+</sup> in the absence of CsA. If VDAC is part of the mPTP channel, it would make sense to observe high level of interaction with CypD following mPTP opening as was the case here, since a CypD-IMM channel-VDAC complex can form and allow CypD to start labelling VDAC. However, what I have also observed was that there was a high level of interaction between VDAC and CypD under resting conditions before mPT occurs. This can be seen across all the proteomics analyses in 4.2 and is also statistically validated, the ANOVA + Tukey's HSD based interactor test repeatedly returned VDAC as a CypD interactor. This interaction has been previously reported long ago when ANT and VDAC were identified together as CypD interactors using an old method involving matrix gels (Martin Crompton et al., 1998). However, the hypothesis then was that VDAC was in complex with ANT which was then in complex with CypD, thus leading to the indirect pull down of VDAC in that screen.

In contrast, the proteomics data here suggest that there was high exposure of VDAC to CypD in intact mitochondrial membranes. This suggests a few possibilities about VDAC or CypD localisation that have not really been explored. VDAC is OMM localised while CypD is matrix localised, so while it makes sense for CypD to interact

with IMM components of the mPTP on their matrix exposed side under resting conditions, it is unlikely for CypD to interact with an OMM protein. This is especially pronounced given the nature of our experimental method where biotin labelling is carried out based on proximity and the biotin ligase enzyme needs physical access to VDAC before labelling can occur, ruling out the possibility of any cross-membrane detection. This means that either CypD is present in the intermembrane space or VDAC is physically exposed to mitochondrial matrix. Presence of CypD in the intermembrane space has not been reported but there is also no evidence against this possibility.

I also note that VDAC is the only OMM protein to show up in the analyses with a few other OMM proteins detected at only insignificant levels indicative of background noise, arguing against non-specific OMM labelling by a mistargeted fusion protein.

### **5.2.2 High levels of steady state CypD interaction**

The proteomics data showed that CypD already had very high levels of interaction with the ATP Synthase, ANT, VDAC and PiC even before mPT induction under resting conditions. This would explain why previous CypD interaction studies have been able to identify these proteins as CypD interactors and possible mPTP channels without having to induce mPT.

I can consider the phenomenon of transient mPTP activity for an explanation of this effect. High levels of CypD interaction with these channel components could be a result of CypD mediating transient mPTP opening during steady state conditions. During mPTP induction, more interaction between CypD and these components occurs, resulting in the observed results. Studies into this phenomenon would also be very interesting.

### **5.2.3 Priority of mPTP Interaction**

In the proteomics data I observed increases in ATP Synthase, ANT and PiC interaction with CypD following mPTP induction. There appears to be some differences in the relative level of increase and statistical robustness of these moves. While I reached

the conclusion that all of these increases are biologically relevant based on a combination of past work and our data, the question remains whether the difference in the relative level of increase in CypD interaction between these proteins following mPTP induction can be interpreted as real preference in CypD binding.

It is entirely possible that the resolution of the proteomics data is not strong enough to differentiate the exact order of preference for mPTP channel formation. However, given that the mPTP can be formed by multiple channels, the preference for particular proteins will become an open question. If the data here are accurate, we are possibly looking at ATP Synthase>ANT>PiC as the order of preference for mPTP formation but more investigations are certainly needed. However, more work is needed to further investigate the exact working of how the multiple proteins form the mPTP.

#### **5.2.4 CsA bound CypD and mPTP**

Perhaps the most intriguing question to emerge from the data was the relationship between CypD-CsA binding and CypD regulation of mPTP. It is normally assumed that CsA completely inhibits CypD's ability to regulate the mPTP. However, my data suggest the possible existence of CypD regulation of the mPTP via an alternative pathway when bound to CsA.

I observed consistent increases in interaction between CypD and HSPE1 (and PRDX6 with weaker statistical support) following mPTP induction under CsA conditions. Normally, if CypD increases its interaction with a particular protein following mPTP induction, it is evidence for that protein's involvement in the mPTP, this is reinforced by the increased interaction with leading mPTP candidates such as the ATP Synthase in my data. However, given that this increase only happens in the presence of CsA or CsA like conditions in the KO cells, it casts doubt on HSPE1 playing a role in mPT, unless a CsA insensitive CypD dependent pathway exists. Further experimental validation is required to clarify this intriguing possibility.

### **5.2.5 CsA mimicking effect from KO cells**

As discussed in section 3, the BE22 CypD KO cells appears to have reached an equilibrium state where the CsA sensitive mPTP pathway was inhibited and a CsA insensitive CypD mediated mPTP pathway was now preferred. This is the hypothesis supported by the proteomics data. As can be seen in Fig 4.13, when CsA was present in WT cells, CypD no longer increases its interaction with the ATP Synthase, ANT, PiC and VDAC following mPTP induction. Instead, CypD increases its binding with HSPE1. The exact same interaction pattern is observed in BE22 CypD KO cells without the addition of any CsA. Furthermore, CsA had no effect on mPTP induced proteomic changes in these KO cells.

I am confident that the KO cells represent shift away from CsA sensitive mPTP. However, as discussed above when it comes to the presence of CsA insensitive CypD mediated mPTP this conclusion is in conflict with our current understanding of the mPTP and requires further validation.

### **5.2.6 CsA insensitive CypD mediated mPTP pathway**

A new area that is worth investigating is the possibility of CypD mediated mPTP in the presence of CsA. My data has provided a very straightforward path here with the discovery that HSPE1 increases interaction with CypD following mPTP opening. Hence, we can do some genetic manipulation of HSPE1 (KD/KO) in the presence of CsA and observe if mPTP activity changes. If it does not, it likely means that CypD does not mediate mPTP in the presence of CsA. This would cast more doubt on the physiological relevance of the KO cell model and increase the likelihood that the response to CypD re-expression in the KO cell line is an artefact. On the other hand, if HSPE1 does modulate mPTP activity, it could open up a whole new area of mPTP research.

### **5.2.7 Defining features of the mPTP channels**

Since the CypD mediated mPTP can be formed by multiple candidate proteins, it immediately begs the question of what is a common feature/defining characteristic of



these proteins that allows them to act as mPTP channels. This would probably involve structural studies of interaction between these candidates and CypD. It is not clear how CypD mediates changes in these proteins to form the mPTP and whether the same pore forming process occurs for every possible channel.

### **5.2.8 Investigating the mPTP pathway in KO cells**

It will be very interesting to investigate the root cause of the change in mPTP regulation in the CypD KO CRISPR cell lines. This is a very strange phenomenon as the plasmid expression ensures no difference in CypD itself but the mPTP pathway have undergone a fundamental shift. The effect of this is unlikely to come from genetic changes due to CRISPR off-target effects as I have discussed earlier. As such, I have formulated some other hypothesis for this phenomenon mostly based upon the concept of cellular adaptation.

The first hypothesis is that the long-term absence of CypD has caused the cell line to undergo potential metabolic adaptation away from CypD mediated mPTP. As discussed earlier, CypD KO has been shown to cause changes in key metabolic enzymes and pathways involved in the TCA cycle, pyruvate metabolism and branch chain amino acid metabolism. The mPTP is also known to be regulated by metabolic substrates and products including ADP/ATP. However, what is missing is the link between how these metabolic changes caused by the absence of CypD might feedback onto the interaction of CypD and mPTP itself.

A potential starting point could be to investigate whether any of the metabolic changes observed in CypD KO models as described in (Elrod et al., 2010; Menazza et al., 2013) affects the mPTP itself. This should be relatively straight forward, and we can study how inhibition/upregulation of specific metabolic enzymes implicated in CypD KO might affect mPTP assay readouts such as the CRC. But it is important to note that what I observed in in my CypD HEK293T KO cells was missing interaction between CypD and mPTP. As such, it will also be important to investigate how metabolic changes can affect this. This could involve manipulating specific metabolic pathways and observing whether CsA continues to have any effect on mPTP assay readouts. Finally, it could also be interesting to characterise the specific metabolic changes in the HEK293T CypD KO cell lines I created. This would involve metabolomic

experiments and potentially measuring several of the monoclonal cell lines to determine if any specific metabolic change is consistently observed.

The second hypothesis is that the monoclonal cell line generation process is responsible for this change. During monoclonal cell line selection, there is actually a high bias for robust growing cells and stress resistant cells due to the nature of the process. The cells undergo multiple different treatment steps before they are grown in plates and I observe <10% survivability and growth of these cells following CRISPR treatment in 3 months' time. Only cells that are resistant to stress and possibly cell death with a good growth rate will even be available for testing of potential KO. This difference might have arisen from single cell differences possibly stemming from CRISPR induced changes. When this happens, following expansion of the monoclonal cell line, the final CypD KO cell line generated will have a host of additional adaptation differences instead of just being a CypD KO line. These host of adaptation changes cannot be reversed simply by CypD re-expression, hence leading to the unexpected CypD rescue effects I observed in the KO cells.

However, I do not have any straightforward ideas for investigating this phenomenon. The difficulty lies with the fact that there is no obvious path to investigate this change. One possibility is to do a large-scale proteomics study to quantify proteome difference between the CypD and the WT cell line. Alternatively, other screening approaches such as whole genome/RNA sequencing and cross comparison between the WT and CypD KO cell lines are possible. The lack of a logical hypothesis means that only screening approaches are possible. These studies are costly, time consuming and do not guarantee any results, which makes any potential investigation here difficult. Apart from curiosity about the reason of the anomalous PTP, I can also envisage that this phenomenon is underlying something genuinely novel regarding the mPTP that we do not yet understand.

## 6 References

- Abramov, A. Y., Fraley, C., Diao, C. T., Winkfein, R., Colicos, M. A., Duchen, M. R., French, R. J., & Pavlov, E. (2007). Targeted polyphosphatase expression alters mitochondrial metabolism and inhibits calcium-dependent cell death. *Proceedings of the National Academy of Sciences*, *104*(46), 18091–18096. <https://doi.org/10.1073/PNAS.0708959104>
- Agarwal, A., Wu, P.-H., Hughes, E. G., Fukaya, M., Tischfield, M. A., Langseth, A. J., Wirtz, D., & Bergles, D. E. (2017). Transient Opening of the Mitochondrial Permeability Transition Pore Induces Microdomain Calcium Transients in Astrocyte Processes. *Neuron*, *93*(3), 587-605.e7. <https://doi.org/10.1016/j.neuron.2016.12.034>
- Alavian, K. N., Beutner, G., Lazrove, E., Sacchetti, S., Park, H. A., Licznerski, P., Li, H., Nabili, P., Hockensmith, K., Graham, M., Porter, G. A., & Jonas, E. A. (2014). An uncoupling channel within the c-subunit ring of the F1F<sub>0</sub> ATP synthase is the mitochondrial permeability transition pore. *Proceedings of the National Academy of Sciences of the United States of America*, *111*(29), 10580–10585. <https://doi.org/10.1073/pnas.1401591111>
- Alcalá, S., Klee, M., Fernández, J., Fleischer, A., & Pimentel-Muiños, F. X. (2007). A high-throughput screening for mammalian cell death effectors identifies the mitochondrial phosphate carrier as a regulator of cytochrome c release. *Oncogene* *2008 27:1*, *27*(1), 44–54. <https://doi.org/10.1038/sj.onc.1210600>
- Altschuld, R. A., Hohl, C. M., Castillo, L. C., Garleb, A. A., Starling, R. C., & Brierley, G. P. (1992). Cyclosporin inhibits mitochondrial calcium efflux in isolated adult rat ventricular cardiomyocytes. <https://doi.org/10.1152/Ajphheart.1992.262.6.H1699>, *262*(6 31-6).
- Angeli, S., Foulger, A., Chamoli, M., Peiris, T. H., Gerencser, A., Shahmirzadi, A. A., Andersen, J., & Lithgow, G. (2021). The mitochondrial permeability transition pore activates the mitochondrial unfolded protein response and promotes aging. *ELife*, *10*, e63453. <https://doi.org/10.7554/eLife.63453>

- Angelin, A., Bonaldo, P., & Bernardi, P. (2008). Altered threshold of the mitochondrial permeability transition pore in Ullrich congenital muscular dystrophy. *Biochimica et Biophysica Acta - Bioenergetics*, 1777(7–8), 893–896. <https://doi.org/10.1016/j.bbabi.2008.03.026>
- Antoniell, M., Jones, K., Antonucci, S., Spolaore, B., Fogolari, F., Petronilli, V., Giorgio, V., Carraro, M., Di Lisa, F., Forte, M., Szabó, I., Lippe, G., & Bernardi, P. (2018). The unique histidine in OSCP subunit of F-ATP synthase mediates inhibition of the permeability transition pore by acidic pH. *EMBO Reports*, 19(2), 257–268. <https://doi.org/10.15252/embr.201744705>
- Argaud, L., Gateau-Roesch, O., Raissy, O., Loufouat, J., Robert, D., & Ovize, M. (2005). Postconditioning inhibits mitochondrial permeability transition. *Circulation*, 111(2), 194–197. <https://doi.org/10.1161/01.CIR.0000151290.04952.3B>
- Assaly, R., De Tassigny, A. D. A., Paradis, S., Jacquin, S., Berdeaux, A., & Morin, D. (2012). Oxidative stress, mitochondrial permeability transition pore opening and cell death during hypoxia-reoxygenation in adult cardiomyocytes. *European Journal of Pharmacology*, 675(1–3), 6–14. <https://doi.org/10.1016/j.ejphar.2011.11.036>
- Azzolin, L., von Stockum, S., Basso, E., Petronilli, V., Forte, M. A., & Bernardi, P. (2010). The mitochondrial permeability transition from yeast to mammals. In *FEBS Letters* (Vol. 584, Issue 12, pp. 2504–2509). <https://doi.org/10.1016/j.febslet.2010.04.023>
- Bagur, R., & Hajnóczky, G. (2017). Intracellular Ca<sup>2+</sup> Sensing: Its Role in Calcium Homeostasis and Signaling. *Molecular Cell*, 66(6), 780–788. <https://doi.org/10.1016/j.molcel.2017.05.028>
- Baines, C. P. (2009). The molecular composition of the mitochondrial permeability transition pore. In *Journal of Molecular and Cellular Cardiology* (Vol. 46, Issue 6, pp. 850–857). Academic Press. <https://doi.org/10.1016/j.yjmcc.2009.02.007>
- Baines, C. P., & Gutiérrez-Aguilar, M. (2018). The still uncertain identity of the channel-forming unit(s) of the mitochondrial permeability transition pore. *Cell Calcium*, 73, 121–130. <https://doi.org/10.1016/J.CECA.2018.05.003>

- Baines, C. P., Kaiser, R. A., Purcell, N. H., Blair, N. S., Osinska, H., Hambleton, M. A., Brunskill, E. W., Sayen, M. R., Gottlieb, R. A., Dorn, G. W., Bobbins, J., & Molkentin, J. D. (2005). Loss of cyclophilin D reveals a critical role for mitochondrial permeability transition in cell death. *Nature*, *434*(7033), 658–662. <https://doi.org/10.1038/nature03434>
- Baines, C. P., Kaiser, R. A., Sheiko, T., Craigen, W. J., & Molkentin, J. D. (2007). Voltage-dependent anion channels are dispensable for mitochondrial-dependent cell death. *Nature Cell Biology*, *9*(5), 550–555. <https://doi.org/10.1038/ncb1575>
- Basso, E., Petronilli, V., Forte, M. A., & Bernardi, P. (2008). Phosphate is essential for inhibition of the mitochondrial permeability transition pore by cyclosporin A and by cyclophilin D ablation. *Journal of Biological Chemistry*, *283*(39), 26307–26311. <https://doi.org/10.1074/jbc.C800132200>
- Bauer, T. M., & Murphy, E. (2020). Role of mitochondrial calcium and the permeability transition pore in regulating cell death. In *Circulation Research* (Vol. 126, pp. 280–293). Lippincott Williams and Wilkins. <https://doi.org/10.1161/CIRCRESAHA.119.316306>
- Bernardi, P. (1999). Mitochondrial transport of cations: Channels, exchangers, and permeability transition. In *Physiological Reviews* (Vol. 79, Issue 4, pp. 1127–1155). American Physiological Society. <https://doi.org/10.1152/physrev.1999.79.4.1127>
- Bernardi, P. (2013). The mitochondrial permeability transition pore: A mystery solved? *Frontiers in Physiology*, *4* MAY, 95. <https://doi.org/10.3389/fphys.2013.00095>
- Bernardi, P. (2018). Why F-ATP synthase remains a strong candidate as the mitochondrial permeability transition pore. *Frontiers in Physiology*, *9*(NOV), 1543. <https://doi.org/10.3389/fphys.2018.01543>
- Bernardi, P., & Forte, M. (2015). Commentary: SPG7 is an essential and conserved component of the mitochondrial permeability transition pore. *Frontiers in Physiology*, *6*(NOV), 320. <https://doi.org/10.3389/fphys.2015.00320>
- Bernardi, P., Krauskopf, A., Basso, E., Petronilli, V., Blalchy-Dyson, E., Di Lisa, F., &

- Forte, M. A. (2006). The mitochondrial permeability transition from in vitro artifact to disease target. In *FEBS Journal* (Vol. 273, Issue 10, pp. 2077–2099). John Wiley & Sons, Ltd. <https://doi.org/10.1111/j.1742-4658.2006.05213.x>
- Beutner, G., Alanzalon, R. E., & Porter, G. A. (2017). Cyclophilin D regulates the dynamic assembly of mitochondrial ATP synthase into synthasomes. *Scientific Reports*, 7(1), 1–12. <https://doi.org/10.1038/s41598-017-14795-x>
- Beutner, G., Alavian, K. N., Jonas, E. A., & Porter, G. A. J. (2017). The Mitochondrial Permeability Transition Pore and ATP Synthase. *Handbook of Experimental Pharmacology*, 240, 21–46. [https://doi.org/10.1007/164\\_2016\\_5](https://doi.org/10.1007/164_2016_5)
- Bezanilla, F. (2008). Ion Channels: From Conductance to Structure. *Neuron*, 60(3), 456–468. <https://doi.org/10.1016/J.NEURON.2008.10.035>
- Bhosale, G., & Duchen, M. R. (2019). Investigating the Mitochondrial Permeability Transition Pore in Disease Phenotypes and Drug Screening. *Current Protocols in Pharmacology*, 85(1), e59. <https://doi.org/10.1002/cpph.59>
- Bhosale, G., Sharpe, J. A., Sundier, S. Y., & Duchen, M. R. (2015). Calcium signaling as a mediator of cell energy demand and a trigger to cell death. *Annals of the New York Academy of Sciences*, 1350(1), 107. <https://doi.org/10.1111/NYAS.12885>
- Bonora, M., Wieckowski, M. R., Chinopoulos, C., Kepp, O., Kroemer, G., Galluzzi, L., & Pinton, P. (2014). Molecular mechanisms of cell death: central implication of ATP synthase in mitochondrial permeability transition. *Oncogene* 2015 34:12, 34(12), 1475–1486. <https://doi.org/10.1038/onc.2014.96>
- Bonora, Massimo, Bononi, A., De Marchi, E., Giorgi, C., Lebedzinska, M., Marchi, S., Patergnani, S., Rimessi, A., Suski, J. M., Wojtala, A., Wieckowski, M. R., Kroemer, G., Galluzzi, L., & Pinton, P. (2013). Role of the c subunit of the FO ATP synthase in mitochondrial permeability transition. *Cell Cycle*, 12(4), 674–683. <https://doi.org/10.4161/cc.23599>
- Bonora, Massimo, Giorgi, C., & Pinton, P. (2021). Molecular mechanisms and consequences of mitochondrial permeability transition. *Nature Reviews Molecular Cell Biology* 2021 23:4, 23(4), 266–285.

<https://doi.org/10.1038/s41580-021-00433-y>

Bonora, Massimo, Morganti, C., Morciano, G., Pedriali, G., Lebedzinska-Arciszewska, M., Aquila, G., Giorgi, C., Rizzo, P., Campo, G., Ferrari, R., Kroemer, G., Wieckowski, M. R., Galluzzi, L., & Pinton, P. (2017). Mitochondrial permeability transition involves dissociation of F<sub>1</sub>F<sub>0</sub> ATP synthase dimers and C-ring conformation. *EMBO Reports*, *18*(7), 1077–1089.

<https://doi.org/10.15252/embr.201643602>

Borutaite, V., Jekabsone, A., Morkuniene, R., & Brown, G. C. (2003). Inhibition of mitochondrial permeability transition prevents mitochondrial dysfunction, cytochrome c release and apoptosis induced by heart ischemia. *Journal of Molecular and Cellular Cardiology*, *35*(4), 357–366.

[https://doi.org/10.1016/S0022-2828\(03\)00005-1](https://doi.org/10.1016/S0022-2828(03)00005-1)

Boyman, L., Coleman, A. K., Zhao, G., Wescott, A. P., Joca, H. C., Greiser, B. M., Karbowski, M., Ward, C. W., & Lederer, W. J. (2019). Dynamics of the mitochondrial permeability transition pore: Transient and permanent opening events. *Archives of Biochemistry and Biophysics*, *666*, 31–39.

<https://doi.org/10.1016/j.abb.2019.03.016>

Branon, T. C., Bosch, J. A., Sanchez, A. D., Udeshi, N. D., Svinkina, T., Carr, S. A., Feldman, J. L., Perrimon, N., & Ting, A. Y. (2018). Efficient proximity labeling in living cells and organisms with TurboID. *Nature Biotechnology*, *36*(9), 880–887.

<https://doi.org/10.1038/nbt.4201>

Briston, T., Lewis, S., Koglin, M., Mistry, K., Shen, Y., Hartopp, N., Katsumata, R., Fukumoto, H., Duchen, M. R., Szabadkai, G., Staddon, J. M., Roberts, M., & Powney, B. (2016). Identification of ER-000444793, a Cyclophilin D-independent inhibitor of mitochondrial permeability transition, using a high-throughput screen in cryopreserved mitochondria. *Scientific Reports*, *6*(1), 37798.

<https://doi.org/10.1038/srep37798>

Briston, T., Roberts, M., Lewis, S., Powney, B., Staddon, J. M., Szabadkai, G., & Duchen, M. R. (2017). Mitochondrial permeability transition pore: Sensitivity to opening and mechanistic dependence on substrate availability. *Scientific Reports*, *7*(1), 10492. <https://doi.org/10.1038/s41598-017-10673-8>

- Briston, T., Selwood, D. L., Szabadkai, G., & Duchen, M. R. (2018). Mitochondrial Permeability Transition: A Molecular Lesion with Multiple Drug Targets. *Trends in Pharmacological Sciences*, 0(0). <https://doi.org/10.1016/j.tips.2018.11.004>
- Brustovetsky, N., & Klingenberg, M. (1996). Mitochondrial ADP/ATP carrier can be reversibly converted into a large channel by Ca<sup>2+</sup>. *Biochemistry*, 35(26), 8483–8488. <https://doi.org/10.1021/bi960833v>
- Brustovetsky, N., Tropschug, M., Heimpel, S., Heidkämper, D., & Klingenberg, M. (2002). A large Ca<sup>2+</sup>-dependent channel formed by recombinant ADP/ATP carrier from *Neurospora crassa* resembles the mitochondrial permeability transition pore. *Biochemistry*, 41(39), 11804–11811. <https://doi.org/10.1021/bi0200110>
- Büttner, S., Ruli, D., Vögtle, F.-N., Galluzzi, L., Moitzi, B., Eisenberg, T., Kepp, O., Habernig, L., Carmona-Gutierrez, D., Rockenfeller, P., Laun, P., Breitenbach, M., Khoury, C., Fröhlich, K.-U., Rechberger, G., Meisinger, C., Kroemer, G., & Madeo, F. (2011). A yeast BH3-only protein mediates the mitochondrial pathway of apoptosis. *The EMBO Journal*, 30(14), 2779–2792. <https://doi.org/10.1038/EMBOJ.2011.197>
- Carraro, M., Carrer, A., Urbani, A., & Bernardi, P. (2020). Molecular nature and regulation of the mitochondrial permeability transition pore(s), drug target(s) in cardioprotection. *Journal of Molecular and Cellular Cardiology*, 144, 76–86. <https://doi.org/10.1016/j.yjmcc.2020.05.014>
- Carraro, M., Giorgio, V., Sileikyte, J., Sartori, G., Forte, M., Lippe, G., Zoratti, M., Szabò, I., & Bernardi, P. (2014). Channel formation by yeast F-ATP synthase and the role of dimerization in the mitochondrial permeability transition. *Journal of Biological Chemistry*, 289(23), 15980–15985. <https://doi.org/10.1074/jbc.C114.559633>
- Carrer, A., Tommasin, L., Šileikytė, J., Ciscato, F., Filadi, R., Urbani, A., Forte, M., Rasola, A., Szabò, I., Carraro, M., & Bernardi, P. (2021). Defining the molecular mechanisms of the mitochondrial permeability transition through genetic manipulation of F-ATP synthase. *Nature Communications* 2021 12:1, 12(1), 1–12. <https://doi.org/10.1038/s41467-021-25161-x>



- Carroll, J., He, J., Ding, S., Fearnley, I. M., & Walker, J. E. (2019). Persistence of the permeability transition pore in human mitochondria devoid of an assembled ATP synthase. *Proceedings of the National Academy of Sciences of the United States of America*, *116*(26), 12816–12821. <https://doi.org/10.1073/pnas.1904005116>
- Chelli, B., Falleni, A., Salvetti, F., Gremigni, V., Lucacchini, A., & Martini, C. (2001). Peripheral-type benzodiazepine receptor ligands: Mitochondrial permeability transition induction in rat cardiac tissue. *Biochemical Pharmacology*, *61*(6), 695–705. [https://doi.org/10.1016/S0006-2952\(00\)00588-8](https://doi.org/10.1016/S0006-2952(00)00588-8)
- Chen, X., Zaro, J. L., & Shen, W. C. (2013). Fusion Protein Linkers: Property, Design and Functionality. *Advanced Drug Delivery Reviews*, *65*(10), 1357. <https://doi.org/10.1016/J.ADDR.2012.09.039>
- Chinopoulos, C. (2018). Mitochondrial permeability transition pore: Back to the drawing board. *Neurochemistry International*, *117*, 49–54. <https://doi.org/10.1016/J.NEUINT.2017.06.010>
- Chinopoulos, C., Konràd, C., Kiss, G., Metelkin, E., Töröcsik, B., Zhang, S. F., & Starkov, A. A. (2011). Modulation of F<sub>0</sub>F<sub>1</sub>-ATP synthase activity by cyclophilin D regulates matrix adenine nucleotide levels. *FEBS Journal*, *278*(7), 1112–1125. <https://doi.org/10.1111/j.1742-4658.2011.08026.x>
- Cho, K. F., Branon, T. C., Udeshi, N. D., Myers, S. A., Carr, S. A., & Ting, A. Y. (2020). Proximity labeling in mammalian cells with TurboID and split-TurboID. *Nature Protocols* *2020 15:12*, *15*(12), 3971–3999. <https://doi.org/10.1038/s41596-020-0399-0>
- Chouchani, E. T., Pell, V. R., Gaude, E., Aksentijević, D., Sundier, S. Y., Robb, E. L., Logan, A., Nadtochiy, S. M., Ord, E. N. J., Smith, A. C., Eyassu, F., Shirley, R., Hu, C. H., Dare, A. J., James, A. M., Rogatti, S., Hartley, R. C., Eaton, S., Costa, A. S. H., ... Murphy, M. P. (2014). Ischaemic accumulation of succinate controls reperfusion injury through mitochondrial ROS. *Nature*, *515*(7527), 431–435. <https://doi.org/10.1038/nature13909>
- Costantini, P., Colonna, R., & Bernardi, P. (1998). Induction of the mitochondrial permeability transition by N-ethylmaleimide depends on secondary oxidation of

critical thiol groups. Potentiation by copper-ortho-phenanthroline without dimerization of the adenine nucleotide translocase. *Biochimica et Biophysica Acta (BBA) - Bioenergetics*, 1365(3), 385–392. [https://doi.org/10.1016/S0005-2728\(98\)00090-5](https://doi.org/10.1016/S0005-2728(98)00090-5)

CROMPTON, M. (1999). The mitochondrial permeability transition pore and its role in cell death. *Biochemical Journal*, 341(2), 233–249. <https://doi.org/10.1042/bj3410233>

Crompton, M., Ellinger, H., & Costi, A. (1988). Inhibition by cyclosporin A of a Ca<sup>2+</sup>-dependent pore in heart mitochondria activated by inorganic phosphate and oxidative stress. *Biochemical Journal*, 255(1), 357–360. </pmc/articles/PMC1135230/?report=abstract>

Crompton, Martin, Virji, S., & Ward, J. M. (1998). Cyclophilin-D binds strongly to complexes of the voltage-dependent anion channel and the adenine nucleotide translocase to form the permeability transition pore. *European Journal of Biochemistry*, 258(2), 729–735. <https://doi.org/10.1046/j.1432-1327.1998.2580729.x>

Cung, T.-T., Morel, O., Cayla, G., Rioufol, G., Garcia-Dorado, D., Angoulvant, D., Bonnefoy-Cudraz, E., Guérin, P., Elbaz, M., Delarche, N., Coste, P., Vanzetto, G., Metge, M., Aupetit, J.-F., Jouve, B., Motreff, P., Tron, C., Labeque, J.-N., Steg, P. G., ... Ovize, M. (2015). Cyclosporine before PCI in Patients with Acute Myocardial Infarction. *New England Journal of Medicine*, 373(11), 1021–1031. <https://doi.org/10.1056/nejmoa1505489>

Davidson, S. M., Adameová, A., Barile, L., Cabrera-Fuentes, H. A., Lazou, A., Pagliaro, P., Stensløkken, K. O., & Garcia-Dorado, D. (2020). Mitochondrial and mitochondrial-independent pathways of myocardial cell death during ischaemia and reperfusion injury. *Journal of Cellular and Molecular Medicine*, 24(7), 3795–3806. <https://doi.org/10.1111/JCMM.15127>

Davidson, S. M., Arjun, S., Basalay, M. V., Bell, R. M., Bromage, D. I., Bøtker, H. E., Carr, R. D., Cunningham, J., Ghosh, A. K., Heusch, G., Ibanez, B., Kleinbongard, P., Lecour, S., Maddock, H., Ovize, M., Walker, M., Wiart, M., & Yellon, D. M. (2018). The 10th Biennial Hatter Cardiovascular Institute

workshop: cellular protection—evaluating new directions in the setting of myocardial infarction, ischaemic stroke, and cardio-oncology. *Basic Research in Cardiology* 2018 113:6, 113(6), 1–11. <https://doi.org/10.1007/S00395-018-0704-Z>

Davidson, S. M., Ferdinandy, P., Andreadou, I., Bøtker, H. E., Heusch, G., Ibáñez, B., Ovize, M., Schulz, R., Yellon, D. M., Hausenloy, D. J., & Garcia-Dorado, D. (2019). Multitarget Strategies to Reduce Myocardial Ischemia/Reperfusion Injury: JACC Review Topic of the Week. *Journal of the American College of Cardiology*, 73(1), 89–99. <https://doi.org/10.1016/J.JACC.2018.09.086>

Davidson, S. M., Foote, K., Kunuthur, S., Gosain, R., Tan, N., Tyser, R., Zhao, Y. J., Graeff, R., Ganesan, A., Duchon, M. R., Patel, S., & Yellon, D. M. (2015). Inhibition of NAADP signalling on reperfusion protects the heart by preventing lethal calcium oscillations via two-pore channel 1 and opening of the mitochondrial permeability transition pore. *Cardiovascular Research*, 108(3), 357–366. <https://doi.org/10.1093/CVR/CVV226>

Davidson, S. M., Hausenloy, D., Duchon, M. R., & Yellon, D. M. (2006). Signalling via the reperfusion injury signalling kinase (RISK) pathway links closure of the mitochondrial permeability transition pore to cardioprotection. *The International Journal of Biochemistry & Cell Biology*, 38(3), 414–419. <https://doi.org/10.1016/J.BIOCEL.2005.09.017>

De Marchi, E., Bonora, M., Giorgi, C., & Pinton, P. (2014). The mitochondrial permeability transition pore is a dispensable element for mitochondrial calcium efflux. *Cell Calcium*, 56(1), 1–13. <https://doi.org/10.1016/J.CECA.2014.03.004>

De Stefani, D., Raffaello, A., Teardo, E., Szabó, I., & Rizzuto, R. (2011). A forty-kilodalton protein of the inner membrane is the mitochondrial calcium uniporter. *Nature* 2011 476:7360, 476(7360), 336–340. <https://doi.org/10.1038/nature10230>

Doczi, J., Torocsik, B., Echaniz-Laguna, A., Camaret, B. M. de, Starkov, A., Starkova, N., Gál, A., Molnár, M. J., Kawamata, H., Manfredi, G., Adam-Vizi, V., & Chinopoulos, C. (2016). Alterations in voltage-sensing of the mitochondrial permeability transition pore in ANT1-deficient cells. *Scientific Reports* 2016 6:1,

6(1), 1–21. <https://doi.org/10.1038/srep26700>

- Doench, J. G., Fusi, N., Sullender, M., Hegde, M., Vaimberg, E. W., Donovan, K. F., Smith, I., Tothova, Z., Wilen, C., Orchard, R., Virgin, H. W., Listgarten, J., & Root, D. E. (2016). Optimized sgRNA design to maximize activity and minimize off-target effects of CRISPR-Cas9. *Nature Biotechnology*, *34*(2), 184–191. <https://doi.org/10.1038/nbt.3437>
- Du, H., Guo, L., Fang, F., Chen, D., Sosunov, A. A., McKhann, G. M., Yan, Y., Wang, C., Zhang, H., Molkentin, J. D., Gunn-Moore, F. J., Vonsattel, J. P., Arancio, O., Chen, J. X., & Yan, S. Du. (2008). Cyclophilin D deficiency attenuates mitochondrial and neuronal perturbation and ameliorates learning and memory in Alzheimer's disease. *Nature Medicine* 2008 *14*:10, *14*(10), 1097–1105. <https://doi.org/10.1038/nm.1868>
- Du, H., Guo, L., Zhang, W., Rydzewska, M., & Yan, S. (2011). Cyclophilin D deficiency improves mitochondrial function and learning/memory in aging Alzheimer disease mouse model. *Neurobiology of Aging*, *32*(3), 398–406. <https://doi.org/10.1016/j.neurobiolaging.2009.03.003>
- Du, H., & Yan, S. S. Du. (2010). Mitochondrial permeability transition pore in Alzheimer's disease: Cyclophilin D and amyloid beta. In *Biochimica et Biophysica Acta - Molecular Basis of Disease* (Vol. 1802, Issue 1, pp. 198–204). Elsevier. <https://doi.org/10.1016/j.bbadis.2009.07.005>
- Duchen, M. R., McGuinness, O., Brown, L. A., & Crompton, M. (1993). On the involvement of a cyclosporin A sensitive mitochondrial pore in myocardial reperfusion injury. *Cardiovascular Research*, *27*(10), 1790–1794. <https://doi.org/10.1093/CVR/27.10.1790>
- Eliseev, R. A., Malecki, J., Lester, T., Zhang, Y., Humphrey, J., & Gunter, T. E. (2009). Cyclophilin D interacts with Bcl2 and exerts an anti-apoptotic effect. *The Journal of Biological Chemistry*, *284*(15), 9692–9699. <https://doi.org/10.1074/jbc.M808750200>
- Elrod, J. W., Wong, R., Mishra, S., Vagnozzi, R. J., Sakthivel, B., Goonasekera, S. A., Karch, J., Gabel, S., Farber, J., Force, T., Brown, J. H., Murphy, E., & Molkentin, J. D. (2010). Cyclophilin D controls mitochondrial pore - Dependent

Ca<sup>2+</sup> exchange, metabolic flexibility, and propensity for heart failure in mice. *Journal of Clinical Investigation*, 120(10), 3680–3687.  
<https://doi.org/10.1172/JCI43171>

Elustondo, P A, Nichols, M., Negoda, A., Thirumaran, A., Zakharian, E., Robertson, G. S., & Pavlov, E. V. (2016). Mitochondrial permeability transition pore induction is linked to formation of the complex of ATPase C-subunit, polyhydroxybutyrate and inorganic polyphosphate. *Cell Death Discovery 2016* 2:1, 2(1), 1–9. <https://doi.org/10.1038/cddiscovery.2016.70>

Elustondo, Pia A., Angelova, P. R., Kawalec, M., Michalak, M., Kurcok, P., Abramov, A. Y., & Pavlov, E. V. (2013). Polyhydroxybutyrate Targets Mammalian Mitochondria and Increases Permeability of Plasmalemmal and Mitochondrial Membranes. *PLOS ONE*, 8(9), e75812.  
<https://doi.org/10.1371/JOURNAL.PONE.0075812>

Eum, H. A., Cha, Y. N., & Lee, S. M. (2007). Necrosis and apoptosis: sequence of liver damage following reperfusion after 60 min ischemia in rats. *Biochemical and Biophysical Research Communications*, 358(2), 500–505.  
<https://doi.org/10.1016/J.BBRC.2007.04.153>

Forte, M., Gold, B. G., Marracci, G., Chaudhary, P., Basso, E., Johnsen, D., Yu, X., Fowlkes, J., Bernardi, P., & Bourdette, D. (2007). Cyclophilin D inactivation protects axons in experimental autoimmune encephalomyelitis, an animal model of multiple sclerosis. *Proceedings of the National Academy of Sciences of the United States of America*, 104(18), 7558–7563.  
<https://doi.org/10.1073/pnas.0702228104>

Fournier, N., Ducet, G., & Crevat, A. (1987). Action of Cyclosporine on Mitochondrial Calcium Fluxes. In *Journal of Bioenergetics and Biomembranes* (Vol. 19, Issue 3).

Fujimoto, K., Chen, Y., Polonsky, K. S., & Dorn, G. W. (2010). Targeting cyclophilin D and the mitochondrial permeability transition enhances  $\beta$ -cell survival and prevents diabetes in Pdx1 deficiency. *Proceedings of the National Academy of Sciences of the United States of America*, 107(22), 10214–10219.  
[https://doi.org/10.1073/PNAS.0914209107/SUPPL\\_FILE/PNAS.200914209SI.P](https://doi.org/10.1073/PNAS.0914209107/SUPPL_FILE/PNAS.200914209SI.P)

DF

- Galluzzi, L., Vitale, I., Aaronson, S. A., Abrams, J. M., Adam, D., Agostinis, P., Alnemri, E. S., Altucci, L., Amelio, I., Andrews, D. W., Annicchiarico-Petruzzelli, M., Antonov, A. V., Arama, E., Baehrecke, E. H., Barlev, N. A., Bazan, N. G., Bernassola, F., Bertrand, M. J. M., Bianchi, K., ... Kroemer, G. (2018). Molecular mechanisms of cell death: recommendations of the Nomenclature Committee on Cell Death 2018. *Cell Death and Differentiation*, 25(3), 486–541. <https://doi.org/10.1038/S41418-017-0012-4>
- Gasteiger, E., Hoogland, C., Gattiker, A., Duvaud, S., Wilkins, M. R., Appel, R. D., & Bairoch, A. (2005). Protein Identification and Analysis Tools on the ExPASy Server. *The Proteomics Protocols Handbook*, 571–607. <https://doi.org/10.1385/1-59259-890-0:571>
- Gerle, C. (2016). On the structural possibility of pore-forming mitochondrial FoF1 ATP synthase. *Biochimica et Biophysica Acta - Bioenergetics*, 1857(8), 1191–1196. <https://doi.org/10.1016/j.bbabi.2016.03.008>
- Giorgio, V., Bisetto, E., Soriano, M. E., Dabbeni-Sala, F., Basso, E., Petronilli, V., Forte, M. A., Bernardi, P., & Lippe, G. (2009). Cyclophilin D modulates mitochondrial F0F1-ATP synthase by interacting with the lateral stalk of the complex. *The Journal of Biological Chemistry*, 284(49), 33982–33988. <https://doi.org/10.1074/jbc.M109.020115>
- Giorgio, V., Burchell, V., Schiavone, M., Bassot, C., Minervini, G., Petronilli, V., Argenton, F., Forte, M., Tosatto, S., Lippe, G., & Bernardi, P. (2017). Ca<sup>2+</sup> binding to F-ATP synthase  $\beta$  subunit triggers the mitochondrial permeability transition. *EMBO Reports*, 18(7), 1065–1076. <https://doi.org/10.15252/embr.201643354>
- Giorgio, V., von Stockum, S., Antoniel, M., Fabbro, A., Fogolari, F., Forte, M., Glick, G. D., Petronilli, V., Zoratti, M., Szabó, I., Lippe, G., & Bernardi, P. (2013). Dimers of mitochondrial ATP synthase form the permeability transition pore. *Proceedings of the National Academy of Sciences of the United States of America*, 110(15), 5887–5892. <https://doi.org/10.1073/pnas.1217823110>
- Gordon, M. D., & Nusse, R. (2006). Wnt signaling: Multiple pathways, multiple

- receptors, and multiple transcription factors. *Journal of Biological Chemistry*, 281(32), 22429–22433. <https://doi.org/10.1074/jbc.R600015200>
- Gray, M. W. (2012). Mitochondrial Evolution. *Cold Spring Harbor Perspectives in Biology*, 4(9). <https://doi.org/10.1101/CSHPERSPECT.A011403>
- Griffiths, E. J., & Halestrap, A. P. (1993). Protection by Cyclosporin A of Ischemia/Reperfusion-Induced Damage in Isolated Rat Hearts. *Journal of Molecular and Cellular Cardiology*, 25(12), 1461–1469. <https://doi.org/10.1006/JMCC.1993.1162>
- Gutiérrez-Aguilar, M., Douglas, D. L., Gibson, A. K., Domeier, T. L., Molkenin, J. D., & Baines, C. P. (2014). Genetic manipulation of the cardiac mitochondrial phosphate carrier does not affect permeability transition. *Journal of Molecular and Cellular Cardiology*, 72, 316–325. <https://doi.org/10.1016/j.yjmcc.2014.04.008>
- Hafner, A. V., Dai, J., Gomes, A. P., Xiao, C.-Y., Palmeira, C. M., Rosenzweig, A., & Sinclair, D. A. (2010). Regulation of the mPTP by SIRT3-mediated deacetylation of CypD at lysine 166 suppresses age-related cardiac hypertrophy. *Aging (Albany NY)*, 2(12), 914. <https://doi.org/10.18632/AGING.100252>
- Halestrap, A. P., Connern, C. P., Griffiths, E. J., & Kerr, P. M. (1997). Cyclosporin A binding to mitochondrial cyclophilin inhibits the permeability transition pore and protects hearts from ischaemia/reperfusion injury. *Detection of Mitochondrial Diseases*, 167–172. [https://doi.org/10.1007/978-1-4615-6111-8\\_25](https://doi.org/10.1007/978-1-4615-6111-8_25)
- Halestrap, Andrew P., & Pasdois, P. (2009). The role of the mitochondrial permeability transition pore in heart disease. In *Biochimica et Biophysica Acta - Bioenergetics* (Vol. 1787, Issue 11, pp. 1402–1415). Elsevier. <https://doi.org/10.1016/j.bbabbio.2008.12.017>
- Halestrap, Andrew P., Woodfield, K.-Y., & Connern, C. P. (1997). Oxidative Stress, Thiol Reagents, and Membrane Potential Modulate the Mitochondrial Permeability Transition by Affecting Nucleotide Binding to the Adenine Nucleotide Translocase \*. *Journal of Biological Chemistry*, 272(6), 3346–3354. <https://doi.org/10.1074/JBC.272.6.3346>

- Halestrap, Andrew P, & Richardson, A. P. (2015). The mitochondrial permeability transition: a current perspective on its identity and role in ischaemia/reperfusion injury. *Journal of Molecular and Cellular Cardiology*, 78, 129–141.  
<https://doi.org/10.1016/j.yjmcc.2014.08.018>
- Hausenloy, D., Duchen, M. R., & Yellon, D. M. (2003). Inhibiting mitochondrial permeability transition pore opening at reperfusion protects against ischaemia–reperfusion injury. *Cardiovascular Research*, 60(3), 617–625.  
<https://doi.org/10.1016/j.cardiores.2003.09.025>
- Hausenloy, D. J., Yellon, D. M., Mani-Babu, S., & Duchen, M. R. (2004). Preconditioning protects by inhibiting the mitochondrial permeability transition. *American Journal of Physiology-Heart and Circulatory Physiology*, 287(2), H841–H849. <https://doi.org/10.1152/ajpheart.00678.2003>
- Haworth, R. A., & Hunter, D. R. (1979). The Ca<sup>2+</sup>-induced membrane transition in mitochondria. II. Nature of the Ca<sup>2+</sup> trigger site. *Archives of Biochemistry and Biophysics*, 195(2), 460–467. [https://doi.org/10.1016/0003-9861\(79\)90372-2](https://doi.org/10.1016/0003-9861(79)90372-2)
- He, J., Carroll, J., Ding, S., Fearnley, I. M., & Walker, J. E. (2017). Permeability transition in human mitochondria persists in the absence of peripheral stalk subunits of ATP synthase. *Proceedings of the National Academy of Sciences of the United States of America*, 114(34), 9086–9091.  
<https://doi.org/10.1073/pnas.1711201114>
- He, J., Ford, H. C., Carroll, J., Ding, S., Fearnley, I. M., & Walker, J. E. (2017). Persistence of the mitochondrial permeability transition in the absence of subunit c of human ATP synthase. *Proceedings of the National Academy of Sciences of the United States of America*, 114(13), 3409–3414.  
<https://doi.org/10.1073/pnas.1702357114>
- He, L., & Lemasters, J. J. (2002). Regulated and unregulated mitochondrial permeability transition pores: a new paradigm of pore structure and function? *FEBS Letters*, 512(1–3), 1–7. [https://doi.org/10.1016/S0014-5793\(01\)03314-2](https://doi.org/10.1016/S0014-5793(01)03314-2)
- Hunter, D. R., Haworth, R. A., & Southard, J. H. (1976). Relationship between configuration, function, and permeability in calcium treated mitochondria. *Journal of Biological Chemistry*, 251(16), 5069–5077.



[https://doi.org/10.1016/s0021-9258\(17\)33220-9](https://doi.org/10.1016/s0021-9258(17)33220-9)

Hunter, Douglas R., & Haworth, R. A. (1979a). The Ca<sup>2+</sup>-induced membrane transition in mitochondria. I. The protective mechanisms. *Archives of Biochemistry and Biophysics*, 195(2), 453–459. [https://doi.org/10.1016/0003-9861\(79\)90371-0](https://doi.org/10.1016/0003-9861(79)90371-0)

Hunter, Douglas R., & Haworth, R. A. (1979b). The Ca<sup>2+</sup>-induced membrane transition in mitochondria. III. Transitional Ca<sup>2+</sup> release. *Archives of Biochemistry and Biophysics*, 195(2), 468–477. [https://doi.org/10.1016/0003-9861\(79\)90373-4](https://doi.org/10.1016/0003-9861(79)90373-4)

Ichas, F., & Mazat, J. P. (1998). From calcium signaling to cell death: Two conformations for the mitochondrial permeability transition pore. Switching from low- to high-conductance state. *Biochimica et Biophysica Acta - Bioenergetics*, 1366(1–2), 33–50. [https://doi.org/10.1016/S0005-2728\(98\)00119-4](https://doi.org/10.1016/S0005-2728(98)00119-4)

Izyumov, D. S., Avetisyan, A. V., Pletjushkina, O. Y., Sakharov, D. V., Wirtz, K. W., Chernyak, B. V., & Skulachev, V. P. (2004). “Wages of Fear”: transient threefold decrease in intracellular ATP level imposes apoptosis. *Biochimica et Biophysica Acta (BBA) - Bioenergetics*, 1658(1–2), 141–147. <https://doi.org/10.1016/J.BBABIO.2004.05.007>

Javadov, S. A., Clarke, S., Das, M., Griffiths, E. J., Lim, K. H. H., & Halestrap, A. P. (2003). Ischaemic Preconditioning Inhibits Opening of Mitochondrial Permeability Transition Pores in the Reperfused Rat Heart. *The Journal of Physiology*, 549(2), 513–524. <https://doi.org/10.1113/jphysiol.2003.034231>

Javadov, S., Jang, S., Parodi-Rullán, R., Khuchua, Z., & Kuznetsov, A. V. (2017). Mitochondrial permeability transition in cardiac ischemia-reperfusion: whether cyclophilin D is a viable target for cardioprotection? *Cellular and Molecular Life Sciences : CMLS*, 74(15), 2795–2813. <https://doi.org/10.1007/s00018-017-2502-4>

Jonas, E. A., Buchanan, J. A., & Kaczmarek, L. K. (1999). Prolonged activation of mitochondrial conductances during synaptic transmission. *Science*, 286(5443), 1347–1350. <https://doi.org/10.1126/SCIENCE.286.5443.1347/ASSET/F12AF57A-9978->

4C92-9C2F-292C71A94A1E/ASSETS/GRAPHIC/SE4597998004.JPEG

Jonas, E. A., Knox, R. J., & Kaczmarek, L. K. (1997). Giga-ohm seals on intracellular membranes: A technique for studying intracellular ion channels in intact cells. *Neuron*, *19*(1), 7–13. [https://doi.org/10.1016/S0896-6273\(00\)80343-8](https://doi.org/10.1016/S0896-6273(00)80343-8)

Jonas, E. A., Porter, G. A. J., Beutner, G., Mnatsakanyan, N., & Alavian, K. N. (2015). Cell death disguised: The mitochondrial permeability transition pore as the c-subunit of the F(1)F(O) ATP synthase. *Pharmacological Research*, *99*, 382–392. <https://doi.org/10.1016/j.phrs.2015.04.013>

Jonas, & Elizabeth. (2006). BCL-xL Regulates Synaptic Plasticity. *Molecular Interventions*, *6*(4), 208. <https://doi.org/10.1124/MI.6.4.7>

Karch, J., Broun, M. J., Khalil, H., Sargent, M. A., Latchman, N., Terada, N., Peixoto, P. M., & Molkentin, J. D. (2019). Inhibition of mitochondrial permeability transition by deletion of the ANT family and CypD. *Science Advances*, *5*(8), eaaw4597. <https://doi.org/10.1126/sciadv.aaw4597>

Karch, J., Kwong, J. Q., Burr, A. R., Sargent, M. A., Elrod, J. W., Peixoto, P. M., Martinez-Caballero, S., Osinska, H., Cheng, E. H.-Y., Robbins, J., Kinnally, K. W., & Molkentin, J. D. (2013). Bax and Bak function as the outer membrane component of the mitochondrial permeability pore in regulating necrotic cell death in mice. *ELife*, *2*, 772. <https://doi.org/10.7554/elife.00772>

Karch, J., & Molkentin, J. D. (2015). Regulated necrotic cell death: The passive aggressive side of Bax and Bak. *Circulation Research*, *116*(11), 1800. <https://doi.org/10.1161/CIRCRESAHA.116.305421>

Kinnally, K. W., Campo, M. L., & Tedeschi, H. (1989). Mitochondrial Channel Activity Studied by Patch-Clamping Mitoplasts. In *Journal of Bioenergetics and Biomembranes* (Vol. 21, Issue 4).

Kinnally, K. W., Lohret, T. A., Campo, M. L., & Mannella, C. A. (1996). Perspectives on the mitochondrial multiple conductance channel. *Journal of Bioenergetics and Biomembranes*, *28*(2), 115–123. <https://doi.org/10.1007/BF02110641>

Kinnally, K. W., Zorov, D. B., Antonenko, Y. N., Snyder, S. H., Mcenery, M. W., & Tedeschi, H. (1993). Mitochondrial benzodiazepine receptor linked to inner

- membrane ion channels by nanomolar actions of ligands. *Proceedings of the National Academy of Sciences of the United States of America*, 90(4), 1374–1378. <https://doi.org/10.1073/pnas.90.4.1374>
- Klintmalm, G. B. G., Iwatsuki, S., & Starzl, T. E. (1981). CYCLOSPORIN A HEPATOTOXICITY IN 66 RENAL ALLOGRAFT RECIPIENTS. *Transplantation*, 32(6), 488. [/pmc/articles/PMC2962575/](https://pubmed.ncbi.nlm.nih.gov/2962575/)
- Klutho, P. J., Dashek, R. J., Song, L., & Baines, C. P. (2020). Genetic manipulation of SPG7 or NipSnap2 does not affect mitochondrial permeability transition. In *Cell Death Discovery* (Vol. 6, Issue 1, pp. 1–3). Springer Nature. <https://doi.org/10.1038/s41420-020-0239-6>
- Kokoszka, J. E., Waymire, K. G., Levy, S. E., Sligh, J. E., Cai, J., Jones, D. P., MacGregor, G. R., & Wallace, D. C. (2004). The ADP/ATP translocator is not essential for the mitochondrial permeability transition pore. *Nature*, 427(6973), 461–465. <https://doi.org/10.1038/nature02229>
- Konrad, C., Kiss, G., Torocsik, B., Adam-Vizi, V., & Chinopoulos, C. (2012). Absence of Ca<sup>2+</sup>-Induced Mitochondrial Permeability Transition but Presence of Bongkrekate-Sensitive Nucleotide Exchange in *C. crangon* and *P. serratus*. *PLOS ONE*, 7(6), e39839. <https://doi.org/10.1371/JOURNAL.PONE.0039839>
- Konr d, C., Kiss, G., T r csik, B., L b r, J. L., Gerencser, A. A., M ndi, M., Adam-Vizi, V., & Chinopoulos, C. (2011). A distinct sequence in the adenine nucleotide translocase from *Artemia franciscana* embryos is associated with insensitivity to bongkrekate and atypical effects of adenine nucleotides on Ca<sup>2+</sup> uptake and sequestration. *The FEBS Journal*, 278(5), 822–836. <https://doi.org/10.1111/J.1742-4658.2010.08001.X>
- Krauskopf, A., Eriksson, O., Craigen, W. J., Forte, M. A., & Bernardi, P. (2006). Properties of the permeability transition in VDAC1<sup>-/-</sup> mitochondria. *Biochimica et Biophysica Acta - Bioenergetics*, 1757(5–6), 590–595. <https://doi.org/10.1016/j.bbabi.2006.02.007>
- Kwong, J. Q., Davis, J., Baines, C. P., Sargent, M. A., Karch, J., Wang, X., Huang, T., & Molkentin, J. D. (2014). Genetic deletion of the mitochondrial phosphate carrier desensitizes the mitochondrial permeability transition pore and causes

- cardiomyopathy. *Cell Death and Differentiation*, 21(8), 1209–1217.  
<https://doi.org/10.1038/cdd.2014.36>
- Kwong, Jennifer Q., Lu, X., Correll, R. N., Schwanekamp, J. A., Vagnozzi, R. J., Sargent, M. A., York, A. J., Zhang, J., Bers, D. M., & Molkentin, J. D. (2015). The Mitochondrial Calcium Uniporter Selectively Matches Metabolic Output to Acute Contractile Stress in the Heart. *Cell Reports*, 12(1), 15–22.  
<https://doi.org/10.1016/j.celrep.2015.06.002>
- Kwong, Jennifer Q., & Molkentin, J. D. (2015). Physiological and pathological roles of the mitochondrial permeability transition pore in the heart. *Cell Metabolism*, 21(2), 206. <https://doi.org/10.1016/J.CMET.2014.12.001>
- Leist, M., Single, B., Castoldi, A. F., Kühnle, S., & Nicotera, P. (1997). Intracellular Adenosine Triphosphate (ATP) Concentration: A Switch in the Decision Between Apoptosis and Necrosis. *Journal of Experimental Medicine*, 185(8), 1481–1486. <https://doi.org/10.1084/JEM.185.8.1481>
- Leung, A. W. C., Varanyuwatana, P., & Halestrap, A. P. (2008). The mitochondrial phosphate carrier interacts with cyclophilin D and may play a key role in the permeability transition. *Journal of Biological Chemistry*, 283(39), 26312–26323.  
<https://doi.org/10.1074/jbc.M805235200>
- Li, F., Leier, A., Liu, Q., Wang, Y., Xiang, D., Akutsu, T., Webb, G. I., Smith, A. I., Marquez-Lago, T., Li, J., & Song, J. (2020). Procleave: Predicting Protease-specific Substrate Cleavage Sites by Combining Sequence and Structural Information. *Genomics, Proteomics & Bioinformatics*, 18(1), 52–64.  
<https://doi.org/10.1016/J.GPB.2019.08.002>
- Li, W., Zhang, C., & Sun, X. (2018). Mitochondrial Ca<sup>2+</sup> retention capacity assay and Ca<sup>2+</sup>-triggered mitochondrial swelling assay. *Journal of Visualized Experiments*, 2018(135). <https://doi.org/10.3791/56236>
- Li, X., Wang, W., Wang, J., Malovannaya, A., Xi, Y., Li, W., Guerra, R., Hawke, D. H., Qin, J., & Chen, J. (2015). Proteomic analyses reveal distinct chromatin-associated and soluble transcription factor complexes. *Molecular Systems Biology*, 11(1), 775. <https://doi.org/10.15252/msb.20145504>

- Littlejohns, B., Pasdois, P., Duggan, S., Bond, A. R., Heesom, K., Jackson, C. L., Angelini, G. D., Halestrap, A. P., & Suleiman, M. S. (2014). Hearts from Mice Fed a Non-Obesogenic High-Fat Diet Exhibit Changes in Their Oxidative State, Calcium and Mitochondria in Parallel with Increased Susceptibility to Reperfusion Injury. *PLOS ONE*, 9(6), e100579. <https://doi.org/10.1371/JOURNAL.PONE.0100579>
- Liu, F., Lössl, P., Rabbitts, B. M., Balaban, R. S., & Heck, A. J. R. (2018). The interactome of intact mitochondria by cross-linking mass spectrometry provides evidence for coexisting respiratory supercomplexes. *Molecular and Cellular Proteomics*, 17(2), 216–232. <https://doi.org/10.1074/mcp.RA117.000470>
- Lu, X., Kwong, J. Q., Molkenin, J. D., & Bers, D. M. (2016). Individual cardiac mitochondria undergo rare transient permeability transition pore openings. *Circulation Research*, 118(5), 834–841. <https://doi.org/10.1161/CIRCRESAHA.115.308093>
- Luongo, T. S., Lambert, J. P., Yuan, A., Zhang, X., Gross, P., Song, J., Shanmughapriya, S., Gao, E., Jain, M., Houser, S. R., Koch, W. J., Cheung, J. Y., Madesh, M., & Elrod, J. W. (2015). The Mitochondrial Calcium Uniporter Matches Energetic Supply with Cardiac Workload during Stress and Modulates Permeability Transition. *Cell Reports*, 12(1), 23–34. <https://doi.org/10.1016/j.celrep.2015.06.017>
- Luisetto, S., Basso, E., Petronilli, V., Bernardi, P., & Forte, M. (2008). Enhancement of anxiety, facilitation of avoidance behavior, and occurrence of adult-onset obesity in mice lacking mitochondrial cyclophilin D. *Neuroscience*, 155(3), 585–596. <https://doi.org/10.1016/J.NEUROSCIENCE.2008.06.030>
- Malkevitch, N. ., Dedukhova, V. ., Simonian, R. ., Skulachev, V. ., & Starkov, A. . (1997). Thyroxine induces cyclosporin A-insensitive, Ca<sup>2+</sup>-dependent reversible permeability transition pore in rat liver mitochondria. *FEBS Letters*, 412(1), 173–178. [https://doi.org/10.1016/S0014-5793\(97\)00666-2](https://doi.org/10.1016/S0014-5793(97)00666-2)
- Malty, R. H., Aoki, H., Kumar, A., Phanse, S., Amin, S., Zhang, Q., Minic, Z., Goebels, F., Musso, G., Wu, Z., Abou-tok, H., Meyer, M., Deineko, V., Kassir, S., Sidhu, V., Jessulat, M., Scott, N. E., Xiong, X., Vlasblom, J., ... Babu, M.

- (2017). A Map of Human Mitochondrial Protein Interactions Linked to Neurodegeneration Reveals New Mechanisms of Redox Homeostasis and NF- $\kappa$ B Signaling. *Cell Systems*, 5(6), 564-577.e12.  
<https://doi.org/10.1016/j.cels.2017.10.010>
- Marchi, U. De, Campello, S., Szabò, I., Tombola, F., Martinou, J.-C., & Zoratti, M. (2004). Bax Does Not Directly Participate in the Ca<sup>2+</sup>-induced Permeability Transition of Isolated Mitochondria \*. *Journal of Biological Chemistry*, 279(36), 37415–37422. <https://doi.org/10.1074/JBC.M314093200>
- Martin, L. J., Gertz, B., Pan, Y., Price, A. C., Molkentin, J. D., & Chang, Q. (2009). The mitochondrial permeability transition pore in motor neurons: Involvement in the pathobiology of ALS mice. *Experimental Neurology*, 218(2), 333–346.  
<https://doi.org/10.1016/J.EXPNEUROL.2009.02.015>
- Marzo, I., Brenner, C., Zamzami, N., Jürgensmeier, J. M., Susin, S. A., Vieira, H. L. A., Prévost, M. C., Xie, Z., Matsuyama, S., Reed, J. C., & Kroemer, G. (1998). Bax and adenine nucleotide translocator cooperate in the mitochondrial control of apoptosis. *Science*, 281(5385), 2027–2031.  
<https://doi.org/10.1126/science.281.5385.2027>
- Matsuda, S., & Koyasu, S. (2000). Mechanisms of action of cyclosporine. *Immunopharmacology*, 47(2–3), 119–125. [https://doi.org/10.1016/S0162-3109\(00\)00192-2](https://doi.org/10.1016/S0162-3109(00)00192-2)
- Mcenery, M. W., Snowman, A. M., Trifiletti, R. R., & Snyder, S. H. (1992). Isolation of the mitochondrial benzodiazepine receptor: Association with the voltage-dependent anion channel and the adenine nucleotide carrier. *Proceedings of the National Academy of Sciences of the United States of America*, 89(8), 3170–3174. <https://doi.org/10.1073/pnas.89.8.3170>
- McGee, A. M., & Baines, C. P. (2011). Complement 1q-binding protein inhibits the mitochondrial permeability transition pore and protects against oxidative stress-induced death. *Biochemical Journal*, 433(1), 119–125.  
<https://doi.org/10.1042/BJ20101431>
- Menazza, S., Wong, R., Nguyen, T., Wang, G., Gucek, M., & Murphy, E. (2013). CypD<sup>-/-</sup> Hearts Have Altered Levels of Proteins Involved in Krebs Cycle,

Branch Chain Amino Acid Degradation and Pyruvate Metabolism. *Journal of Molecular and Cellular Cardiology*, 56(1), 81.

<https://doi.org/10.1016/J.YJMCC.2012.12.004>

Menze, M. A., Hutchinson, K., Laborde, S. M., & Hand, S. C. (2005). Mitochondrial permeability transition in the crustacean *Artemia franciscana*: absence of a calcium-regulated pore in the face of profound calcium storage.

<https://doi.org/10.1152/Ajpregu.00844.2004>, 289(1 58-1), 68–76.

<https://doi.org/10.1152/AJPREGU.00844.2004>

Millay, D. P., Sargent, M. A., Osinska, H., Baines, C. P., Barton, E. R., Vuagniaux, G., Sweeney, H. L., Robbins, J., & Molkenin, J. D. (2008). Genetic and pharmacologic inhibition of mitochondrial-dependent necrosis attenuates muscular dystrophy. *Nature Medicine*, 14(4), 442–447.

<https://doi.org/10.1038/nm1736>

Mnatsakanyan, N., Beutner, G., Porter, G. A., Alavian, K. N., & Jonas, E. A. (2016). Physiological roles of the mitochondrial permeability transition pore. *Journal of Bioenergetics and Biomembranes* 2016 49:1, 49(1), 13–25.

<https://doi.org/10.1007/S10863-016-9652-1>

Murphy, E., & Steenbergen, C. (2008). Mechanisms underlying acute protection from cardiac ischemia-reperfusion injury. *Physiological Reviews*, 88(2), 581–609.

<https://doi.org/10.1152/PHYSREV.00024.2007/ASSET/IMAGES/LARGE/Z9J0030824730011.JPEG>

Murphy, E., & Steenbergen, C. (2011). What makes the mitochondria a killer? Can we condition them to be less destructive? In *Biochimica et Biophysica Acta - Molecular Cell Research* (Vol. 1813, Issue 7, pp. 1302–1308). Elsevier.

<https://doi.org/10.1016/j.bbamcr.2010.09.003>

Nakagawa, T., Shimizu, S., Watanabe, T., Yamaguchi, O., Otsu, K., Yamagata, H., Inohara, H., Kubo, T., & Tsujimoto, Y. (2005). Cyclophilin D-dependent mitochondrial permeability transition regulates some necrotic but not apoptotic cell death. *Nature*, 434(7033), 652–658. <https://doi.org/10.1038/nature03317>

Narita, M., Shimizu, S., Ito, T., Chittenden, T., Lutz, R. J., Matsuda, H., & Tsujimoto, Y. (1998). Bax interacts with the permeability transition pore to induce

permeability transition and cytochrome c release in isolated mitochondria.

*Proceedings of the National Academy of Sciences*, 95(25).

Nazareth, W., Yafei, N., & Crompton, M. (1991). Inhibition of anoxia-induced injury in heart myocytes by cyclosporin A. *Journal of Molecular and Cellular Cardiology*, 23(12), 1351–1354. [https://doi.org/10.1016/0022-2828\(91\)90181-K](https://doi.org/10.1016/0022-2828(91)90181-K)

Neginskaya, M. A., & Pavlov, E. V. (2023). Investigation of Properties of the Mitochondrial Permeability Transition Pore Using Whole-Mitoplast Patch-Clamp Technique. <https://Home.Liebertpub.Com/Dna>, 42(8), 481–487. <https://doi.org/10.1089/DNA.2023.0171>

Neginskaya, M. A., Solesio, M. E., Berezhnaya, E. V., Amodeo, G. F., Mnatsakanyan, N., Jonas, E. A., & Pavlov, E. V. (2019). ATP Synthase C-Subunit-Deficient Mitochondria Have a Small Cyclosporine A-Sensitive Channel, but Lack the Permeability Transition Pore. *Cell Reports*, 26(1), 11-17.e2. <https://doi.org/10.1016/j.celrep.2018.12.033>

Neher, E., & Sakaba, T. (2008). Multiple Roles of Calcium Ions in the Regulation of Neurotransmitter Release. *Neuron*, 59(6), 861–872. <https://doi.org/10.1016/J.NEURON.2008.08.019>

Novgorodov, S. A., Gudz, T. I., Milgrom, Y. M., & Brierley, G. P. (1992). The permeability transition in heart mitochondria is regulated synergistically by ADP and cyclosporin A. *Journal of Biological Chemistry*, 267(23), 16274–16282. [https://doi.org/10.1016/S0021-9258\(18\)41996-5](https://doi.org/10.1016/S0021-9258(18)41996-5)

Ong, S.-G., Lee, W. H., Theodorou, L., Kodo, K., Lim, S. Y., Shukla, D. H., Briston, T., Kiriakidis, S., Ashcroft, M., Davidson, S. M., Maxwell, P. H., Yellon, D. M., & Hausenloy, D. J. (2014). HIF-1 reduces ischaemia–reperfusion injury in the heart by targeting the mitochondrial permeability transition pore. *Cardiovascular Research*, 104(1), 24–36. <https://doi.org/10.1093/cvr/cvu172>

Osellame, L. D., Blacker, T. S., & Duchen, M. R. (2012). Cellular and molecular mechanisms of mitochondrial function. *Best Practice & Research. Clinical Endocrinology & Metabolism*, 26(6), 711. <https://doi.org/10.1016/J.BEEM.2012.05.003>



- Palma, E., Tiepolo, T., Angelin, A., Sabatelli, P., Maraldi, N. M., Basso, E., Forte, M. A., Bernardi, P., & Bonaldo, P. (2009). Genetic ablation of cyclophilin D rescues mitochondrial defects and prevents muscle apoptosis in collagen VI myopathic mice. *Human Molecular Genetics*, *18*(11), 2024–2031. <https://doi.org/10.1093/hmg/ddp126>
- Pan, X., Liu, J., Nguyen, T., Liu, C., Sun, J., Teng, Y., Fergusson, M. M., Rovira, I. I., Allen, M., Springer, D. A., Aponte, A. M., Gucek, M., Balaban, R. S., Murphy, E., & Finkel, T. (2013). The Physiological Role of Mitochondrial Calcium Revealed by Mice Lacking the Mitochondrial Calcium Uniporter. *Nature Cell Biology*, *15*(12), 1464–1472. <https://doi.org/10.1038/ncb2868>
- Parks, R. J., Menazza, S., Holmström, K. M., Amanakis, G., Fergusson, M., Ma, H., Aponte, A. M., Bernardi, P., Finkel, T., & Murphy, E. (2019). Cyclophilin D-mediated regulation of the permeability transition pore is altered in mice lacking the mitochondrial calcium uniporter. *Cardiovascular Research*, *115*(2), 385–394. <https://doi.org/10.1093/cvr/cvy218>
- Pavlov, E., Zakharian, E., Bladen, C., Diao, C. T. M., Grimbly, C., Reusch, R. N., & French, R. J. (2005). A Large, Voltage-Dependent Channel, Isolated from Mitochondria by Water-Free Chloroform Extraction. *Biophysical Journal*, *88*(4), 2614–2625. <https://doi.org/10.1529/BIOPHYSJ.104.057281>
- Petronilli, V., Miotto, G., Canton, M., Brini, M., Colonna, R., Bernardi, P., & Di Lisa, F. (1999). Transient and long-lasting openings of the mitochondrial permeability transition pore can be monitored directly in intact cells by changes in mitochondrial calcein fluorescence. *Biophysical Journal*, *76*(2), 725–734. [https://doi.org/10.1016/S0006-3495\(99\)77239-5](https://doi.org/10.1016/S0006-3495(99)77239-5)
- Petronilli, V., Miotto, G., Canton, M., Colonna, R., Bernardi, P., & Di Lisa, F. (1998). Imaging the mitochondrial permeability transition pore in intact cells. *BioFactors (Oxford, England)*, *8*(3–4), 263–272. <https://doi.org/10.1002/BIOF.5520080314>
- Petronilli, V., Nicolli, A., Costantini, P., Colonna, R., & Bernardi, P. (1994). Regulation of the permeability transition pore, a voltage-dependent mitochondrial channel inhibited by cyclosporin A. *Biochimica et Biophysica Acta (BBA) - Bioenergetics*, *1187*(2), 255–259. <https://doi.org/10.1016/0005->

- Pfeiffer, D. R., Gudz, T. I., Novgorodov, S. A., & Erdahl, W. L. (1995). The Peptide Mastoparan Is a Potent Facilitator of the Mitochondrial Permeability Transition (\*). *Journal of Biological Chemistry*, 270(9), 4923–4932.  
<https://doi.org/10.1074/JBC.270.9.4923>
- Piot, C., Croisille, P., Staat, P., Thibault, H., Rioufol, G., Mewton, N., Elbelghiti, R., Cung, T. T., Bonnefoy, E., Angoulvant, D., Macia, C., Raczka, F., Sportouch, C., Gahide, G., Finet, G., André-Fouët, X., Revel, D., Kirkorian, G., Monassier, J.-P., ... Ovize, M. (2008). Effect of Cyclosporine on Reperfusion Injury in Acute Myocardial Infarction. *New England Journal of Medicine*, 359(5), 473–481.  
<https://doi.org/10.1056/nejmoa071142>
- Precht, T. A., Phelps, R. A., Linseman, D. A., Butts, B. D., Le, S. S., Laessig, T. A., Bouchard, R. J., & Heidenreich, K. A. (2005). The permeability transition pore triggers Bax translocation to mitochondria during neuronal apoptosis. *Cell Death and Differentiation*, 12(3), 255–265. <https://doi.org/10.1038/SJ.CDD.4401552>
- Ran, F. A., Hsu, P. D., Wright, J., Agarwala, V., Scott, D. A., & Zhang, F. (2013). Genome engineering using the CRISPR-Cas9 system. *Nature Protocols*, 8(11), 2281–2308. <https://doi.org/10.1038/nprot.2013.143>
- Rasmussen, T. P., Wu, Y., Joiner, M. L. A., Koval, O. M., Wilson, N. R., Luczak, E. D., Wang, Q., Chen, B., Gao, Z., Zhu, Z., Wagner, B. A., Soto, J., McCormick, M. L., Kutschke, W., Weiss, R. M., Yu, L., Boudreau, R. L., Abel, E. D., Zhan, F., ... Anderson, M. E. (2015). Inhibition of MCU forces extramitochondrial adaptations governing physiological and pathological stress responses in heart. *Proceedings of the National Academy of Sciences of the United States of America*, 112(29), 9129–9134. <https://doi.org/10.1073/pnas.1504705112>
- Rasola, A., Sciacovelli, M., Chiara, F., Pantic, B., Brusilow, W. S., & Bernardi, P. (2010). Activation of mitochondrial ERK protects cancer cells from death through inhibition of the permeability transition. *Proceedings of the National Academy of Sciences*, 107(2), 726–731. <https://doi.org/10.1073/PNAS.0912742107>
- Reutenauer, J., Dorchies, O. M., Patthey-Vuadens, O., Vuagniaux, G., & Ruegg, U. T. (2008). Investigation of Debio 025, a cyclophilin inhibitor, in the dystrophic

mdx mouse, a model for Duchenne muscular dystrophy. *British Journal of Pharmacology*, 155(4), 574–584. <https://doi.org/10.1038/bjp.2008.285>

Richardson, A. P., & Halestrap, A. P. (2016). Quantification of active mitochondrial permeability transition pores using GNX-4975 inhibitor titrations provides insights into molecular identity. *Biochemical Journal*, 473(9), 1129–1140. <https://doi.org/10.1042/BCJ20160070>

Richter, R., Rorbach, J., Pajak, A., Smith, P. M., Wessels, H. J., Huynen, M. A., Smeitink, J. A., Lightowlers, R. N., & Chrzanowska-Lightowlers, Z. M. (2010). A functional peptidyl-tRNA hydrolase, ICT1, has been recruited into the human mitochondrial ribosome. *EMBO Journal*, 29(6), 1116–1125. <https://doi.org/10.1038/emboj.2010.14>

Rizzuto, R., Pinton, P., Ferrari, D., Chami, M., Szabadkai, G., Magalhães, P. J., Di Virgilio, F., & Pozzan, T. (2003). Calcium and apoptosis: facts and hypotheses. *Oncogene* 2003 22:53, 22(53), 8619–8627. <https://doi.org/10.1038/sj.onc.1207105>

Rolland, T., Taşan, M., Charloteaux, B., Pevzner, S. J., Zhong, Q., Sahni, N., Yi, S., Lemmens, I., Fontanillo, C., Mosca, R., Kamburov, A., Ghiassian, S. D., Yang, X., Ghamsari, L., Balcha, D., Begg, B. E., Braun, P., Brehme, M., Broly, M. P., ... Vidal, M. (2014). A proteome-scale map of the human interactome network. *Cell*, 159(5), 1212–1226. <https://doi.org/10.1016/j.cell.2014.10.050>

Roth, G. A., Abate, D., Abate, K. H., Abay, S. M., Abbafati, C., Abbasi, N., Abbastabar, H., Abd-Allah, F., Abdela, J., Abdelalim, A., Abdollahpour, I., Abdulkader, R. S., Abebe, H. T., Abebe, M., Abebe, Z., Abejie, A. N., Abera, S. F., Abil, O. Z., Abraha, H. N., ... Murray, C. J. L. (2018). Global, regional, and national age-sex-specific mortality for 282 causes of death in 195 countries and territories, 1980–2017: a systematic analysis for the Global Burden of Disease Study 2017. *The Lancet*, 392(10159), 1736–1788. [https://doi.org/10.1016/S0140-6736\(18\)32203-7](https://doi.org/10.1016/S0140-6736(18)32203-7)

Rottenberg, H., & Hoek, J. B. (2017). The path from mitochondrial ROS to aging runs through the mitochondrial permeability transition pore. *Aging Cell*, 16(5), 943–955. <https://doi.org/10.1111/ACEL.12650>

- Rottenberg, H., & Marbach, M. (1990). Regulation of Ca<sup>2+</sup> transport in brain mitochondria. II. The mechanism of the adenine nucleotides enhancement of Ca<sup>2+</sup> uptake and retention. *BBA - Bioenergetics*, 1016(1), 87–98.  
[https://doi.org/10.1016/0005-2728\(90\)90010-2](https://doi.org/10.1016/0005-2728(90)90010-2)
- Roux, K. J., Kim, D. I., Burke, B., & May, D. G. (2018). BioID: A Screen for Protein-Protein Interactions. In *Current Protocols in Protein Science* (Vol. 91, Issue 1, pp. 19.23.1-19.23.15). John Wiley & Sons, Inc. <https://doi.org/10.1002/cpps.51>
- Roux, K. J., Kim, D. I., Raida, M., & Burke, B. (2012). A promiscuous biotin ligase fusion protein identifies proximal and interacting proteins in mammalian cells. *The Journal of Cell Biology*, 196(6), 801–810.  
<https://doi.org/10.1083/jcb.201112098>
- Rück, A., Dolder, M., Wallimann, T., & Brdiczka, D. (1998). Reconstituted adenine nucleotide translocase forms a channel for small molecules comparable to the mitochondrial permeability transition pore. *FEBS Letters*, 426(1), 97–101.  
[https://doi.org/10.1016/S0014-5793\(98\)00317-2](https://doi.org/10.1016/S0014-5793(98)00317-2)
- Shanmughapriya, S., Rajan, S., Hoffman, N. E., Higgins, A. M., Tomar, D., Nemani, N., Hines, K. J., Smith, D. J., Eguchi, A., Vallem, S., Shaikh, F., Cheung, M., Leonard, N. J., Stolakis, R. S., Wolfers, M. P., Ibeti, J., Chuprun, J. K., Jog, N. R., Houser, S. R., ... Madesh, M. (2015). SPG7 Is an Essential and Conserved Component of the Mitochondrial Permeability Transition Pore. *Molecular Cell*, 60(1), 47–62. <https://doi.org/10.1016/j.molcel.2015.08.009>
- Shen, K., Pender, C. L., Bar-Ziv, R., Zhang, H., Wickham, K., Willey, E., Durieux, J., Ahmad, Q., & Dillin, A. (2022). Mitochondria as Cellular and Organismal Signaling Hubs. *Annual Review of Cell and Developmental Biology*, 38, 179–218. <https://doi.org/10.1146/ANNUREV-CELLBIO-120420-015303>
- Shum, L. C., White, N. S., Nadtochiy, S. M., Bentley, K. L. de M., Brookes, P. S., Jonason, J. H., & Eliseev, R. A. (2016). Cyclophilin D Knock-Out Mice Show Enhanced Resistance to Osteoporosis and to Metabolic Changes Observed in Aging Bone. *PLOS ONE*, 11(5), e0155709.  
<https://doi.org/10.1371/journal.pone.0155709>
- Šileikyte, J., Blachly-Dyson, E., Sewell, R., Carpi, A., Menabò, R., Di Lisa, F.,

- Ricchelli, F., Bernardi, P., & Forte, M. (2014). Regulation of the mitochondrial permeability transition pore by the outer membrane does not involve the peripheral benzodiazepine receptor (translocator protein of 18 kDa (TSPO)). *Journal of Biological Chemistry*, 289(20), 13769–13781. <https://doi.org/10.1074/jbc.M114.549634>
- Šileikyte, J., Petronilli, V., Zulian, A., Dabbeni-Sala, F., Tognon, G., Nikolov, P., Bernardi, P., & Ricchelli, F. (2011). Regulation of the inner membrane mitochondrial permeability transition by the outer membrane translocator protein (peripheral benzodiazepine receptor). *Journal of Biological Chemistry*, 286(2), 1046–1053. <https://doi.org/10.1074/jbc.M110.172486>
- Skyschally, A., Schulz, R., & Heusch, G. (2010). *Cyclosporine A at Reperfusion Reduces Infarct Size in Pigs*. <https://doi.org/10.1007/s10557-010-6219-y>
- Sokolove, P. M., & Kinnally, K. W. (1996). A Mitochondrial Signal Peptide from *Neurospora crassa* Increases the Permeability of Isolated Rat Liver Mitochondria. *Archives of Biochemistry and Biophysics*, 336(1), 69–76. <https://doi.org/10.1006/ABBI.1996.0533>
- Solesio, M. E., Elustondo, P. A., Zakharian, E., & Pavlov, E. V. (2016). Inorganic polyphosphate (polyP) as an activator and structural component of the mitochondrial permeability transition pore. *Biochemical Society Transactions*, 44(1), 7–12. <https://doi.org/10.1042/BST20150206>
- Staat, P., Rioufol, G., Piot, C., Cottin, Y., Cung, T. T., L'Huillier, I., Aupetit, J. F., Bonnefoy, E., Finet, G., André-Fouët, X., & Ovize, M. (2005). Postconditioning the human heart. *Circulation*, 112(14), 2143–2148. <https://doi.org/10.1161/CIRCULATIONAHA.105.558122>
- Stockburger, C., Miano, D., Pallas, T., Friedland, K., & Müller, W. E. (2016). Enhanced Neuroplasticity by the Metabolic Enhancer Piracetam Associated with Improved Mitochondrial Dynamics and Altered Permeability Transition Pore Function. *Neural Plasticity*, 2016. <https://doi.org/10.1155/2016/8075903>
- Stoolman, J. S., Porcelli, A. M., & Martínez-Reyes, I. (2022). Editorial: Mitochondria as a hub in cellular signaling. *Frontiers in Cell and Developmental Biology*, 10, 981464. <https://doi.org/10.3389/FCELL.2022.981464/BIBTEX>

- Szabó, I., & Zoratti, M. (1992). The mitochondrial megachannel is the permeability transition pore. *Journal of Bioenergetics and Biomembranes*, 24(1), 111–117. <http://www.ncbi.nlm.nih.gov/pubmed/1380498>
- Szabó, Ildikó, Pinto, V. De, & Zoratti, M. (1993). The mitochondrial permeability transition pore may comprise VDAC molecules. *FEBS Letters*, 330(2), 206–210. [https://doi.org/10.1016/0014-5793\(93\)80274-X](https://doi.org/10.1016/0014-5793(93)80274-X)
- Tanveer, A., Virji, S., Andreeva, L., Totty, N. F., Hsuan, J. J., Ward, J. M., & Crompton, M. (1996). Involvement of cyclophilin D in the activation of a mitochondrial pore by Ca<sup>2+</sup> and oxidant stress. *European Journal of Biochemistry*, 238(1), 166–172. <https://doi.org/10.1111/j.1432-1033.1996.0166q.x>
- Tatsumi, T., Shiraishi, J., Keira, N., Akashi, K., Mano, A., Yamanaka, S., Matoba, S., Fushiki, S., Fliss, H., & Nakagawa, M. (2003). Intracellular ATP is required for mitochondrial apoptotic pathways in isolated hypoxic rat cardiac myocytes. *Cardiovascular Research*, 59(2), 428–440. [https://doi.org/10.1016/S0008-6363\(03\)00391-2/2/59-2-428-FIG9.GIF](https://doi.org/10.1016/S0008-6363(03)00391-2/2/59-2-428-FIG9.GIF)
- Urbani, A., Giorgio, V., Carrer, A., Franchin, C., Arrigoni, G., Jiko, C., Abe, K., Maeda, S., Shinzawa-Itoh, K., Bogers, J. F. M., McMillan, D. G. G., Gerle, C., Szabó, I., & Bernardi, P. (2019). Purified F-ATP synthase forms a Ca<sup>2+</sup>-dependent high-conductance channel matching the mitochondrial permeability transition pore. *Nature Communications*, 10(1), 1–11. <https://doi.org/10.1038/s41467-019-12331-1>
- Varanyuwatana, P., & Halestrap, A. P. (2012). The roles of phosphate and the phosphate carrier in the mitochondrial permeability transition pore. *Mitochondrion*, 12(1), 120–125. <https://doi.org/10.1016/j.mito.2011.04.006>
- Vaseva, A. V., Marchenko, N. D., Ji, K., Tsirka, S. E., Holzmann, S., & Moll, U. M. (2012). P53 opens the mitochondrial permeability transition pore to trigger necrosis. *Cell*, 149(7), 1536–1548. <https://doi.org/10.1016/j.cell.2012.05.014>
- Walker, J. E., Carroll, J., & He, J. (2020). Reply to Bernardi: The mitochondrial permeability transition pore and the ATP synthase. In *Proceedings of the National Academy of Sciences of the United States of America* (Vol. 117, Issue

6, pp. 2745–2746). National Academy of Sciences.

<https://doi.org/10.1073/pnas.1921409117>

Weinbrenner, C., Liu, G. S., Downey, J. M., & Cohen, M. V. (1998). Cyclosporine a limits myocardial infarct size even when administered after onset of ischemia. *Cardiovascular Research*, 38(3), 676–684. [https://doi.org/10.1016/S0008-6363\(98\)00064-9](https://doi.org/10.1016/S0008-6363(98)00064-9)

Whelan, R. S., Konstantinidis, K., Wei, A. C., Chen, Y., Reyna, D. E., Jha, S., Yang, Y., Calvert, J. W., Lindsten, T., Thompson, C. B., Crow, M. T., Gavathiotis, E., Dorn, G. W., O'Rourke, B., & Kitsis, R. N. (2012). Bax regulates primary necrosis through mitochondrial dynamics. *Proceedings of the National Academy of Sciences of the United States of America*, 109(17), 6566–6571. [https://doi.org/10.1073/PNAS.1201608109/SUPPL\\_FILE/PNAS.201201608SI.PDF](https://doi.org/10.1073/PNAS.1201608109/SUPPL_FILE/PNAS.201201608SI.PDF)

Woodfield, K., Rück, A., Brdiczka, D., & Halestrap, A. P. (1998). Direct demonstration of a specific interaction between cyclophilin-D and the adenine nucleotide translocase confirms their role in the mitochondrial permeability transition. *Biochemical Journal*, 336(2), 287–290. <https://doi.org/10.1042/bj3360287>

Zhou, B., Kreuzer, J., Kumsta, C., Hansen, M., Haas, W., Soukas Correspondence, A. A., Brief, I., Wu, L., Kamer, K. J., Cedillo, L., Zhang, Y., Li, S., Kacergis, M. C., Webster, C. M., Fejes-Toth, G., Naray-Fejes-Toth, A., Das, S., & Soukas, A. A. (2019). Mitochondrial Permeability Uncouples Elevated Autophagy and Lifespan Extension The role of autophagy in lifespan extension depends on modulation of mitochondrial permeability via the action of the kinase SGK1. Article Mitochondrial Permeability Uncouples Elevated Autophagy and Lifespan Extension. *Cell*, 177, 299–314. <https://doi.org/10.1016/j.cell.2019.02.013>

Zhou, W., Marinelli, F., Nief, C., & Faraldo-Gómez, J. D. (2017). Atomistic simulations indicate the c-subunit ring of the F1Fo ATP synthase is not the mitochondrial permeability transition pore. *ELife*, 6. <https://doi.org/10.7554/eLife.23781>

Zoratti, M., & Szabò, I. (1995). The mitochondrial permeability transition. *BBA -*

*Reviews on Biomembranes*, 1241(2), 139–176. [https://doi.org/10.1016/0304-4157\(95\)00003-A](https://doi.org/10.1016/0304-4157(95)00003-A)

Zoratti, M., Szabò, I., & De Marchi, U. (2005). Mitochondrial permeability transitions: how many doors to the house? *Biochimica et Biophysica Acta (BBA) - Bioenergetics*, 1706(1–2), 40–52.  
<https://doi.org/10.1016/J.BBABIO.2004.10.006>



# Appendix 1: Review of past CypD interactor hits

## Analysis of CypD interactor list

The interactors here are grouped according to their respective likely complexes/function in vivo. This is because the protein complexes and functions determine how close they are in vivo, which is what is used to carry out most screens. By grouping the interactors according to complexes we can consider the complexes as a whole in terms of how likely they are to be involved in mPTP. The full summary table of interactors is included at the end of the analysis.

### Group 1: Apoptosis regulators

#### Interest level: Low

BCL2

TP53/p53

AIFM1

Previous work has been done on p53 (Vaseva et al., 2012) and BCL2 (Eliseev et al., 2009), 2 genes identified here.

P53 has been suggested to form a complex with CypD to open mPTP (Vaseva et al., 2012).

CypD is suggested to interact with BCL2 to serve an apoptosis inhibitory function (Eliseev et al., 2009) that doesn't have anything to do with the mPTP. However, it should be noted that the work did not fully investigate the effect of BCL2 on mPTP, no CRC assays etc is done. The authors hypothesized that this was independent of MPT because the effects were opposite to that of MPT. The CypD-BCL2 interaction produced an anti-cell death effect while MPT is a pro-cell death pathway.

In addition to the apoptosis genes identified here, Bax and Bak has also been suggested to form the mPTP as the outer membrane component (Karch et al., 2013). Given that Bax and Bak has extensive interaction with BCL2, there might be more to the BCL2 story.

Although AIFM1 is also involved in apoptosis it is also an NAD enzyme with metabolic roles. AIFM1 doesn't have much interaction with BCL2, Bak or Bax. Its role in apoptosis might be to act as a apoptosis signal when it is detected outside the mitochondria. In this sense, its interaction with CypD might not be connected to that of BCL2/Bax/Bak.

## **Group 2: Mitochondria transcription regulators**

### **Interest level: Low**

MTRES1  
MTERF3  
TEFM  
TFAM  
EXD2

There has not been reports of CypD been involved in regulation of mt-DNA transcription. It is possible that these genes could have other functions in addition to their transcription roles, which might be involved in mPT or other CypD functions. However, these seems somewhat unlikely given a large number of transcription factors are found, it is more likely that CypD has some unknown role in mt-DNA transcription.

## **Group 3: Mitochondria ribosome/translation complex**

### **Interest level: None**

MRPS12  
MRPS26  
MRPL11  
FASTKD2  
MRRF  
METTL17  
MTIF2  
MTIF3  
MTRF1  
MTRF1L  
RMND1  
TRMT61B  
MTG2  
MRPL58  
TSFM  
TUFM  
TRUB2  
MRM1  
RPUUSD4  
TRMT61B  
METTL15  
TACO1  
CHCHD1  
GRSF1  
RPUUSD3  
GFM1

GFM2  
C1QBP

CypD is a PPIase that assist in protein folding and catalyzes the cis-trans isomerization of proline imidic peptide bonds in oligopeptides. As such it is very likely that extensive association with the ribosome/translation complex is due to its function to assist in protein and has little to do with mPT. However, one of the proteins, C1QBP, has been reported to be an inhibitor of mPT in an isolated study (McGee & Baines, 2011). Despite this, the ribosome/translation complex is unlikely to be involved in mPT.

#### **Group 4: MCU complex**

**Interest level: High**

CCDC90B  
MCUR1  
MCUB  
HINT2

Cardiac specific inducible MCU KO in adult mice is associated with a reduction in cardiac I/R injury and mPT (Jennifer Q. Kwong et al., 2015; Luongo et al., 2015). However, adult mice lacking MCU or expressing a myocardial-specific dominant-negative MCU from birth are not protected from cardiac I/R injury compared to WT mice (Pan et al., 2013; Rasmussen et al., 2015).

In all KO models, CsA sensitivity of the pore is lost. It should also be noted that in the 2 inducible KO models, very small amounts of MCU are still present while there are no MCU protein present in the MCU KO mice with KO from birth (from analysis of western blot data from mice hearts).

A recent study suggest an explanation for the above phenomenon by proposing that reduction in Ca<sup>2+</sup> levels due to MCU KO results in alterations via phosphorylation of CypD such that mPTP sensitivity is increased. This accounts for the observed lack of protection in germline KO mice. The group also show that mPT can occur in the presence of a Ca<sup>2+</sup> ionophore using CRC. They explain the observed lack of CsA sensitivity as due to increased CypD sensitivity that rendered CsA ineffective (Parks et al., 2019).

I would think that the lack of CsA sensitivity is the one that is hard to reconcile. No other KO (ATP Synthase/ANT) has this effect. Only CypD KO resulted in loss of CsA effect. Would seem a little unlikely that increased Ca<sup>2+</sup> sensitivity completely counteracted any effect of CsA. In addition, inducible KO are also CsA insensitive, but protects against mPT, but this could be due to the fact that maximum protection is already afforded by MCU inducible KO.

It still seem possible that MCU could be the mPTP, but it would also need to explain why ATP Synthase/ANT would have an effect on mPTP. Maybe due to effect of ADP?

The idea that MCU is the mPTP has never been investigated, because mPTP is highly Ca<sup>2+</sup> sensitive so any disturbance due to mPTP cannot be determined to come from altered Ca<sup>2+</sup> levels or the pore itself. Very interesting but might not be feasible to investigate.

### **Group 5: ATP Synthase complex**

**Interest level: None**

TMEM70  
Atp5f1b  
ATP5F1A  
ATP5PB  
ATP5PF  
ATP5B

ATP Synthase complex has been extensively investigated as a candidate for mPTP, with no conclusive results. Further work unlikely to yield anything new.

### **Group 6: Electron Transport Chain regulators**

**Interest level: Medium**

ACAD9  
SURF1  
ETFRF1

No previous reports of CypD interacting with the ETC. Additionally, these proteins are ETC regulators and not complex components, so it is possible the interaction with CypD does not occur at the ETC. Not to mention they regulate different complexes, further bringing down the chance any one complex could be involved in mPT. So if they are involved in mPT it would be likely due to non-etc related functions.

### **Group 7: Metabolic enzymes and their regulators**

**Interest level: Medium**

MDH2  
AUH  
OTC  
PDK1

PDK1 was investigated as part of a paper investigating the role of HIF-1a on mPT. However, its role in mPT was suggested to be that of contributing to metabolic regulation and ETC usage which would affect osphos/ROS stress generation and hence mPT, instead of any direct roles in mPT (Ong et al., 2014).

There is no indication these enzymes could be directly involved in mPTP formation. However, they could potentially act as up/down stream signalling proteins for CypD to induce mPT given we do not know how CypD induces mPT.

### **Group 8: MTS cleavage and imported protein processing**

**Interest level: Low**

HSPD1  
PMPCA  
PMPCB  
HSPE1  
IMMP2L

CypD is known to have PPlase activity that assist in protein folding, so it would make sense for CypD to interact with the mito-protein import machinery. As such, it is unlikely that the interactions observed here has anything to do with mPT. However, the mito-protein import machinery do have multiple transmembrane channel proteins and could very easily form a channel if it is the mPTP. As such the targets here are a little more interesting than the ribosome complex, which is also related to PPlase function but has no obvious way to form a pore or interact with any channel proteins.

### **Group 9: RNA processing and binding**

**Interest level: Low**

SLIRP  
FASTKD5  
TBRG4  
LRPPRC  
FASTKD3

No previous report of CypD being involved in RNA processing. Seems unlikely that these proteins could be involved in mPT. This could yet be related to the ribosome complex/translation, and PPlase's folding role. However, as previously mentioned, due to our lack of knowledge in CypD mPT induction mechanism, we cannot discount the possibility they could potentially act as up/down stream signalling proteins for CypD to induce mPT.

### **Group 10: Individual roles/no complex or functional group**

**Interest level: None**

Slc25a4  
VDAC1  
ATF2

The ADP/ATP translocator and VDAC are original candidates for mPTP and have been extensively investigated with no conclusive findings. New work unlikely to discover anything new.

**Interest level: Low**

HTT  
APP

HTT and APP are implicated in Huntington's and Alzheimer's respectively and while not impossible, it would appear rather unlikely for them to be part of mPTP. Although mPTP has been linked to both diseases in studies. So it would be unlikely but not impossible for APP and HTT to be somehow involved. Especially since both proteins' functions has yet to be determined.

**Interest level: Medium**

CLPP  
CDC34  
SIRT3  
LRRK2  
SSBP1  
CIDEB  
PARL

These proteins do not belong to any functional complexes. They are also not transmembrane so the only way for them to be involved is to act as an intermediary between CypD and the pore/change conformation and undergo membrane insertion (which seems unlikely).

**Group 11: Too little information available for proper function/complex deduction**

**Interest level: Medium**

FAM25C  
C12orf65  
VWA8

Proteins with unclear functions, might be worth investigating. But they not membrane proteins so most likely only regulatory roles in mPT at best

Summary  
table

Biogrid, Intact, String and APID databases are curated. Only Biogrid and Intact relevant to our question. String is more focused on network analysis and does not include publication based list of interactors to consider. All APID interactors were result of curation of the Biogrid and Intact databases

Notes: with the original 2 databases having a more extensive list.

In addition, the following publication that were not included in the databases were curated: <https://dx.doi.org/10.1074%2Fmcp.RA117.000470>

2H = 2 hybrid assay, PDB = Proximity dependent biotinylation, ACMS = Affinity capture mass spectroscopy, PD = Proximal ligation, CL =  
Study type: Crosslinking, PD = Pull down, COIP = Co-immuno precipitation, DA = deacetylase assay, SPR = Surface plasma resonance

Groups: genes of interest are grouped according  
to their function/protein complexes

None = Non mitochondrial genes	Priority
1 = Apoptosis regulation	Low
2 = Mito transcription regulation	Low

3 = Mito-ribosomal/translation complex	None
4 = MCU Complex	High
5 = ATP Synthase complex	None
6 = Electron Transport Chain	Medium
7 = Metabolic enzymes and their regulators	Medium
8 = MTS cleavage and imported protein processing	Low
9 = RNA processing and binding	Low
10 = Individual roles/no complex or functional group	None/Low/Medium
11 = Too little information available for proper function/complex deduction	Medium



Previous screen: Refers to the CRC screen on a selection of Mito proteins (Shanmughapriya et al., 2015).

Mito-localization prediction: Carried out using deeploc1.0 (<http://www.cbs.dtu.dk/services/DeepLoc/>), the localization probability of the predicted compartment and that of mitochondria is given

Gene	Uniprot Identifier	Database	Mito-Localization (literature)	Mito-localization(prediction by deeploc1.0)	Gene function	Study type and no. of hits	Previous work	Transmembrane	Group	Interest level	Previous screen
CCDC90B	Q9GZT6	Biogrid	Yes		MCU regulator	PDB:1	No	Yes	4	High	No
MCUR1	Q96AQ8	Biogrid	Yes		MCU regulator	PDB:1	No	Yes	4	High	No
MCUB	Q9NWR8	Biogrid	Yes		MCU regulator	PDB:1	Yes	Yes	4	High	No
HINT2	Q9BX68	Biogrid	Yes		Possible MCU regulator	PDB:1	Yes	No	4	High	No
ACAD9	Q9H845	Biogrid	Yes		Complex I assembly factor	PDB:1	No	No	6	Medium	No
ETFRF1	Q6IPR1	Intact	Yes		ETC flavoprotein regulator	COIP:2	No	No	6	Medium	No
MDH2	P40926	Biogrid	Yes		Malate dehydrogenase	PDB:1, CL:1	No	No	7	Medium	No
AUH	Q13825	Biogrid	Yes		Methylglutaconyl-CoA hydratase	PDB:1	No	No	7	Medium	No
OTC	P00480	Biogrid	Yes		Ornithine carbamoyltransferase	PDB:1	No	No	7	Medium	No
PDK1	Q15118	Intact, Biogrid	Yes		Pyruvate dehydrogenase regulator	PDB:1	Yes	No	7	Medium	No
CIDEB	Q9UHD4	Intact, Biogrid	No/Yes	Mito: 0.4963	Lipid metabolism	2H:3	No	No	10	Medium	No
PARL	Q9H300	Biogrid	Yes		Mitophagy	PDB:1	No	No	10	Medium	No
CLPP	Q16740	Biogrid	Yes		Clp protease proteolytic subunit	PDB:1	No	No	10	Medium	No
CDC34	P49427	Biogrid	Yes		Ubiquitin-conjugating enzyme	ACMS:1	No	No	10	Medium	No

SIRT3	Q9NTG7	Intact	Yes		NAD-dependent protein deacetylase	DA:1	Yes	No	10	Medium	No
LRRK2	Q5S007	Intact, Biogrid	Yes		protein kinase, regulator of RAB GTPases	COIP:2, ACMS:1	No	No	10	Medium	No
SSBP1	Q04837	Biogrid	Yes		mtDNA maintenance	PDB:1	Yes	No	10	Medium	No
FAM25C	B3EWG5	Intact, Biogrid	Unknown/Yes	Mito: 0.878	Unknown	2H:3	No	No	11	Medium	No
C12orf65	Q9H3J6	Biogrid	Yes		Little info, Leigh Syndrome related, neurological phenotype in mutants	PDB:1	No	No	11	Medium	No
VWA8	A3KMH1	Biogrid	Yes		Little info, has ATPase activity	PDB:1	No	No	11	Medium	No
SURF1	Q15526	Biogrid	Yes		cytochrome c oxidase regulator	PDB:1	No	Yes	6	Medium	Yes-little effect
TP53/p53	P04637	Intact	Yes		Cell death regulator	2H:4, COIP:2	Yes	No	1	Low	
AIFM1	O95831	Intact, Biogrid	Yes		NADH and apoptosis regulation	PDB:1	No	No	1	Low	
MTRES1	Q9POP8	Biogrid	Yes		Mito transcription reguator	PDB:1	No	No	2	Low	
MTERF3	Q96E29	Biogrid	Yes		Transcription regulator	PDB:1	No	No	2	Low	
TEFM	Q96QE5	Biogrid	Yes		Transcription regulator	PDB:1	No	No	2	Low	
TFAM	Q00059	Biogrid	Yes		Transcription regulator	PDB:1	Yes	No	2	Low	
EXD2	Q9NVH0	Biogrid	Yes		Exonuclease	PDB:1	No	Yes	2	Low	

HSPD1	P10809	Intact, Biogrid	Yes		Protein import/assembly chaperon	PDB:1	No	No	8	Low	
PMPCA	Q10713	Biogrid	Yes		Mitochondrial-processing peptidase subunit	PDB:1	No	No	8	Low	
PMPCB	O75439	Biogrid	Yes		Mitochondrial-processing peptidase subunit	PDB:1	No	No	8	Low	
HSPE1	P61604	Pub1	Yes		Protein import/assembly chaperon	CL:1	No	No	8	Low	
IMMP2L	Q96T52	Biogrid	Yes		Transit peptide removal	PDB:1	No	Yes	8	Low	
SLIRP	Q9GZT3	Biogrid	Yes		Mito RNA binding protein	PDB:1	No	No	9	Low	
FASTKD5	Q7L8L6	Biogrid	Yes		mRNA processing	PDB:1	No	No	9	Low	
TBRG4	Q969Z0	Biogrid	Yes		RNA processing	PDB:1	No	No	9	Low	
LRPPRC	P42704	Biogrid	Yes		RNA metabolism	PDB:1	Yes	No	9	Low	
FASTKD3	Q14CZ7	Biogrid	Yes		mRNA regulation/translation induction	PDB:1	No	No	9	Low	
HTT	P42858	Intact	Yes		Huntington's disease gene	2H:2	Yes	No	10	Low	
APP	P05067	Intact	Yes		Alzheimers' disease	SPR:4	Yes	No	10	Low	
MRPS12	O15235	Biogrid	Yes		28S ribosomal protein	PDB:1	No	No	3	None	
MRPS26	Q9BYN8	Biogrid	Yes		28S ribosomal protein	PDB:1	No	No	3	None	
MRPL11	Q9Y3B7	Biogrid	Yes		39S ribosomal protein	PDB:1	No	No	3	None	
FASTKD2	Q9NYY8	Biogrid	Yes		Mito ribosome assembly	PDB:1	No	No	3	None	
MRRF	Q96E11	Biogrid	Yes		Mito ribosome assistor	PDB:1	No	No	3	None	

METTL1 7	Q9H7H 0	Biogrid	Yes		Mito translation	PDB:1	No	No	3	None	
MTIF2	P46199	Biogrid	Yes		Mito translation	PDB:1	No	No	3	None	
MTIF3	Q9H2K 0	Biogrid	Yes		Mito translation	PDB:1	No	No	3	None	
MTRF1	O7557 0	Biogrid	Yes		Mito translation	PDB:1	No	No	3	None	
MTRF1L	Q9UGC 7	Biogrid	Yes		Mito translation	PDB:1	No	No	3	None	
RMND1	Q9NW S8	Biogrid	Yes		Mito translation	PDB:1	No	No	3	None	
TRMT61 B	Q9BVS 5	Intact	Yes		Mito tRNA methyltransferase	PDB:1	No	No	3	None	
MTG2	Q9H4K 7	Biogrid	Yes		mitochondrial ribosome assembly	PDB:1	No	No	3	None	
MRPL58	Q1419 7	Biogrid	Yes		Peptidyl-tRNA hydrolase	PDB:1	No	No	3	None	
TSFM	P43897	Biogrid	Yes		Ribosome complex	PDB:1	No	No	3	None	
TUFM	P49411	Biogrid	Yes		Ribosome complex	PDB:1	No	No	3	None	
TRUB2	O9590 0	Biogrid	Yes		RNA processing/ribosome complex	PDB:1	No	No	3	None	
MRM1	Q6IN8 4	Biogrid	Yes		rRNA methyltransferase	PDB:1	No	No	3	None	
RPUSD4	Q96CM 3	Biogrid	Yes		rRNA/tRNA modification	PDB:1	No	No	3	None	
TRMT61 B	Q9BVS 5	Biogrid	Yes		tRNA methyltransferase	PDB:1	No	No	3	None	
METTL1 5	A6NJ78	Biogrid	Yes		N4-methylcytidine methyltransferase	PDB:1	No	No	3	None	
TACO1	Q9BSH 4	Biogrid	Yes		Translational activator of cytochrome c oxidase 1	PDB:1	No	No	3	None	

CHCHD1	Q96BP2	Biogrid	Yes		Little info, Possible mt-ribosome related protein	PDB:1	No	No	3	None	
GRSF1	Q12849	Biogrid	Yes		Post-transcription regulator, ribosome assembly	PDB:1	No	No	3	None	
RPUSD3	Q6P087	Biogrid	Yes		post-transcriptional regulation, mito rRNA/ribosome role	PDB:1	No	No	3	None	
GFM1	Q96RP9	Biogrid	Yes		Mitochondrial GTPase, catalyzes the GTP-dependent ribosomal translocation	PDB:1	No	No	3	None	
GFM2	Q969S9	Biogrid	Yes		Mitochondrial GTPase, ribosome/translation regulation roles	PDB:1	No	No	3	None	
C1QBP	Q07021	Intact, Biogrid	Yes		Multiple functions, mito ribosome and translation regulation	PD:3, COIP:1, PDB:1	Yes	No	3	None	
TMEM70	Q9BUB7	Biogrid	Yes		ATP synthase biogenesis	PDB:1	No	Yes	5	None	
Atp5f1b	P56480	Intact	Yes		ATP synthase subunit beta	CL:1	Yes	Yes	5	None	
ATP5F1A	P25705	Pub1	Yes		ATP synthase subunit	CL:1	Yes	No	5	None	
ATP5PB	P24539	Pub1	Yes		ATP synthase subunit	CL:1	Yes	No	5	None	
ATP5PF	P18859	Pub1	Yes		ATP synthase subunit	CL:1	Yes	No	5	None	
ATP5B	Q0QEN7	Pub1	Yes		ATP synthase subunit	CL:1	Yes	No	5	None	
Slc25a4	Q05962	Intact, Biogrid	Yes		Mito ADP/ATP transport	PD:1	Yes	Yes	10	None	
VDAC1	P21796	Intact	Yes		Mito ion transport	PD:1	Yes	Yes	10	None	

ATF2	P15336	Intact, Biogrid	Yes		VDAC interactor	COIP: 1	No	No	10	None	
BCL2	P10415	Intact	Yes		Apoptosis regulation/NADH enzyme	PD:1, COIP: 1, 2H:1	Yes	Yes	1, 7		
MAGEA11	P43364	Intact, Biogrid	No	Cytoplasm: 0.5159, Mito: 0.0074	Androgen receptor coregulator	2H:3	No	No	None		
AGTRAP	Q6RW13	Intact, Biogrid	No	Golgi: 0.4696, Mito: 0.002	Angiotensin receptor regulator	2H:3	No	Yes	None		
PRB3	Q04118	Intact, Biogrid	No	Extracellular: 1, Mito: 0	Bacterial defense	2H:3	No	No	None		
BCAR1	P56945	Biogrid	No	Cytoplasm: 0.8993, Mito: 0	Breast cancer anti-estrogen resistance protein	ACMS :1	No	No	None		
ABI2	Q9NYB9	Intact, Biogrid	No	Cytoplasm: 0.9322, Mito: 0.0001	Cytoskeleton regulation	2H:4	No	No	None		
ITPR1	Q14643	Intact	No	ER: 0.6111, Mito: 0.0002	ER Ca <sup>2+</sup> release regulator	PL:2	No	Yes	None		
ESR2	Q92731	Biogrid	No	Nucleus: 0.9971, Mito: 0	Estrogen receptor beta	ACMS :1	No	No	None		
FNTA	P49354	Intact	No	Cytoplasm: 0.558, Mito: 0.0039	farnesyl/geranylgeranyltransferase	AP:1	No	No	None		
MGST3	O14880	Intact	No	ER: 0.5968, Mito: 0.0436	Fatty acid oxidation	PDB:1	No	Yes	None		
ARHGAP31	Q2M1Z3	Intact, Biogrid	No	Cytoplasm: 0.4361, Mito: 0.0004	GTPase-activating protein	COIP: 1	No	No	None		
PPIA	P62937	Intact, Biogrid	No	Cytoplasm: 0.8224, Mito: 0.0773	Multiple functions	CL:1	No	No	None		

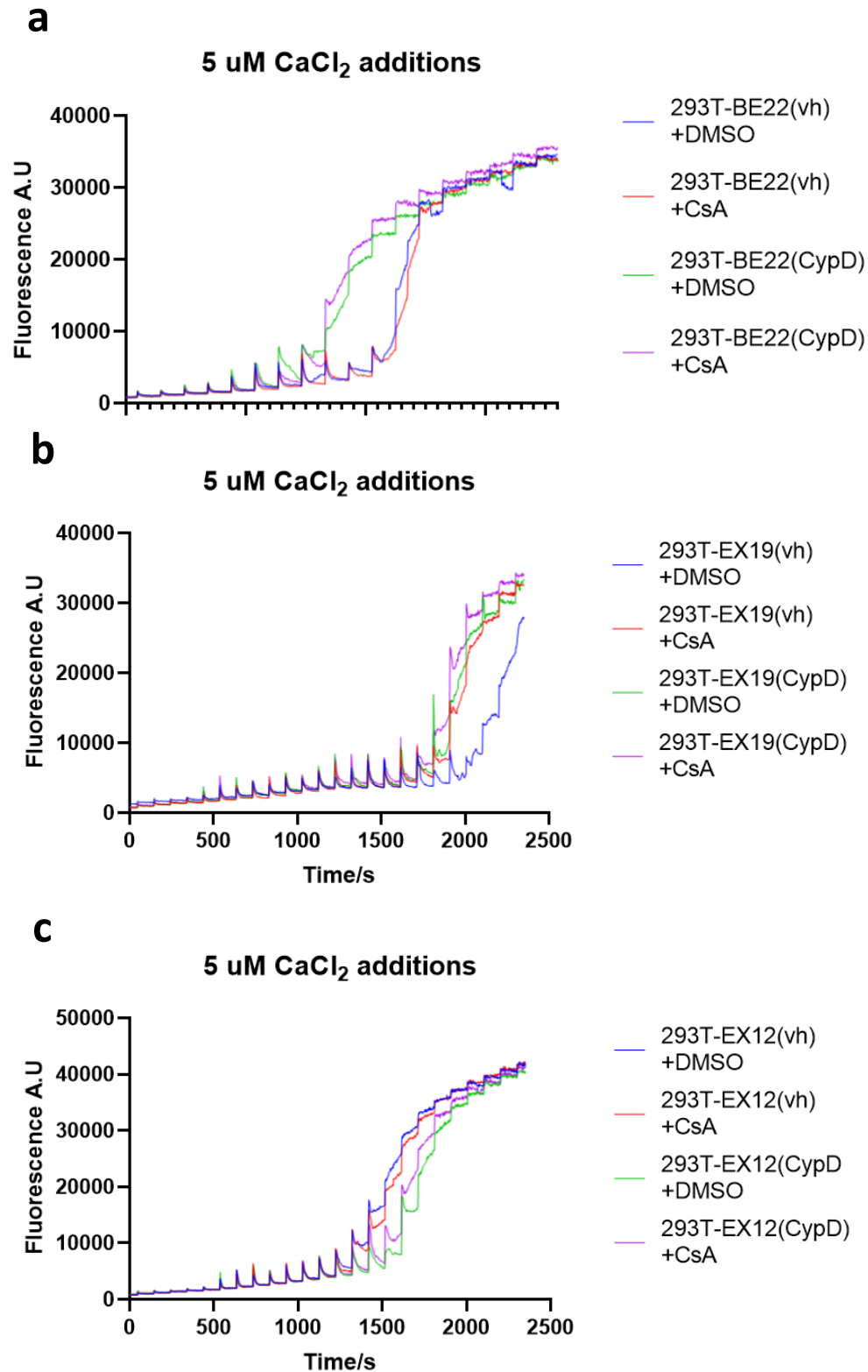
PLEKHA4	Q9H4M7	Biogrid	No	Cytoplasm: 0.9411, Mito: 0.0001	phosphatidylinositol 3-phosphate binding	ACMS:1	No	No	None		
MUC1	P15941	Intact, Biogrid	No	Cell membrane: 0.9328, Mito: 0.0004	Possible multiple functions	2H:3	No	Yes	None		
ARFIP2	P53365	Intact, Biogrid	No	Nucleus: 0.7797, Mito: 0.0008	Possible multiple functions	2H:3	No	No	None		
BANP	Q8N9N5	Intact, Biogrid	No	Nucleus: 0.9805, Mito: 0	Possible multiple functions	2H:3	No	No	None		
SYP	P08247	Intact, Biogrid	No	Cell membrane: 0.5871, Mito: 0.0011	Possible Plasma membrane vesicle	2H:5	No	Yes	None		
YIF1A	O95070	Intact, Biogrid	No	ER: 0.5675, Mito: 0.0004	Possible role in ER/Golgi transport	2H:3	No	Yes	None		
A2M	P01023	Intact	No	Extracellular: 0.994, Mito: 0	Proteinase inhibitor	2H:3	No	No	None		
CRYZ	Q08257	Biogrid	No	Cytoplasm: 0.4689, Mito: 0.0671	Quinone oxidoreductase	PDB:1	No	No	None		
NRAS	P01111	Biogrid	No	Cell membrane: 0.9997, Mito: 0	Ras GTPase	PDB:1	No	No	None		
HRAS	P01112	Biogrid	No	Cell membrane: 0.9997, Mito: 0	Ras protein signaling	PDB:1	No	No	None		
Ophn1	O60890	Intact	No	Cytoplasm: 0.845, Mito: 0.001	Rho family GTP hydrolysis	COIP:1	No	No	None		
MEPCE	Q7L2J0	Biogrid	No	Nucleus: 0.9701, Mito: 0	snRNA methylphosphate capping enzyme	ACMS:1	No	No	None		
KNG1	P01042	Intact	No	Extracellular: 0.8816, Mito: 0	Thiol proteases inhibitor	PL:1	No	No	None		
SERPINB5	P36952	Biogrid	No	Cytoplasm: 0.7193, Mito: 0.0491	Tumor suppressor	2H:1	No	No	None		



CS	O75390	Biogrid	Yes		Citrate synthase	PDB:1	No	No	None		
SYPL1	Q16563	Intact, Biogrid	Unknown	Lysosome/Vacuole: 0.3814, Mito: 0.001	Little info, Cell proliferation/apoptosis regulation, upregulated in some cancers	2H:3	No	Yes	None		
CMTM5	Q96DZ9	Intact, Biogrid	Unknown	Golgi: 0.73, Mito: 0.0007	Little info, Cell proliferation/apoptosis regulation, upregulated in some cancers	2H:3	No	Yes	None		
FKBP7	Q9Y680	Intact, Biogrid	Unknown	ER: 0.9816, Mito: 0.0036	Little info, Translation regulation, PPlases	2H:3	No	No	None		
KLK1	P06870	Intact	No	Extracellular: 0.9717, Mito: 0	Cleaves kininogen	PL:1	Yes	No	None		
KRAS	P01116	Biogrid	No	Cell membrane: 0.0006, Mito: 0	GTPase	PDB:1	Yes	No	None		
DNM2	P50570	Intact	No	Cytoplasm: 0.9818, Mito: 0.0002	Microtubule roles	2H:3	Yes	No	None		

**Table A1: Summary of past CypD protein-protein interaction hits**

## Appendix 2: Screening results of CypD KO cell lines



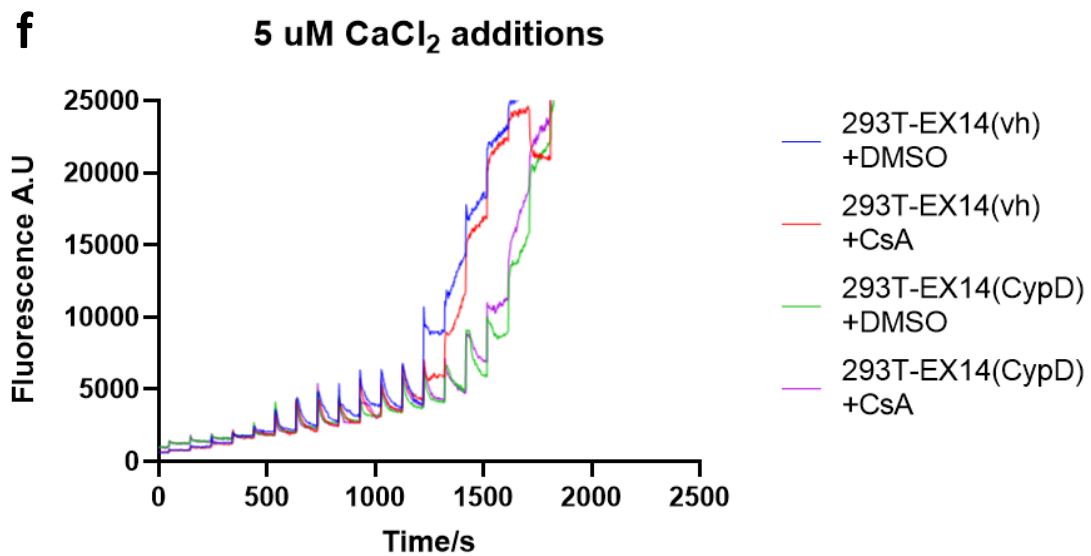
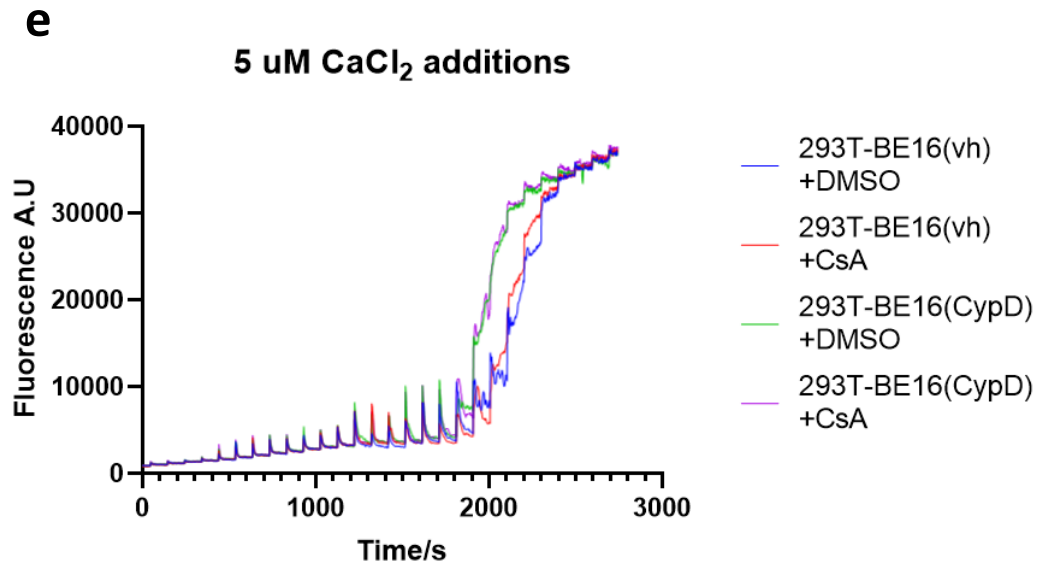
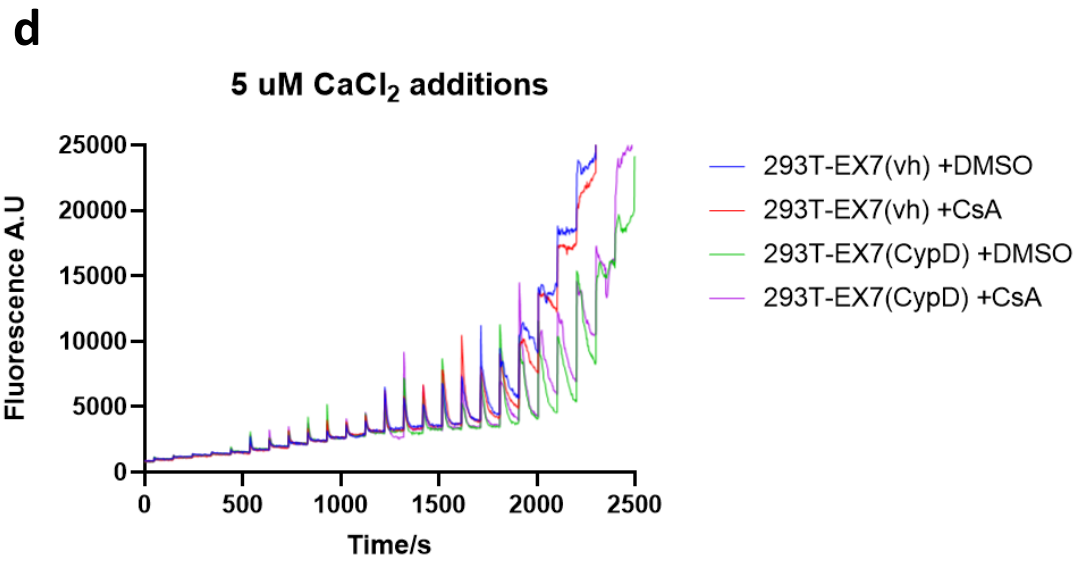


**Figure A2: Screening for response to CypD expression in HEK293T CypD KO lines**

a) Representative CRC assay data for BE22 cells transfected with CypD (in pcDNA3.1+) or vh (vehicle control: an empty plasmid backbone of pcDNA3.1+) with 1uM CsA or an equivalent volume of DMSO added prior to measurement, n=3

b) Quantification of CRC assay data for EX19 cells transfected with CypD (in pcDNA3.1+) or vh (vehicle control: an empty plasmid backbone of pcDNA3.1+) with 1uM CsA or an equivalent volume of DMSO added prior to measurement, n=3

a) Representative CRC assay data for EX12 cells transfected with CypD (in pcDNA3.1+) or vh (vehicle control: an empty plasmid backbone of pcDNA3.1+) with 1uM CsA or an equivalent volume of DMSO added prior to measurement, n=3

b) Quantification of CRC assay data for EX7 cells transfected with CypD (in pcDNA3.1+) or vh (vehicle control: an empty plasmid backbone of pcDNA3.1+) with 1uM CsA or an equivalent volume of DMSO added prior to measurement, n=3

a) Representative CRC assay data for BE16 cells transfected with CypD (in pcDNA3.1+) or vh (vehicle control: an empty plasmid backbone of pcDNA3.1+) with 1uM CsA or an equivalent volume of DMSO added prior to measurement, n=3

b) Quantification of CRC assay data for EX14 cells transfected with CypD (in pcDNA3.1+) or vh (vehicle control: an empty plasmid backbone of pcDNA3.1+) with 1uM CsA or an equivalent volume of DMSO added prior to measurement, n=3

All quantification analysis are represented as mean  $\pm$  SD and were analysed using paired t-test for effect of drug treatments (DMSO vs CsA) and unpaired t-test for differences between cellular conditions, (\*:  $p < 0.05$ ).

Following the second round of CypD KO in HEK293T cells using CRISPR, I proceeded to screen the cells line with successful CypD KO (as verified by western blotting) for changes in CRC assay profile in response to re-expression of CypD. The results of 6 cell lines with good CRC assay response are displayed in Figure A1.